ETHANOL FERMENTATION IN A GAS-LIFT BIOREACTOR SYSTEM

MASSOUD JANEKEH

THESIS SUBMITTED FOR THE QUALIFICATION OF

DOCTOR OF PHILOSOPHY

TO

HERIOT-WATT UNIVERSITY

DEPARTMENT OF CHEMICAL AND PROCESS ENGINEERING

EDINBURGH

SEPTEMBER 1988

INDEX

Abstract

In recent years the fermentation of ethanol from cellulosic waste to overcome possible future energy shortages has received much attention. Although many well established processes can be applied to completely utilise the dextran content of cellulose, the economics of the process may not be fully justified unless the xylan fraction of hemicellulose is also converted to ethanol. In this study, a fermentation system featuring anaerobic digestion of xylose at 60 °C for potential large scale conversion of hemicellulose to ethanol is considered. Under optimum conditions of pH and temperature, *Clostridium thermosaccharolyticum* NCIB 9385 ferments a wide range of carbon sources mainly to ethanol and acetic acid with yields in order of $Y_E \approx$ 35-50% and $Y_A \approx$ 15-30%. Growth on xylose supports marginally higher yields than growth on glucose. The low ethanol productivity was improved by developing an ethanol tolerant strain CTM 3, and by cell entrapment on a variety of Biomass Support Particles (BSPs). Maximum productivity of 0.5 g ethanol/l/h was observed with BSPs in continuous culture. Operation of a gas-lift fermenter (GLF) with a concentric draught tube is found suitable for the scale-up of this bench fermentation. A circulating three-phase system is considered for the potential use of BSPs in the fermenter. The natural characteristics of fermentation broth support a homogeneous two-phase flow in the fermenter with increased interfacial area. Under such conditions an extractive fermentation system based on desorption of ethanol is proposed.

Acknowledgement

I wish to thank my supervisors; Dr W J Mitchell, Dr M Kennard and Dr L R Weatherly for their invaluable guidance and advice throughout this work.

I am equally indebted to Professor C W Nutt and Professor C M Brown for provisions of the research facilities and generous contributions towards the project.

I am also grateful to all academic and technical staff of the departments of Chemical and Process Engineering and Brewing and Biological Sciences, whose help made this work possible.

Finally I would like to thank all my friends not mentioned above, especially Joseph Aduse-Opoku for his excellent freindship.

List of Figures

List of Tables

Nomenclature

Symbol	Definition	Dimension
a	Interfacial area	L^2
A	S^*/K_m (Equation 2.3)	-
A_o	Cross-sectional area of gas nozzle	L^2
A_d	Cross-sectional area of downcomer	L^2
A_r	Cross-sectional area of riser	L^2
Bo	Bodenstein number	-
B	Bond number	-
C_o	Initial cell concentration	ML^{-3}
C	Cell concentration	ML^{-3}
C_{fL}	Coefficient of friction for liquid	-
C_{fM}	Coefficient of friction for fluid mixture	-
Crk^2/σ_L	Parameter of bubble coelescence prposed by Marrucci (1969)	-
C_s	$p_s\epsilon_s/(\epsilon_L+\epsilon_s)$, average solid concentration in gas free slurry	ML^{-3}
c, c_i, c_ϕ	Tracer concentration	ML^{-3}
C_r	c/c_∞	-
D	Coefficient of diffusivity	L^2T^{-1}
	Dilution rate	T^{-1}
D_c	Column diameter	L
D_d	Draught tube diameter	L
D_f	Diffusivity of micrbial film	L^2T^{-1}
D_{max}	Maximum dilution rate	T^{-1}
D_T	Axial dispersion coefficient	L^2T^{-1}
d_b	Diameter of a bubble	L
d_e	Equivalent diameter of a sphere	L
d_m	Diameter of a microbial film	L
d_{max}	Maximum diameter of a particle (or bubble)	L
d_{op}	Diameter of orifice	L
d_p	Diameter of a particle	L
d_s	Sauter mean diameter	L
E	Total energy dissipated in the fermenter	ML^2T^{-3}
E_N	Effectiveness factor (Equation 2.5)	-
Eo	Eotvos (Ertvesh) number	-
Eu	Euler number	-
Fr	Froude number	-
g	Acceleration due to gravity	LT^{-2}
Ga	Galileo number	-
H	Height	L
H_r	Liquid height in the fermenter	L
h_c	Heat transfer coefficien of liquid	$MT^{-3}\Theta^{-1}$
h_i	height of gas-jet nozzle	L
J_G	Superficial gas velocity	LT^{-1}
J_{Gr}	Superficial gas velocity in the riser	LT^{-1}
J_{Gf}	Fluidisation superficial gas velocity	LT^{-1}
J_L	Superficial liquid velocity	LT^{-1}

Symbol	Definition	Dimension
J_{mf}	Minimum fluidisation fluid velocity	LT^{-1}
K_1, K_2, K_3	Reaction rate coefficients (Table 2.5)	ML^{-3}
K_i	Substrate inhibition coefficient	ML^{-3}
K_m	Half-saturation (Monod) constant	ML^{-3}
K_o	Coefficient similar to K_m (Equation 2.13)	ML^{-3}
k_2	Biological Rate Equation Coefficient	-
K_f	Thermal conductivity of gas film	$MLT^{-3}\theta^{-1}$
K_{or}	Coefficient of orficie	-
K_v	Volumeteric mass transfer coefficient	L^3T^{-1}
k_L	Mass transfer coefficient	LT^{-1}
L	Length	L
L_e	Equivalent length of fermenter (Equation 3.14)	L
L_f	Thickness of microbial film	L
L_H	Latent heat vapourisation	L^2T^{-2}
M_1	Mass through flow	MT^{-1}
M_2	Mass circulation flow	MT^{-1}
M_3	Total mass flow = M_1+M_2	MT^{-1}
M_g	Molecular weight of gas	M
M_s, M_p	Mass of cell per unit volume of immobilised cells	M
M	Morton number	-
m_p	Amount of Biomass associated with a particle	M
m_{po}	Maximum mount of Biomass associated with a particle	M
N_s	Substrate flux	ML^{-1}
n_u	Circulation number	-
Pe	Peclet number	-
P	Product concentration	ML^{-3}
P^o	Maximum Productivity	$ML^{-3}T^{-1}$
P_o	Initial product concentration	ML^{-3}
P_m	Maximum product concentration above which cells do not grow (Equation 2.18)	ML^{-3}
	Power dissipated by turbulence by unit mass of liquid (Equation 3.20)	ML^2T^{-3}
P_m'	Maximum product concentration above which cells do not produce products	ML^{-3}
p	Pressure	$ML^{-1}T^{-2}$
Ph	Pressure in the head space	$ML^{-1}T^{-2}$
Q_G	Volumetric gas flowrate	L^3T^{-1}
Q_{Gm}	Gas time-mean flowrate	L^3T^{-1}
Q_L	Volumetric liquid flowrate	L^3T^{-1}
R	Reaction rate	T^{-1}
	Gas constant (Equation 3.1)	$ML^2T^{-2}mol^{-1}\theta^{-1}$
Re	Reynold number	-
Re_{mf}	Minimum fluidisation Reynold number	-
R_s	Specific rate of substrate removal	T^{-1}
R_{so}	Maximum specific rate of substrate removal	T^{-1}
r_c	Circulation rate	T^{-1}
S	Substrate concentration	ML^{-3}
S^*	Interfacial substrate concentration	ML^{-3}
Sc	Schmidt number	-
Sh	Sherwood number	-

Symbol	Definition	Dimension
T	Temperature	θ
T_A	Specific rate of attrition	T^{-1}
T_a	Air (Gas) Tenmperature	θ
T_c	Transition Temperature for crystallisation	θ
T_o	Initial temperature (or condition at t=0)	θ
T_s	Surface or equilibrium temperature	θ
t_b	Batch time	T
t_c	Circulation time	T
t_m	Mixing time	T
t_r	Riser time	T
U_{mr}	Liquid mean realtive velocity	LT^{-1}
U_t	Terminal velocity of particles	LT^{-1}
u_G	Gas velocity	LT^{-1}
u_L	Liquid velocity	LT^{-1}
u_m	Mean liquid velocity	LT^{-1}
V_c	Volume of gas distributor chamber	L^3
V_L	Liquid volume	L^3
V_R	Effective reactor volume	L^3
v_i	Specific rate of ethanol formation in the presence of exogenous ethanol	T^{-1}
v_o	Maximum specific rate of ethanol formation in the presence of exogenous ethanol	T^{-1}
We	Weber number	-
Z	Power per unit volume	$ML^{-1}T^{-2}$

Greek Letters

α	Shape factor	-
δ	Penetration factor	-
ϵ	Porosity of particle	-
	Hold-up (or voidage) of fluid bed	-
ϵ_G	Gas hold-up	-
ϵ_L	Liquid hold-up	-
ϵ_m	Mean fluid hold-up	-
ϵ_{mf}	Gas hold-up at minimum fluidisation	-
ϵ_s	Solid hold-up	-
μ	Viscosity,	$ML^{-1}T^{-1}$
	Specific growth rate of cells	T^{-1}
μ_o	Maximum specific growth rate of cells	T^{-1}
μ_i	Maximum specific growth rate of cells in the presence of ethanol	T^{-1}
ρ	Liquid density	ML^{-3}
ρ_f	Biofilm density	ML^{-3}
ρ_s	Solid density	ML^{-3}
ρ_{em}	Mean liquid density	ML^{-3}
ρ_m	Fluid mixture density	ML^{-3}
ρ_{op}	Microbial density	ML^{-3}
σ	Surface Tension	MT^{-2}
τ	Mean residence time of the fermenter	T
τ_m	Residence time of fluid in a mixed flow reactor	T
τ_p	Residence time of fluid in a plug flow reactor	T

Subscripts

b	Bubble
c	Cell
d	Downcomer
e	Equivalent
f	Microbial film
G	Gas
i	Inhibition condition
L	Liquid
m	Mixture, mean
p	Particle
r	Riser
s	Solids, substrate

Abbreviations

ALF	Air-lift Fermenter
BC	Bubble Column
BRE	Biological Rate Equation
BSP	Biomass Support Particle
CDT	Concentric Draught Tube
CTM 3	3% (w/v) Ethanol Tolerant Mutant of *C. thermosaccarolyticum*
GLF	Gas-lift Fermenter
LIC	Lignocellulosic Material
LR	Loop Reactor
MCR	Revised Clostridial Medium
PNA	The Brazilian National Alcohol Programme
RCM	Reinforced Clostridial Medium
RTD	Residence Time Distribution

TO MY PARENTS

Chapter One

Ethanol Fermentation

Ethanol Fermentation

1.1 Background

The chemical industry has been the main supplier of solvents and fuels to the industrial world for the past few decades. The exploitation of oil and the advent of petroleum cracking ensured firm and substantial economic prospects for the industry's future. The dramatic oil crisis of the early 1970's upset the balance books of the healthy petrochemical industries and also signalled a warning to many energy ministers worldwide to review their future energy strategies and alternative resources. Ever since, complex and unpredictable oil economics have followed an overall positive trend and throughout the 1970's and the 1980's the oil prices have steadily increased to a maximum of $40 US per barrel and current value of $16 US per barrel. Despite such large price variations contemporary industrial society remains a petroleum economy. In 1978, overall organic chemical production was 340 million tons and this was almost entirely based on petroleum (3% originated from coal). It is now clear that an oil crisis is not only an energy crisis, but also a crisis of chemical resources.

The second world war heralded a new era in the field of science and technology. It laid the foundations of many industries such as petrochemicals, computers, nuclear energy, and microbial technology. In the latter industry Penicillium fermentation proved to be of vital importance both in times of war and peace. Solvent production by fermentative micro-organisms such as the acetone/butanol fermentation by *Clostridium acetobutylicum* and fermentation of ethanol by *Saccharomyces cerevisiae* also proved indispensible in overcoming the shortages brought about by the war.

Ethanol fermentation has been known to man for thousands of years and it is at the heart of the brewing industry. Traditionally, industrial ethanol

was produced as a by-product of the sugar industry. Until the early 1940's the production of ethanol by fermenting crops was widespread in Europe, chiefly using corn, potatoes, and sugar beets. After 1945, fermentation in the industrial chemical market was replaced by petroleum based sources. By 1950 nearly all government facilities for ethanol fermentation were terminated except in a few countries such as Argentina, Brazil, and India. From the experience of the world oil market, it is evident that dependence on non-renewable fossile energy resources can only be relatively short term. With rapid development in "industrial" countries, in little over 100 years, the fuels accumulated in the earth over millions of years would be consumed. The concept of renewable energy resources has been subject of numerous studies which have examined the utilisation of such alternatives as solar , tidal, and wind energies. A more attractive and easily utilised alternative is the use of feedstocks containing sugar, starch, cellulose, and hemicellulose. Photosynthesis in plants maintains the perpetual availability of this energy source. Table 1.1 compares the fossil energy with photosynthetically fixed energy. It is worth noting that living plants trap more than ten times the total energy consumed by man, but only a fraction of this energy could be tapped.

Table 1.1 World Energy Balance and Photosynthesis

Source : Faust *et al* (1983)

Solar energy on earth	3.0×10^{24} J per annum
Fossil fuel reserves (Proven)	4.3×10^{22} J per annum
Energy use (1970)	3.0×10^{20} J per annum
Photosynthetically fixed energy (2×10^{11} ton)	3.0×10^{21} J per annum
Food consumption (4×10^{9} people)	1.5×10^{19} J per annum

With such potential, biofuel fermentation processes may become economically viable both in the short term and in the long term.

In the short term they can provide fuel energy resources for those countries without or with inadequate fossil fuel reserves (for example Brazil). In the long term it may help to overcome the eventual global energy shortages. In recent years there has been much renewed investigation into industrial ethanol fermentation as a biofuel source.

The use of alcohol as an automotive fuel created a euphoria of interest in the 1970's and early 1980's. The technology is well established and it is currently practised in Brazil and the United States. In the US the "Gasohol Program" took a major step after the 1970's oil crisis and the federal government funded much research for its development and optimisation. In the US, alcohol blended with gasoline at a 10% inclusion is called gasohol. The programme was encouraged by introducing attractive economic measures for both producers and consumers. The Brazilian approach however has had a stronger impact on the biofuel industry. Prior to the creation of their national alcohol programme, *Programa Nacional do' Alcool* (PNA), much of the alcohol produced in the country was a by-product of the sugar industry. Brazil is a third world country particularly deficient in fossil energy. Almost 45% of its energy needs are imported (Rothman *et al* 1983). The objectives of the PNA is to reduce the petroleum imports and gradually replace gasoline as car fuel. In addition to the PNA, the Brazilian government have considered various other energy programmes and alternative resources to overcome their energy crisis. New measures have been taken in locating and exploiting new petroleum producing areas. Hydroelectricity, coal, wood, biogas, and shale oil are amongst other abundant sources of energy under an extensive and systematic study. The country's vast agricultural potential however provides an ideal natural resource for alcohol fermentation and indeed Brazil is one of the largest

alcohol producing countries in the world (Rothman *et al* 1983). Following the American and the Brazilian experience, many other countries began their own alcohol programme, and operating plants now exist in Canada, New Zealand, and Philippines. At a time when the research interest diverted its attention from ethanol production Lyons (1983) carried out a survey of ethanol production in the US. The report indicated that the American government is proceeding with full emphasis towards their target level of 1.8 billion gal per annum of ethanol by the mid 1980's. However the programme has had its casualties especially in the small size plant operation. This was mainly due to more emphasis on the capital costs rather than budgeting for operating capital. Lack of technical expertise also affected some of the small operations. The Brazilian progress was reported by Barretts de Menzes (1982). The government's committment towards the target level of 10.7 billion liters per annum of alcohol by the mid 1980's is demonstrated by commissioning fermentation plants for the conversion of starchy feedstocks such as cassava, sweet potato and babassu nuts to alcohol. Bu'lock (1983) investigated the potential of cellulosic materials in the U.K for alcohol fermentation. They concluded that the most probable economic choice of substrate would be the by products of paper (the pulping process) and dairy (cheese whey) industries. Indeed the feasibility of ethanol fermentation is to some extent determined by the availability and cost of biomass raw material and on the local conditions. This cost factor amounts to 50-70% of the total production cost of ethanol. It is therefore of prime importance to assess the availability and to analyse the energy yields of the various raw materials.

1.2 Energy Crops

The vast variety of renewable biomass resources used in fermentation are collectively referred to as energy crops. There are three main catagories

namely; Sugars, Starches and Cellulose. They all can give rise to alcoholic fermentation with varying pretreatment requirements and yields. By far the most abundant is cellulose as it constitutes much of the plant material on earth. In practice however the sugar and starch crops are primarily used. This is mainly due to their present availability, costs, and relative ease of processing. Table 1.2 shows some of the more common types of energy crops currently employed in various fermentation plants for production of alcohol.

1.2.1 Ethanol Manufacture from Sugars and Sugar Crops

Monosaccharides and disaccharides obtained from such diverse sources as sugar cane, sweet sorghum, sugar beets, molasses, and cheese whey can be fermented to ethanol. These common fermentable sugars include glucose, fructose, galactose, sucrose and lactose.

Sugar is produced in moderate climatic regions in the form of beet and in tropical regions from sugar cane with about the same areal efficiency for both crops. Often pretreatment by way of extraction and concentration usually by evaporation in order to reduce the microbial content to a tolerable level, may be necessary. The sugar solutions must sometimes be deproteinised or demineralised to optimize fermentation. The sugar from cane or beet extraction usually contains 12-16 percent saccharose. While *Saccharomyces cerevisiae* is widely used to convert glucose, fructose, and sucrose to equimolar amounts of ethanol and carbon dioxide, *Kluyveromyces fragilis* is primarily used to convert lactose from whey. Yields of ethanol typically are 45-50 percent of sugar weight.

Table 1.2 Energy crop - ethanol yields

Source : Humphreys and Glasgow Ltd., (1983)

	Sugar cane	Sugar beet	Cassava (Manioc) (Tapioca)	Potatoes	Maize	Paddy rice	Wheat	Sweet sorghum (stems only)[3]	Grain sorghum (grains only)[2]	Starch[4]	Molasses[5]
Crop Yield t/ha/a[1]											
Commercial mean	80	50	10	13.99	2.95	2.57	1.66	35	7.5[2]		
Realistic range	50-120	30-80	6-30+	11-32	1-5.1	1.83-5.3	1.1-4.8	15-60	6-12		
Ethanol: ton of crop required to give 1 ton ethanol.											
Equivalent mean	18.9	15	8.5	8.5	4.1	3.6	4.3	18.9	3.1	2.2	4.3
range	14-30	12-17	6-11	7-14	3.6-4.4		3.5-4.8	14-30	2.7-3.8		3.5-6.0
Ethanol: liters of ethanol produced by 1 ton of crop.											
Equivalent mean	70	100	170	130	300	350	300	70	400	580	290
range	60-75	70-110	160-180		270-350				-		220-320
Ethanol: ton ethanol /ha/a											
Equivalent mean	4.7	3.3	1.2	1.76	0.7	0.71	0.4	2.0	2.4		
range	3-9.5	1.8-6.2	1-6	0.8-3.5	0.2-1.5	0.4-1.5	0.2-0.9	1-4	2-4		
Ethanol: liters/ha/a											
Equivalent mean	6000	4200	1600	2000	900	900	500	2500	3000		
range	3800-12000	2300-7800	500-4000	1000-4400	250-2000	500-1900	250-1200	1000-5000	2000-5000		
Carbohydrate content% mean	Sucrose 15	Sucrose 17	Starch 28	Starch 28	Starch 59	Starch 67	Starch 56	Sucrose 15	Starch 74	Starch 100	Sucrose 50
range	12-17	14-20	25-32	16-30	55-67		50-70	12-17	60-85		42-60

1: This does *not* imply that crop takes one year to grow and that it may be cropped throughout the year, but only that the land will give these approximate yields at an average annual rate.
2: Grain sorghum figures based on dry weight basis (i.e *not* as cropped)
3: Average growing period 120 days so possibility of double cropping exists.
4: Not a crop as such, but extracted from starch crops.
5: Not strictly a crop but a by-product from cane or beet after removal of sugar for conventional sugar production.

By-products from these processes include crop wastes such as sugar cane bagasse, beet pulp, or sorghum pith, aqueous stillage containing the plant's net yeast cell production mixed with the unfermented sugar solution from the still bottoms, carbon dioxide and fusel oils. For economic production of bioethanol the choice of a suitable substrate is of basic importance, especially when a sugar substrate is used, as the price is the main part of the production costs. Unfortunately compared with starchy and cellulosic raw materials sugar substrates are more expensive (Table 1.3).

Table 1.3 Cost of Feedstock for Ethanol Fermentation in the U.S

Source : Faust *et al* (1983)

	Cost ($ US/gal ethanol)		
	Sugar cane	Maize	Cellulose
Feedstock	1.31	0.93	0.57
Operating	0.47	0.58	0.76
Capital charges	0.56	0.46	0.54
Total costs	2.34	1.97	1.87
Capital charges	0.56	0.46	0.54
Total costs	2.34	1.97	1.87

Sugar crop cultivation relies strongly on the local climatic conditions. The availability of sugar crops limits itself to the abundant regions of the tropics. There are only few locations in the world where sugar cane can be harvested all year round. This disadvantage of sugar raw materials means either expensive evaporation and facilities to allow storage of the juice together with molasses produced or alternatively operating on a part-time or multisubstrate basis. Ethanol from sugar is not usually produced independently in industry but in combination with a sugar refinery where the available infrastructure can be made use of more

economically. The production of 95 vol % ethanol on a base of molasses is estimated to have substrate costs of 68% (Esser & Schmidt, 1982). Despite the high substrate costs molasses is perhaps the simplest and globally the most widely used raw material for alcohol production. However its use in the developed countries is discouraged and whey has come to be a more widely used source. Lyons (1983) reported on some 11 million tons of cheese whey available each year in the U.S, and according to estimates this could produce as much as 90 million gal (U.S.) of ethanol at a cost of only 22¢/gal. The use of whey as a substrate is limited to fermentation by micro-organisms that can metabolise lactose (the predominant sugar in whey). Lactose is a disaccharide consisting of glucose and galactose. Since glucose and galactose are more universally fermentable sugars than lactose, it has been suggested that a lactase treated whey would make a better raw material for fermentation.

1.2.2 Ethanol Manufacture from Grain and Non-Grain Starches

The lack of availability of sugar crops worldwide and its highly fluctuating market as a food commodity has diverted much attention into seeking other substrate sources. Starch is a naturally occurring glucose polymer present in such grain feedstocks as the cereals, maize, rice and wheat, and non-grain feedstocks (tuberous roots) potatoes and cassava. Starchy raw materials make up the majority of classical feedstocks for ethanol fermentation. Their wide availability and good storage properties have allowed all year fermentation. In Brazil, the PNA has commissioned fermentation plants to use Cassava, Babassu nuts, and Sweet Sorghum (Barretts de Menzes 1982). Margaritus and Bajpai (1982) investigated the potential fermentation of Jerusalem artichoke tubers in Canada for fuel alcohol production. They found that *Kluyveromyces marxianus* produced higher yields of alcohol (Y_p=0.45, or 88% of the theoretical) than *Saccharomyces sp.* Substrates containing starch, however, require a very

expensive and elaborate pretreatment. Classical processes for hydrolysing starch involve acid conditioning of the starch slurry prepared by milling and washing and heating it to 70-100 ^{o}C to gelatinize (Figure 1.1). The exposed β.1-4 linkages of the starch polymer are then attacked enzymatically by the action of a thermostable amylase. The resulting product is a mixture of different chain length dextrins and these are then degraded by amyloglucosidase to glucose. Larger operations employ a continuous hydrolysis system. During the second world war Unger *et al* (1944) developed a continuous cooking system for the production of alcohol from corn starch. More recently Lyons (1983) described the system developed by Alltech for plants producing in excess of 1/2 million gallons (US) of ethanol per annum. In a more common and a simpler practice, in the distilling industry, the enzyme derived from *Asperigillus niger* or *Rhizopus niveous* is added directly to the fermenter with the yeast at 33 ^{o}C (Faust *et al* 1983). Ziffer *et al* (1982) reported on ethanol yields of 14%(v/v) and stillage solid levels of 23%(w/v) when whole corn mashes were fermented with *Asperigillis oryzea* . The fermentation was 74-90 hours long and involved a mild acid pretreatment. The stillage solid is often sold as animal feed. The hydrolysis of starch is rather energy consuming and from Table 1.4 it is evident that with the exception of molasses the starch-based ethanol processes produce less net energy than sugar or cellulose based processes. In this view many investigators have developed optimised systems to reduce energy expenditure. Korn and Harper (1982) examined the extrusion and conventional cooking of corn for ethanol production. They showed that with extrusion cooking especially at low moisture contents (15% w/w), ethanol yields increased by 33%. Uncooked potatoes have a very large moisture content and show particularly low yields of ethanol upon fermentation (Table 1.5).

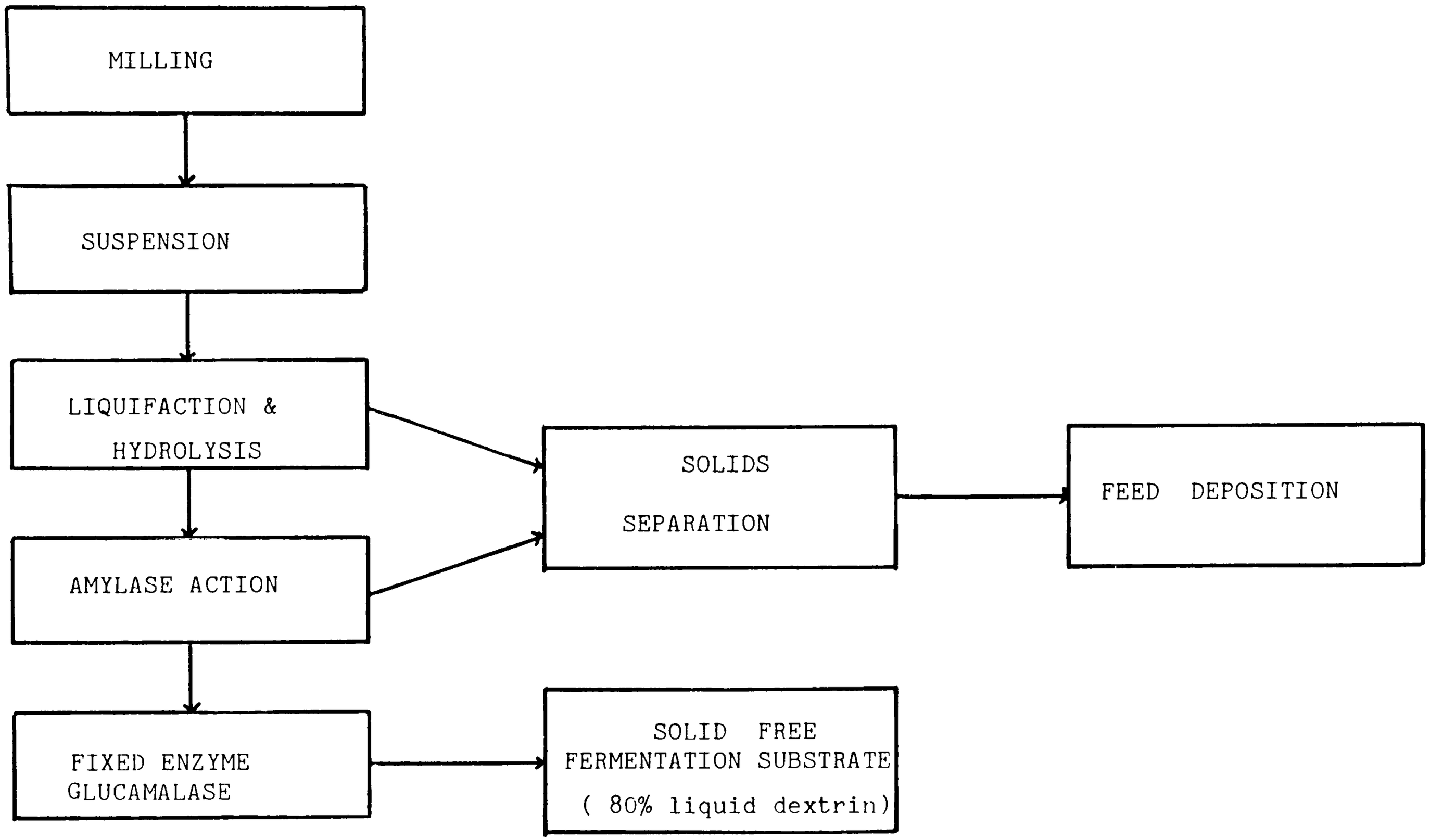

Figure 1.1 Continuous hydrolysis of starch (Faust et al, 1983).

Table 1.4 Net Energy Analysis of Ethanol Production from Sugar, Starch, and Cellulosic Feedstocks.
(MJ/m^3 Anhydrous Ethanol)

Source : Michaels and Blanch (1981)

Feedstock	**DEBIT:** Energy to Produce Feedstocks	**DEBIT:** Ethanol Process Energy Requirements	**CREDIT:** Ethanol Product	**CREDIT:** By-Product Energy	**NET:** Energy Yield
Sugar Cane	4680	12230	21210	19800[1]	24200
Molasses	14530	9620	21210	-	-2940
Sweet Sorghum	6260	12880	21210	14920[1]	16990
Sugar Beet	10220	12500	21210	29410[1]	23870
Whey	10[2]	9620	21210	-	11580
Potatoes	-[3]	14210[4]	21210	-	7000
Cassava	4110	14200	21210	-	2900
Wood (Fir)	10[5]	14650[6]	21210	17160[7]	23710
Waste Paper	370[8]	14650	21210	17070[9]	23260
Agricultural Residues	10	14650	21210	11120[10]	17670

1: Energy of combustion of crop waste.
2: Estimate of energy to concentrate whey permeate to 15 weight percent solids by evaporation. No energy debit is made for whey permeate production as agricultural energy input is allotted to milk products not milk wastes.
3: Culled potatoes used at site of potato processor; energy to grow potatoes is debited to the food products not the potato wastes.
4: Extra energy for potato processing is required for removal of the larger amount of moisture contained in potatoes.
5: Additional energy to collect and transport culled wood, wood chips, or agricultural residues during normal harvesting operations.
6: Plus 5030 $MJ/m^3$for cellulose and hemicellulose hydrolysis.
7: Based on composition of 27% legnin and heat of combustion of 11500 Btu/lb lignin.
8: Energy to separate municipal solid waste into fermentable/combustable and non-combustable components is 50 kWh/ton.
9: Based on composition of 21% lignin.
10:Based on composition of 15% lignin

Table 1.5 Comparison of Alcoholic Fermentation between Cooked and Uncooked Starch[1].

Starch	Total Reducing Sugar[2]		End - Products		Ethanol
	Initial (g)	Final (g)	CO_2 (g)	Ethanol (g)	Yield (%)
Uncooked Corn	20	1.7	9.0	9.2	90.0
Cooked Corn	20	1.2	9.3	9.6	93.9
Uncooked Cassava	20	1.6	9.0	9.1	89.0
Cooked Cassava	20	1.3	9.2	9.4	92.0
Uncooked Babassu	20	6.1	6.2	5.0	48.9
Cooked Babassu	20	4.1	7.7	7.5	73.0
Uncooked Potato	20	11.6	1.1	1.2	11.4
Cooked Potato	20	1.3	9.1	9.3	91.0

1: Mixture of starch (20g of reducing substances), 10g of *Aspergillus awamori* bran enzyme (equivalent to 52.3 units), amd 6 mL of 15% yeast suspension was fermented at 30°C, pH 3.5 for 5 days. In case of cooked starch, liquified by bacterial α-amylase.
2: Amounts show sugar content before and after fermentation.

By simultanously incubating the starch with a glucoamylase preparation of *Rhizopus* sp. and *Saccharomyces cerevisiae* Matsuoko *et al* (1982) demonstrated a one step fermentation of starch to alcohol with yields reaching 94%. In most cases the net costs for the starch substrate are lower compared to those of molasses, in particular when by products of economic value such as distillers light grain are available. In the cost analysis carried out by Michaels and Blanch (1981), starch fermentations were similar in production costs to sugar cane fermentation, and more expensive than producing ethanol from sweet sorghum or whey.

1.2.3 Ethanol Manufacture from Cellulosic Feedstocks

The future world energy shortage is overshadowed by the present food crisis. Only recently the outcry of the African famine victims once again shocked the world. The controversial issue of "Food or Fuel" was elegantly argued by Brown (1980), and it was pointed out that competition with the world's cropland for biofuel production would lend itself to the misuse of fertile land, and directed the attention towards the available biomass

that presently does not feed humans. These are alternative sources of alcohol which are not obtained at the expense of food crops, such as organic waste, forage, wood, crop residue etc.. While over the next few years alcohol for use will undoubtedly come from cereal and sugar crops, it will not be long before a virtually untapped source of energy is utilised, namely saccharification of cellulosic waste. Invariably if the alcohol industry is to survive , alcohol must be produced from such cheap and abundant sources.

Cellulose is the backbone of all plant structures. Most cellulosic solids contain three major components: Cellulose, Hemicellulose and Lignin in ratios of roughly 4:3:3 (Tsao *et al* 1978). Cellulose is a homogeneous polymer of glucose characterised by the β-1,4 glycosidic linkage. Hemicellulose molecules are often polymers of a five-carbon sugar xylose (arabinose and some hexoses are also present). These polysaccharides are bound into a chemical matrix by lignin, a phenylpropane network polymer. Together with the highly ordered crystalline structure of cellulose, lignin protects the cellulosic structure from enzymatic or chemical attack under ambient conditions.

The easily hydrolysable portion of cellulose is often referred to as the amorphous region of cellulose, and the resistant residue the crystalline cellulose. On average celluose is 15% amorphous and 85% crystalline. Crystalline cellulose is hydrolysed under conditions of strong acid and high temperature which makes the chemical and equipment costs prohibitively high.

Hemicelluose is an amorphous polysaccharide that readily hydrolyses in dilute acids to mono- and oligo- saccharides. Hardwood hemicellulose is comprised primarily of partially acetylated xylan and upon hydrolysis breaks up into xylose and acetic acid. Woodchip and saw dust are hydrolysed in batch or continuous percolation reactors. Acid hydrolysis

follows apparent first order kinetics, and increases in acid concentration or temperature result in higher yields. Such processing conditions may be optimised by simulation of the process cost function (Maloney *et al* 1986). Solvents such as Cadoxen (tris (ethylenediamine) cadmium hydroxide), CMCS (an aqueous solution of 17% sodium tartrate, 6.6% ferric chloride, 7.8% caustic, and 6.2% sodium sulphite) and concentrated sulphuric acid are used to dissolve cellulose once the hemicellulose fraction is removed. During the second world war several processes which utilised excess volumes of dilute sulphuric acid at high temperature to hydrolyse wood were developed. In the U.S both the Madison process and the TVA process have used such an approach. In a low temperature operation for hydrolysis of corn cobs suggested by Dunning and Lanthorp (1945), hemicellulose is hydrolysed by the action of dilute acid at 98°C for a period up to three hours. The residue containing lignin and cellulose (often referred to as "lignocellulose" or LIC) is dried and preheated with 85% sulphuric acid. Upon dilution of this material with water to an 8% acid concentration followed by hydrolysis at 120° to 130°C for 7 to 10 minutes a slurry containing dextrans is obtained. Under laboratory scale yields of 90% for conversion to glucose and 85% to xylose were obtained. The Peoria process employs this method at large scale, with yields of 36% (18.2 lb glucose/100lb cobs) and 85% (29.1 lb xylose/100 lb cobs) for glucose and xylose respectively (Tsao *et al* 1982). The lower yield of glucose is thought to be due to its degradation by the action of strong acids used in the process.

From Table 1.4 it may be observed that the net energy yields based on feedstock availability are more favourable for cellulose compared to starch. These results have encouraged research into cellulosic material in two major areas. Firstly optimisation and development of more energy efficient processes for hydrolysis of cellulose. Dale and Moreira (1982)

studied a "Freeze-Explosion" technique for increasing cellulose hydrolysis. This method relies on the treatment of cellulosic material with a volatile liquid under pressure followed by pressure release to evaporate and reduce the temperature. Yields greater than 90% of theoretical conversion were reported. The second area of research concentrates on utilisation of xylose as a sugar source. Many yeasts cannot ferment pentoses. Research is being carried out in order to develop new yeast strains (by genetic manipulation or otherwise) able to ferment "non-fermentable" sugars (Tsao *et al* ,1982). Strains of *Candida* , *Kluyveromyces* , *Pachysolen* , and *Pichia* show varying degree of fermentation of xylose to ethanol. Ethanol productivities of yeast fermentations based on xylose are notably lower than those based on glucose. This is primarily due to metabolic changes induced by different substates (see Chapter 2). So far *Candida shehatae* has proved to be the most promising organism by producing the highest ethanol concentration (24 g/l) from xylose (Skoog and Hahn-Hägerdal, 1988). However research has shown that changes in substrate concentration and pH could improve yields. In a study carried out by Detroy *et al* (1982), *Pachysolen tannophilus* was used to ferment xylose derived from hydrolysis of wheat straw hemicellulose. Xylose was liberated by acid hydrolysis and fermented by the yeast to produce 8.2 g/l ethanol from 47 g/l xylose in four days. In a separate study Dekkar (1982) was able to demonstrate an ethanol yield of 0.3 g ethanol per 1 g xylose by optimising the conditions to a maximum sugar concentration of 10% w/v and an operating pH of 2.75-2.5. More recently Parekh *et al* (1987) showed the ability of *Picha stipitis* **R** to ferment sugars in spent sulphur liquor -a by product of the pulping process. In a comparitive study ethanol yields based on substrate consumed for both *S.cerevisiae* and *P.stipitis* **R** were approximately similar at around 0.45g EtOH/g sugar. The ability of *P.stipitis* **R** to metabolise

pentoses however resulted in a far superior conversion of 95.6% of total sugars compared to *S.cerevisiae* at 68.7%. A single step conversion of cellulose to ethanol was suggested by Khan and Murray (1982). Under anaerobic digestion they employed a coculture of saccharolytic anaerobic bacteria (*Clostridium saccharolyticum* strains) to ferment a variety of cellulosic materials such as ball-milled pulp, cheese cloth, cotton battings, computer paper and news prints. Yields reaching 41% based on glucose and 31% based on xylose were reported.

The difficulty of cellulose hydrolysis be it chemical, thermal or enzymatical, has certainly inhibited its large scale application for ethanol fermentation. High temperature processing in corrosion resistant vessels is a technology not favoured by many critics and has deterred its present use yet by comparison with drilling of oil or catalytic cracking it is a very simple and modest process.

1.3 Economics of Ethanol Fermentation

In common with all other industries, the process economics of ethanol fermentation governs any management decision in commissioning or continuing operation of a plant. The two major factors in production of alcohol are its cost and energy balance (Tables 1.3 & 1.4). As indicated in Table 1.4 the cost of feedstocks for ethanol fermentation increases with the degree of availability of utilisable sugars. Maloney *et al* (1986) analysed the cost of producing 10% (w/v) xylose solution from hardwood hemicellulose. For batch and counter-current continuous treatment processes the cost was estimated at $0.88 US per gallon ethanol. If the same capital charges as with cellulose hydrolysis apply (Table 1.3), then the total cost of xylose would be $1.42 US per gallon ethanol. The relative low cost of xylose production is set back by low ethanol productivities of micro-organisms utilising this substrate. It should be pointed out that energy crops with higher alcohol content per hectare

cultivated land do not necessarily result in the cheapest alcohol. Factors such as exploitation cost should be considered in the overall balance. The other significant cost is due to downstream processing and product recovery. Distillation from the low concentrations of about 5-10% to pure 100% alcohol is particularly energy intensive. In a continuous process of an ethanol plant producing (approx.) 100 million liters of ethanol per year from cheese whey and corn Kalter *et al* (1981) estimated that distillation would account for 63% of the total energy costs, and 8.7% of the total annual operating costs. Moreover it was illustrated that 45% of the latter cost was due to azeotropic distillation of 95% ethanol to its pure anhydrous form which is the only acceptable form of ethanol for fuel. Energy savings can be achieved by alternative separation schemes such as solvent extraction, selective membrane extraction, and flash vapourisation. High conversion rates could also reduce energy costs. A fermentation broth containing 200 g/l ethanol requires little over half the energy needed for distilling 40 g/l (Rothmans *et al* 1983). A broth containing such high levels of ethanol requires a carbohydrate feed of 400 g/l which imposes yet another restriction due to substrate inhibition of culture growth. Higher sugar loads however could also result in savings in stillage handlings, cell separation, and feed sterilisation.

The value of energy is a function of how it is presented - place, time, convenience, cleanliness, continuity of supply etc.. Table 1.6 outlines the various cost aspects of ethanol production worldwide. Presently 95% synthetic ethanol is priced at £508/ton and 100% synthetic ethanol at £544/ton (BP Chemicals, 1988). Recently Wecker and Zall (1987) reported on the price of ethanol manufactured by fermentation at 0.16-0.19 US$/lb 100 % ethanol (equivalent to £187-£222/ton).

Table 1.6 Fuel ethanol production costs :basis and assumptions

Source: Rothmans *et al* (1983)

Case	A	B	C	D	E	F
Location	Brazil	USA	Europe	Europe	Europe	Europe
Feedstock	Sugarcane	Maize	Wheat	Sugarbeet	Sugarbeet & green crops	Woodwaste
Status	Proven	Proven	Development	Development	Development	Research
Hourly Capacity (t/h)	10	10	10	10	10	10
Operating hours (h/a)	5040	8000	8000	4320	7200	8000
Annual capacity (t/a)	50400	80000	80000	43200	72000	80000
Fermentables (wt%)	14	61	66	12	av.12	38
(as carbohydrates)	Sucrose	Starch	Starch	Sucrose	Sucrose	Cellulose
Carbohydrate:ethanol (wt/wt)	1.86	1.76	1.86	1.86	1.86	1.76
Yield % of ideal	84	82.5	82.5	88	av.85	70
Feed:Product (t/t)	15.8	3.50	3.23	17.6	av.18.2	6.6
Feed unit cost ($/t)	10	100	200	20	av.18	30
By-product (type)	None	DDG	Protein	Protein	Protein	Various
Quantity:product (t/t)	-	1.24	0.45	0.25	0.25	0.5
unit price ($/t)	-	150	300	300	300	200
Fuel (type)	With	Coal	Straw	"Tops"	"Tops"	With
Via (conversion)	Feed	Direct	Biogas	Biogas	Biogas	Feed
Fuel use (product/t(dry)/t)	-	1.00	0.425	0.4	0.2	-
Fuel unit cost ($/t(dry))	-	40	35	20	20	-
Export electricity (kWh/t)	None	1000	660	600	600	1000
Unit price (¢/kWh)	-	3.0	5.0	5.0	5.0	5.0
Water + chemicals ($/t)	6	5	6	6	6	20
Fixed capital ($ million)	35	50	55	50	50	80
Production costs ($/t)						
Feed	158	350	646	352	328	198
Fuel	-	40	15	8	4	-
Water + chemicals	6	5	6	6	6	20
By-product credits	-	186	135	75	75	100
Electricity credits	-	30	33	30	30	50
30% p.a x fixed capital	208	188	206	347	208	300
Total $/t	372	367	705	608	441	368
Total ¢/l	29.8	29.4	56.4	48.6	35.3	29.4

Notes : **A** = sugar cost at $10/ton covering also disposal of stillage cost. The plant is assumed to self-supporting in Steam and Electricity. Estimated capital cost $35 million for 10t/day/210days/yr.

B = Fuel is assumed to be coal.

C = It is assumed that only a protein-rich fraction separated from the digester effluent is sold as a by-product.

D = Development status refers to inclusion of an anaerobic digestion step.

E = A more speculative example assuming a successful development of a system of crops and farm management which supplies a succession of sugar-rich leafy crops on a regular basis during most of the summer, and at a unit cost slightly below that of beet.

F = Assumed some significant advances over established methods of hydrolysis of wood in respect of ethanol yield, and consumption of fuel and chemical. Capital cost is considered to be 60% higher than for cases **B** to **E**.

However such favourable terms could change with oil prices. Should the price of oil collapse or gradually decline, synthetic ethanol produced by the petrochemical companies (and sometimes as a by product) would also reduce in price. Hence the competitiveness is clearly marked by the world economics.

As an end-product ethanol is also in competition with other end-products of economic value. This fact was highlighted by Wacker and Zall (1987), as they identified a potential market for production of acetaldehyde by fermentation. Presently the price of acetaldehyde is twice that of ethanol and due to its highly volatile state it can be readily removed from the fermentation broth by air stripping. They employed a mutant of *Zymomonas mobilis* to carry out this fermentation. Moreira *et al* (1979) indicated another alternative strategy to ethanol fermentation. They showed while utilisation of such woods as Eucalyptus and Pinus for ethanol fermentation was 3-5 times more efficient than sugar or starch crops (sugar cane, cassava and sweet sorghum), the net energy yield was even higher, by 50% if the final product was methanol. In a review article Wodzinski *et al* (1987) indicated the economic advantages of bioconversion of waste material to biogas. Indeed this approach is vital for a net energy gain in many alcohol fermentation processes (Table 1.6). This argument therefore could only emphasise the versatility of the fermentation process and dictate flexible process strategy in response to the potential demand and supply market.

1.4 Aims

The significance of ethanol fermentation and the potential contribution of cellulosic materials towards its future is already illustrated. Currently the main areas of research in this field are;

1- Enhanced saccharification of cellulosic materials.

- Physical treatment e.g Freeze Explosion Technique (Dale and Moreira,

1982).

- Enzymatic treatment e.g Thermotolerant Cellulases (Tsao *et al* , 1982).
- Chemical treatment e.g Acid Hydrolysis (Maloney *et al* ,1986).

2- Direct saccharolytic fermentation of cellulose.

- Cellulose e.g *Clostridium thermocellum* (Zertuche & Zall 1982).
- Hemicellulose fermentation (mainly xylose) e.g *Picha stipitis* Parekh *et al* (1987).
- Both (Usually carried out in a coculture) e.g *C.thermocellum* and *Clostridium thermohydrosulphuricum* (Zeikus 1980).

3- Reactor design.

- Hydraulics, Mixing and Mass Transfer studies e.g Air-Lift Fermenters (Onken, 1980).
- Novel designs for specific processes e.g Jet Loop Fermenters (Blenke, 1979).
- *In situ* product recovery e.g Selective Sorption-Desorption (Pitt *et al* , 1983).

4- Downstream processing.

- Membrane Technology e.g Perstraction (Matsumara and Märkl, 1986).
- Solvent Extraction e.g Electrically Enhanced Solvent Extraction (Weatherley, 1985)

As already indicated for cellulosic fermentation to produce alcohol, over 67% of the total unit cost of the product is due to pretreatment and downstream processing costs. It was thought that such costs may be minimised by a single step process. The aim of this project therefore was to design a novel bioreactor system able to carry out single step fermentation of cellulosic materials. In this view a bioreactor system with the following features is desired;

1- Simple in construction and scale-up.

2- Able to minimise mass transfer limitations.

3- Low shear mixing.

4- Able to circulate solids.

5- Facilitate *in situ* product recovery.

The outline of the proposal will be fully discussed in Chapter 3.

In order to carry out the fermentation studies, the test micro-organism was selected with respect to its ability to;

1- Ferment cellulosic hydrolysates to ethanol.

2- Grow at elevated temperatures.

3- Grow in the absence of oxygen.

Clostridium thermosaccharolyticum , a thermophilic anaerobe, was selected based on the above criteria and its ability to ferment a wide range of substrates mainly to ethanol and acetic acid. The feasibility of the proposal was investigated by undertaking the following studies;

1- Growth and physiological studies of *C. thermosaccharolyticum* .

2- Ethanol fermentation studies of *C.thermosaccharolyticum* .

3- Strain development and selection for a an ethanol tolerant mutant of *C.thermosaccharolyticum* .

4- Immobilisation of *C.thermosaccharolyticum* on inert support particles.

5- Design and construction of a pilot gas-lift fermenter.

6- Rheological studies of the fermentation broth.

7- Hydrodynamic studies of the gas-lift fermenter.

8- Product recovery from the fermenter.

Full details of these studies are discussed in the next two chapters. The kinetic parameters were determined by growth and fermentation studies of the micro-organisms. The mixing studies indicated the flow behaviour of the fluids in the reactor and their residence time distributions. The

experiments were carried out almost in the same order as proposed. The design and construction of the 50 liter gas lift fermenter, however, was concurrent with the microbiological studies. The microbiological studies listed above were also complemented by a number of other studies such as development of a suitable growth medium for the system, and investigation of ethanol inhibition and stress factors on *C.thermosaccharolyticum* . The mixing studies of the pilot gas-lift fermenter examined different fermenter systems containing a range of fluids including the air/simulated broth (1% (w/v) ethanol + 0.5% (w/v) CMC mixture) and the multiphase mixing of porous solid particles. The different approaches of trace analysis are discussed in Chapter 3.

1.5 General Methodology

In the following sections, the general methodology employed in this work is discussed. Chapters two and three outline the more specific materials and methods used in their respective experiments described.

1.5.1 Sterilisation

A : Media Sterilisation

The basis of current sterilisation strategy was developed in the food industry where spores of *Clostridium botulinum* proved to be of considerable health hazard. In heat processing of canned foods, inadequate heating could leave many spoilage organisms viable or otherwise provide a sufficient heat shock required to germinate spores. It was found that by heat processing at 121.1°C (250°F) the number of spores of *C.botulinum* was reduced by a factor of ten every 0.22 minutes (Esty and Meyer 1922). Moss and Smith (1977) reported on the death rate of a variety of bacterial spores including those of *C.thermosaccharolyticum* where at 132°C a decimal reduction of 4.4 minutes was observed. Such exponential death rate implies that one hundred percent sterility is never achieved and an acceptable level should be defined. Experience and much research in the food industry and general microbiology has shown that in general a heat treatment at fifteen psi of saturated steam for fifteen minutes (15/15) kills all spores and provides the required level of sterility. Although this rule is generally practised for most bench sterilisations in domestic pressure cookers, larger vessels require longer periods of sterilisation. Bottles up to one litre were sterilised with their caps loose in a bench pressure cooker (Prestige, U.K) at 15/15. Twenty litre aspiraters (Pyrex, U.K) where autoclaved (Astell 2000, U.K) at fifteen psi for ninety minutes. Some media components were sterilised separate from the bulk of the medium due to caramelisation, reaction with other components at high temperatures, and denaturation. Sugars, phosphate buffers, and vitamins

could be named as respective examples. Concentrated solutions of these components were filter sterilised using 0.5 micron mesh membrane filters (Bioseparations, U.K). All other filters for inlet gas streams and outlet effluent gases were made from non-absorbant cotton wool. As an alternative millidisk sterilisable filters (Millipore, U.K) were also used. These had the advantage of durability and ease in connections.

B : Equipment and Vessels

All glassware, subaseals, contaminated vessels, contaminated disposables, small one litre fermentation vessels, tubing and pump heads were sterilised at fifteen psi. Depending on their size some were sterilised for fifteen minutes in a bench pressure cooker or in an autoclave for twenty minutes. For larger fermentation vessels such as 1.5 litre fermenter (Bioenegineering, Swiss) and the pilot 50 litre vessel, an *in situ* operation was installed. The vessels were sterilised by heating distilled water inside the vessel to 121 °C and holding for thirty minutes. After cooling the distilled water was drained and replaced by sterile medium. Equipment which was not heat sterilised was chemically sterilised. PH electrodes were sterilised in concentrated HCl. Electrodes were dipped in a measuring cylinder containing the concentrated acid overnight. This was also beneficial in regeneration of the electrode's membrane. Chloros was used as a general disinfectant for spillages or contaminated vessels. It was also used in the gas traps to disinfect the effluent vapours.

Any attachment to the fermentation vessel was made through a rubber septum. A few drops of ethanol or isopropanol were usually added to cover the exterior of the septum before making the connection. Any leaks in the surrounds were observed by bubbles in the alcohol pool.

1.5.2 Anaerobic Techniques

A : Bottle Cultures

Many anaerobic studies employ the so called Hungate technique after Hungate (1969). This bench method involves the replacement of head space of a long tube containing medium by an inert gas such as carbon dioxide. It is cumbersome to operate and carries a high risk of oxygen contamination upon inoculation. The use of anaerobic cabinets overcomes many of these difficulties by providing an ample work space in an anaerobic environment. After autoclaving the bottles containing hot medium (approx. at 60 °C) were transferred to the interchange chamber of the cabinet (Forma Scientific, U.S.A) where their head space vapour was removed under vacuum and replaced by the anaerobic gas. This special gas contained 85% Nitrogen, 10% Hydrogen and 5% CO_2 (BOC, U.K). The cabinet atmosphere was maintained anaerobic by catalytic removal of trace oxygen by Platinum wafers. The cabinet was routinely tested for anaerobiosis by colour indicators (BRL, U.K). Due to the presence of hydrogen in the cabinet all electrical connections were made spark proof. Thus loop inoculations were carried out by an electric loop (Forma Scientific, U.S.A). Once inoculated the bottles were sealed by Sub-a-seals (Gallenkamp, U.K) and placed in an appropriate incubator.

B : Plate Cultures

Solid media plates were prepared by adding 1% Technical Agar No. 3 (Oxoid, U.K) to the medium. Any additives such as ethanol or medium components that were separately sterilised were added to the plates prior to pouring. Set plates were dried in an oven before storing in the anaerobic cabinet. After inoculation plates were transferred to an anaerobic jar (Oxoid, U.K) containing dessicants and catalyst sachets and placed in an incubator.

C : Batch and Continuous Fermentation

Anaerobic operation of the one litre fermenter was achieved by continuous flow of Oxygen Free Nitrogen, OFN, (BOC, U.K) at approximately 30 ml/ minute through the system. The operating temperature of 60 °C also ensured minimum solubility of oxygen in the bulk of the medium. Any trace quantity of oxygen contaminating the OFN was removed catalytically (Suppelchem, U.K). Gaseous end-products of the fermentation too contributed towards maintaing the medium in a reduced form thus providing some degree of autoanaerobiosis. The anaerobic status of the medium was reflected by its redox potential or alternatively indicated by using a suitable colour indicator. Resazurin solution at 0.1% (w/v) addition produced a pink colouration in the presence of trace oxygen.

Anaerobic operation of the gas-lift fermenter was designed on the basis of the above experimental studies. For scale-up however the gas source was suggested to be dry ice which was considerably cheaper than OFN and would lead to the same processing conditions. It was further thought that upon removal of solvent vapours by condensation part of the gas could be recycled to the vessel to make the overall process more cost effective.

1.5.3 Fermentation Methods

A : Bottle Cultures

Basic growth studies were carried out in 20 ml McCartney and 100 ml Medical Flat bottles. The cultures were started up in the morning by inoculating from a fresh overnight cell culture of an optical density between A_{650} = 0.8 - 1.0. The lag period prior to exponential phase varied from one experiment to another. It was however observed that if the carbon source was changed from glucose to xylose a longer lag occured. Bottle cultures were essentially employed for qualitative observations. The experiments undertaken are listed as follows;

- Growth in the presence of different carbon sources.
- Growth at different sugar concentrations.

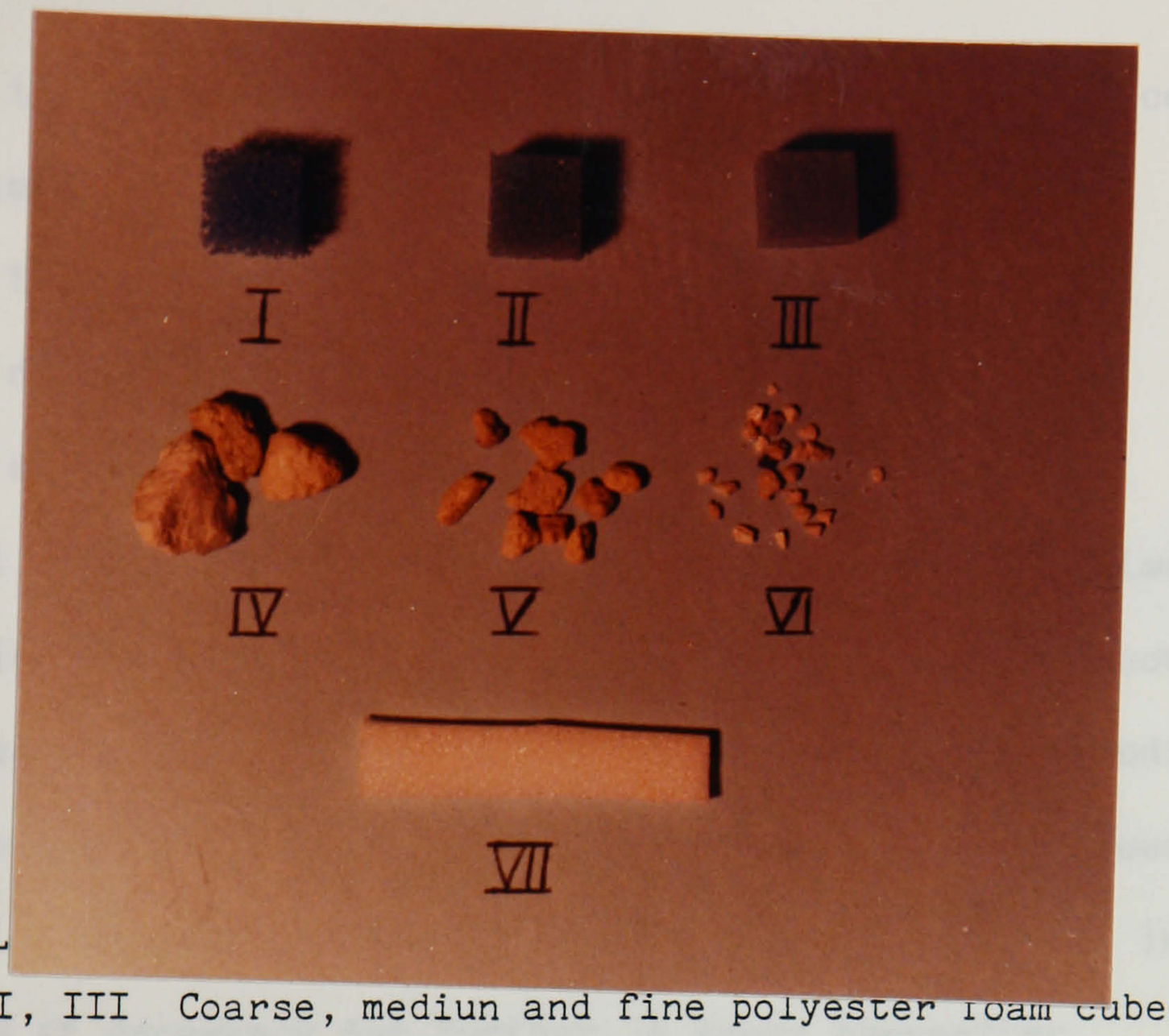

(a) L

I, II, III Coarse, mediun and fine polyester foam cubes

IV, V, VI Coarse, medium and fine PERLAG (volcanic agglomerate)

VII A strip of packing foam

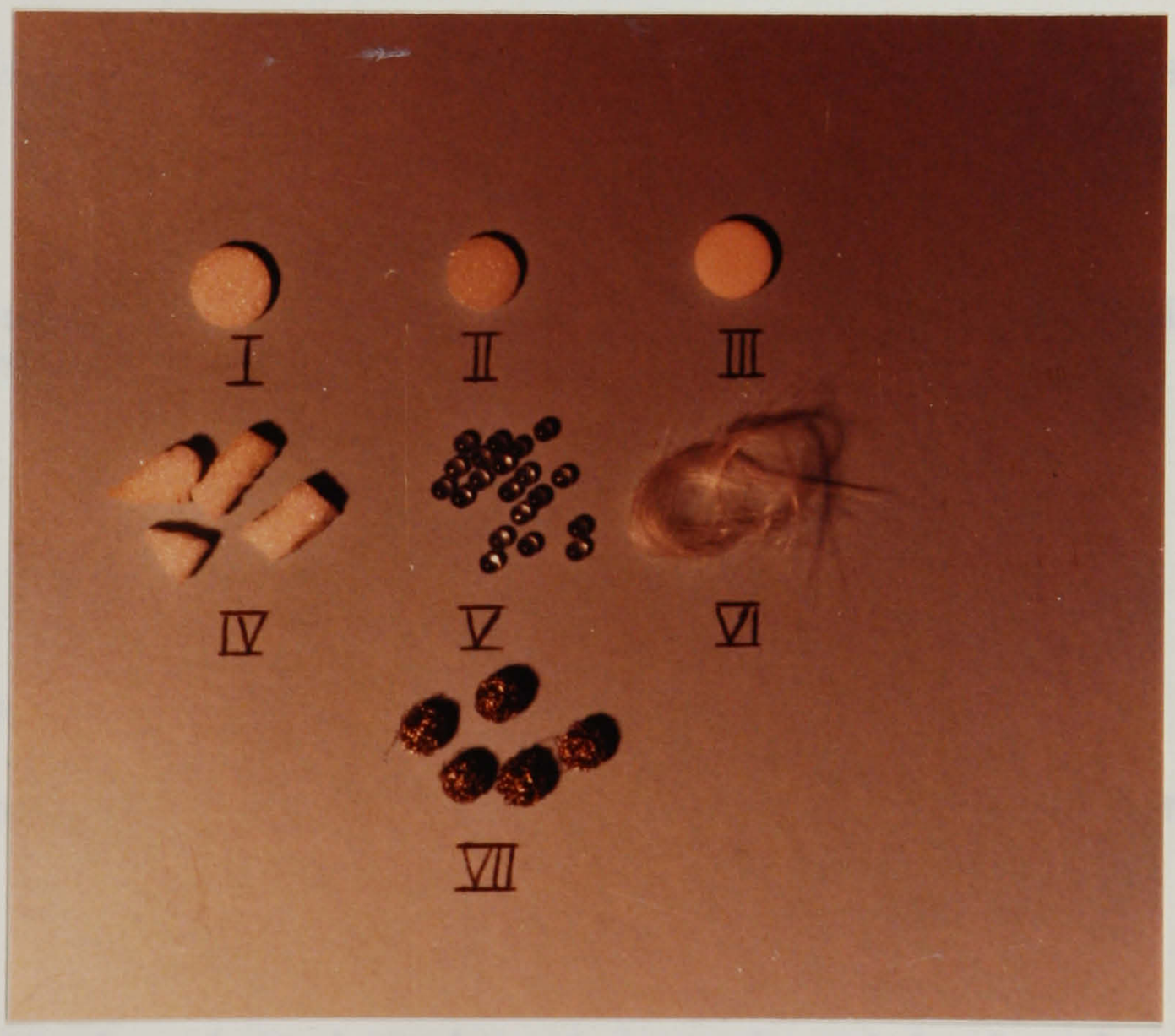

(b) High density particles

I, II, III Coarse, medium and fine sintered glass discs

IV Glass chippings, V Glass beads, VI Glass fibre, VII Stainless steel wire mesh

Figure 1.2 Examples of inert support particles employed in the studies of cell immobilisation (see text for details)

- Growth in the presence of varying concentration of medium components to achieve optimum conditions.
- Growth in the presence of inert solid particles.
- Growth at different ethanol concentrations.
- Growth at different pH.

The optical density was the main variable parameter with time. For many growth studies the exponential growth lasted for about 6-8 hours depending upon the inoculum size and the carbon source. For other studies mentioned above the bottles were inoculated with 1 ml of a freshly grown culture of the optical density around A_{650}= 0.8-1.0. The bottles were incubated for 24 hours and if necessary for further 24 hours thereafter.

Inert solid support particles were autoclaved in the bottles with the bulk of the medium. The various type of support particles used are shown in Figure 1.2. Table 1.7 indicates some of their physical properties related to this study.

Table 1.7 Inert solid support particles used in the immobilisation of *C.thermosaccharolyticum* .

Type	Density kg/m^3	Voidage	Supplier
Glass beads	1430	0	Gallenkamp ,U.K
Polyester foam	84	0.99	Delcon Plastic Ltd, U.K
Perlite	450-500	0.7-0.8	Silvaperl Ltd, U.K
Stainless steel mesh	200	0.8	Dr. N. Smart, University of Sheffield

All these materials showed good resistant towards wet heat and extreme pH conditions.

B : Batch and Continuous Culture in one litre Fermentation Vessel

The equipment used is shown schematically in Figure 1.3a. All parts were autoclaved or alternatively sterilised as previously described. Prior to

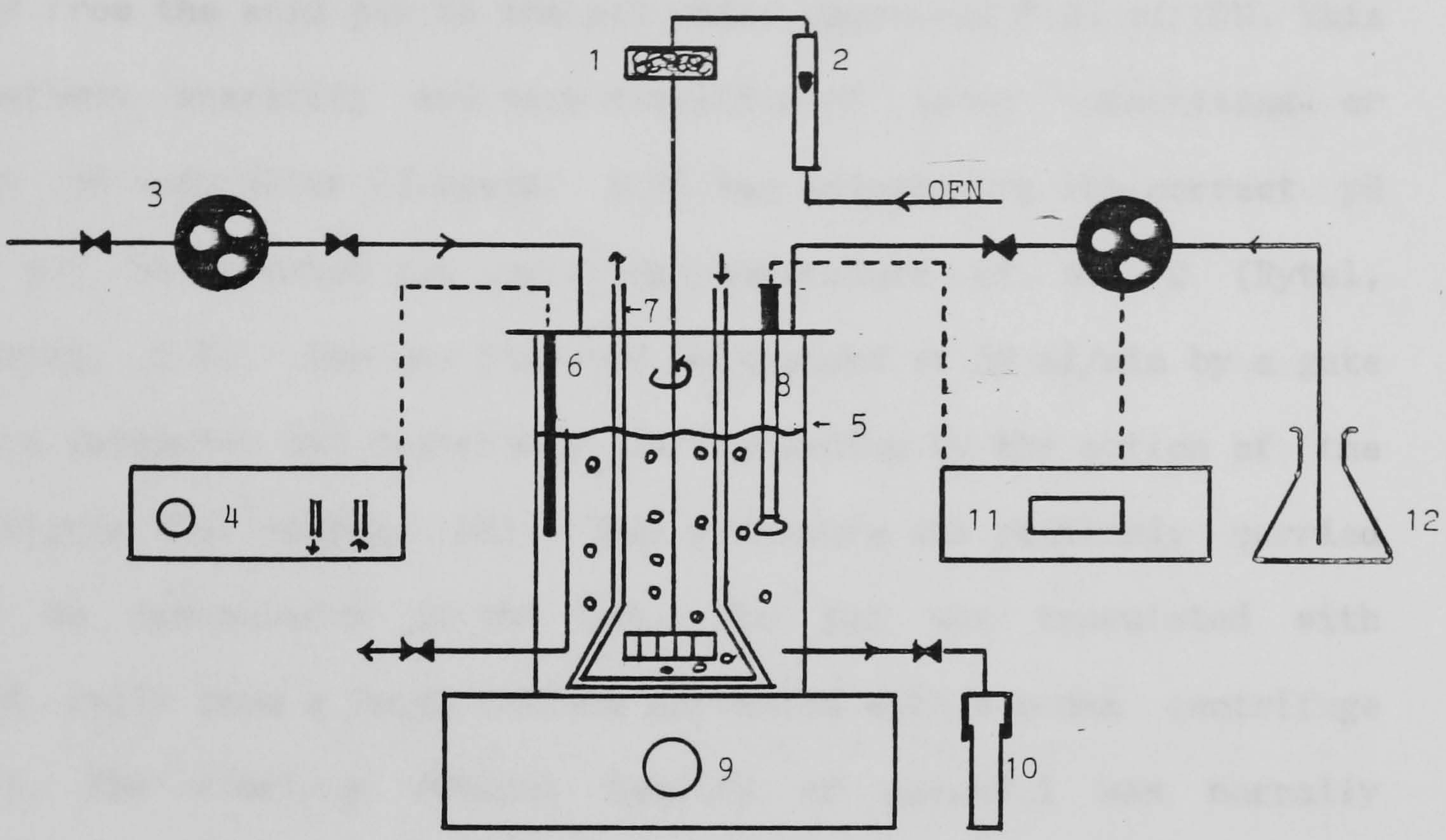

(a)

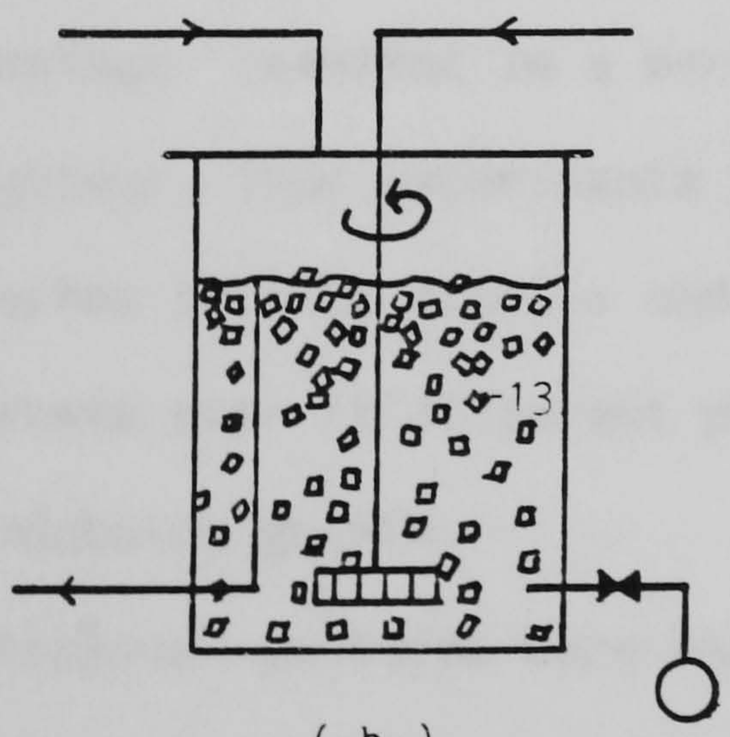

(b)

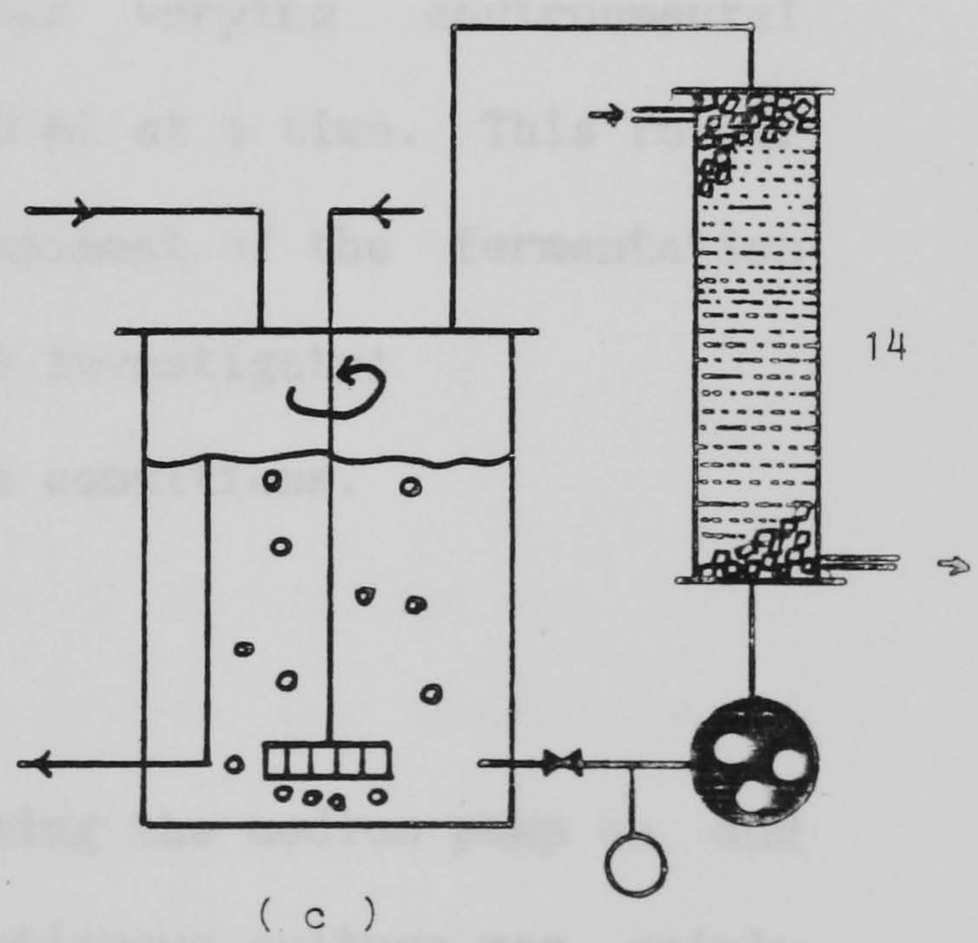

(c)

Figure 1.3 Shematic Diagram of 1 litre Bench Fermenter

1 : Air filter, 2: Air flowmeter, 3: Peristaltic pump, 4: Water circulater, 5: Fermenter vessel, 6: Thermocouple, 7: Heating Coil, 8: PH electrode, 9: Magnetic stirrer, 10: Sampling port, 11: PH controller, 12: Alkali supply, 13: Biomass support particles, 14: Packed column

pumping sterile medium in to the vessel, the whole system was flushed with filter sterilised OFN. The medium was delivered to the pot by a metering pump (DCL, U.K). The pH electrode (Russell PH, U.K) was aseptically transferred from the acid jar to the pot under increased flow of OFN. This ensured maximum sterility and easy detection of loose connections or leaks. The pH controller (Jencons, U.K) was adjusted to the correct pH once the pot had reached the operating temperature of 60 °C (Rytel, Control Master, U.K). The gas flow was maintained at 30 ml/min by a gate valve and a rotameter and distributed in the medium by the action of the magnetic stirrer (Gallenkamp, UK). This procedure was routinely carried out prior to inoculation of the pot. The pot was inoculated with resuspended cells from a fresh culture harvested with a bench centrifuge (MSE, U.K). The start-up optical density of A_{650}=0.1 was normally practised. The cells were then allowed to grow batchwise in the controlled environment for 24 hours. In the case of short lag, the pump was switched on to 50 ml/hour delivery for continuous culture. Batch cultures in the one litre fermenter allowed operation under varying environmental conditions and larger sample volumes of upto 20 ml at a time. This former advantage resulted in a more quantitative assessment of the fermentation behaviour. Thus experiments were carried out to investigate;

- Carbon balance studies under different growth conditions.
- Growth rate at different pH.
- Fed-batch growth.

Continuous cultures were carried out by switching the medium pump on and setting it to the required dilution rate. Continuous culture was mainly employed to maintain or adapt microbial cultures for a given set of environmental conditions. As a general guide, four fermenter volume changes was accepted to be the minimum time period required for the bacterial culture to adapt to their new environment. Thus batch growth at

different pH or ethanol concentration was carried out after continuous period of adaptation.

Cells were grown on inert support particles in two ways; in a stirred tank system, and in a packed column. These two systems are schematically shown in Figures 1.3b and 1.3c.

For the suspended solid system in the stirred tank, 20% working volume of the vessel (160 ml) was filled with particles and sterilised in the same manner as a normal vessel described earlier. The packed column operation involved the use of 30 cm tall QVF glass columns (Corning, U.K) of various internal diameters. The various packed column systems used are shown in Table 1.8.

Table 1.8 Different packed columns employed in the immobilised cell studies.

Packed column diameter cm	Packing type	Liquid hold-up ml	Voidage
2.54	glass beads (3 mm diameter)	52	0.35
5.08	glass (3 mm diameter)	198	0.34
2.54	Polyester foam (3 mm cubes)	135	0.92
5.08	Polyester foam (8 mm cubes)	542	0.92
5.08	Medium Grade "Perlag"	350	0.59

The packed column operated upflow by a recycle stream from the one litre fermentation pot (Figure 1.3b). The recycle stream was pumped by a metering pump (DCL, U.K) at a rate ten times greater than the maximum dilution rate of the growth culture. This minimised the dead space in the column with a smaller mean residence time.

Immobilised batch and continuous cultures were carried out in the same fashion as for the free suspended cell cultures.

1.5.4 Sampling

A : Bottle cultures

Samples were taken with a one ml disposeable plastic syringe through the subaseal. The bottles were normally under positive pressure due to the accumulation of fermentation gases in the head space and thus the syringe was filled with relative ease. Care was however taken to minimise any possible leaks as a result of the puncture made.

B : One litre fermenter cultures

The fermenter was equipped with a sample port situated at the bottom of the vessel near the stirrer. Samples were taken by opening a gate valve and drawing out a sample into a sterile universal bottle. Depending on the nature of the experiment one ml of the contaminated broth was centrifuged to remove cells, and supernatant kept frozen for further analysis. Samples were also routinely checked for pH to ensure accurate operation of the control equipment. The temperature of the pot was independently checked by dip thermometer inserted in the vessel through a stainless steel sleeve. Anaerobic samples were taken by a needle arrangement at the end of the sampling tube. The growth culture was then injected into a bottle previously made anaerobic in the anaerobic cabinet.

For the packed column operation samples were taken on the recycle stream, before entering the column. Occasionally samples were also taken at the top of the column to check for the mixing inside the column. Sampling from the pilot scale fermenter was achieved by the operation of a sample valve (Life Science Laboratories, U.K). The lever action of the valve drew samples with an adjustable flow control.

1.5.5 Calibration

All control equipment, pumps, and measuring equipment were calibrated prior to use. These were essentially carried out by the manufacturer and

the equipment was mainly adjusted for their zero points.

PH meters were calibrated against a standard buffer solution of pH 7, with the gradient adjusted at pH 4. A resistor was placed in the pH controller to compensate for 60 °C pot temperature. Due to acid incubation, the sterile electrode normally maintained a very active membrane and responded rapidly to a change of pH. Once placed in the pot, it would quickly stabilise. During continuous culture film growth on the outer wall of the electrode was thought to influence its sensitivity and response. It was therefore necessary to check the pH of samples regularly with an independent pH meter and adjust the controller to compensate for the drift.

The thermocouples and temperature controller were also adjusted by using a reference resistor for ice point. All thermocouples were chromoalumel type K and operated through controller via a multichannel distributor. It was found that despite different lengths and makes they all gave similar consistent response.

The conductivity meters (Model 220, Corning, U.K) were calibrated against a standard 2M solution of KCl, according to the manufacturers specifications.

Peristaltic pumps were calibrated each time used since the tubing slightly expanded and/or streched after autoclaving or continuous use. On line calibration was achieved by shutting off the reservoir supply and timing the transfer of 10 ml sterile medium from a pipette to the vessel. This was repeated at different pump speeds and a linear calibration was always observed. Similar technique was employed with the metering pumps.

All analytical equipment was "zeroed" where necessary by using an appropriate blank. The gas chromotograph was operated through an integrater with an automatic zeroing facility. The use of analytical equipment will be discussed in the next chapter.

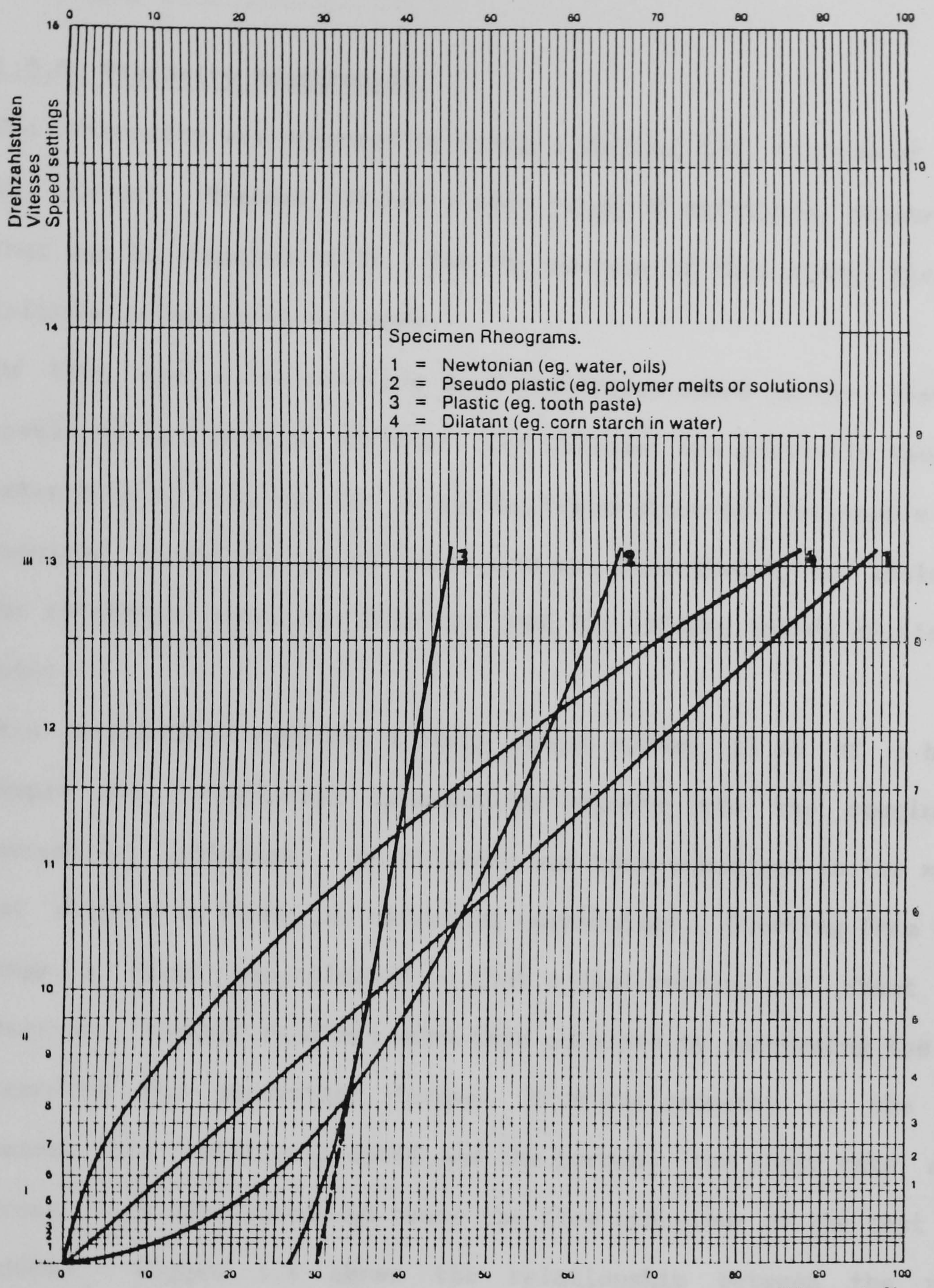

Figure 1.4 Flow Characteristics of Different Liquids

Source : Contraves AG, Switzerland

1.5.6 Viscosity Measurement

The Viscosity was measured by using a Rheomat 15T viscometer (Contraves AG, Swiss). Rheomat 15T has a wide range of rotational measuring systems that can be attached to it. For the purpose of this study, the concentric cylinder arrangement was used.

In this system the rotating part was driven round in the test material enveloped in a holding cylinder. The cylinder was partially submerged in a water bath to maintain the measuring temperature of test sample.The torque required to maintain a certain speed was indicated by an analogue dial. The rotational speed was selected from the fifteen speeds available on the motor.

This measurement required a large sample volume. 15 ml of a homogenised sample was transferred by a pasteur pipette into the spacing of the concentric cylinders. The cylinder was then submerged in the water bath and allowed to reach the operating temperature. Starting frrm the lower range, a speed was selected so that a dial reading of about 10% was observed. Further readings were then obtained by increasing the speed and recording the percentage torque. From the geometry of the measuring system, the rotational speed and the torque, the shear rate and shear stress were calculated and hence the flow behaviour of the test material deduced. Figure 1.4 shows the relationship between the percentage torque (analogue reading) and the speed setting for a number of fluids with different flow behaviour. Figure 1.5 shows a semi-logarithmic plot of the latter versus the shear rate.

Hydraulics of gas-lift fermenter were examined under different viscous sytems. Solutions containing CMC and starch were employed in order to simulate broth conditions in the fermenter. Figure 1.6 shows the variations of shear rate with torque for a number of solutions at room temperature. It is notable that at low concentrations, all solutions

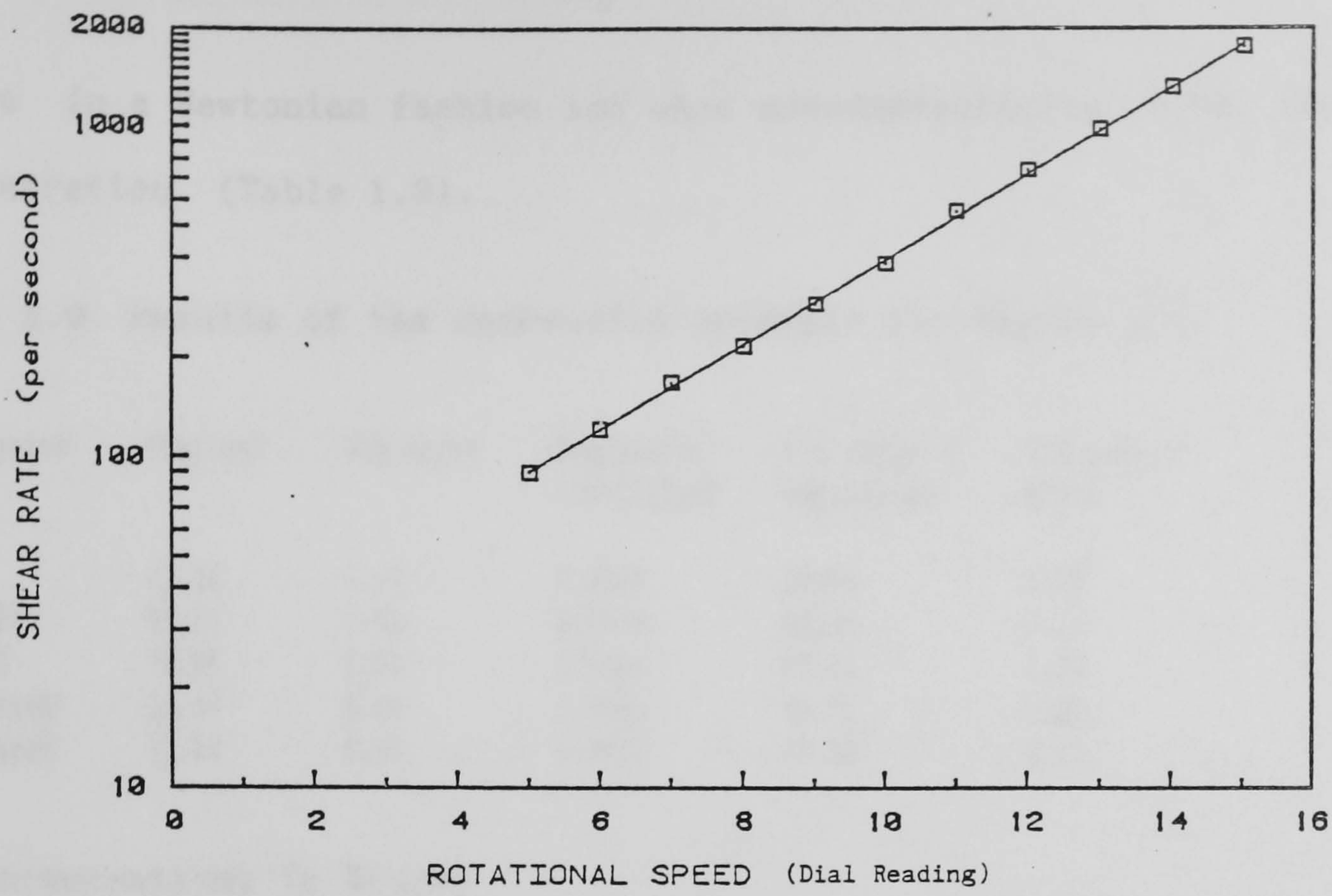

Figure 1.5 Standard calibration for speed settings of RHEOMAT 15 viscometer.

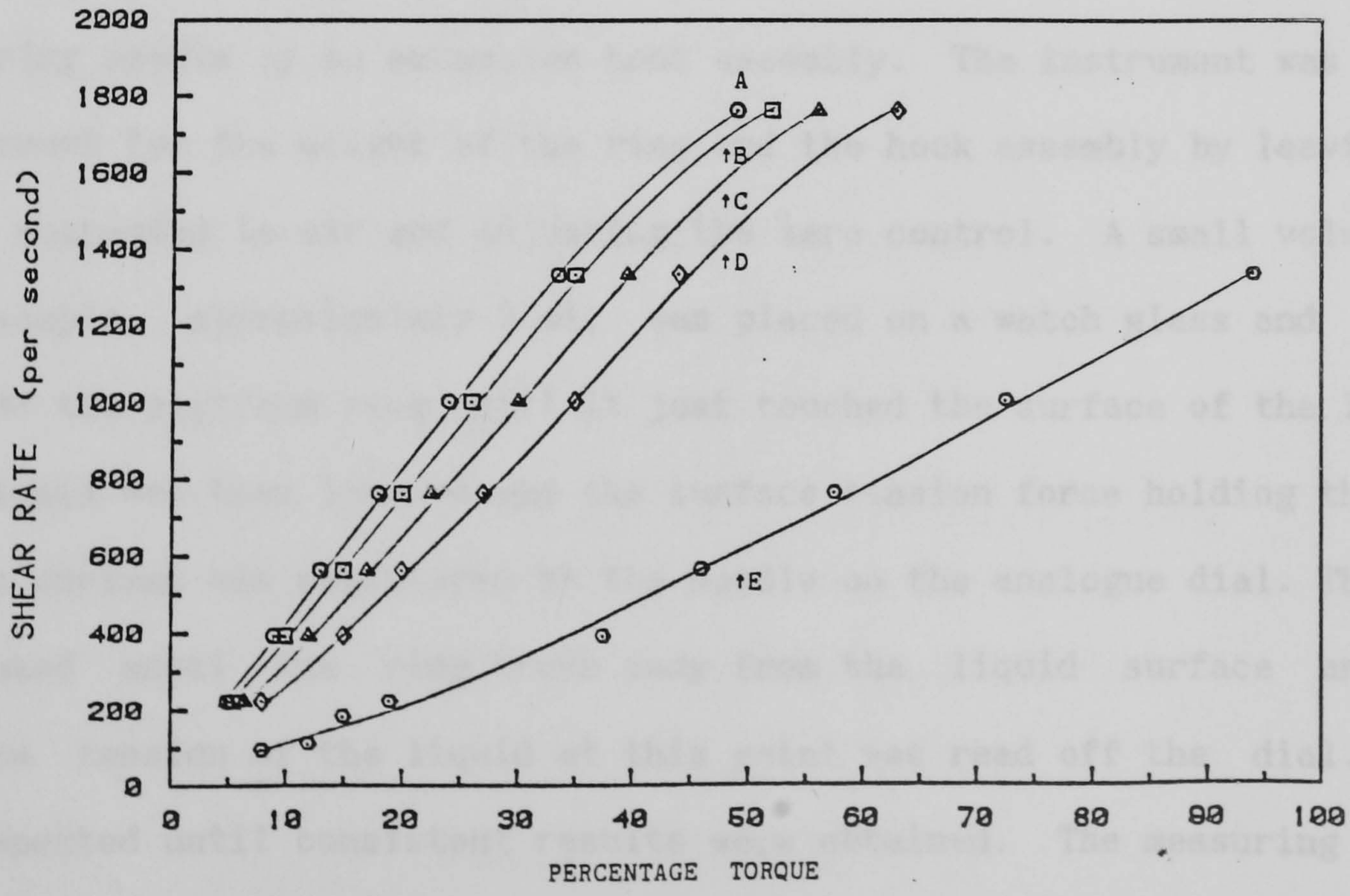

Figure 1.6 Standard calibration for viscosity measurements of various solutions
A : Distilled water; B : 0.1% (w/v) CMC; C : 0.1% (w/v) starch; D : 1% (w/v) CMC
E : 1% (w/v) starch.

behave in a Newtonian fashion and show pseudoplasticity with increasing concentration (Table 1.9).

Table 1.9 Results of the regression analysis for Figure 1.6

Fluid system	Gradient	Std error	Regression coefficient	Std error of regression	Viscosity mPa.s
Water	38.18	1.17	0.9944	80.44	1.05
0.1% CMC[1]	35.78	0.95	0.9958	69.54	1.12
1.0% CMC	28.64	0.52	0.9980	47.71	1.39
0.1% starch[1]	32.63	0.50	0.9986	40.56	1.23
1.0% starch	12.80	0.43	0.9921	49.00	3.13

1: Concentrations in %(w/v)

1.5.7 Surface Tension Measurement

The measurement of surface tension of fermentation broth, and other test liquids for hydrodynamic studies of the GLF were carried out by a torsion balance (White Electrical Instrument Co. Ltd, U.K). This instrument provided a direct reading of the surface and interfacial tension by means of a platinum ring having a circumference of 4 cm, connected to a measuring needle by an extension hook assembly. The instrument was zeroed to account for the weight of the ring and the hook assembly by leaving the ring suspended in air and adjusting the zero control. A small volume of test sample, approximately 2 ml, was placed on a watch glass and raised towards the platinum ring until it just touched the surface of the liquid. The liquid was then lowered and the surface tension force holding the ring to the surface was registered by the needle on the analogue dial. This was continued until the ring broke away from the liquid surface and the surface tension of the liquid at this point was read off the dial. This was repeated until consistent results were obtained. The measuring range of 0-0.12 N/m (1 N/m = 1000 Dynes/cm) was found adequate for all experimental values. Figures 1.7 and 1.8 show the calibration curves for

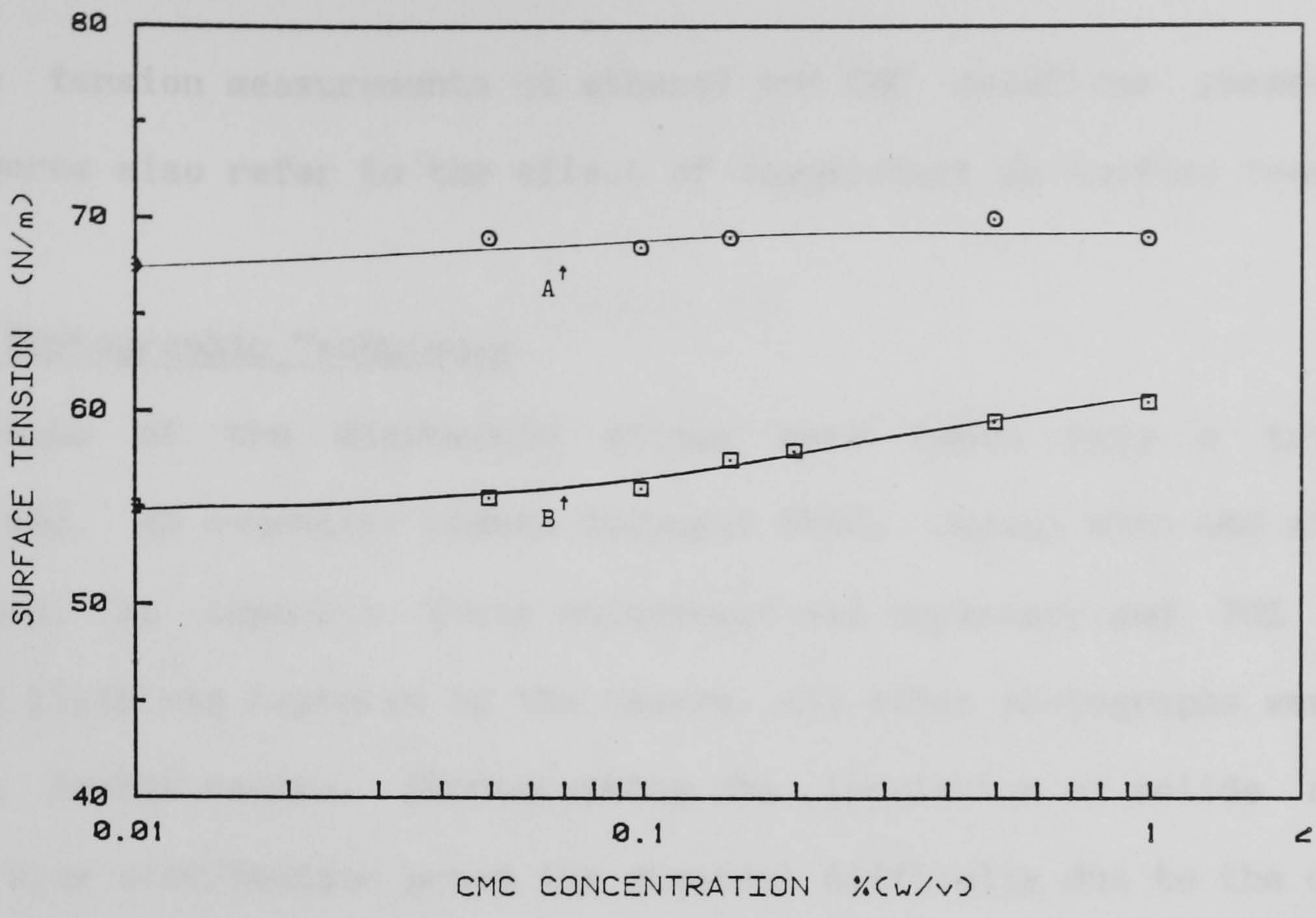

Figure 1.8 Standard calibration for surface tension measurement of CMC solutions

A : Room temperature (20'C); B : 60'C measurements

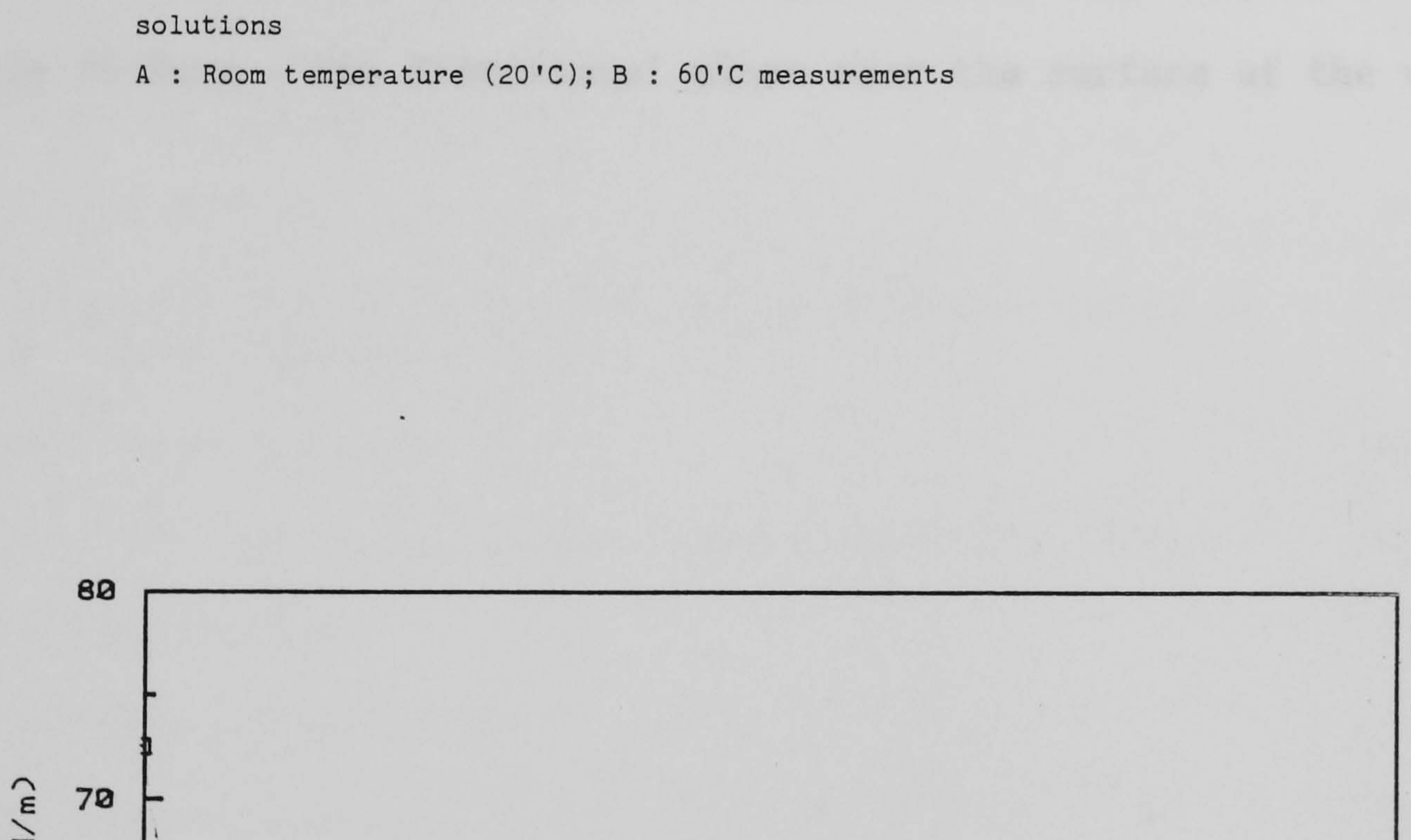

Figure 1.7 Standard calibration for surface tension measurement of ethanol solutions.

A : Room temperature (20'C); B : 60'C measurements.

surface tension measurements of ethanol and CMC solutions respectively. The figures also refer to the effect of temperature on surface tension.

1.5.8 Photographic Techniques

Photographs of the microscope slides were taken from a trinocular microscope. An automatic camera (Olympus OM10, Japan) with 400 ASA film was used. No separate focus adjustment was necessary and 70% of the viewing field was captured by the camera. All other photographs were taken with a Pentax camera. Photographing the circulation of solids and the bubble size distribution posed the greatest difficulty due to the depth of field. This problem was minimised by adjusting the lighting on the rig at 90° angle to form a two dimensional plane near the surface of the vessel.

Chapter Two

Ethanol Fermentation by *C. thermosaccharolyticum*

Ethanol Fermentation by *C. thermosaccharolyticum*

2.1 Background

Almost all present industrial fermentation of ethanol is carried out by yeast. Different strains of *Saccharomyces cerevisiae* are employed in the brewing industry to produce alcoholic beverages. The ability of this yeast to grow at low pH (~4) and its high ethanol tolerance (8-9% w/v), has made it a robust choice which allows crude fermentations of ethanol to be carried out with relative ease. Indeed yeast plays a major rôle in the alcohol fuel programme and much of the ethanol produced in Brazil is fermented by strains of *S.cerevisiae* from a glucose or sucrose containing substrate.

The economic importance of cellulosic substrate for alcohol production has already been discussed and it became evident that a successful fuel alcohol program would have to include the utilisation of a wide range of substrates to overcome the problems of availability and cost. *S.cerevisiae* has a very narrow substrate range, only able to ferment hexoses and disaccharides. This limitation together with an inherent slow growth rate has led to the introduction of strain improvement programmes, and also a search for other micro-organisms able to ferment polysaccharides and pentoses. Attempts to provide a thermotolerant strain of yeast are reviewed by van Uden (1984). Temperature profiles show a decreasing yield with increasing incubation temperatures. The highly complex genetics of yeasts also has retarded the attempts to obtain a strain of yeast with a broader substraté range (Campbell, 1981). In exploring potential micro-organisms for ethanol fermentation it will be desirable to include the criteria for both thermophilic growth and saccharolytic substrate utilisation. Operating at elevated temperature would enhance the fermentation kinetics and minimise the contamination risks. It is also economically favourable due to savings in cooling and downstream

processing costs. The utilisation of a saccharolytic organism would overcome the substrate limitation problems and reduce the pretreatment costs. A further criterion that could also be considered is with regard to the method of digestion. An organism fermenting under anaerobic conditions would certaintly nullify the aeration requirements. At elevated temperatures of growth (>50°C) oxygen shows very low solubility in water and as a result many thermophiles are facultative or obligate anaerobes and meet the latter criterion.

Apart from yeasts bacteria are the main micro-organisms considered for fermentation of ethanol. This fact was perhaps boosted by the concentrated publications in the late 1970's on the ability of *Zymomonas mobilis* to produce ethanol. The reports of 120-200 g/l ethanol production were controversial and eventually discredited by Zajic *et al* (1982). Table 2.1 summarises the productivity and substrate range of *Z.mobilis* and other bacteria of potential interest. As indicated in Table 2.1 the substrate range of mesophilic bacteria is relatively inferior to that of the thermophiles. *Z.mobilis* shows a very high ethanol tolerance and the highest ethanol yield (97% w/v). The organism however mainly utilises glucose and fructose as sugar source. The use of the thermophiles to produce ethanol is a relatively recent development and much of the work carrried out in this area is still at laboratory scale. In a review article Sonnleitner and Fiechter (1983) describe the use of thermophilic organisms for large scale production of thermotolerant and caldoactive enzymes. Apart from thermostability these organisms offer more resistance to denaturing agents such as solvents, and more tolerance to high solute concentrations. Other advantages such as fast growth rate and high productivity also make them favourable for exploitation as solvent producers.

Table 2.1 Productitvity and substrate range of ethanol producing bacteria. As reference, corresponding data for yeast are shown.

Source: Esser and Karsch (1983)

Organism	T_{opt}	Y_{EtOH}	Ethanol tolerance	Hexoses	Disacch-arides	Cellulose	Starch	Hemi-Cellulose	Special Substrate
	°C	(%)	(% w/v)						
Mesophilic (20-40°C)									
Erwinia amulovorans	27-30	60	?	x	x	-	-	-	-
Sarcina ventriculi	30-37	50	?	x	x	-	-	-	-
Leuconostoc mesenteroides	20-30	55	?	x	x	-	-	-	Lactose
Zymomonas mobilis	30	97	7	x	x	-	-	-	-
Thermophilic (40-65°C)									
Clostridium thermosacch-arolyticum	60	55	5	x	x	-	x	x	Xylan
Clostridium thermocellum	65	50	5	x	x	x	-	-	-
Extreme thermophiles(>65°C)									
Thermoanaerobacter ethanolicus	69	90	?	x	x	-	x	x	Xylose Cellobiose
Clostridium thermo-hydrosulphuricum	69	80	?	x	x	-	x	-	Xylose Pectin Cellobiose
Thermoanaerobium brockii	65-70	48	?	x	x	-	x	x	Lactose Cellobiose
Saccharomyces species	30-35	89	x	x	-	-	-	-	-

It is notable that most organic solvents produced by fermentation such as ethanol, butanol, and acetic acid are relatively volatile in nature. This fact gives rise to an elegant means of *in situ* end-product recovery. Under reduced pressure or high gas throughputs volatile components of the fermentation broth simply either boil off or strip off the vessel. Therefore by applying this technique the end-product inhibition effects on the growth of the culture are minimised. High temperature operation has also a significant effect on the rheological parameters of the fermentation broth and may influence its flow behaviour. Both viscosity and the surface tension decrease with increasing temperature and hence reduce the overall shear in the vessel.

Classically, fermentation processes were considered to be the catabolic conversion of sugar substrates to generate reduced end-products. Ethanol, lactic acid, butyric acid, etc. may all be produced in the absence of molecular oxygen, provided cellular functions remain active, and hence are more commonly referred to as "anaerobic fermentation products". In recent years the definition of the fermentation process has changed to mean any microbial process which yields a useful (saleable) product. Consequently anaerobic fermentation is more specifically referred to those fermentation processes that can be carried out in the absence of molecular oxygen.

With the exception of some heterolactic acid species most anaerobic bacteria employ the Embden-Meyerhof pathway (glycolysis) and Warburg-Dickens pathway (xylolysis) for hexose and pentose metabolism respectively (Doelle, 1975). The different pathways for glucose and xylose conversion are shown in Figure 2.1. In all cases the main end-product is formed by reduction of pyruvic acid. The yields of ethanol obtained from glucose fermentation by any of these pathways depend upon specific cultural conditions that control the carbon and electron flow during the fermentation time course. The most common fermentation pathway to ethanol employed by a wide range of anaerobes (including clostridia) is the phosphoclastic pathway (Zeikus, 1980).

Unlike the ketoclastic pathway (used by lactic acid bacteria), the decarboxyclastic pathway gives rise to very high ethanol yields and has ethanol as its only solvent end-product. This pathway present in yeast is not common to bacteria and has only been reported in the facultative *Zymomonas* species (Zeikus, 1980).

Fermentation of pentoses is mainly associated with bacteria. Yeasts generally ferment xylulose (an isomer of xylose) rather than xylose. This is due to the absence of the enzyme xylose isomerase. Some yeasts ferment xylose by reducing xylose to xylitol followed by a combination of

xylose by reducing xylose to xylitol followed by a combination of enzymatic reactions to xylulose-5-phosphate. In many bacteria, including the genus *clostridia* (Booth and Mitchell, 1987) the activity xylose isomerase is controlled by catabolic repression. Aduse-Opoku and Mitchell (1988) observed glucose-grown cells of *C. thermosaccharolyticum* do not transport xylose, and extracts lack xylose isomerase and xylulokinase activity. As indicated in Table 2.2 mycelial fungi ferment xylose in the same manner as yeasts.

Table 2.2 General comparison of pentose metabolism for bacteria, yeasts and fungi

Source : Manderson (1985)

Organism	Stage 1 Xylose to Xylulose-5-P	Stage 2 Xylulose-5-P Pyruvate	Stage 3 Pyruvate to End-products
Bacteria	Isomerisation	Xylolysis + glycolysis	Ethanol+ acid Ethanol+butandiol Ethanol+acetone/ butanol
Yeasts	Oxidation reduction	Xylolysis + glycolysis	Ethanol
Mycelial Fungi	Oxidation reduction	Xylolysis + glycolysis	Ethanol Acetic acid and lactic acid

Xylose fermentation has been recently reviewed by Skoog and Hahn-Hägerdal (1988). Their paper indicated large variations in the reported data with regard to ethanol yield and production. It has been shown that the availibility of oxygen, xylose concentration, and pH have a more significant influence on xylose fermentation when compared to the classical glucose fermentation by yeast. For example under aerobic conditions *Pachysolen tannophilus* produces cell mass, while under anaerobic or oxygen limited conditions xylitol and ethanol are produced

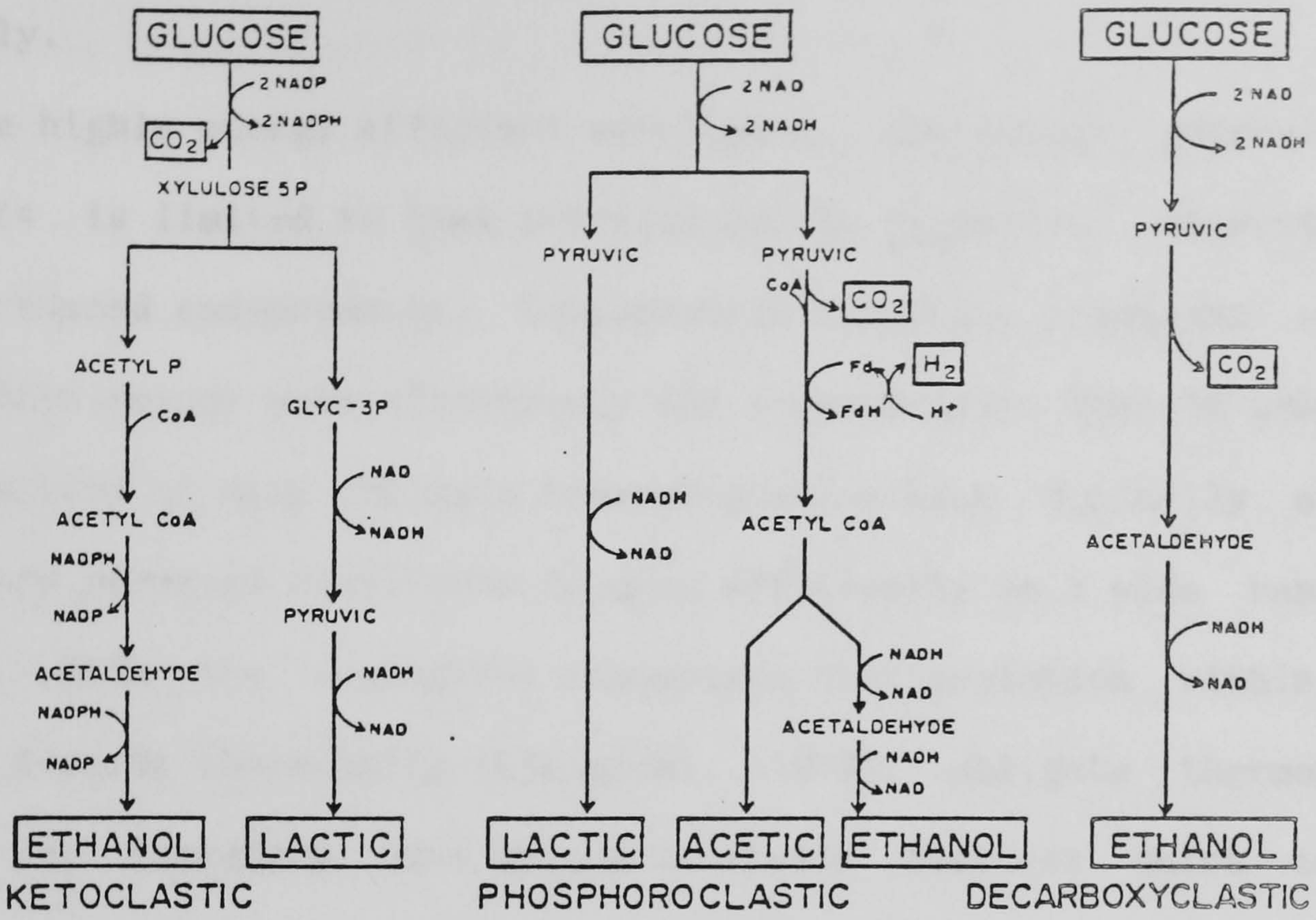

(a) Ethanolic fermentation pathways for glucose

Zeikus (1980)

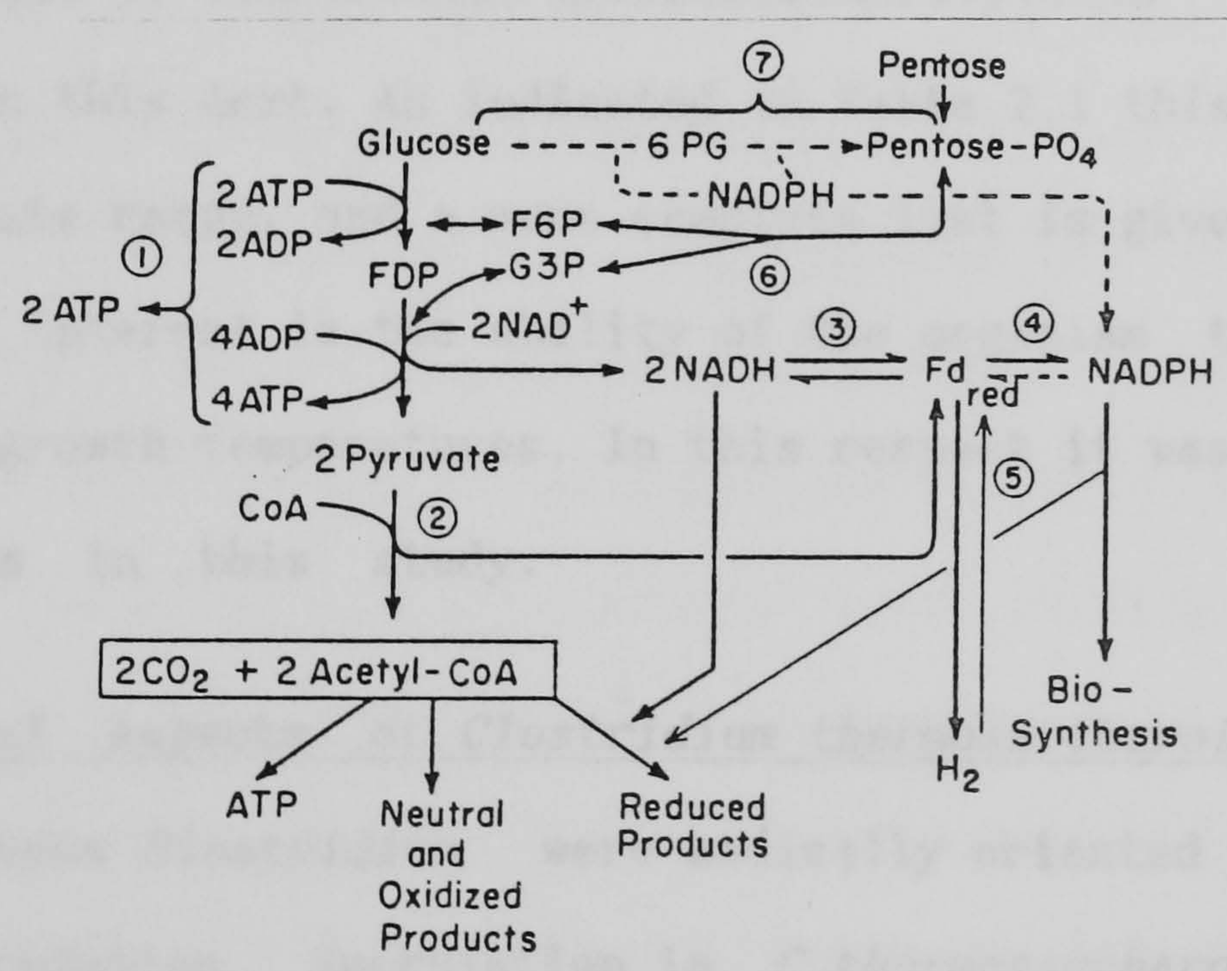

(b) The clostridial fermentation strategy

Rogers (1986)

Figure 2.1 Ethanol fermentation pathways for glucose and xylose

respectively.

Unlike the highly energy efficient aerobiosis, the energy generated in anaerobiosis is limited to that provided by the catabolic conversion of sugars to reduced end-products. Consequently anaerobic organisms require to spend their energy more effectively and economically. This is exhibited by the ability of many obligate anaerobes which have optimally adapted under energy stressed conditions to grow efficiently on a wide range of substrates. With the ecological assumption that evolution within most groups is towards thermophily (Ljungdahl, 1979), obligate thermophilic anaerobes may therefore have unique metabolic features which can be utilised in the large scale production of reduced end-products for use as chemicals and fuels.

Some of the features of *Clostridium thermosaccharolyticum* have already been referred to in this text. As indicated in Table 2.1 this organism has a very wide substrate range, and a more complete list is given in Appendix 1. Of particular interest is the ability of the organism to metabolise xylan at elevated growth temperatures. In this respect it was chosen to be the test organism in this study.

2.1.1 Physiological Aspects of *Clostridium thermosaccharolyticum*

Early studies of genus *Clostridium* were medically oriented towards their toxicity and sporulation. Sporulation in *C.thermosaccharolyticum* was extensively studied in the late 1960's (Phiel and Ordal, 1967; Hsu and Ordal, 1969a; Hsu and Ordal, 1970). Generally the spore development resembles the mechanism in the genus *Bacillus* . Various "stress factors" thought to be involved in the onset of sporulation are recently reviewed by Woods and Jones (1987). In *C.thermosaccharolyticum* , stress factors such as extreme pH, catabolic repression due to a change of substrate, and high concentrations of substrate or end-products have been shown to

stimulate sporulation (Hsu and Ordal, 1970). Moreover such conditions were also thought to be responsible for morphological and metabolic changes observed with different strains of *C.thermosaccharolyticum* (Phiel and Ordal (1967), Hsu and Ordal (1969a), and Landuyt *et al* (1983)). Spore formation in many clostridia is often accompanied by characteristic changes in cell shape. Such changes in *C.thermosaccharolyticum* are marked by a characteristic continued elongation (Phiel and Ordal 1969a, Landuyt *et al* ,1983). During sporulation the turbidity of the culture may continue to increase for some hours after cell division has stopped. The reasons for such unusual morphological changes are not understood. Possible explanations may be inhibition of enzymes involved in binary fission under stress conditions or accumulation of storage products prior to the dormant phase. The studies of Hsu and Ordal (1969b and 1970) and more recently Landuyt *et al* (1983) and Landuyt and Hsu (1984), have shown a shift in metabolism in *C.thermosaccharolyticum* concomitant with cell elongation. Under conditions of restricted growth, the organism was found to go through an intermediate non-dividing form that produced mainly ethanol instead of acetate. Such growth restrictions are prompted by limiting supply of substrate (continuous culture only), less readily utilisable substrates e.g starch, and growth under extreme environmental conditions e.g acid pH. Growth restrictions in effect reduce the specific growth rate of the organisms and thus induce catabolic (and perhaps anabolic) changes. These observations are in common with other solvent producing clostridia. Acetone/butanol fermentation by *C.acetobutylicum* is onset by a pH breakpoint as a result of initial acid production by the organism (Jones *et al* , 1982).

There are only a limited number of reports on sugar fermentation by *C.thermosaccharolyticum* . An early study by Sjolander (1937) indicated that the main end-products formed are CO_2, H_2, acetic, butyric, and lactic

acids, but no significant amount of ethanol. Production of ethanol at the stationary phase of growth was reported by Lee and Ordal (1967). Later Hsu and Ordal (1970) qualitatively showed ethanol production by slow growing (sporulating) cells . Fang (1980) analysed the fermentation end-products of cells growing on xylose and reported maximum ethanol yields of 55%. Landuyt *et al* (1983) also found ethanol to be the main end-product of fermentation with the highest concentration of 0.048 moles (≈ 2.2 g/l) in a 6 hour culture. Improved productivities have been reported with an ethanol tolerant mutant of *C. thermosaccharolyticum* (Fang, 1980; Landuyt and Hsu, 1984; Rothstein, 1986). The ethanol tolerant mutants were obtained by environmental adaptation rather than genetic manipulation. Continuous subculturing into a medium containing increasing concentrations of ethanol would naturally select for the surviving organisms. It is generally believed that these survivors are good solvent producers. The relative ease and speed of such selective technique coupled with inadequate genetic information on clostridia, has led to its popular use by a number of workers. Solvent tolerant strains of *C.thermocellum* (Herrero *et al* , 1982), *C.acetobutylicum* (Jones *et al* ,1982), and *C.thermohydrosulphuricum* (Lovitt *et al* ,1984) have been obtained by employing selective adaptation. Fermentation studies of the ethanol tolerant strain of *C.thermosaccharolyticum* (Fang 1980) showed encouraging improvements over the wild-type with an increase in ethanol productivity by three fold. Landuyt *et al* (1984) also reported on significant ethanol production by their ethanol tolerant mutant. These observations and results will be more carefully analysed and discussed at a later stage.

2.1.2 Ethanol Fermentation by Immobilised Cell Systems

The maximum throughput in continuous microbial processes based on free suspended cells is defined by the maximum dilution rate of the system. Dilution rate is a kinetic parameter equivalent to the specific growth

rate of the micro organism. Operation beyond the maximum growth rate therefore results in "washout", a condition where cells are removed faster than they can grow. Thus many early scale-ups involved extremely large fementers such as the activated sludge tanks used in the water treatment plants. This situation was rapidly improved by the introduction of cell recycle on fermenters, in order to maintain a large microbial population within the fermenter. Recycling of cells however required external loops and costly physical separation methods such as membranes or centrifugation. Utilisation of immobilised cells did not receive much attention until the early 1970's; although immobilised systems were developed even prior to immobilisation of enzymes (Webb *et al* , 1986).

An immobilised cell system is generally interpreted as the presence of organisms, either on surfaces or within particles, under conditions allowing maintenance of their catalytic activity and - if possible or even necessary - viability, and one which can be used repeatedly and continuously. Analogous to heterogenous porous catalysis, where extended surface and increased flux (transport per unit area) enhance the reactor performance, cell immobilisation has brought about a new concept in fermenter design. The features associated with such a system are listed in Table 2.3. Improvements in fermenter productivity could be achieved by operating at higher cell densities and dilution rates. On the other hand diffusional limitations together with mixing difficulties could create concentration gradients which may upset the stoichiometric balance of the system and influence the growth rate. Every fermentation system however should be judged by its own merit . For example in the acetone/butanol fermentation by *C.acetobutylicum* the latter limitation may prove to be beneficial whereby a pH gradient induces solvent production.

Four major groups of immobilised cells are distinguished in terms of the immobilisation procedure used : adhesion to a surface; entrapment in a

polymer matrix; retention behind membranes and flocculation or aggregation by cross-linkage between cells (Figure 2.2).

Any material capable of interacting with cells physically or via polar links may be employed as support for cellular adhesion. This simple technique is further enhanced by use of surface active porous materials such as porous glass, charcoal, resins, and wood chips. Various mechanisms involved in adhesion are reviewed by Ho (1986). Both dispersion forces (or van der Waals energy) and electrostatic forces become significant due to the mutual proximity of the surfaces, and thereby influence the interaction energy, V_L. This is generally defined as the energy required

Table 2.3 Applications of immobilised cells in fermentation

Source : Various

Advantages	*Disadvantages*
-Increased cell concentration with in the reactor	-Mainly suitable for extracellular products
-Operation of continuous fermenters independent of the dilution rate	-Mass transfer limitations
-Operation of batch fermenters on a drain and fill basis	-Mixing limitations
-facilated cell separation	-Formation of internal gradients (e.g pH)
-Protection against contamination	-Alterations in growth behaviour
-Manipulation of cells as a discrete phase	
-Possibility of carrying out sequential reactions in series with different microbial population	

to bring the particle from the bulk aqueous phase a distance L to the surface. Therefore for adhesion to occur , V_L must be negative for at least some value of L. Various factors such as age of the culture, zeta potential, and pore size could also affect the interaction energy (Nùñez and Lema, 1987). Physico-chemical changes as a result of growth or otherwise may result in desorption. Gammack and Brown (1986) reported on the influence of pH upon loss of bacterial adhesion to glass surfaces.

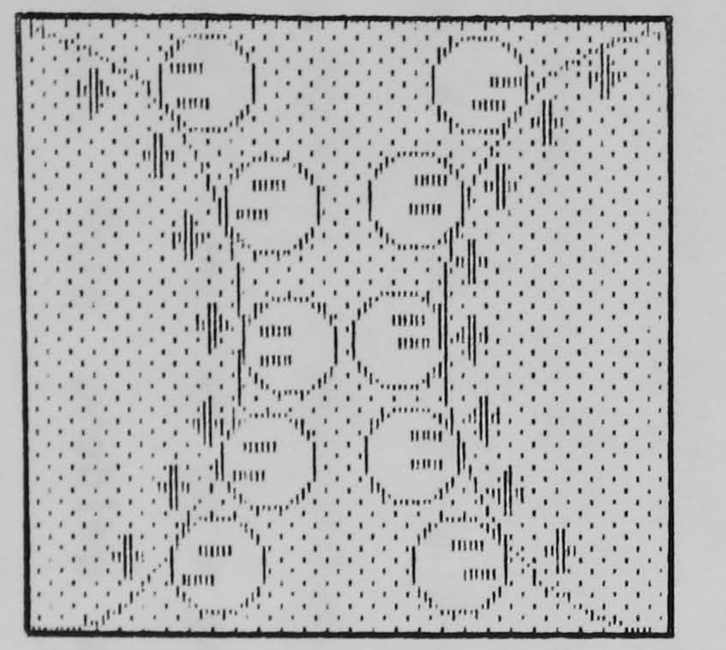

ADSORPTION

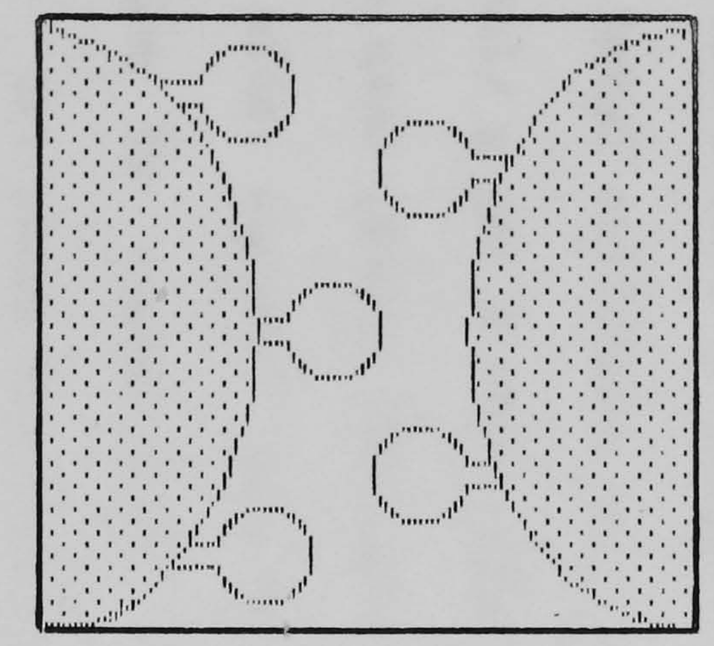

COVALENT ATTACHMENT

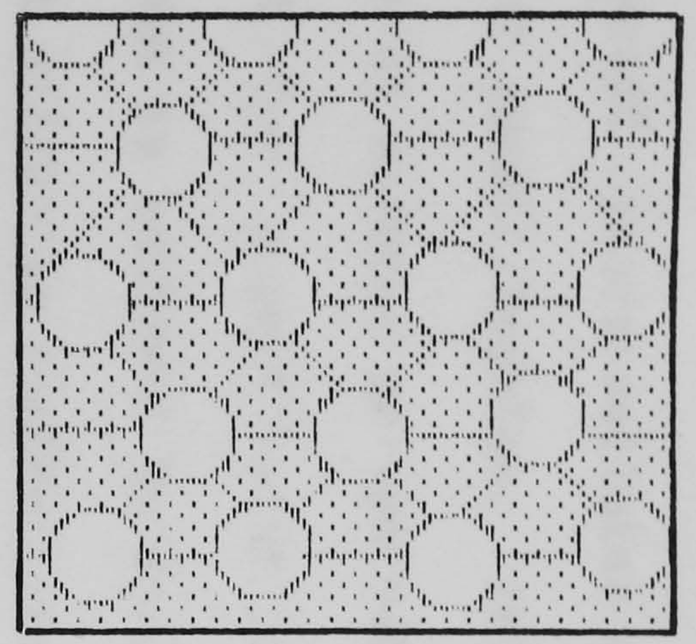

CROSS-LINKING

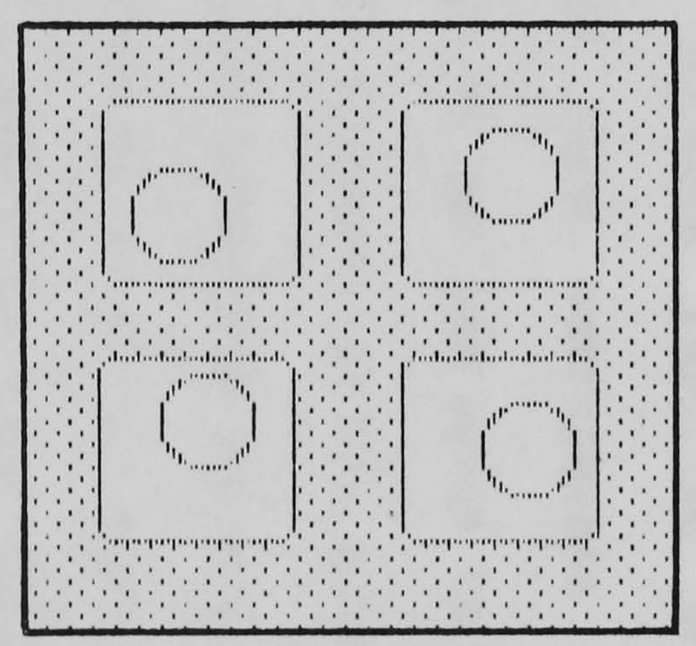

ENTRAPMENT

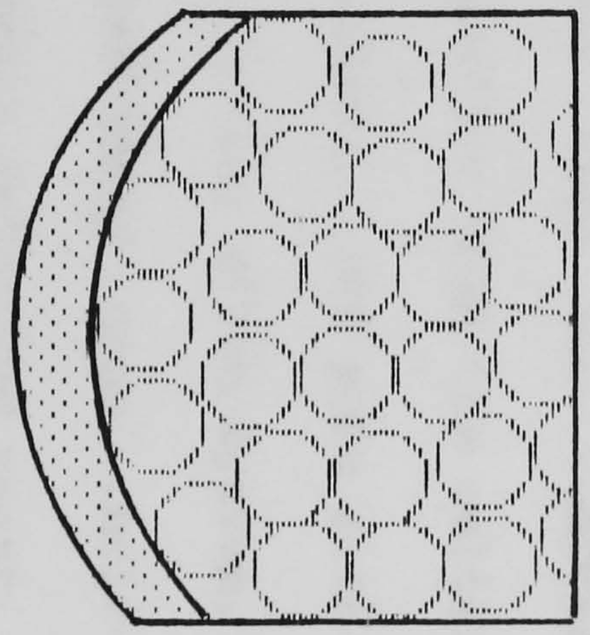

MEMBRANE CONFINEMENT

Figure 2.2 Techniques Commonly Employed for Cell Immobilisation

Addition of surfactants or cross-linking agents such as gluteraldehyde promotes covalent bonding (Bucke, 1986).

Over recent years cellular entrapment has proved to be a more popular choice of immobilisation. It essentially involves encapsulation of cells in beads of natural or synthetic gels. Gel support matrices can easily be designed for a particular porosity, shape, size and compressibility. Entrapment is achieved by designing pores smaller than the cells. With the inherent diffusion limitations of immobilisation, the pore size therefore becomes a critical design parameter. Hence for any given system, different gels show different productivity values depending upon their chemical nature and method of preparation. For example entrapped yeast cells in acetyl butyl cellulose only produce 14 mg ethanol/g gel.h compared to 40 mg ethanol/ g gel.h when natural gels such as Ca-alginate, carageenan and agar are used (Nùñez and Lema, 1987). Indeed the use of natural gels has gained wide support and the majority of the work reported on ethanol production by immobilised cells is based upon entrapments in these systems. Gel beads are produced by addition of gelling agent to cell (or spore) suspension followed by collection of droplets of the mixture in a "hardening" solution. Classically solutions of potassium and calcium salts were used for this purpose. However recently use of Al^{3+}, Ti^{4+}, and Zr^{4+} has been shown to be more effective (Bucke, 1986). Cellular entrapment in gels has a finite life as the support matrix ruptures in response to two opposing forces; compression and expansion. Gels are very compressible in nature and if operated in a packed column may limit the loading or size of the column. This problem may be overcome by the use of intermediate support trays or bed fluidisation. Gas formation by the micro-organisms has an expansive effect and is more difficult to overcome. Gas bubbles grow with cell numbers and as the matrix becomes saturated with cells, its diffusivity reduces and entraps bubbles even further. Accumulation of

bubbles is relieved as the particle explodes. In many cases cell immobilisation is "voluntary" and the cells prefer to grow on the surface of solids rather than to grow in free suspension.

Atkinson *et al* (1980) observed such behaviour by cellular colonisation within porous support particles. Organisms became immobilised as a natural consequence of their own growth and perhaps in combination with aggregation, entrapment and adsorption. These support particles are exremely robust and could be of any shape or size . Figure 1.2 shows some of the more popular particles employed in immobilisation studies. Large scale application of such a system has been employed in the waste water treatment industry (Atkinson and Mavituna, 1983).

A : Ethanol Production by Immobilised Cells

Many of the features listed in Table 2.3 indicate that cell immobilisation can greatly enhance the productivity of ethanol in many conventional processes. Kolot (1984) reviewed a number of yeast and bacterial fermentation studies where both free and immobilised cells were examined for ethanol productivity, yield, and product cost. Generally, for similar continuous conditions, the mentioned parameters of the immobilised systems were found to be the same as the free suspended systems with cell recyle and superior to the batch systems or those without cell recycle. The potential exploitation of immobilised systems however lies with operations at high dilution rates and substrate concentrations. In a recent extensive survey Gõdia *et al* (1987) have examined the efficiency of fermentation processes employing different methods of immobilisation. The majority of the reported data is based upon fermentation studies using *S.cerevisiae* and *Z.mobilis* . Studies involving cells adsorbed to support surfaces were mainly carried out in vertical packed beds. The research on *Z.mobilis* indicates shorter reactor residence time and higher ethanol productivities

when compared with the yeast. Both organisms have shown stable immobilised forms over a long period of fermentation. Similar trends were observed with other types of immobilisation based on entrapment and membrane confinement. The application of a packed bed with the entrapped cells of *S.cerevisiae* in Ca alginate gel showed improved ethanol productivities by a number of different studies (G dia *et al* ,1987). The stability of the gel support was estimated from its half-life in the reactor measured as the time taken for the cell activity/viability to reduce by half. There was no such data available for clogging of membranes. Hollow fibres have a very large surface and are most commonly employed for cellular immobilisation. The ethanol productivities however are much lower than the other immobilised systems used.

B : Kinetics of Immobilised Cells

The reaction kinetics of microbial systems is systematically studied and reviewed by Atkinson (1974). The famous work by Monod (1949) set the basis for much of the microbial kinetic studies carried out since and is best marked by the basic two parameter microbial growth equation named after him.

$$\frac{dC}{dt} = \mu C \qquad \textbf{(2.1a)} \qquad ; \qquad \mu = \mu_o \frac{S}{K_m + S} \qquad \textbf{(2.1b)}$$

Where C is the concentration of the cells; μ is the specific growth rate ; μ_o is the maximum specific growth rate; S is the limiting substrate concentration; K_m is the Monod constant equivalent to the substrate concentration where the rate is is one-half of the maximum, otherwise known as the half-saturation constant.

Microbial growth of free suspended cells generally follows first order kinetics and it is adequately described by the parameters in Equation 2.1. In order to determine these parameters, the reciprocal of Equation 2.1 (b)

would result a linear plot (Lineweaver-Burk plot). Thus;

$$\frac{1}{\mu} = \frac{1}{\mu_o} + \frac{K_m}{\mu_o}\,\frac{1}{S} \qquad (2.2)$$

where $1/\mu$ and $1/S$ need to be determined experimentally for a given microbial system.

Monod kinetics however fails to account for two limiting conditions often encountered in microbial fermentations viz., diffusion and inhibition. Hence it may be regarded as a special case of a more general rate form. When a system is not limited by diffusion the growth may halt irrespective of substrate concentration due to formation of end products. The mechanism and kinetics of ethanol inhibition play a major part in bacterial fermentation and will be discussed in a separate section. Diffusional limitations however may arise by immobilisation of cells. Generally in a fermenter system micro-organisms occur either as flocs freely suspended, or as films adhered to a support surface. Atkinson (1974) constructed a model for a single organism, and by analysing the rate limiting steps in the substrate transport to the cells provided a generalised equation for susbtrate take up by the cell.

$$R_s = R_{so}\,\{1+ k_2^2+A - [(1+k_2^2- A)^2 + 4A]^{1/2}\} \qquad (2.3)$$

where R_o and R are the maximum and the specific rate of substrate removed respectively ; $A = S^*/K_m$; k_2 is the solid phase diffusion limitation; and S^* is the concentration of substrate at solid/liquid interface.

Equation 2.3 was derived on the basis of molecular diffusion theory described by Fick's law and the assumption that the flux of substrate N_s, through diffusion limited zones is equal to the rate of consumption in the metabolic zone. On these grounds a model was developed for microbial mass by further assuming ;

- under steady-state conditions, the composition of total microbial mass remains invariant with respect to time in spite of the fact that growth of each micro organism does not fit this criterion,
- the cell is a unit whose functions are invariant with time and which has average gross properties that are functions of the local environment,
- for the microbial mass as a whole, the age distribution of the population and such biological properties as viability, mutation, selection, adaptation, and competition are time variant.

Thus for a microbial film or floc , the transport at the interface is described by the following parameters,

$$N_s = -D_f \frac{dS}{dx} = f\ (D_f,\ a\alpha,\ K_m,\ L,\ S^*) \qquad (2.4)$$

where N is the rate of transport of substrate per unit area; D_e is diffusivity, dS/dx is the substrate concentration gradient across the film or floc, $a\alpha$ is a constant describing the shape and geometry of the film or floc, and L is the thickness of the film. Atkinson (1974) described Equation 2.4 as the Biological Rate Equation (BRE). Atkinson and Davies (1974) solved Equation 2.4 for for both microbial films and flocs by introducing an effectiveness factor, E_N which accounts for deviations from the flux. The model takes the general half order reaction kinetics given by;

$$R = E_N R_o \frac{S}{K_m + S} \qquad (2.5)$$

Hence from Equation 2.4 for microbial flocs we have,

$$R_p = \frac{6R_o}{\alpha k_{2p} d_p} \frac{(1 + A_p)^{1/2}}{(1 + A_p)} A_p \qquad (2.6)$$

and for films,

$$N_s = \frac{R_o}{k_{2f}} \frac{(1 + 2A_f)^{1/2}}{(1 + A_f)} A_f \qquad (2.7)$$

where $k_{2i} = [\rho_{oi} R_o / K_m D_f]^{1/2}$, $A_i = S^*_i / K_m$, ρ_{oi} is the density of microbial film or floc (dry weight per unit volume).

Equations 2.6 and 2.7 contain most of the characteristic design parameters and are of fundamental importance . In a later work Atkinson *et al* (1984) analysed the kinetics of microbial growth in Biomass Support Particles (BSP). It was thought that the overall rate of substrate removal R_f, in the fermenter results from the combined effect of the support particles, films and suspended flocs. Hence;

$$R_f = R_p M_p + a N_s + R_s M_s \qquad (2.8)$$

which in effect is the combination of Equations 2.1, 2.6 and 2.7. Thus ;

$$R_f = \frac{R_o}{k_{2i}} \left\{ \frac{(1+A_p)^{1/6} A_p}{(1+A_p)\, \alpha d_p} + a \frac{(1+2A_f)^{1/2} A_f}{(1+A_f)} + \frac{A}{1+A} \right\} \qquad (2.9)$$

As $A_i \gg 1$ then;

$$R_f = \frac{R_o}{k_{2i}} \left\{ \frac{6 A_p^{1/2}}{\alpha d_p} + A_f^{1/2} \right\} \qquad (2.10)$$

By defining the effective microbial density throughout the 'free' space within the support particle as $\rho_{oe} = m_p / \epsilon V_p$, then

$$k_{2p} = k_{2f} = k_{2i} = [\rho_{oe} R_o / K_m D_f]^{1/2} \qquad (2.11)$$

where V_p is the volume of the particle; ϵ is the particle porosity; m_p is the biomass associated with the particle.

The assumptions made for deriving Equations 2.1 to 2.11 are experimentally justified by Atkinson *et al* (1984). Many fermentation systems operate on unlimited supply of substrate in the feed stream hence Equation 2.10 has many practical advantages over the more general form given by Equation

2.9. It is notable that in the absence of microbial films and flocs, the specific substrate removal rate is given by the maximum rate R_o, as originally described by Monod's equation.

C : Particle Biomass Hold-up

The rate at which micro-organisms grow within their support particles is dependent upon their specific growth rate, μ , and the specific rate of attrition, T_A. Thus;

$$\frac{dm_p}{dt} = (\mu - T_A)m_p \qquad (2.12)$$

For the maximum rate, $dm_p/dt = 0$ and hence $\mu = T_A$.

Thus the maximum biomass concentration is achieved where there is a steady state balance between growth and removal of the cells. It may therefore be deduced that at low biomass hold-ups, m_p increases according to Monod kinetics, i.e $m_p \alpha \mu$, and hence;

$$m_p = m_{po} \frac{S^*}{K_o + S^*} \qquad (2.13)$$

where K_o is a constant similar to K_m, and m_{po} is the maximum biomass hold-up in the support particle.

Atkinson *et al* (1984) experimentally determined the constants K_o and m_{po} and found a good correlation between the model and the experimental data. Shieh and Chan (1984) determined a biomass hold-up correlation for BSPs in a fluidised bed fermenter. They employed the Richardson-Zaki solid-liquid fluidisation correlation (Coulson *et al* ,1978) in association with the Galileo number, Ga, to obtain;

$$m_p = p(1-\epsilon)\ [1- (d_m/d_p)^3] \qquad (2.14)$$

and for $d_p \gg d_m$;

$$m_p = p(1-\epsilon) \qquad (2.15)$$

where ϵ is the bed porosity defined by the Richardson-Zaki equation; d_m is the diameter of microbial film; d_p is the diameter of the particle. Equation 2.14 was found to give an excellent fit to all experimental observations made by Shieh and Chen (1984).

2.1.3 Ethanol Inhibition

It has long been recognised that industrial fermentations terminate prematurely despite an unlimiting supply of substrates. Early studies on *S.cerevisiae* demonstrated that inhibition was due to a "staling effect" which refers to accumulation of toxic products resulting from the fermenting organism's own metabolism (Ingram and Buttke, 1984). Premature termination limits the final concentration of alcohol and hence lowers the productivity. Inhibitory effects of ethanol have been extensively studied on both bacteria and yeast (mainly *S.cerevisiae*). Such physiological studies have provided new insights into the mechanisms of end-product inhibition and lead to reduced manufacturing costs.

Product tolerant organisms that can sustain a high rate of growth in the presence of high product concentration would be ideally suited for industrial fermentation. It is widely believed that since accumulation of all anaerobic fermentation products is closely related to the rate of growth, a tolerant organism will also be a good producer in the presence of high product concentration. Such adaptation however is very difficult to achieve and as will be indicated later, has led to much controversy in the recent literature.

End-product inhibition in solvent producing bacteria is perhaps the main limiting factor for their use in industry. Much research has been carried out in order to identify the main mode of inhibition and thence to develop tolerant strains. Jöbses and Roels (1986) investigated such effects on *Z.mobilis* . Although changes in cellular membrane stucture were thought to

be the main inhibiting factor, it was not the only mechanism that retarded growth. At extracellular ethanol concentrations above 50 g/l, deactivation of proteins and inhibition of the transport system were thought to occur. Herrero *et al* (1982) studied the membrane lipid composition of wild-type and an ethanol tolerant strain (**C9**) of *C.thermocellum* . They found a marked difference in the lipid composition of the two strains, and concluded that membrane disorder caused by introduction of ethanol is the main mode of inhibition. Fang (1982) selected for a highly ethanol tolerant (5% w/v) strain of *C.thermosaccharolyticum* , and reported high ethanol productivity (30 g/l) under a fed-batch system. Studies on another thermophile by Lovitt *et al* (1986) showed that ethanol does not affect the cellular membrane of *C.thermohydrosulphuricum* , but changes the fermentation pattern of the organism. Both physical and chemical means have also been employed in reducing the inhibitory effect of end-products. Dekker (1986) reported on enhanced ethanol production from xylose by *P. tannophilus* by supplementing the growth medium with a lipid mixture. Matsumara and Märkl (1985) attempted to eliminate ethanol inhibition in *S. cerevisiae* growth culture by perstraction (membrane-aided solvent extraction). They used a hollow fibre membrane module to separate cells and nutrient solids from the fermentation broth , followed by solvent extraction. There is little information in the literature regarding *C.thermosaccharolyticum* . The foregoing survey , examines the various modes of ethanol inhibition related to the genus *Clostridia* with a possible suggestion for the inhibitory mechanism in *C.thermosaccharolyticum* .

A : Modes of Ethanol Inhibition

Membrane disorders and deactivation of enzymes are thought to be the main modes of ethanol inhibition. It is generally believed that a combination

of both modes contribute to the overall inhibitory effect- the mechanisms of which are not clearly understood.

Biological membranes are very thin (~ 100 A in width) and are mainly composed of proteins , lipids, and metal ions. The amphiphilic nature of membrane lipids allow the formation of a bilayer structure in an aqueous form. Bacterial membranes in general fit the "fluid mosaic" model. This model proposes a dynamic structure of the membrane where lipids and proteins are able to move laterally. Such dynamic behaviour is explained by the physicochemical nature of the phospholipids. Based on a glycerol molecule, phospholipids have two non-polar fatty acid chains and a polar amino acid chain. It has been shown that there are many different fatty acids invloved in the membrane but this variety does not contribute to the chemical functions of the membrane. Depending upon the water activity and temperature, the association of fatty acid chains influence the fluid behaviour of the membrane. The transition temperature from gel (solid) to liquid crystalline form is called the phase transition temperature, T_c, and it is dependent upon the length, branching and saturation of the hydrocarbon chains. Maximal growth temperature of micro-organisms is related to the lipid phase transition. Bacteria change their lipid fatty acids composition in response to variation in their growth temperature to achieve a constant membrane fluidity. This process is called "homoviscous adaptation". Micro-organisms can adjust to growth at higher temperature as long as they can produce clusters (mainly protein) or domains in their membranes instead of producing an unrestrictive , randomising two-dimensional fluid. The relevance of membrane fluidity or viscosity in such thermal adaptation is less clear, partially because of difficulties encountered in measurement of the fluidity of membranes. Although micro-organisms have the ability to synthesise lipids with higher melting points to achieve a constant fluidity, the concomitant alterations in volume,

length, and packing capabilities could terminate a successful matching of lipids, proteins, and ions in the membrane. Studies of *C.thermocellum* (Herrero *et al*, 1982) and *Z.mobilis* (Jöbses and Roels, 1985) have indicated that the mechanism of solvent inhibition in bacteria is similar to thermal adaptation.

Table 2.4 Fatty acid distribution pattern of different clostridial membrane lipids.

Source : Chan *et al* (1971).

Fatty acid	Organism			
	A	**B**	**C**	**D**
Straight chain				
C_{10}	T[2]	1.4	-	-
C_{12}	1.5	T	T	T
C_{14}	13.9	8.6	3.2	19.5
C_{15}	1.4	-	-	-
C_{16}	10.0	16.1	32.1	21.3
C_{18}	1.1	1.8	2.0	-
Branched chain				
a-C_{13}	1.0	T		
i-C_{15}	44.1	37.5	1.7	-
a-C_{17}	3.3	3.0	-	-
i-C_{17}	6.4	7.7	-	-
Cyclopropane				
C_{13}	2.8	1.8	T	1.0
C_{15}	3.9	8.7	10.7	1.0
C_{17}	-	-	5.2	-
C_{19}	-	-	2.2	-
Monounsaturated				
$C_{14:1}$	-	-	-	5.2
^{9}-$C_{16:1}$	-	-	20.0	14.8
^{11}-$C_{16:1}$	-	-	-	13.8
$C_{18:1}$	T	1.5	7.4	-
Unsaturated cyclo-propane	7.8	10.9	9.8	18.2
% Higher melting fatty acids	78.4	73.1	39.0	40.8
% Lower melting fatty acids	18.8	25.9	55.3	54.0

1: **A:** *C.thermosaccharolyticum* ; **B:** *C.tatrtarivorum* ; **C:** *C.pateurianum* ; **D:** *Clostridium* sp. srain 69.
2: Trace (less than 1%)

In a recent review article Ingram and Buttke (1984) clearly showed that in all studies reviewed , the addition of relevant concentrations of alcohol increases the freedom of motion within membrane, lowers the phase transition temperature, and decreases the membrane order. Thus like thermophily, solvent tolerance in organisms is controlled under complex genetic systems and on this basis resembles the thermophilic evolution of many mesophiles (Ljungdahl, 1979).

It appears therefore that isolation of tolerant strains cannot be achieved with a single mutation step due to the number of variables involved. Structurally thermophiles are very similar to their mesophilic cousins, with the added advantage of thermostability. Chan *et al* (1971), reported on the fatty acid composition of the lipid membrane of thermophilic, mesophilic, and psychrophilic clostridia. The data showed (Table 2.4) notable differences with thermophiles containing the highest amount of saturated- and branched-chain fatty acids. The mesophiles and psychrophiles were characterised by having a higher proportion of unsaturated fatty acids. Sleyter and Thorne (1976) reported on the presence of surface (S) layer on the cells of *C.thermosaccharolyticum* and *C.thermohydrosulphuricum* . They found that the sub-units of the S-layer are glycoproteins that interact with each other through ionic and hydrophobic bonds, and with the underlying cell wall by means of hydrogen bonds. From this data it is evident that the membrane structure of *C.thermosaccharolyticum* is highly evolved for thermophilic growth and as with *C.thermohydrosulphuricum* (Lovitt *et al* , 1984) should be able to tolerant solvents.

The relative potency of ethanol on the biological membrane is thought to be due to its polar nature. It is generally believed that the hydrophobic interior of the membrane acts as a permeability barrier to exchange of polar, water soluble molecules. Ethanol partitions very poorly into a

hydrophobic environment. However at high concentrations it can interact with the membrane and thereby increase the polarity and weaken the barrier. In this view it was proposed that a lipid supplement to the cells could maintain the hydrophobicity (cf homoviscosity) and thus strengthen the lipid membrane. Studies with *E.coli* showed that addition of vaccinic acid ($C_{18:1}$) resulted in an increase in the growth of an alcohol intolerant mutant (Ingram and Buttke, 1984). More evidence on the effect of lipid supplements and inhibition is presented by Herrero *et al* (1982) and Rose and Beaven (1981). The combined effect of ethanol concentration and temperature was demonstrated for different strains of *C.thermohydrosulphuricum* (Lovitt *et al* , 1984) and *C.thermocellum* (Herrero and Gomez, 1980). In both cases the optimum temperature of the wild type organism decreased with increasing ethanol concentration. The ethanol tolerant mutant of *C.thermohydrosulphuricum* grew at ethanol concentrations reaching 8% (w/v) at 45°C, but only up to 3.3% (w/v) at 68°C. The growth of the ethanol tolerant mutant of *C.thermocellum* at 60°C was inhibited at ethanol concentrations above 3% (w/v). Unlike *C.thermocellum* , *C.thermohydrosulphuricum* was found to have a unique membrane lipid composition which contained a C_{30} dicarboxylic acid.

The effect of ethanol on enzymes and metabolic activity is well documented. Ethanol differs from other end-products of catabolic pathways in that it is known to denature proteins non-specifically. Certainly Rose and Beaven (1981) have identified the action of ethanol on the proteins of *S.cerevisiae* as the main mode of inhibition. The studies of Linden and Moreira (1983) on *C.acetobutylicum* also indicate some deactivation of membrane-bound proteins. Organisms with protein structure resistant to ethanol can live and metabolise at higher ethanol concentrations. There are no specific target sites for the ethanol molecule. Therefore in practical terms it is not possible to mutate the receptor structure and

thus develop strains that tolerate higher concentrations of ethanol. The inhibitory effect of ethanol upon glycolytic enzymes was demonstrated by Miller *et al* (1982). They observed that at ethanol concentrations greater than 12% (w/v), the activity of enzymes decreased by an average 10%. This observation lent itself to two different arguments. Firstly the low tolerance of the organism at lower ethanol concentration could be due to other modes of inhibition such as membrane fluidisation. And secondly the ethanol produced by the organismr could be accumulated inside the cell at much higher ethanol concentrations than measured extracellularly. This could bring about a sharp concentration gradient across the membrane affecting much of the protein structure of the cell. The latter could be particularly damaging to anaerobes. Anaerobes degrade sugars through oxidative pathways to obtain chemical energy for growth. Because only a small number of ATP molecules are produced during the anaerobic catabolism, the growth of anaerobes is said to be limited by the rate of energy producing reactions. ATP molecules are either used in membrane energisation (H^+ pump) or biosynthesis. A net reduction in the amount of ATP going to biosynthesis will inhibit growth. There is evidence that product inhibitors upset this energy balance and limit the supply of energy for growth. Membrane bound ATPase activity, and uptake of alanine and 3-O-methyl glucose in *C.acetobutylicum* showed significant sensitivity to butanol (Linden and Moreira, 1983).

Ethanol inhibition is affected by a number of other factors. Vega *et al* (1987) showed that increasing the inoculum level decreases the severity of ethanol inhibition on *S.cerevisiae* . They argued that much controversy in the literature concerning the various tolerance levels could be due to different initial inoculum sizes. Their study also indicated that tolerance levels achieved by extracellular additions of ethanol to the growth medium are not representative values and often misleading, and only

autogenously produced concentrations can provide a real estimate (often much lower than the former). In an earlier study based on extracellular addition of ethanol to the growth medium of *S.cerevisiae* , Brown *et al* (1981) found that the growth and viability effects had different inhibition constants and ethanol was less inhibitory towards fermentation than towards growth. This work can offer a plausible explanation to the findings of Vega *et al* (1987) when they observed that the specific production rate at cell concentrations above 1.3 g/l was independent of the inoculum size. The effect of type and concentration of substrate on ethanol inhibition was investigated by Moulin *et al* (1981). Their fermentation studies with *Candida pseudotropicalis* revealed that at relatively high ethanol and substrate concentration the inhibitory effect is very different according to whether the fermented sugar is a monosaccharide (glucose) or a disaccharide (lactose). Perhaps this can be explained by the different osmotic pressures imparted on the cell membrane by the different sugar solutions.

Despite the continuing work on the mechanisms of solvent inhibition the only breakthrough expected is by a better understanding of the genetics of the micro-organisms. Recombinant DNA technology can then be employed to produce a more tolerant or super producer strain. However the recent survey by Rogers (1986) shows just how little is known about genetics of clostridia.

From the description of the main modes of ethanol inhibition it is of no suprise to see how closely they are inter-related. No unique mode or mechanism can be solely associated with inhibition. However the evidence so far certainly supports the contention that membranes are involved, and their mosaic protein/lipid arrangement serves as a prime site for solvent attacks.

B : Kinetics of Ethanol Inhibition

The various views on the modes of ethanol inhibition also reflects on the various approaches employed in the kinetic studies of the subject. In the presence of excess substrate, the main rate limiting step associated with all types of inhibitory mechanisms is the rate of growth of micro-organisms. Monod kinetics have been successfully applied to many different growth systems where inhibition plays no role. In the alcoholic fermentation, the presence of ethanol decreases the value of the specific growth rate, and Equation 2.1(b) must be extended to include such effects. In other words;

$$\mu = f\,(S,P) \qquad \textbf{(2.16)}$$

where P is the concentration of the inhibitory product (i.e ethanol).

Early studies on the kinetics of ethanol inhibition (Aiba *et al* , 1968) have indicated that ethanol inhibition only affected the maximum specific growth rate, μ_o, and not the saturation constant, K_m. This would imply that ethanol inhibition is non-competitive (cf enzyme kinetics) and hence specific growth rate can be expressed as;

$$\mu = \mu_i \frac{S}{K_m + S} \qquad \textbf{(2.17)}$$

where $\mu_i < \mu_o$. From Equations 2.17 and 2.1(b) it is clear that in the absence of inhibition $\mu_i = \mu_o$. In this respect a relationship between μ_i and μ_o indicates the degree of inhibition for any given system. Such relations invariably include empirical constants to describe a particular system (Table 2.5). Hinshelwood (1946) suggested a linear relationship incoporating a finite value of the maximum ethanol concentration above which cells do not grow. This simple relation between μ_i and end-product concentration P, has been successfully applied to many experimental data where fermentation is not nutrient or substrate limited (Ghose and Tyagi,

1979; Holzberg *et al* ,1967). The non-linear models described by Aiba *et al* (1968) and Aiba and Shoda (1969) however imply that cells are capable of growing and producing ethanol indefinitely. This is contrary to what is observed in reality since with all alcoholic fermentations there exists a definite ethanol concentration limit above which both cell growth and fermentation cease. Moreover it has been shown that inhibition only takes effect if a threshold concentration of ethanol is reached (Holzberg *et al* , 1967). The threshold concentration however is rendered insignificant and does not come into any of the models listed in Table 2.5. Other non-linear models such as the parabolic relationship suggested by Bazua and Wilke (1977) describe the deviations form the original model proposed by Hinshelwood (1946). Perhaps the most general model is offered by Levenspiel (1979). In his work a general non-linear equation (Eq. 2.18) with only one empirical constant was proposed.

$$\mu_i = \mu_o \left(1 - \frac{P}{P_m}\right)^n \qquad (2.18)$$

where P_m is the concentration of ethanol above which cells do not grow; and n is the "toxicity power" governing the linearity of the system, determined as the gradient of a plot of *ln* (μ_i/μ_o) Vs. $(1- P/P_m)$. From Equation 2.18 all models in Table 2.5 can be derived. For example when n=1 Hinshelwood's linear relation is obtained and when n>1 or n<1 the hyperbolic and the parabolic relations are derived.

More recently Luong (1985) extended the equation proposed by Levenspiel to distinguish the specific rate of ethanol production from that of growth by;

$$\frac{\mu_i}{\mu_o} = 1 - \left(\frac{P}{P_m}\right)^{\alpha} \qquad (2.19a)$$

$$\frac{v_i}{v_o} = 1 - \left(\frac{P}{P'_m}\right)^{\beta} \qquad \textbf{(2.19b)}$$

where v_i is the specific rate of ethanol production in the presence of ethanol; and v_o is the maximum specific rate of ethanol production at zero ethanol concentration. This work is analogous with the earlier proposal by Brown *et al* (1981) where they observed rates for growth and fermentation of *S.cerevisiae* . More recently Daugulis and Swaine (1987) further included the effect of substrate concentration in the Levenspiel's general equation and suggested;

Table 2.5 Kinetics of Ethanol Inhibition

Source : various

Microbiol System	Conditions	Relationship	References
S.cerevisiae + exogenous EtOH	Unlimiting Substrate	$\mu_i=\mu_o-K_1P$ $K_1=\mu_o/P_m$	Hinshelwood (1946)
S.cerevisiae + exogenous EtOH	Limiting substrate	$\mu_i=\mu_o\ \exp(-K_2P)$	Aiba & Shoda (1968)
S.cerevisiae + exogenous EtOH	Limiting substrate	$\mu_i=\mu_o(1+[P/K_3])^{-1}$ (Hyperbolic)	Aiba & Shoda (1981)
S.cerevisiae + exogenous EtOH	Unlimiting substrate	$\mu_i=\mu_o-\frac{aP}{b-P}$ (Parabolic)	Bazua & Wilke (1977)
Applied examples to justify the generality of the correlation.		$\mu_i=\mu_o\ (1-[P/P_m])^n$	Levenspiel (1979)
S.cerevisiae + exogenous EtOH	Unlimiting substrate	$\mu_i=\mu_o\ (1-[P/P_m])^{\alpha}$ $v_i=v_o\ (1-[P/P'_m])^{\beta}$	Luong (1985)
S.cerevisiae + endogenous EtOH	Unlimting substrate	$\mu_i=\mu_o(1+[P/K_3])^{-1}$ (Same as Aiba & Shoda)	Hoppe & Hansford (1982)

$$\frac{dP}{dt} = \frac{\mu_o CS}{K_S + S + S^2/k} \left(1 - \frac{P}{P_m}\right)^n \qquad (2.20)$$

where k is a constant.

The effect of substrate concentration in incorporated in Equation 2.20 is in fact due to an earlier work by Klecke and Maier (1985) on *S.cerevisiae*.

All kinetic relationships described so far were initially based upon experimental studies under the effects of exogenous ethanol on the growth and fermentation of micro-organisms. The inhibitory effects of autogenous ethanol were studied by Hoppe and Hansford (1982). By observing fermentation behaviour of *S.cerevisiae* under different inhibitory conditions, they successfully demonstrated that added ethanol was not as inhibitory to growth as was the ethanol produced by the cells. They applied the proposed inhibition model by Aiba and Shoda (1969) (see Table 2.5) and for the same microbial system, estimated the value for the inhibition constant, K_p, to be one-tenth of that determined originally by Aiba and Shoda (1969). They concluded such parameters as K_p, P_m and μ_i are unrealistic measures if determined in terms of exogenous ethanol concentrations. As we shall see later in the results section such observations are in common with this study where a similar type of kinetics is employed.

At this point it essential to make one simplifying assumption in the effect that every unit of substrate consumed will produce the same amount of cells, and of products, at all conditions. In other words it is assumed that the system will hold a constant yield at all times. In terms of concentration of products P, and cells C, the performance expression for a batch or a plug-flow reactor is then given by;

$$t_b = \tau_p = \int_{Po}^{P} dp/dt \int_{Co}^{C} dC/\mu C \qquad (2.21)$$

Thus substituting for μ_i in terms of μ_o we have;

$$\mu = \mu_o \left(1 - \frac{P}{P_m}\right)^n \frac{S}{K_S + S} \qquad \textbf{(2.22a)}$$

for n=1 and $S \gg K_S$;

$$\mu = \mu_o \left(1 - \frac{P}{P_m}\right)^n \qquad \textbf{(2.22b)}$$

Thus by integration;

$$\mu_o t_b = \mu_o \tau_P = \frac{P_m}{P_m - P_o + [P/C]C_o} \ln \frac{C(P_m - P_o)}{C_o(P_m - P)} \qquad \textbf{(2.23)}$$

where $[P/C] = (P-P_o)/(C-C_o)$.

A similar expression can also be derived for the continuous mixed system;

$$\mu_o \tau_m = \frac{P_m}{(P-P_o + [P/C]C_o)(1- P/P_m)^n} \qquad \textbf{(2.24)}$$

For a sterile feed $C_o = 0$, hence;

$$\mu_o \tau_m = (1 - P/P_m)^{-n} \qquad \textbf{(2.25)}$$

Both Equations 2.24 and 2.25 can be used for reactor design and are of fundamental importance.

2.2 Materials and Methods

2.2.1 Organism and Growth Conditions

Freeze dried *Clostridium thermosaccharolyticum* NCIB 9385 was resuscitated in Reinforced Clostridial Medium RCM, (Oxoid, U.K) at 60 °C. Working stock cultures were prepared in 20 % glycerol and stored at -20 °C. Upon prolonged storage cell viability loss was observed by poor resuscitation. As a result stocks were regenerated every two months. The mutant strain of *C.thermosaccharolyticum* CTM 3, was also maintained as stock cultures in similar fashion. The cell viability however deteriorated more rapidly than the wild type strains and stocks were regenerated every month.

Experimental cultures were started by inoculating 20 ml of RCM or MCR media (see below) with 0.2 ml of the stock culture followed by incubation at 60 °C. These culture were used to "seed" larger volumes of the experimental cultures.

Experiments involving xylose as the carbon source were seeded by cells grown on xylose. This minimised the lag frequently encountered in the growth studies.

2.2.2 Growth Medium

Initial growth studies were carried out by growing cells on RCM or synthetic RCM which allowed use of different carbon sources. Fang (1980) developed an optimum medium for the growth of *C.thermosaccharolyticum* and proposed a partially defined medium CM4, and a chemically defined medium CCM4. In the latter yeast extract was replaced with trace quantities of vitamins riboflavin, nicotinic acid and biotin, and amino acids methionine, histidine, and cysteine.

Preparation of CM4 medium resulted in precipitation of minerals upon addition of phosphate buffer before or after autoclaving. Sequential omission and stepwise addition of minerals revealed magnesium ions to be responsible. The problem was overcome by addition of 30 mM disodium EDTA

(BDH, U.K). Table 2.6 shows the growth of *C.thermosaccharolyticum* in the presence of different concentration of minerals. Optimum concentrations relate to the maximum growth at the lowest concentration. Thus the new revised medium MCR had a composition as follows; Yeast Extract (Oxoid) 5g/l, $(NH_4)_2SO_4$ 1.5 g/l, $MgCl_2.6H_2O$ 0.3 g/l, $CaCl_2.2H_2O$ 0.15 g/l, $FeSO_4.7H_2O$ 5 mg/l, Na_2EDTA 0.558 g/l, Na thioglycolate 0.5 g/l. Addition of the latter two components acidified the medium and a few drops of 2N NaOH was added to adjust the pH at 6.8. Buffer consisted of KH_2PO_4 1.5 g/l, and Na_2HPO_4 3.0 g/l, and was added after autoclaving. The type and quantity of carbon source was added depending on the experimental requirements.

Table 2.6 Growth of *C.thermosaccharolyticum* at different mineral concentrations.

$[(NH_4)_2SO_4]$ %(w/v)	Max Growth %	$[MgCl_2]$ %(w/v)	Max Growth %	$[FeSO_4]$ %(w/v) x10^{-4}	Max Growth %	$[Na_2EDTA]$ %(w/v)	Max Growth %
0	54	0	78	0	91	0	95*
0.1	79	0.01	86	1.0	85	0.1	98*
0.3	96	0.03	100	3.0	88	0.5	89
0.5	100	0.05	92*	5.0	100	1.0	96
0.7	84	0.07	89*	10.0	94	1.5	85
1.0	93	0.1	96*	15.0	78	2.0	100

* : At these concentrations precipitation upon addition of buffer was observed.

2.2.3 Selection Procedure for an Ethanol Tolerant Mutant of *C. thermosaccharolyticum*

Isolation of 3% (w/v) ethanol tolerant mutant of *C.thermosaccharolyticum* was achieved by growth in the presence of increasing ethanol concentrations. This technique has been successfully adapted in selecting for tolerant strains of *C.thermocellum* (Herrero and Gomez, 1980), *C.thermohydrosulfuricum* (Lovitt *et al* , 1984) and *C.thermosaccharolyticum* (Fang, 1980; Landuyt and Hsu, 1984). In the preliminary studies wild type

cells were used to inoculate bottle cultures containing ethanol concentrations ranging from 0-5% (w/v). The optical density of the cultures after 24 and 48 hours was measured and recorded. This revealed the maximum tolerance of the wild type cells without any changes in growth activity, and the ethanol concentration above which cells cease to grow. Up to the concentration of 1% (w/v) ethanol showed little effect on the cells and thereafter, a decline in the cell number and the growth rate with increasing ethanol concentration was observed. Three sequential subcultures in medium containing 1% (w/v) ethanol proved adequate for isolation of the 1% tolerant strain. Pure cultures were obtained by plating out the cells and isolating single colonies that had survived the ethanol concentration. Stock cultures were prepared by growing these colonies in liquid medium containing the required level of ethanol and storing at -20 °C in the presence of 20% (v/v) glycerol. The isolated 1% tolerant strain was used to inoculate medium containing 1.5% (w/v) ethanol. Further subculturing , stock preparation and transfers yielded cells growing at 3% ethanol concentration (Figure 2.3). The growth rate of cells at 3% (w/v) ethanol concentration was significantly lower than the wild type cells with doubling time of 2.15 hours with glucose and 3 hours with xylose. Thus the period of incubation for each subculture was increased from 24 to 48 hours.

2.2.4 Microbial Assessments

A : Morphological Observation

Changes in cell shape were observed by microscopic examination of gram stain preparations of the organism. Wild type cells of *C. thermosaccharolyticum* appeared as Gram positive rods about 3-4 μ in length. On plates they form convex white colonies of the order of 1-2 mm in diameter. The mutant or stressed cells appeared much longer in length than their wild type parents. Size distributions were determined by taking

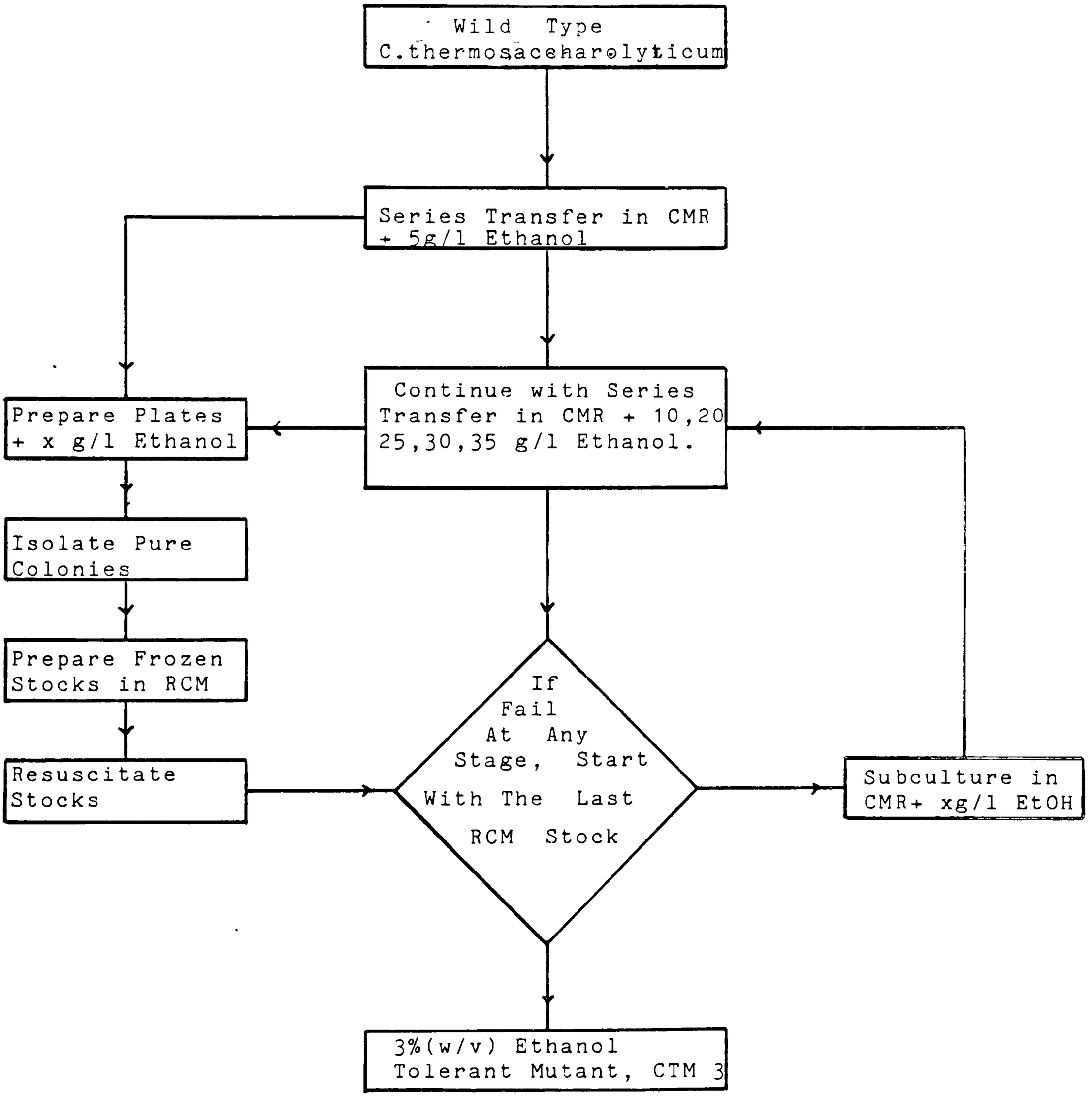

Figure 2.3 Selection Procedure For Isolation Of 3% (w/v) Ethanol Tolerant Mutant of C. thermosaccharolyticum

photographs from the slide preparations followed by image analysis on a MOP video plan analyser (Bildanalyser; Kontron, W.Germany). The only parameter analysed was the organisms' length. Figure 2.4 shows a typical size distribution for a mutant strain of *C.thermosaccharolyticum* .

B : Optical Density Determination

The cell number is thought to be in direct relationship with the turbidity of the growth culture. Thus cell growth can be directly followed by measuring the optical density of the broth at a specific wave band against a suitable blank. The broth culture was diluted by 10% formalin solution and placed in a 1 ml path cuvette. The absorbance was measured at 650 nm by spectophotometer (SP8-100, Pye Unicam, U.K).

C : Dry Weight Determination

As an alternative to optical density measurement the dry weight of the cell culture may be reported to represent the biomass yield. Figure 2.5 shows a calibration curve relating the optical density to the dry weight. Steps involved were broth filtration and drying. A rapid technique involving microwave drying was suggested by Wardell (1985) and is outlined as follows;

1- Dry filter (47 mm diameter; 0.45μ mesh; Bioseparations, U.K)for three minutes in microwave oven (Creda, U.K). Cool in a dessicator and weigh to four decimal places.

2- Disinfect and wash filter in 1% (v/v) Teepol.

3- Transfer the filter to the Buchner funnel and wash under vacuum with 2 ml distilled water followed by 2x10 ml distilled water.

4- Pipette 10 ml of the cell culture onto the filter, followed by 1 ml of 10% formalin.

5- Apply vacuum to remove the liquid, then wash with 3x10 ml distilled water.

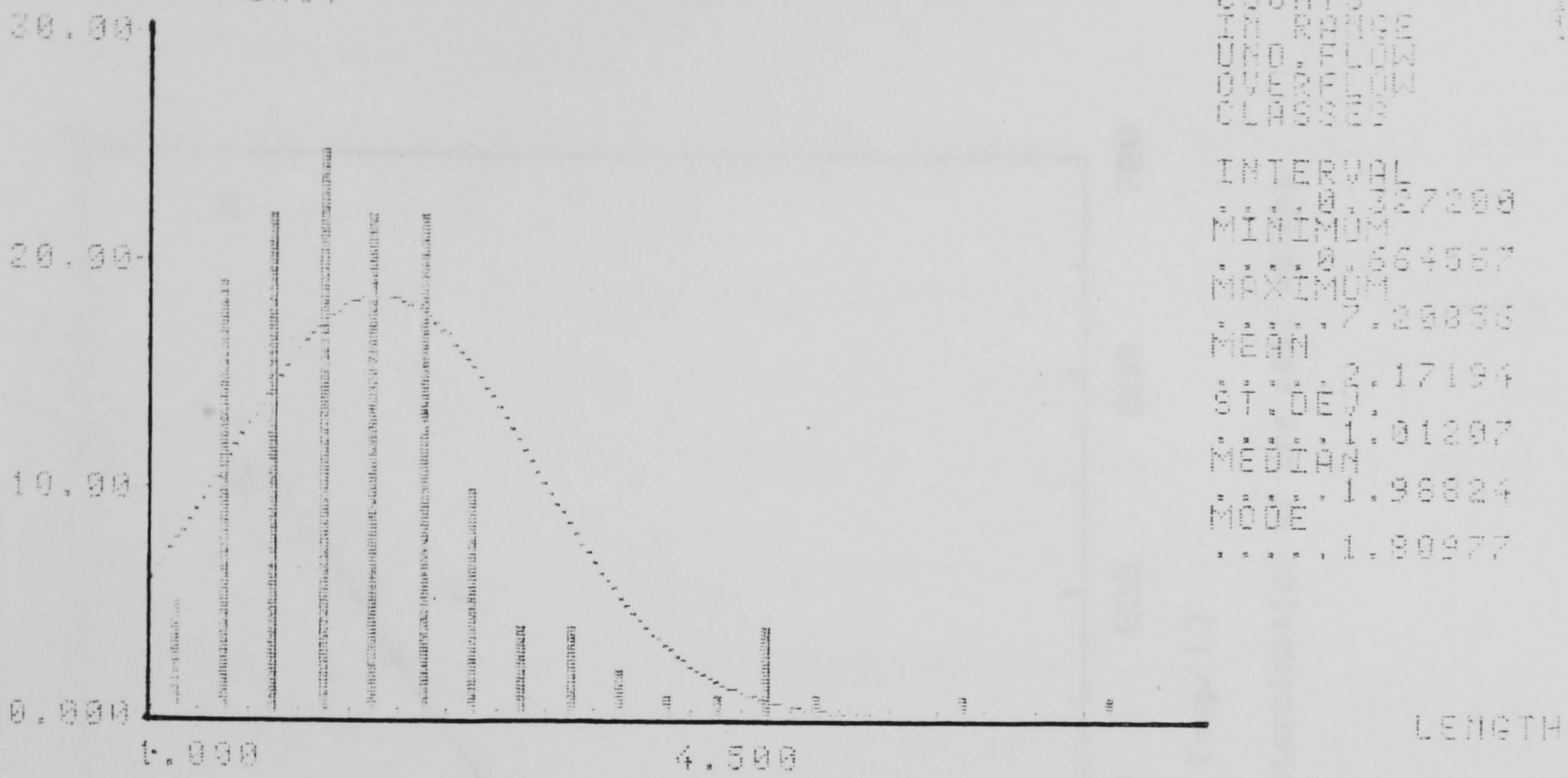

(a) Wild Type C. thermosaccharolyticum

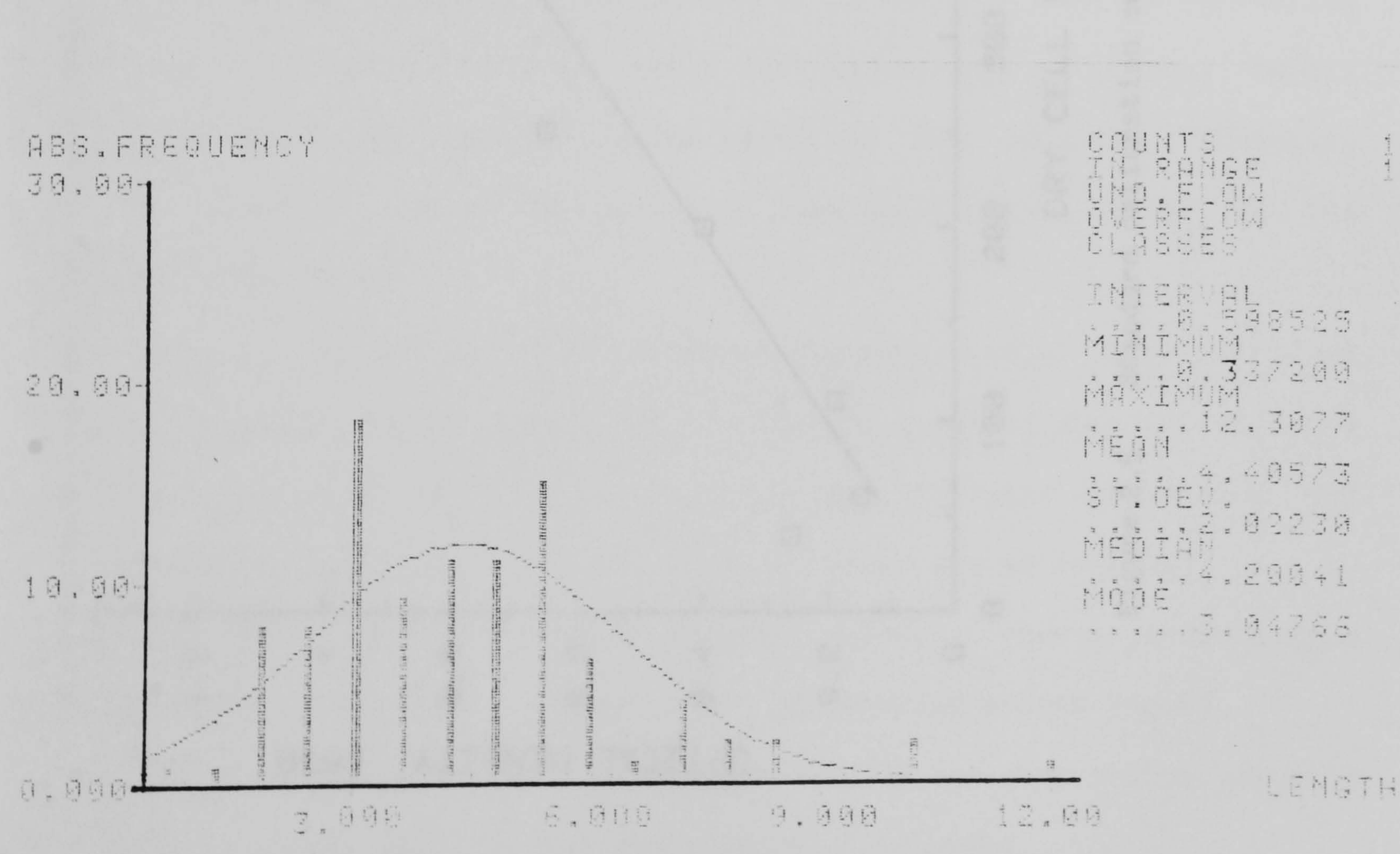

(b) C. thermosaccharolyticum in the presence of 2% (w/v) exogenous ethanol

Figure 2.4 Typical size distributions for C. thermosaccharolyticum

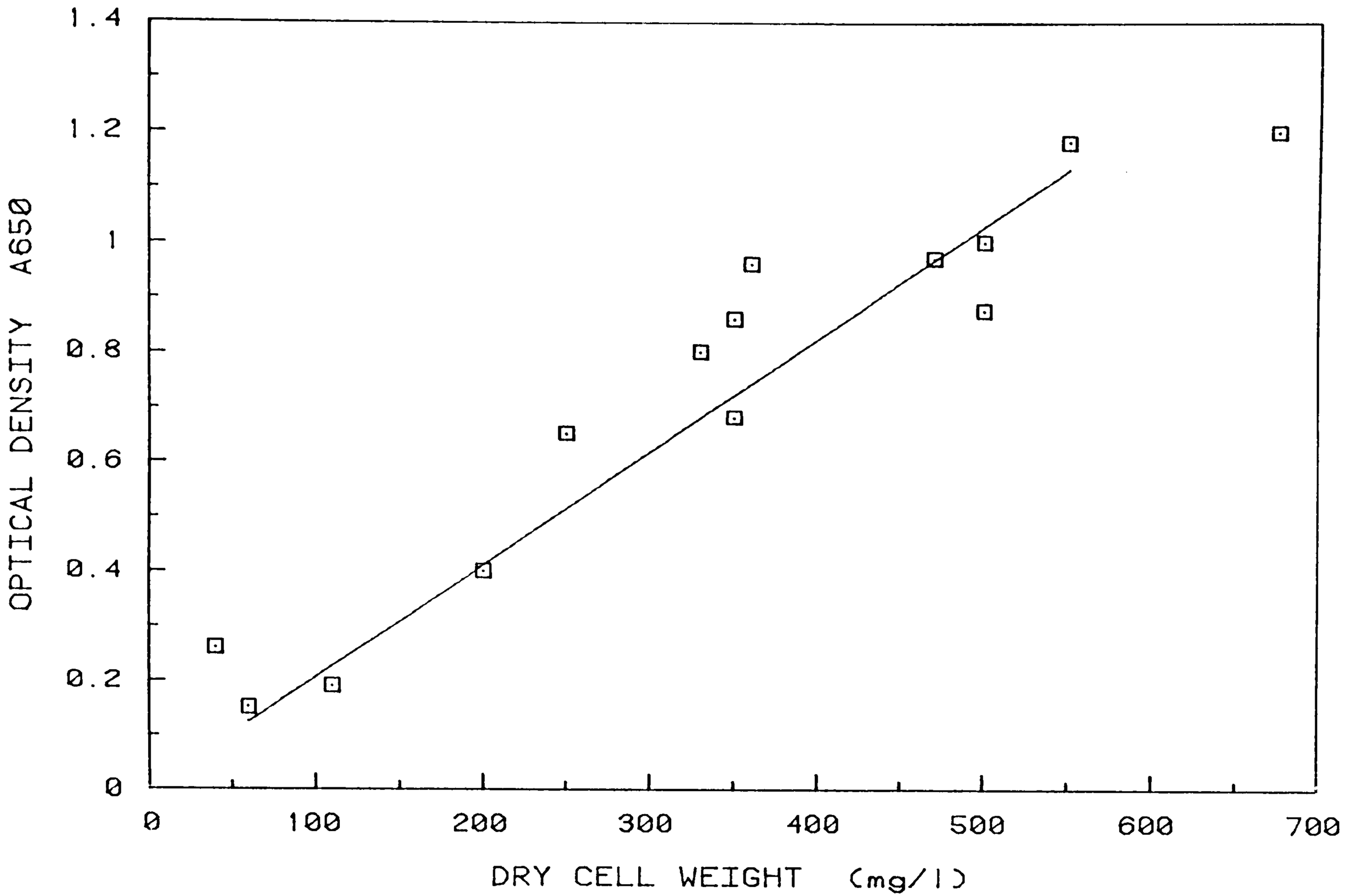

Figure 2.5 Standard calibration curve for determination of dry cell weight

6- Dry filter in microwave oven for four minutes. Cool in a dessicator and weigh to four decimal places.

Notes : a) to avoid superheating, always place a 500 ml bottle of cold water in the microwave.

b) dried filter paper is extremely fragile. Place in a glass petri dish and heat with the lid half open.

c) for dilute cell suspensions use multiples of the 10 ml sample.

2.2.5 Cell Entrapment in Biomass Support Particles (BSPs)

For all porous BSPs investigated, cell entrapment occured by natural colonisation of cells inside the particle. In bottle cultures this was achieved by incubation of inoculated broth in presence of BSPs, and for larger volumes by recycling contaminated broth through a column containing the BSPs. In batch cultures, after the initial lag , gradual bubble formation by active cells within the particles was observed. Excessive bubble formation caused the polyester foam particles to float to the surface of the broth.

The effect of agitation and attrition on disengagement of the entrapped cells from their support matrix was examined by a method whereby cells are physically "shaken off" the particle. Steps involving expression and mechanical agitation for polyester foam particles are as follows;

1- Under aseptic conditions in an anaerobic cabinet, remove particle from contaminated broth with a pair of tongs and express excess liquid.

2- Transfer expressed particle to 20 ml fresh MCR (or RCM) medium and hold bottle on a Whirly mixer at maximum speed for 2 minutes.

3- Repeat the above step for the required number of treatments.

Notes : a) For all other support particles remove excess liquid by drip drying.

b) Use 20 ml Universal bottles for particle transfers.

2.2.6 Carbon Balance

A : Glucose Assay

Concentration of glucose in liquid medium was rapidly determined by the use of a commercial assay kit (Sigma, U.K). The enzymatic assay system was based on oxidation of residual glucose in the presence of glucose oxidase coupled with a colour reaction as follows;

$$\text{Glucose} + 2H_2O + O_2 \xrightarrow{\textit{Glucose oxidase}} \text{Gluconic acid} + 2H_2O_2$$

$$H_2O_2 + \underset{\text{(COLOURLESS)}}{\text{O-Dianisidine}} \xrightarrow{\textit{Peroxidase}} \underset{\text{(BROWN)}}{\text{Oxidised O-Dianisidine}}$$

Batches of 100 ml of enzyme/colour reagent were prepared in accordance with Sigma directions of use and stored at 2-6 °C for up to one month. The assay was carried out by incubating 105 μl of not more than 30 nmol glucose concentration with 1 ml of enzyme reagent at 37 °C for thirty minutes. The absorbance of the colour developed was read at 450 nm. Figure 2.6 shows the calibration curve for the glucose standards.

B : Xylose Assay

The method for determination of xylose concentration is adopted from Ashwell (1957). This method relies on the hydrolysis of the reducing sugar upon the action of concentrated acid and heat. This is followed by a colour reaction involving ferric chloride and orcinol.

The colour reagent was prepared fresh for every assay as follows : Weigh out 0.01 g orcinol and 0.03 g $FeCl_3$ and add 3.5 ml distilled water. In a fume cupboard, gently add 20 ml 10N HCl and mix. Samples were diluted to contain no more than 125 nmol of xylose. 125 μl of each dilution was incubated with 1 ml of the colour reagent for twenty minutes in a boiling water bath. After cooling to room temperature a further 2.5 ml distilled water was added to every test sample. The absorbance of the green colour

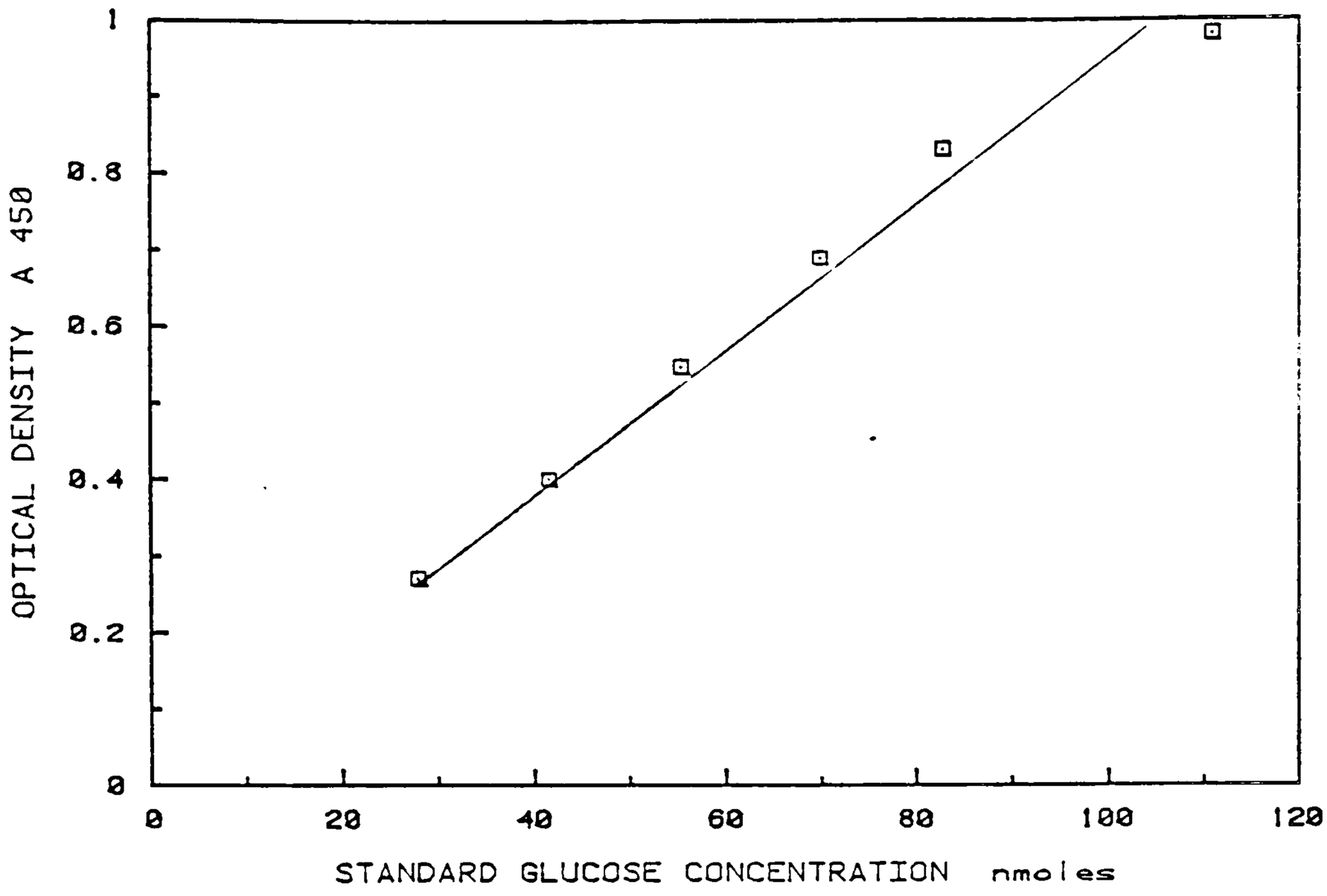

Figure 2.6 Standard calibration for determination of glucose solutions.

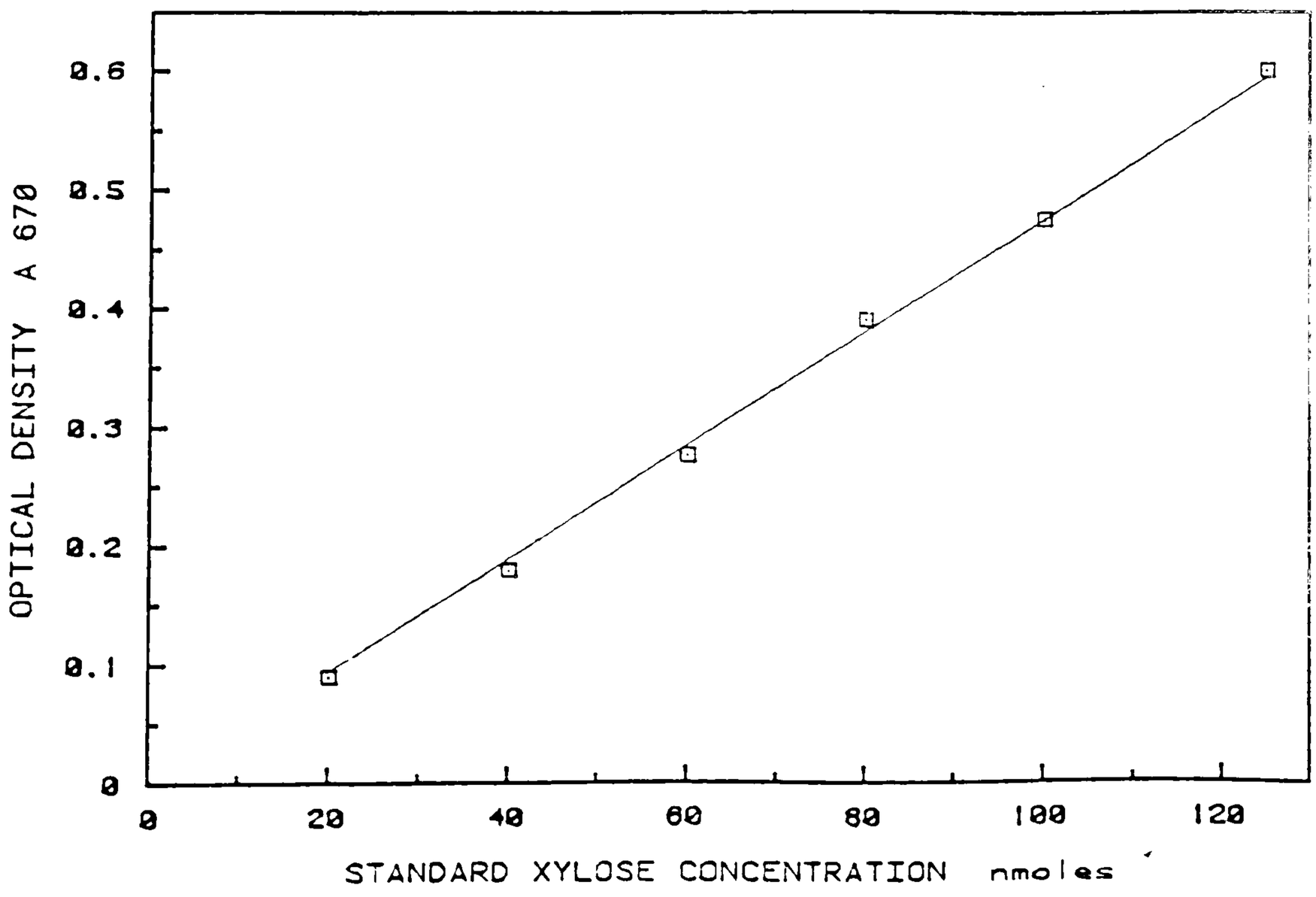

Figure 2.7 Standard calibration for determination of xylose concentration.

developed was read at 670 nm. Figure 2.7 shows the calibration curve for xylose standards.

C : Lactic Acid Assay

Concentration of lactic acid was determined by chemical (Baker, 1957) and enzymatic techniques (Sigma, U.K). Enzymatically the presence of D-Lactic acid was measured by the yield of the following reversible reaction to the left;

$$\underset{\text{(HIGH A340)}}{\text{Pyruvic acid + NADH}} \xrightleftharpoons{LDH} \underset{\text{(LOW A340)}}{\text{Lactic acid + NAD}}$$

In the presence of excess NAD the reaction is carried from right to left. To force the reaction to completion in this direction, pyruvic acid is trapped with hydrazine. The increased absorbance at 340 nm due to NADH formation becomes a measure of lactic acid present.

The assay was accomplished by applying a commercial assay kit (Sigma, U.K). Samples were diluted ten fold before incubating with the enzyme-hydrazine mixture at 37 °C for thirty minutes. Figure 2.8 shows the calibration curve for the lactic acid standards.

The chemical method described by Barker and Simmerson (1941) assayed for both L- and D- lactic acid. In principle it invovles quantitative conversion of lactic acid to acetaldehyde on being heated with concentrated sulphuric acid. The acetaldehyde is determined by measurement of the purple colour formed with p-hydroxydiphenol at 670 nm. The method was carried out according to the procedure outlined by Barker and Simmerson (1941). The calibration curve for a lactic acid mixture containing equal amounts of both isomers is shown in Fig. 2.9.

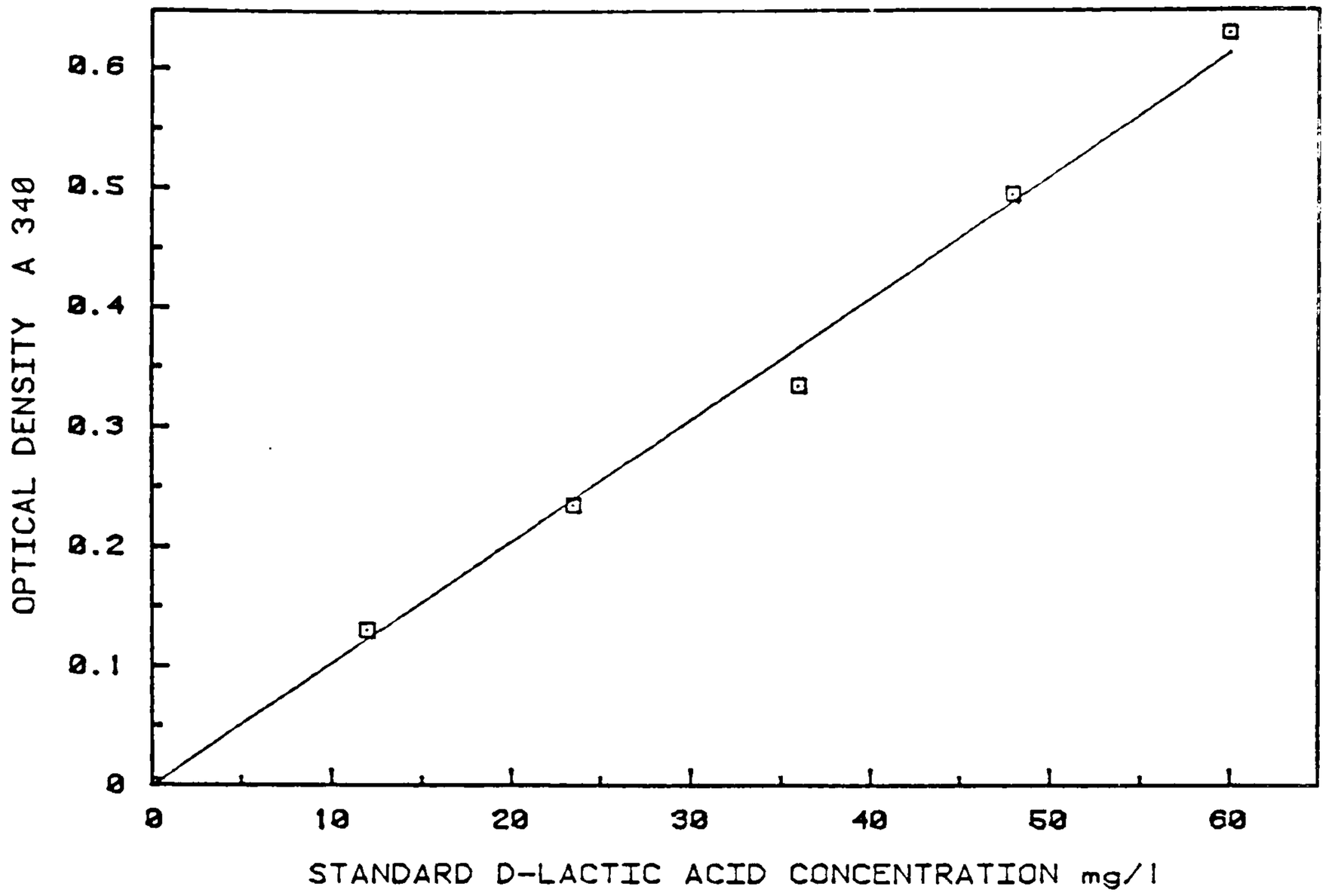

Figure 2.8 Standard calibration for determination of D- Lactic acid (Enzymatic method).

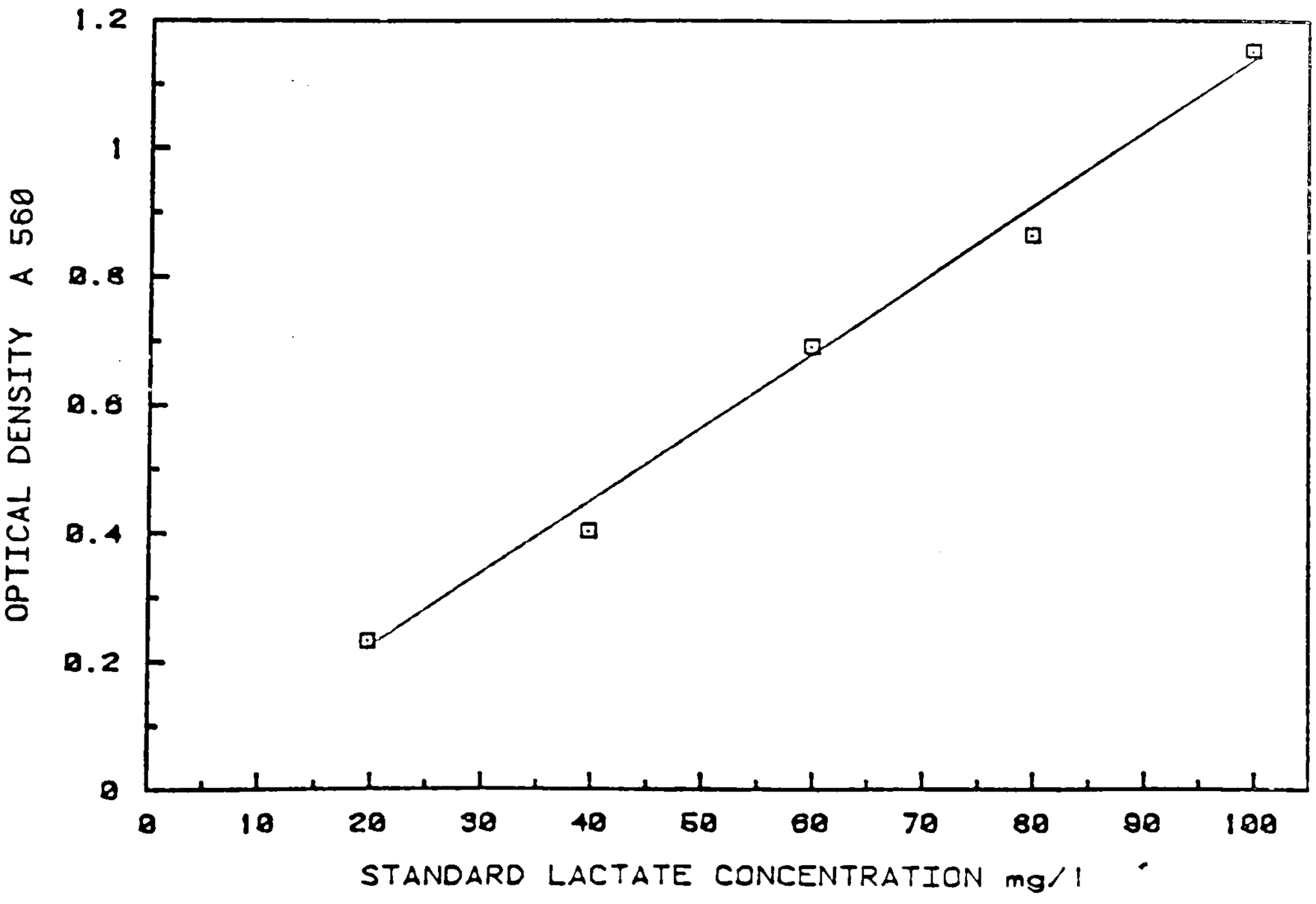

Figure 2.9 Standard calibration for determination of L- and D- Lactic acid concentration (Chemical method).

D : Chromatographic Assay for Ethanol, n-Butanol, Acetic and Butyric Acids

Volatile organic end-products are normally assayed by chromatoghraphic means (Supelchem Reporter, 1985). All main liquid end-products viz. ethanol, n-butanol, acetic acid, and butyric acid but not lactic acid, were adequately separated on a Graphpac GC support medium (Alltech, U.K) for quantitative assessment. GC analysis of lactic acid required a esterification step and in this respect the chemical and enzymatic analysis were preferred. Gas chromatograph (Packard 428, U.S.A) was operated through an integrater with multicalibration abilities (Spectra Physics SP 4270, U.S.A). The operational specifications are given as follows;

	Packard 428			**Column**
Temperatures	Oven	120 °C	*Support*	Graphpac GC
	Detector	160 °C		
	Injection	160 °C	*Mesh Range*	60/80 μ
Flowrates	Nitrogen	30 ml/min	*Liquid Phase*	C-20 M + H_3PO_4
	Hydrogen	25 ml/min		
	Oxygen	250 ml/min		

Prior to use the GC and the column were allowed 12 hours to stabilise at the oven temperature with N_2 flowing through.

A rapid phase separation was achieved as 1 μl of the centrifuged broth was injected inside the column. The flame ionisation detector (FID) responded linearly to the varying concentration of organic components of the medium. The attenuation was automatically programmed so that all peaks could be easily observed on the trace output.

The method of external standards was employed for calibration. Standard solutions of alcohol and acid mixtures were injected in the column and the voltage signal was transulated into concentration units by the integrater. The standard calibration curve was stored on a data file for future use. The standard solutions contained; 0-0.5% (w/v) ethanol, 0-0.5% (w/v)

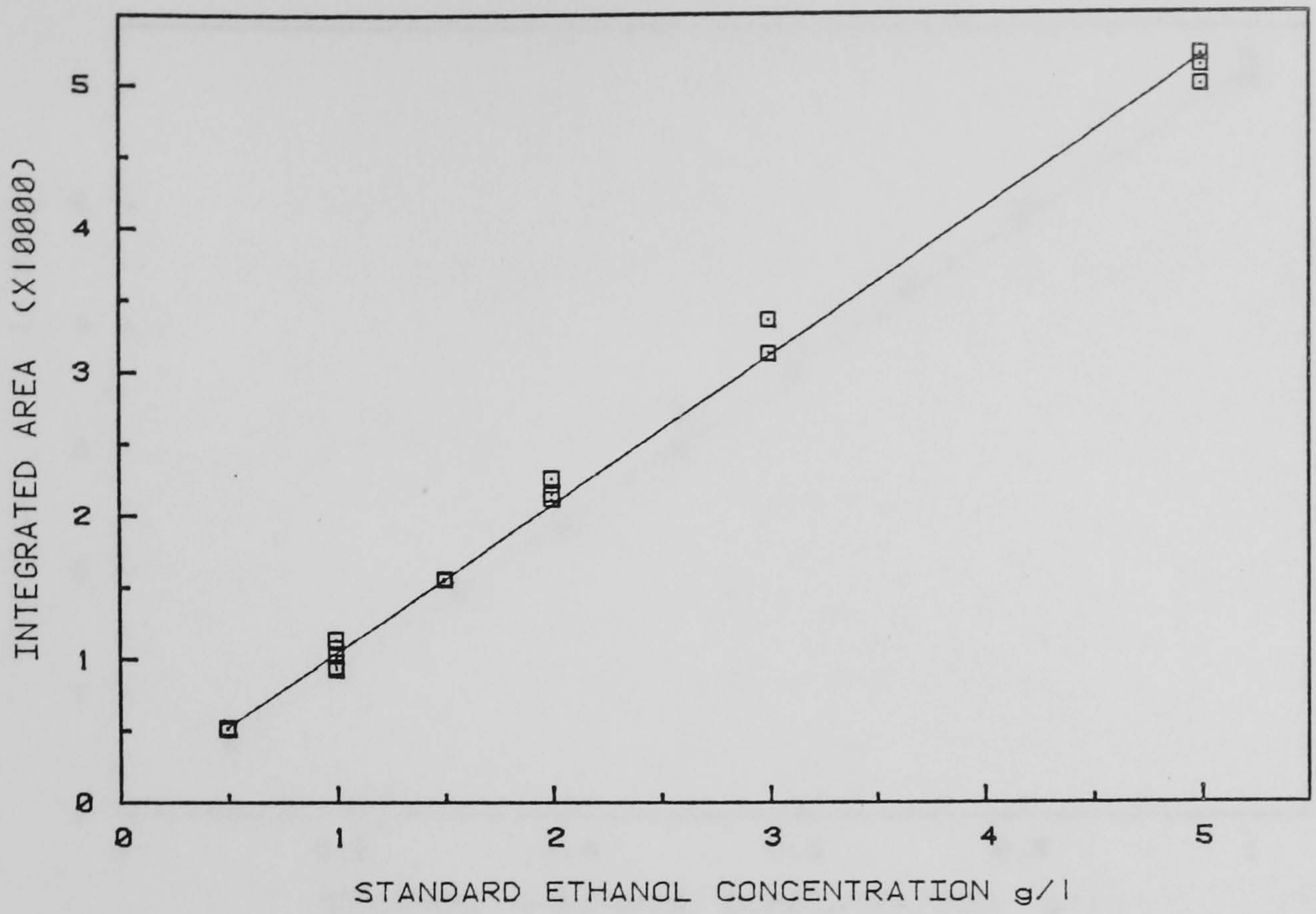

Figure 2.10 Standard calibration for determination of ethanol concentration.

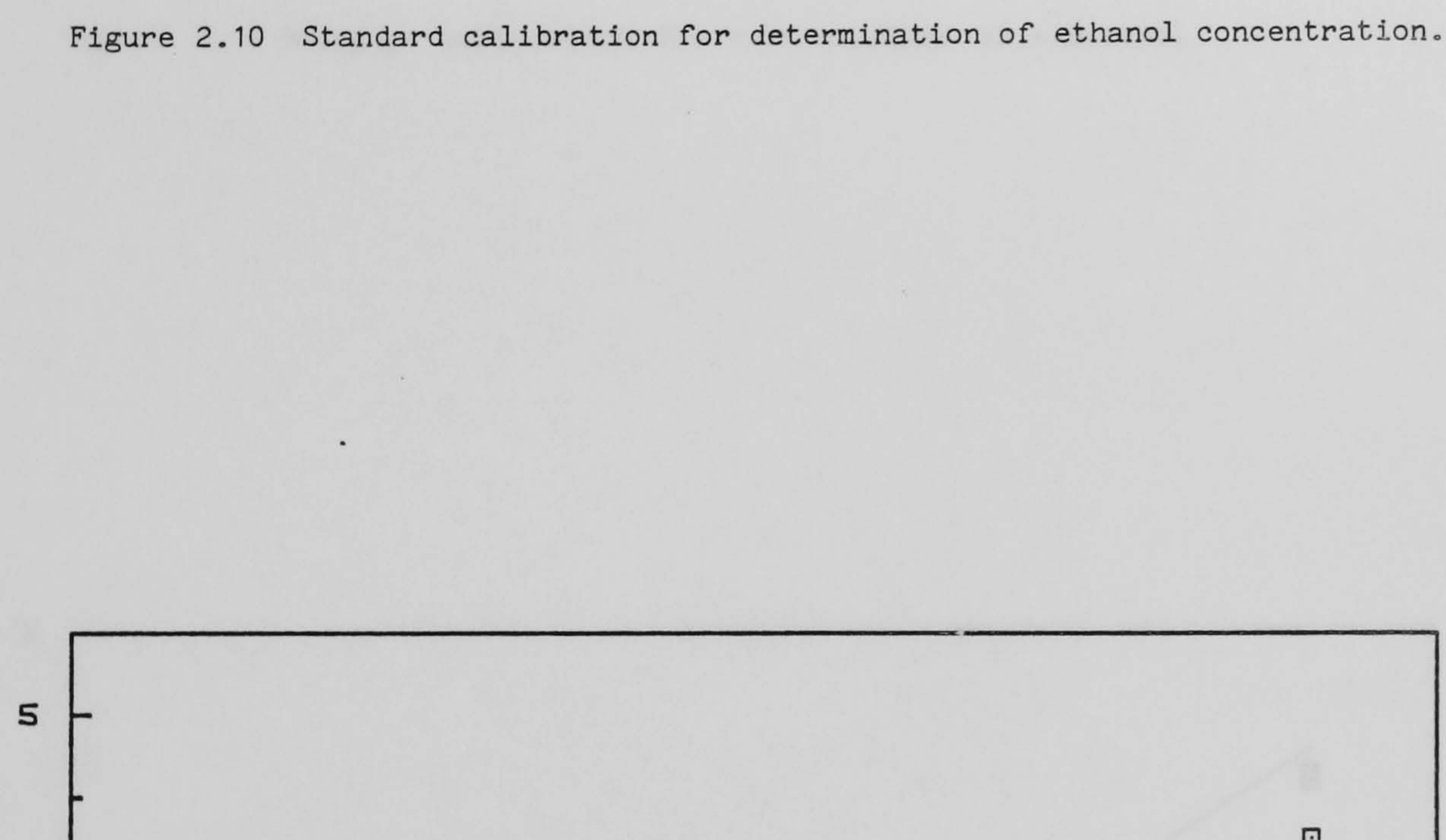

Figure 2.11 Standard calibration for determination of Acetic acid.

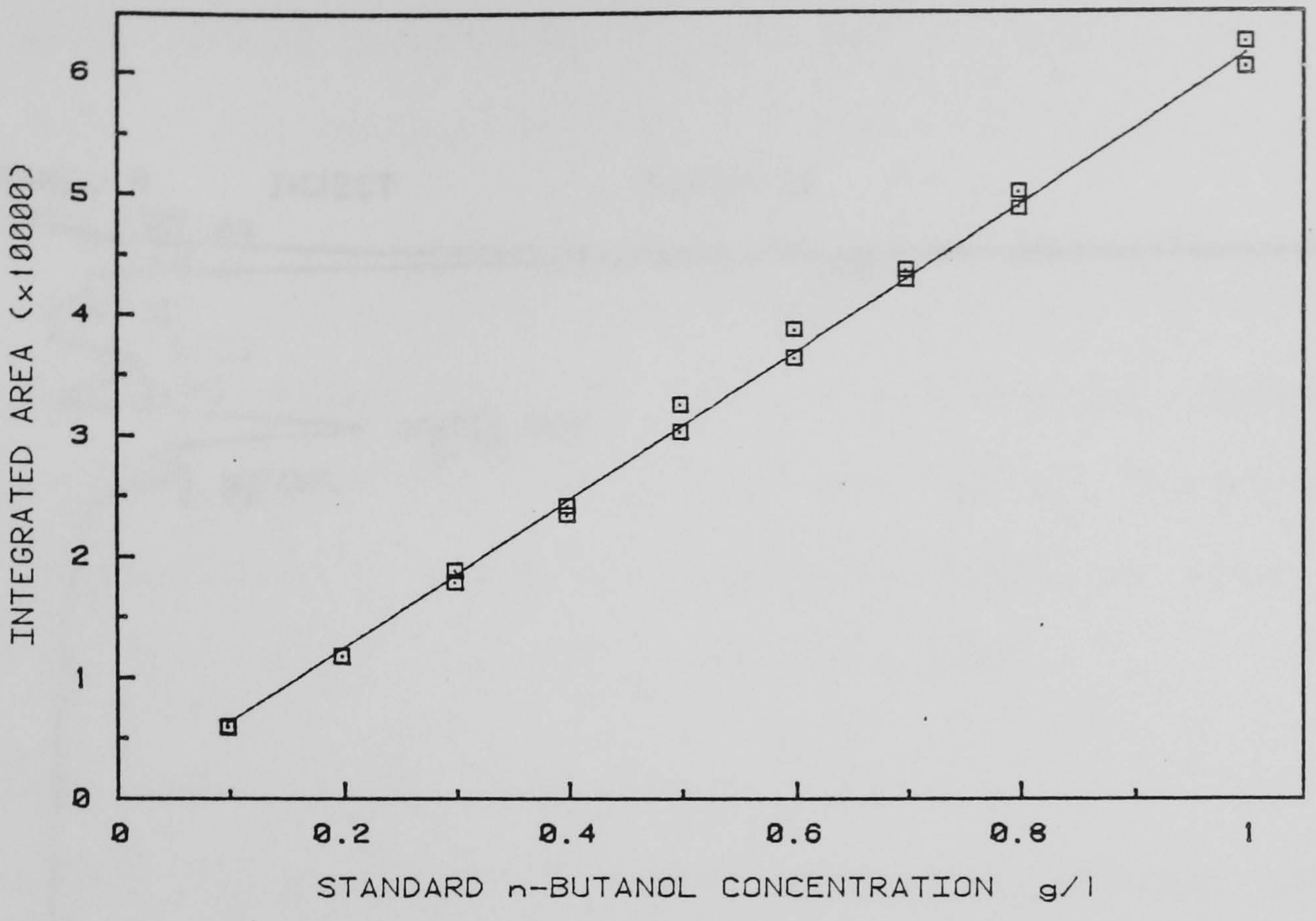

Figure 2.12 Standard calibration for determination of n-Butanol.

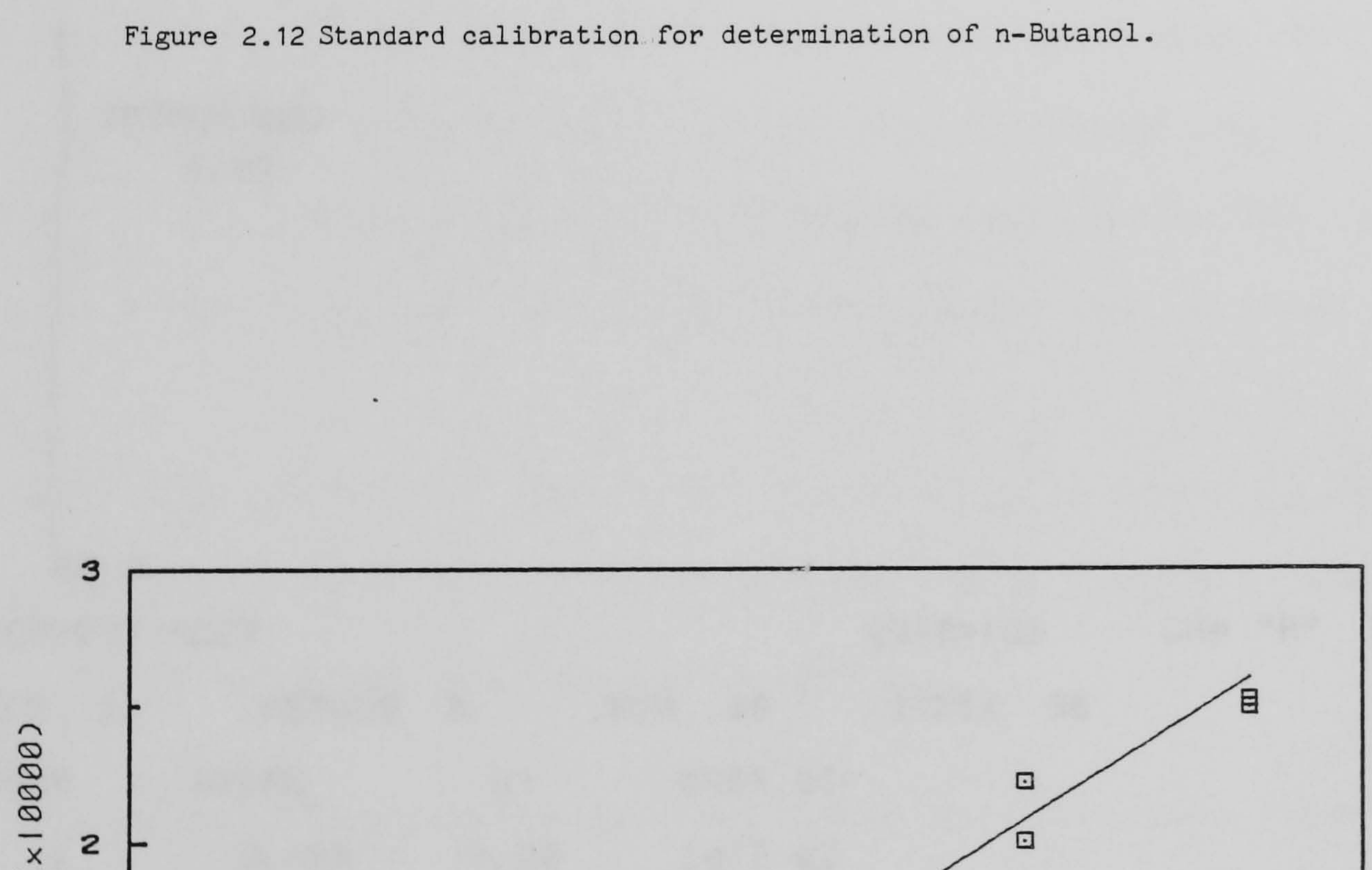

Figure 2.13 Standard calibration for determination of Butyric acid.

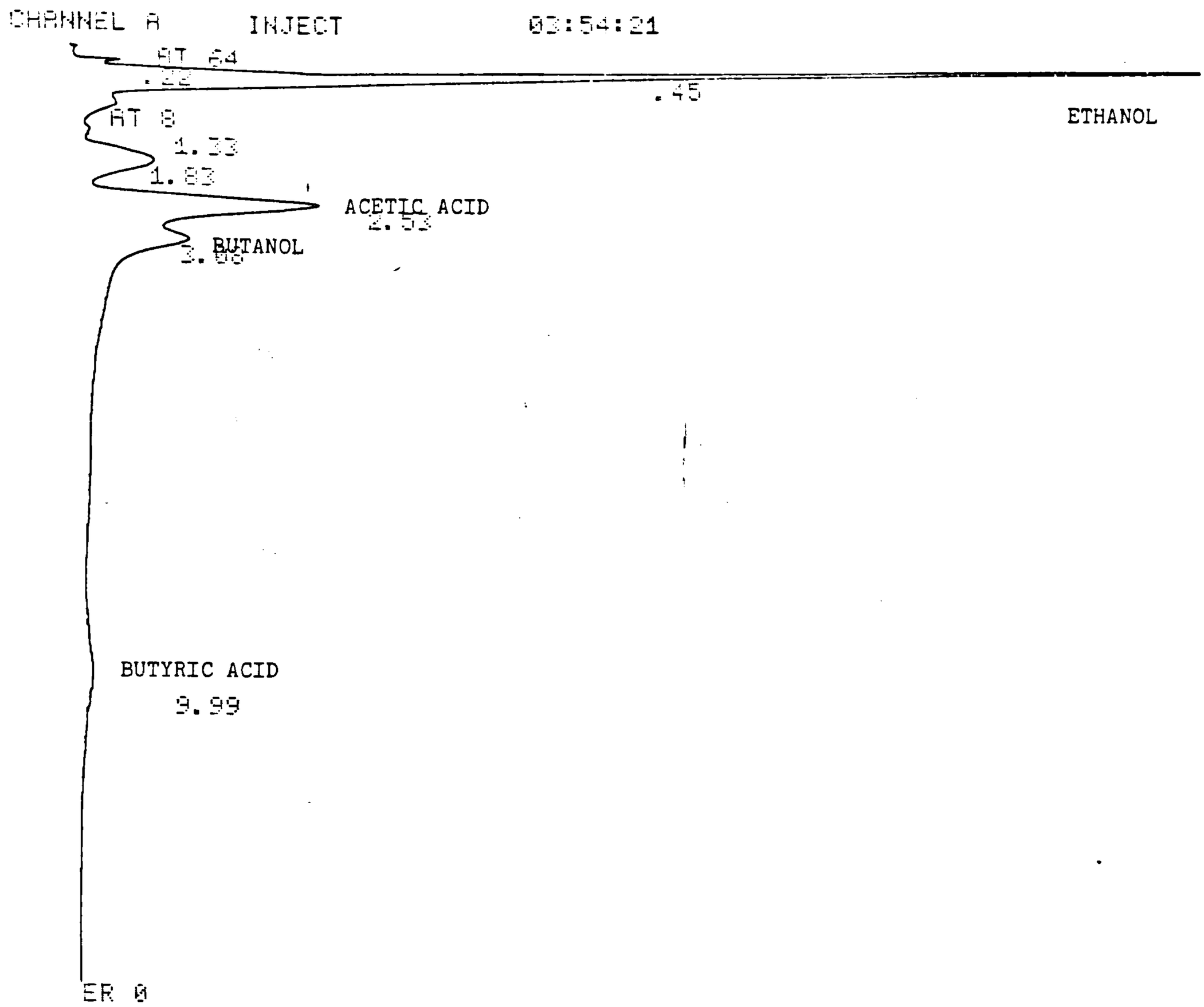

ETOH/BUT/ACET 03:54:21 CH= "A" PS= 1.

FILE 1. METHOD 0. RUN 86 INDEX 86

PEAK#	AREA%	RT	AREA BC
1	0.699	0.22	1073 02
2	47.684	0.45	73187 02
3	2.572	0.92	3947 02
4	0.486	1.33	746 02
5	7.847	1.83	12044 02
6	21.71	2.53	33321 02
7	15.796	3.08	24244 03
8	3.206	9.99	4921 01
TOTAL	100.		153483

Figure 2.14 An example of the recorder output for the chromatogrphic analysis of the end-products of fermentation

acetic acid, 0-0.1% (w/v)n-butanol, 0-0.1% (w/v) butyric acid. Figures 2.10, 2.11, 2.12, and 2.13 show the standard calibration curves obtained by this method.

Three 1 μl injections per test sample produced a weighted average at all concentrations. Normally only trace quantities of butyric acid and butanol were observed and frequently such amounts were ignored. Figure 2.14 is a trace output from the integrator showing the retention times and the percentage area for all respective compounds present.

F : Carbon Dioxide Assay

Quantitative determination of carbon dioxide in the effluent gas stream was achieved by barium carbonate precipitation technique described by Vogel (1979). The effluent gas stream was dispersed in a gas trap containing 1 litre Byreta solution (10% barium hydroxide). The percentage conversion was determined by weighing the amount of barium carbonate formed.

The statistical analysis of the calibration curves is shown on Table 2.7. All calibrations were carried out in the linear regions and a good regression in analysing the data was observed.

Table 2.7 Regression results for the standard calibration curves for the carbon balance.

Assay system	Gradient	Std error	Regression coefficient	Std error of regression
Glucose	0.0094	2.85E-4	0.9954	0.0185
Xylose	0.0051	1.61E-4	0.9960	0.0135
Lactic acid (Chemical)	0.0012	5.25E-4	0.9938	0.0332
D-Lactic acid (Enzymatic)	0.0104	4.98E-4	0.9932	0.0189
Ethanol	1.0297	0.01475	0.9971	0.0897
Acetic acid	0.8076	0.01783	0.9932	0.1210
n-Butanol	6.3324	0.11598	0.9953	0.1205
Butyric acid	2.4375	0.08475	0.9904	0.0758
Dry cell weight	0.0021	8.56E-5	0.9780	0.1237

2.3 Results and Observations

2.3.1 Basic Growth Studies

Wild type *C. thermosaccharolyticum* was successfully grown on RCM at 60°C and starting pH of 6.8. The optical density and pH at the final stages of growth were in the order of A_{650}=0.8-1.0 and 4.8-5.1 respectively, when the medium contained 0.5% (w/v) carbon source. Unless otherwise stated all growth measurements and observations were made after 24 hours' incubation at 60°C.

A : Growth with Different Carbon Sources

The organism's ability to grow on different carbon sources was demonstrated by growth on synthetic RCM where glucose was replaced by xylose. Figure 2.15 shows the batch growth of wild type cells in 100 ml medical flat bottles. The maximum growth refers to the highest optical density observed during the course of growth. The doubling time of cells growing on glucose is approximately 60 minutes and the maximum growth rate, μ_{oG}= 0.69 h^{-1}. The corresponding values for growth on xylose are 90 minutes and μ_{oX}= 0.46 h^{-1}. In this experiment the lag observed with growth on xylose is due to inoculation with cells grown on glucose.

The effect of sugar concentration on growth is illustrated in Figure 2.16. A significant reduction in cell number, about 75% with xylose and 50% with glucose, is observed at sugar concentrations greater than 2% (w/v). The difference is less marked at higher sugar concentrations and over the investigated range, 0-10% (w/v), the number of the surviving cells remains at a constant level. Batch growth at 0% (w/v) sugar concentration was thought to be supported by undefined carbon constituents of yeast extract, lab lemco or bacterial peptone used in making up of the synthetic RCM. Although cells appear to respond better to the excess presence of glucose than xylose, at lower sugar concentrations the same growth profile is

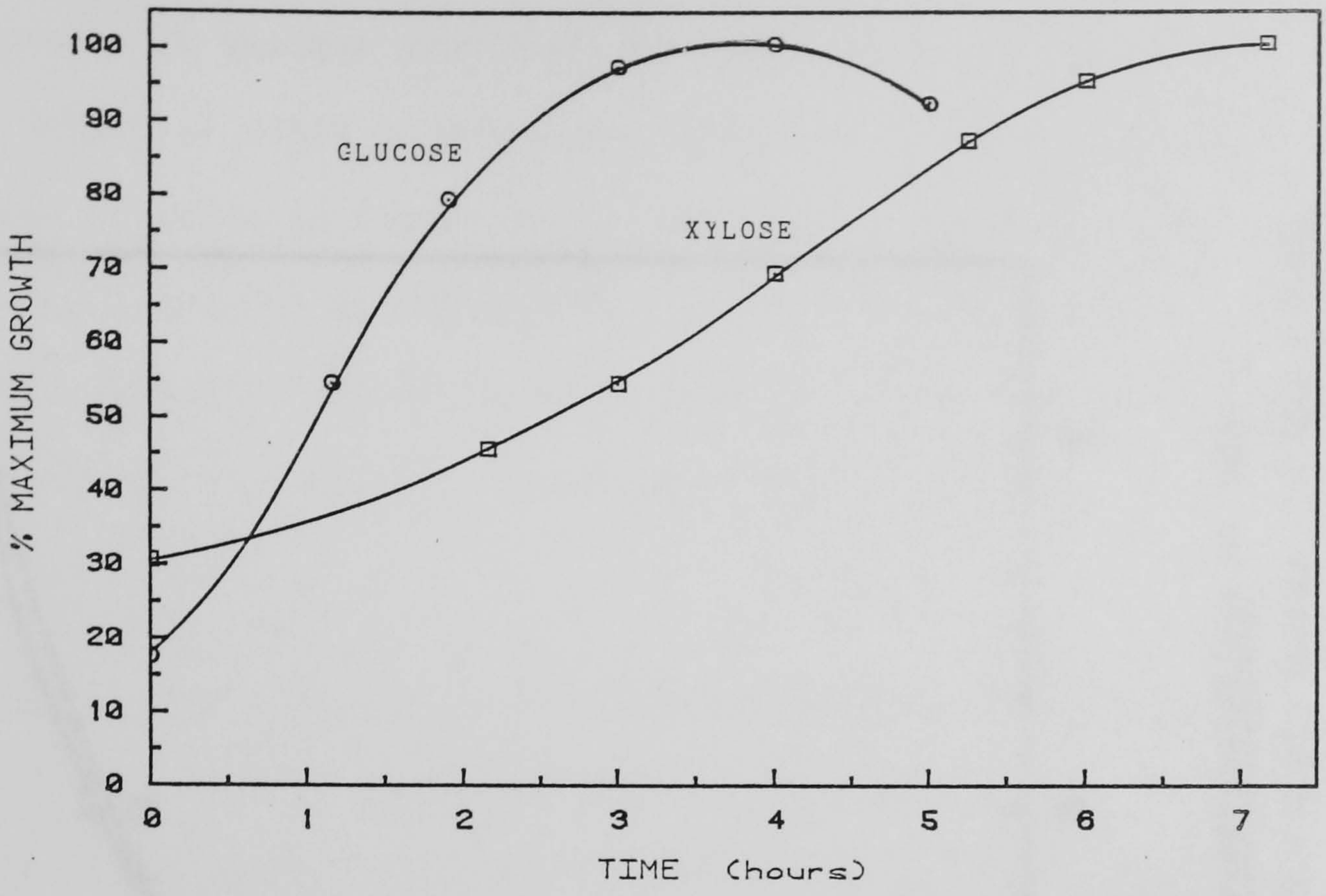

Figure 2.15 Batch growth of wild type C.thermosaccharolyticum on synthetic RCM containing 0.5% carbon source.

Maximum optical density observed; Glucose : A 650 = 0.88 ; Xylose : A650 = 0.73

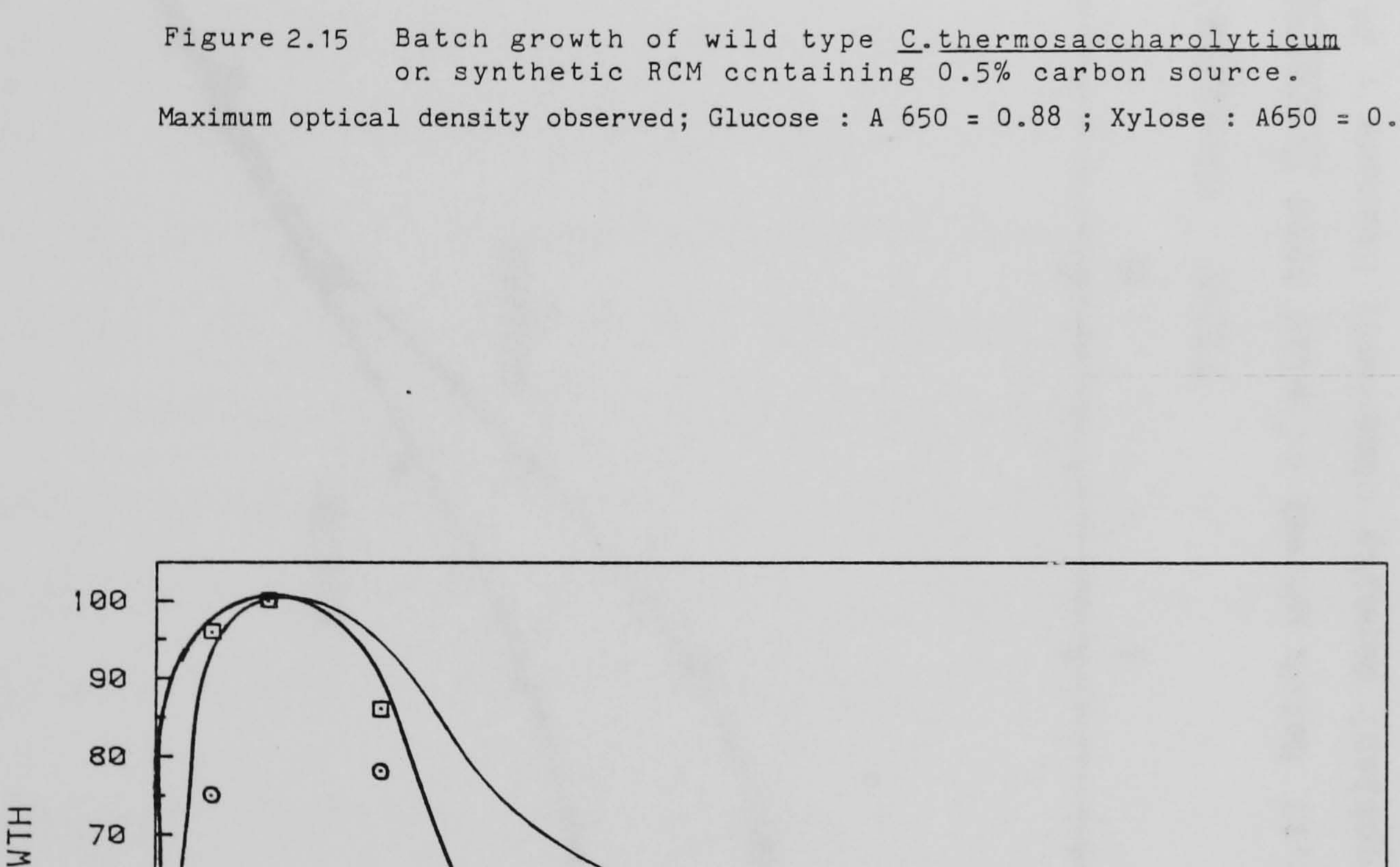

Figure 2.16 Batch Growth of wild type C. thermosaccharolyticum at different sugar concentrations in synthetic RCM.

Maximum optical density observed; Glucose : A 650 = 0.76; Xylose : A 650 = 0.68

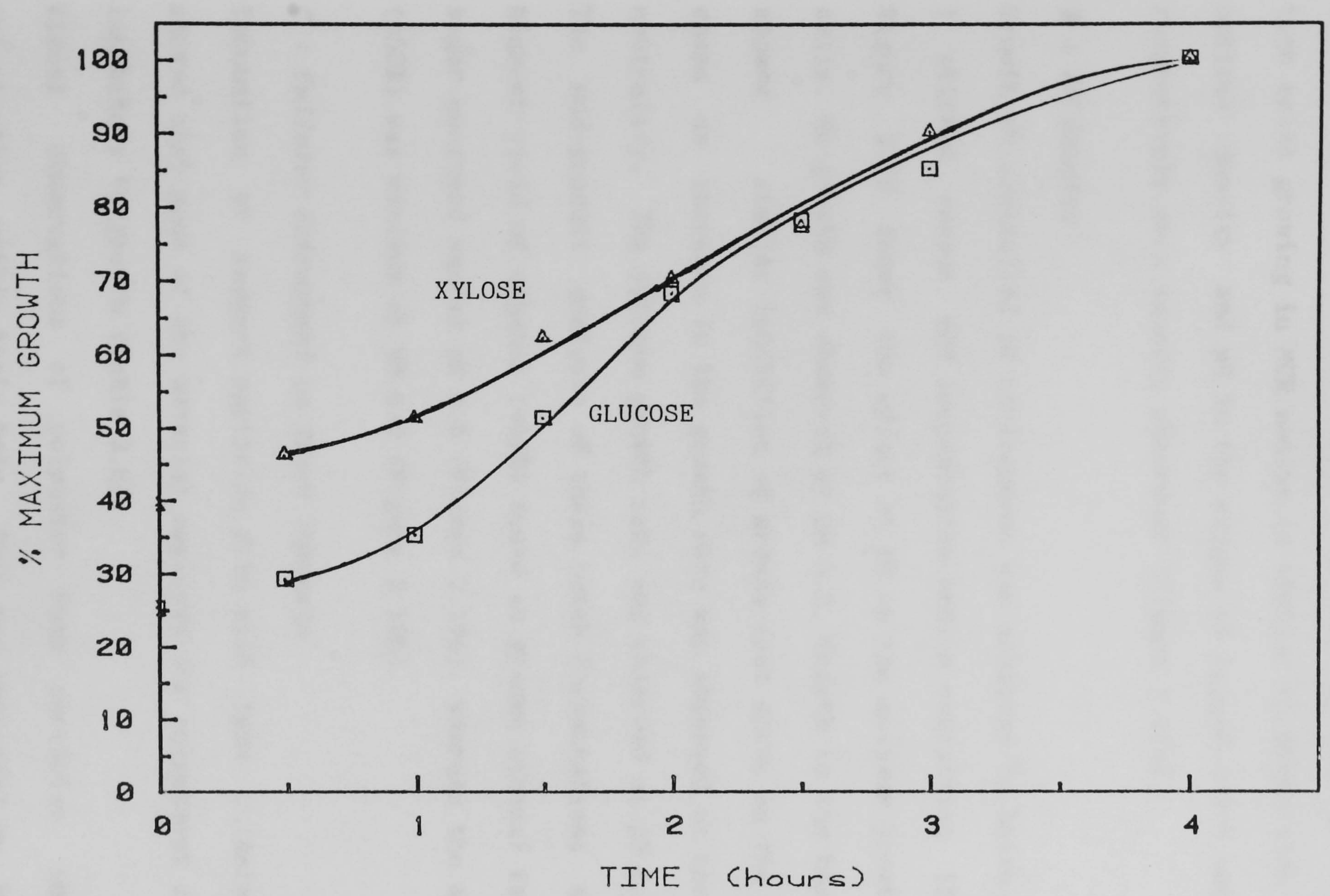

Figure 2.17 Batch growth of wild type C.thermosaccharolyticum on MCR.
Maximum optical density observed; Glucose : A650 = 0.67; Xylose : A 650 = 0.64

observed with maximum growth at 1% (w/v) sugar concentration.

The growth of cells on MCR media contaning 1% (w/v) glucose and 1% (w/v) xylose is shown in Figure 2.17. The mean generation times for the wild type cells growing in MCR medium is similar to those with RCM. Both final optical density and pH in the ranges of A_{650}=0.6-0.8 and pH = 4.9-5.2 respectively were usually obsereved (Figure 2.17b).

B : PH Studies

Growth at controlled pH environment was achieved by batch growth in a 0.8 l stirred vessel and fermentation medium containing 1% (w/v) xylose. Figure 2.18 shows the effect of pH on the maximum growth rate of the cells. No growth was observed at pH 4.5. Growth in the basic range at pH 8 showed similar inhibition of growth (not shown on the graph). In all cases an increase in the growth rate was observed as the pH approached neutrality. The optimum growth rate was observed at pH 6.8 with μ°_{X}=0.46.

The end-product analysis of these batch fermentations showed that the highest yield of ethanol (≈55%) based on gramme ethanol formed per gramme sugar consumed was at pH 6.8 (Figure 2.19a), whereas the acetic acid yield (≈50%) was maximum at pH 6.0 (Figure 2.19b).

C : Cellular Entrapment on Inert Supports

Incubation of support particles with wild type *C.thermosaccharolyticum* showed that none of the material employed for entrapment of the cells were inhibitory to growth (Table 2.8).

Visual observations of polyester foam particles showed bacterial colonisation within their body. This was indicated by bubble formation within the support particle prior to suspended growth. This phenomenon resulted in a net reduction in the overall density of the support particles and in the case of polyester foams, they rose to the surface of the medium.

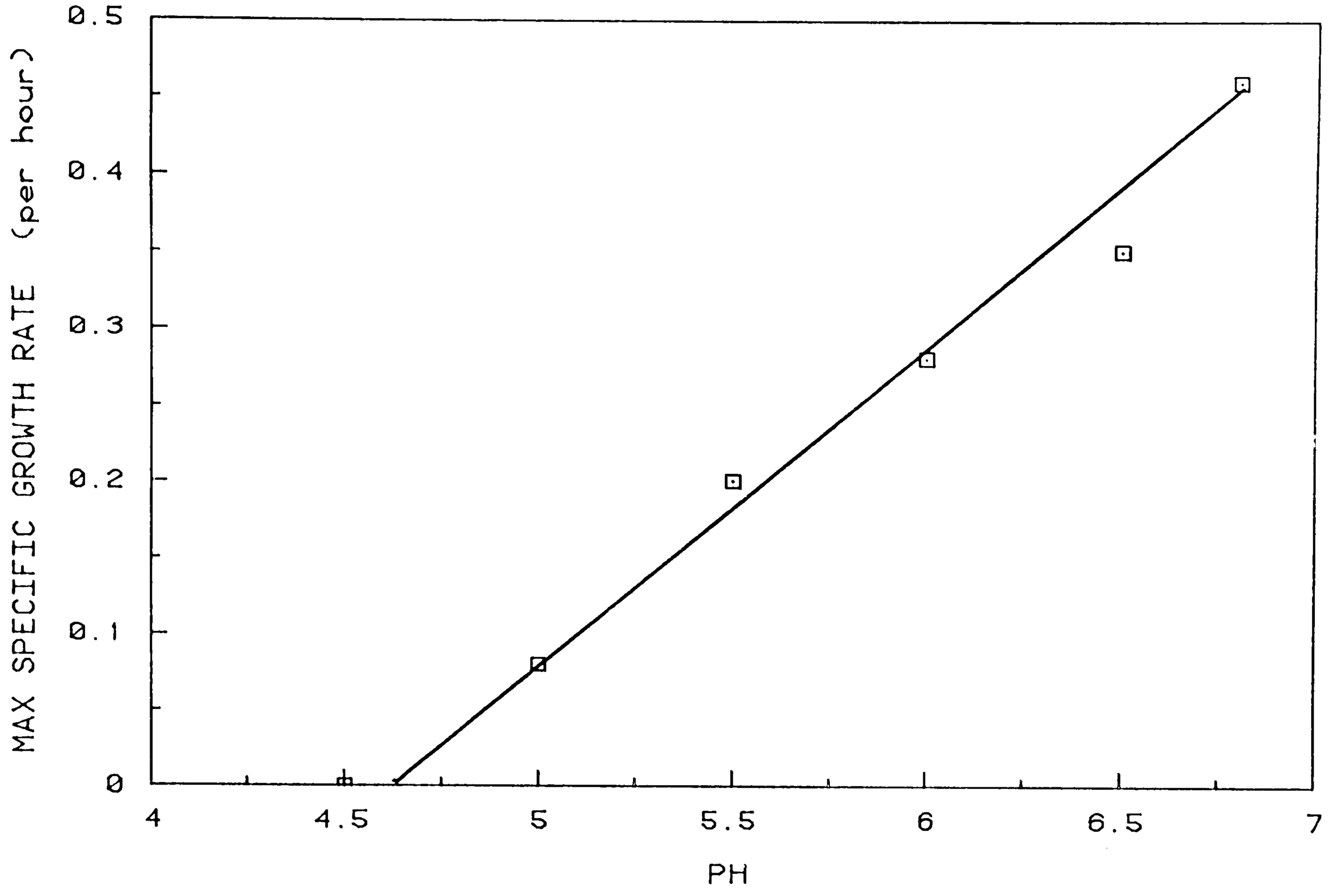

Figure 2.18 Batch growth of wild type C. thermosaccharolyticum at different pH.

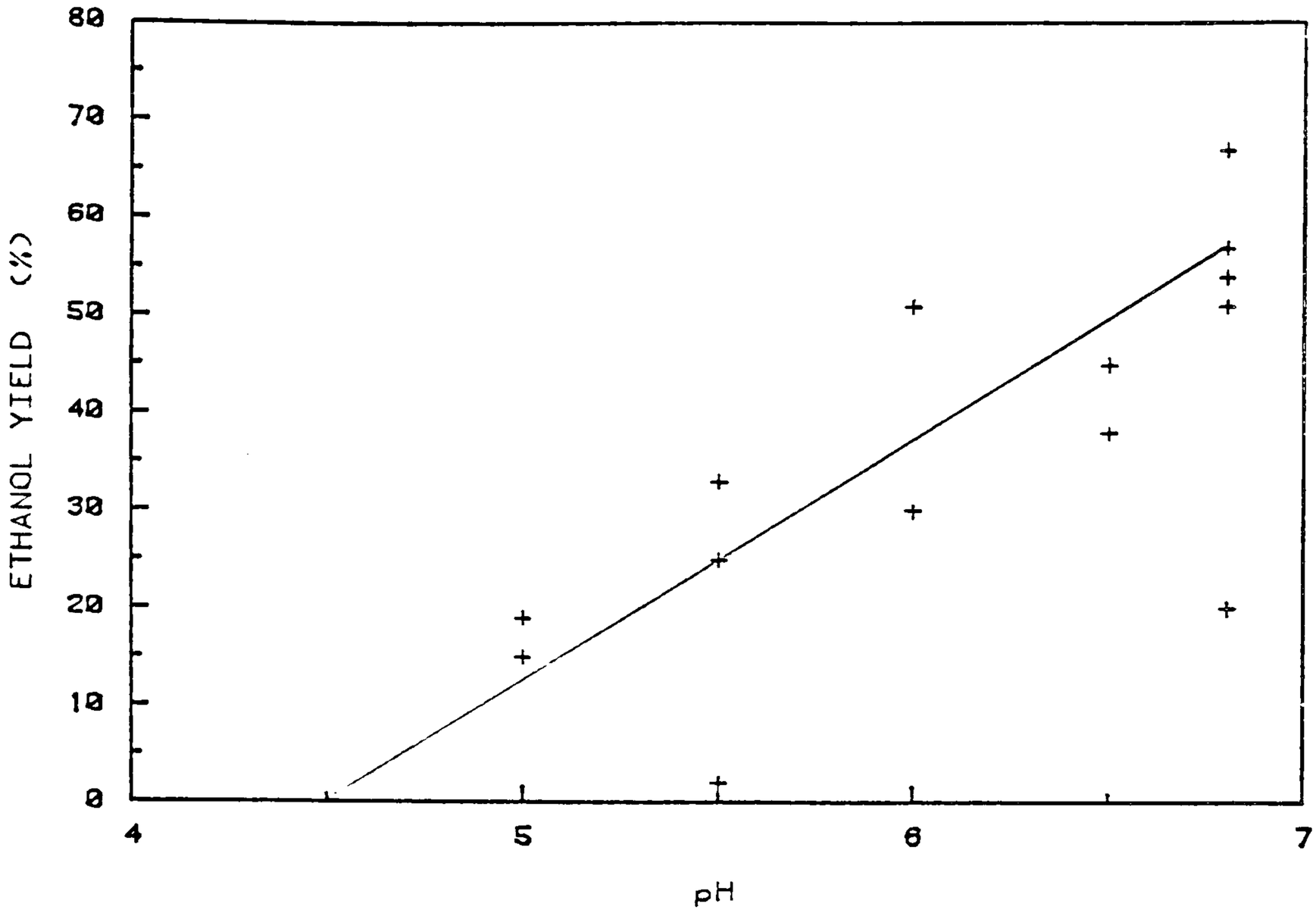

Figure 2.19 Batch growth of wild type C.thermosaccharolyticum at different pH - (a) variations of ethanol yield.

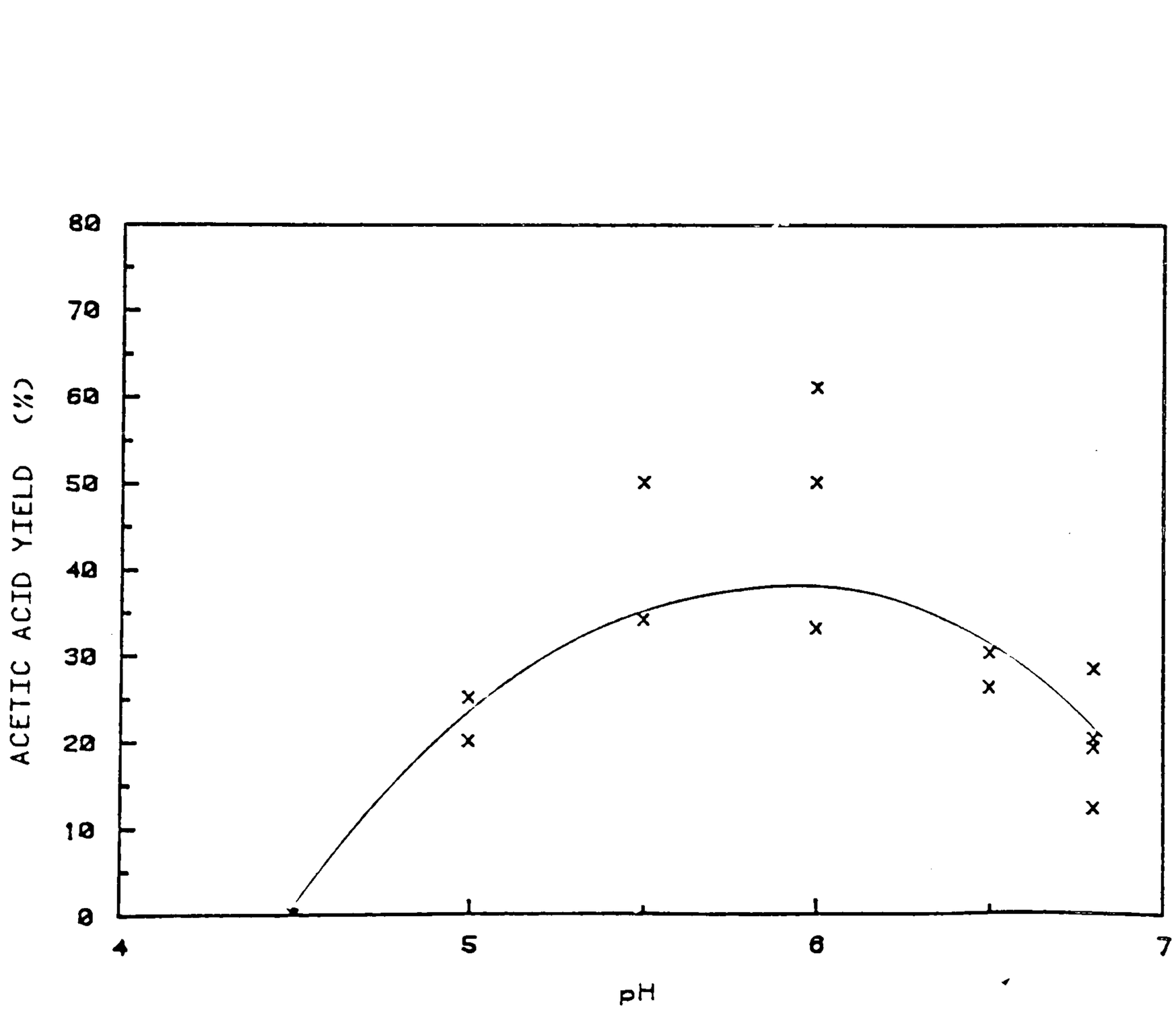

Figure 2.19 Batch growth of wild type C.thermosaccharolyticum at different pH - (b) variations of acetic acid yield.

Table 2.8 Batch growth of *C.thermosacchrolyticum* on inert support particles[1].

Support Matrix	Optical Density[2] A_{650}
Control	1.08
Polyester foam (medium)	1.31
Perlag (medium grade)	0.96
Glass beads (3 mm o.d)	0.92
Sintered glass (5 mm o.d, 50μ mesh)	0.88
Stainless steel wire mesh (200μ mesh)	1.14

1 : Growth after 24 hours incubation with 10% solids in RCM (0.5% xylose)
2 : The refers to the concentration of the cells in the liquid medium

The degree of entrapment was examined qualitatively by physically removing the cells from their support matrix. In Figure 2.20 curve A refers to the growth of cells retained in polyester foam cubes after disengagement steps of sequential expression and sterile washing. These results show that the shear force effects on polyester particles (≈4.5mm cubes) are minimal. Curve B shows the growth of the residual cells that were removed from the supports by washing. The results show that after two washes the main bulk of the loose cells are removed.

D : Carbon Balance

Table 2.9 shows the carbon balance for the wild type cells grown on glucose and xylose. The estimated yields are based on the gramme product formed per gramme substrate removed. Within reasonable experimental approximations and errors due to measurements usually over 80% carbon can be accounted for. Ethanol, acetic acid and carbon dioxide constitute over two-thirds of the carbon uptake. Lactic acid, butyric acid, n-butanol and cell mass account for the rest. The yield of ethanol varied considerably from one experiment to another in the range 20-65%. The yields of acetic

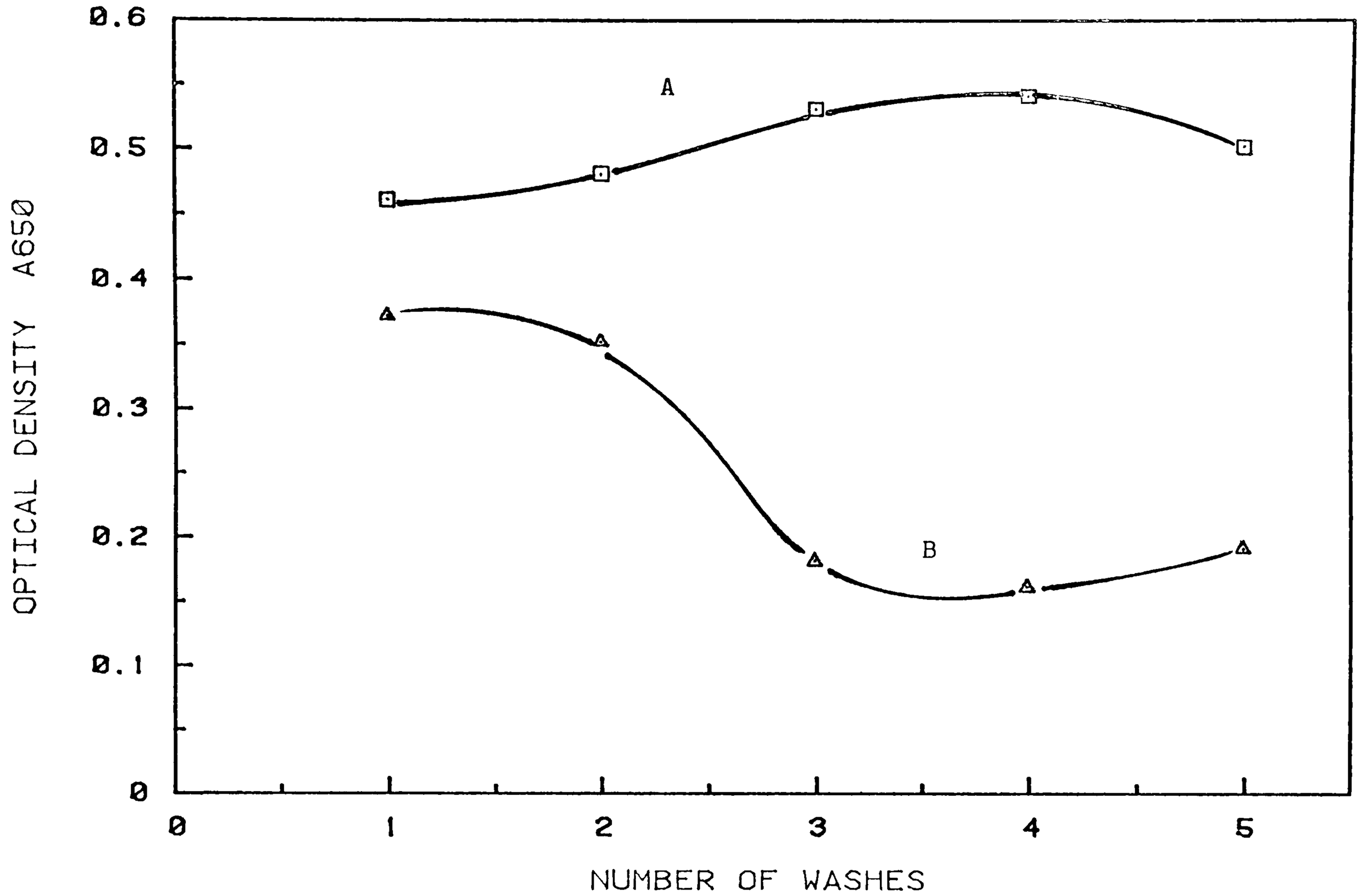

Figure 2.20 Batch growth study of entrapped cells of wild type C.thermosaccharolyticum on polyester foam support particles.

A : Batch growth of entrapped cells after washing

B : Batch growth of disengaged cells upon washing

acid at about 18% and CO_2 at 20% were more consistent.

Table 2.9 Carbon balance of wild type *C.thermosaccharolyticum* .

Carbon Source		End-Product Break-Down							
Type	Amount Consumed g/l	Ethanol Y_E %	Acetic Acid Y_{AA} %	Lactic Acid Y_L %	n-Butanol Y_{nB} %	Butyric Acid Y_{BA} %	Carbon Dioxide Y_{CO2} %	Dry Cell Y_C[1] %	Total Yield %
Glucose	2.78	26	14	6	3	4	21	6	80
Xylose	1.46	51	16	12	4	-[2]	14	10	107
Glucose + Xylose	2.21 } 0.61	31	13	5	6.5	-[2]	22	8	86

1 : Based on 30% carbon contribution.
2 : Less than 1%.

The sugar source and concentration are important factors influencing the final concentration of end-products. In general for sugar concentrations around 0.25-1% (w/v) complete utilsation of glucose in batch cultures was observed while utilisation of xylose was frequently incomplete. In both cases the end-product concentrations nontheless are of the same order. As a result, despite higher cell mass production in presence of glucose, the estimated cell mass yield Y_C, based on consumed sugar in the broth, is lower than the comparable values for xylose. Growth on medium containing both sugars shows similar yields as with the growth on the individual sugars. Figures 2.21a and 2.21b how typical fermentation profiles for cells growing on ≈1% (w/v) glucose and xylose respectively. In these experiments the pH was maintained at 6.8.

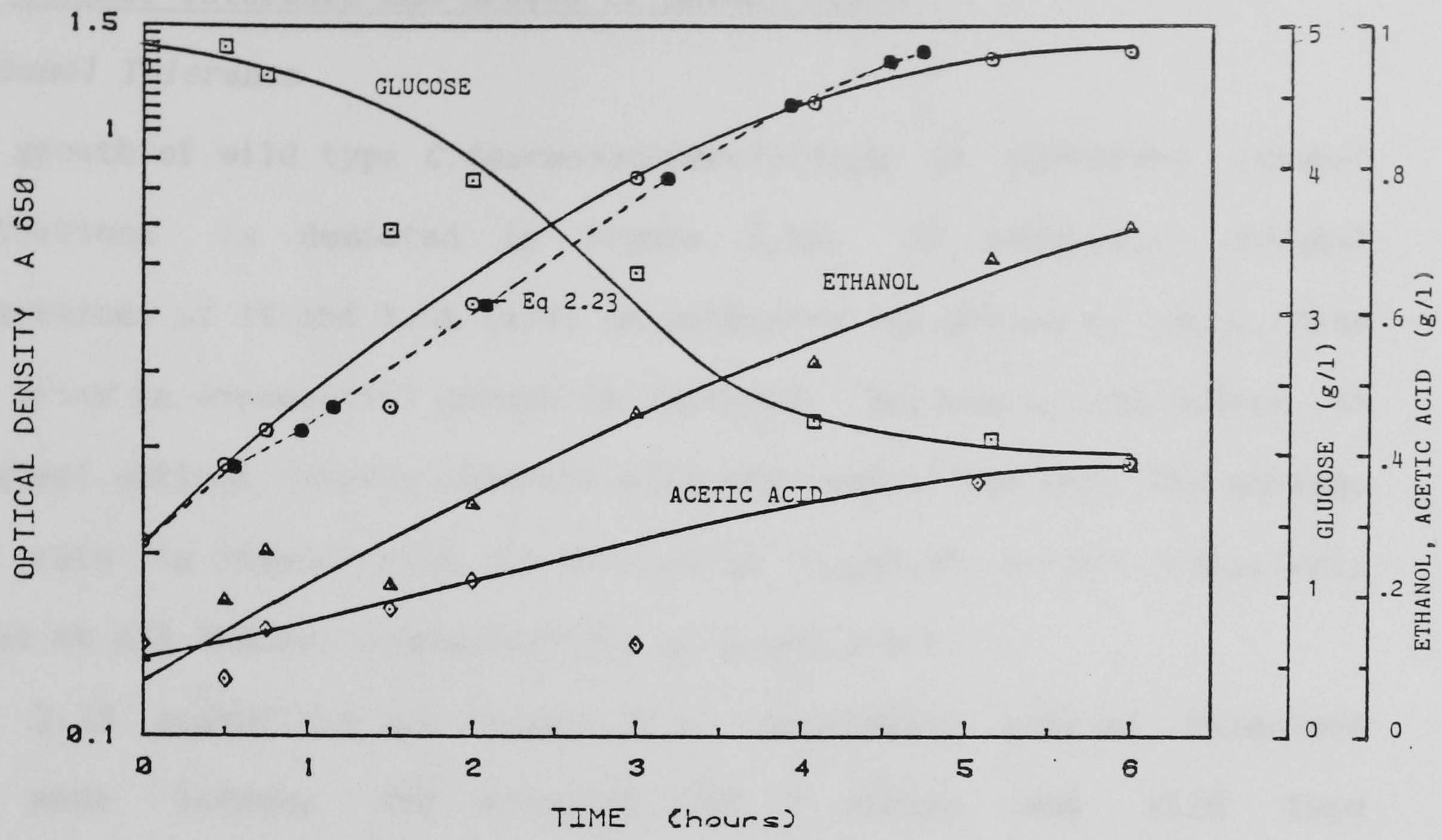

Figure 2.21 Fermentation Profile of wild type C.thermosaccharolyticum grown ; (a) on glucose.

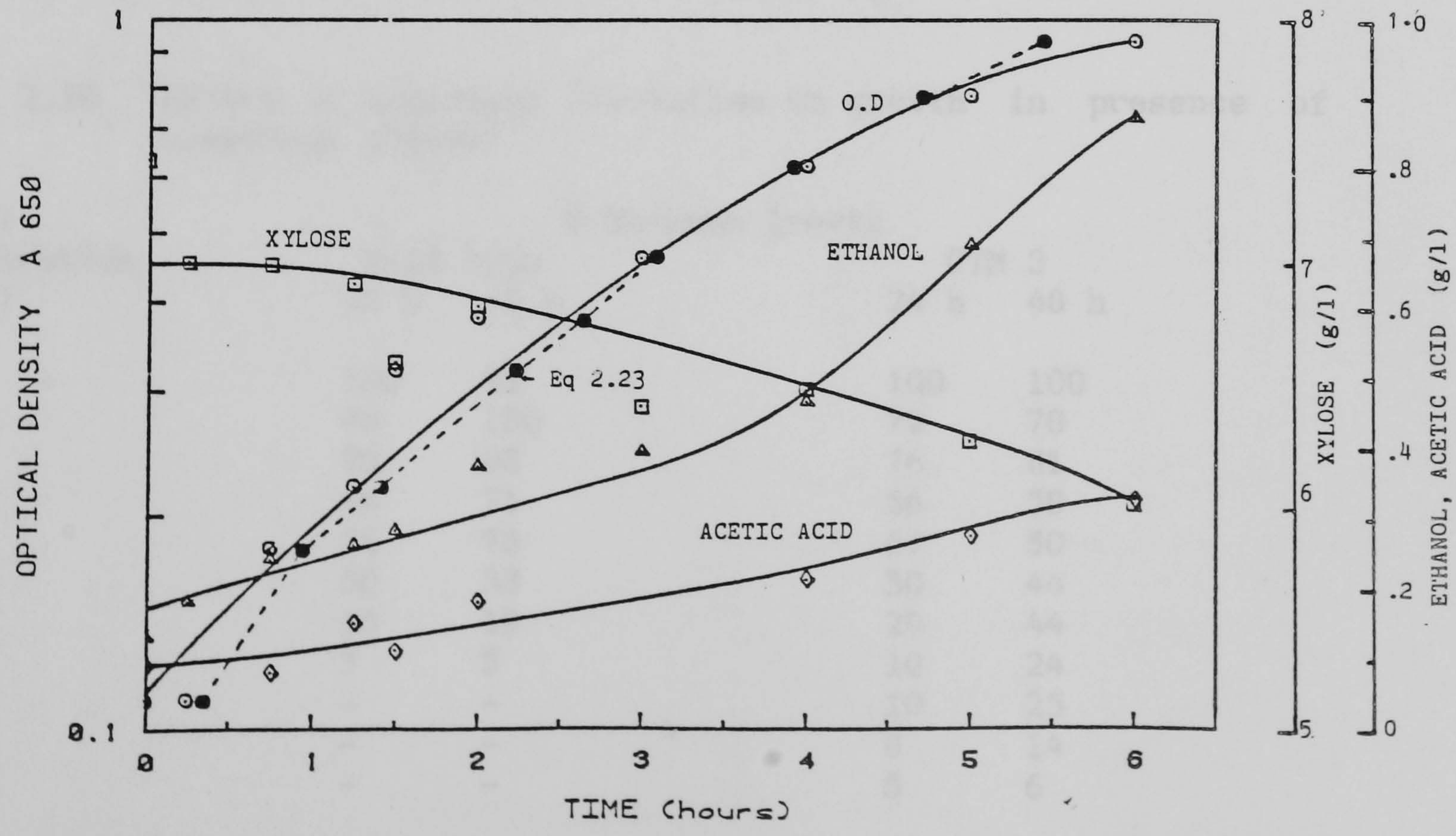

Figure 2.21Fermentation profile of wild type C.thermosaccharolyticum grown; (b) on xylose.

2.3.2 Alcohol Tolerance and Growth of Mutant CTM 3

A : Ethanol Tolerance

Batch growth of wild type *C.thermosaccharolyticum* at different ethanol concentrations is depicted in Figure 2.22. At exogenous ethanol concentrations of 1% and 1.5% (w/v) an extensive lag period of about five hours prior to exponential growth is observed. Maximum growth refers to the highest optical density observed with the control culture. The maximum growth rate is highest with the control at μ_{ox}=0.35 $h^{-1}$and relatively constant at all ethanol concentrations at $\mu_{ox}\approx$0.2 h^{-1}.

Figure 2.23 summarises the results of a comparative ethanol tolerance study made between the selected CTM 3 strain and wild type *C.thermosaccharolyticum* . From the curves it may be observed that at ethanol concentrations greater than 1.5% (w/v) there is a significant reduction in the growth of the wild type cells and complete cessation at 4% (w/v). The CTM 3 strain generally showed slower growth (μ_{ox}= 0.2 h^{-1}). It is notable however that at 3% (w/v) ethanol concentration the number of surviving organisms is double that of the wild type.

Table 2.10 Effect of prolonged incubation on growth in presence of exogenous ethanol.

Ethanol Concentration % (w/v)	% Maximum growth			
	Wild type		CTM 3	
	24 h	48 h	24 h	48 h
0	100	92	100	100
0.5	96	100	72	70
1	95	88	76	81
1.5	86	71	56	50
2	74	75	67	50
2.5	50	33	50	44
3	15	18	29	44
3.5	5	5	10	24
4	-	-	10	25
4.5	-	-	8	14
5	-	-	5	6

In Table 2.10 the effect of prolonged incubation of the mutant cells is shown. The effect is most notable at higher ethanol concentrations when

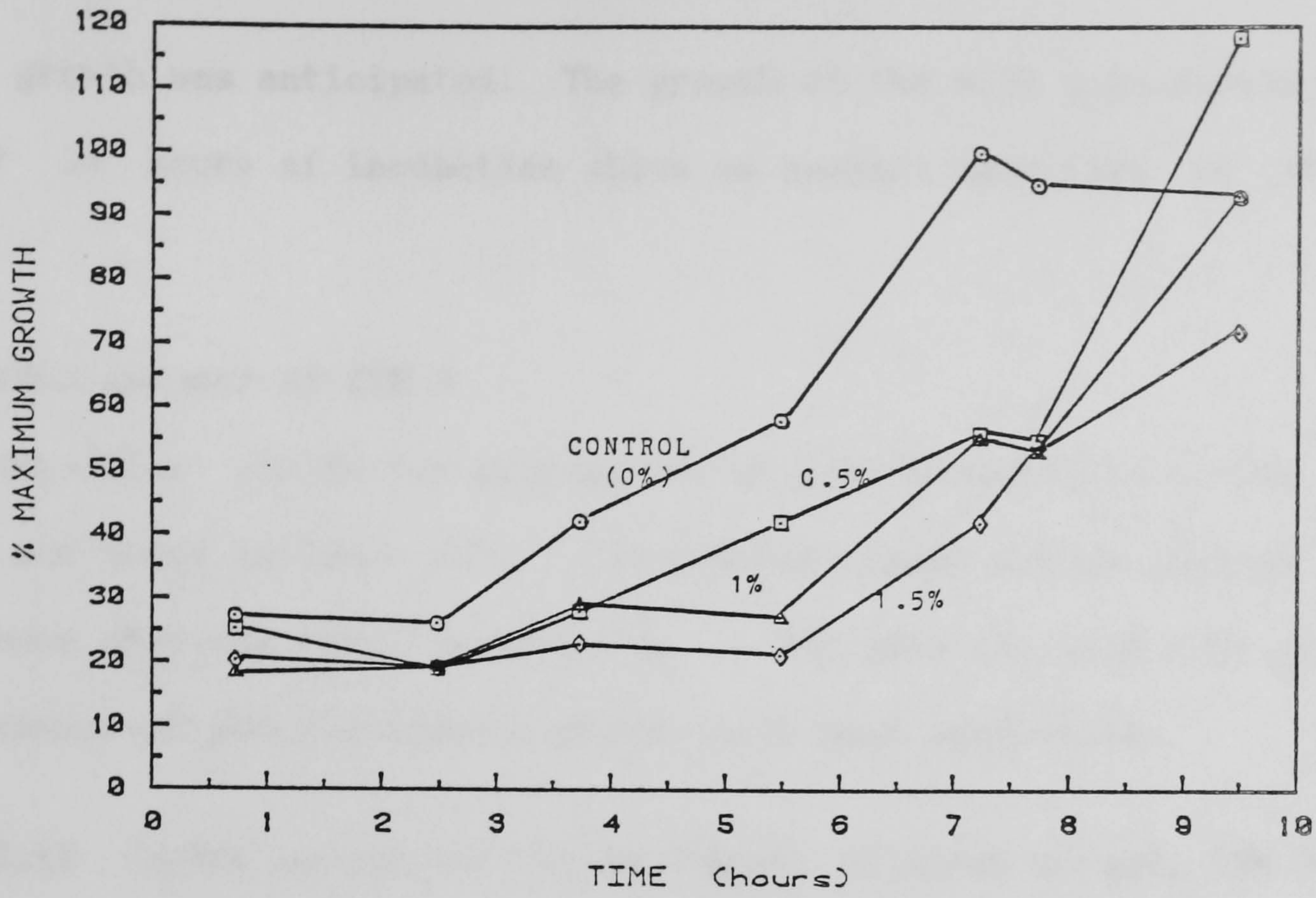

Figure 2.22 Batch growth of wild type C.thermosaccharolyticum at different ethanol concentrations (% w/v).

Maximum optical density observed; A 650 = 0.82

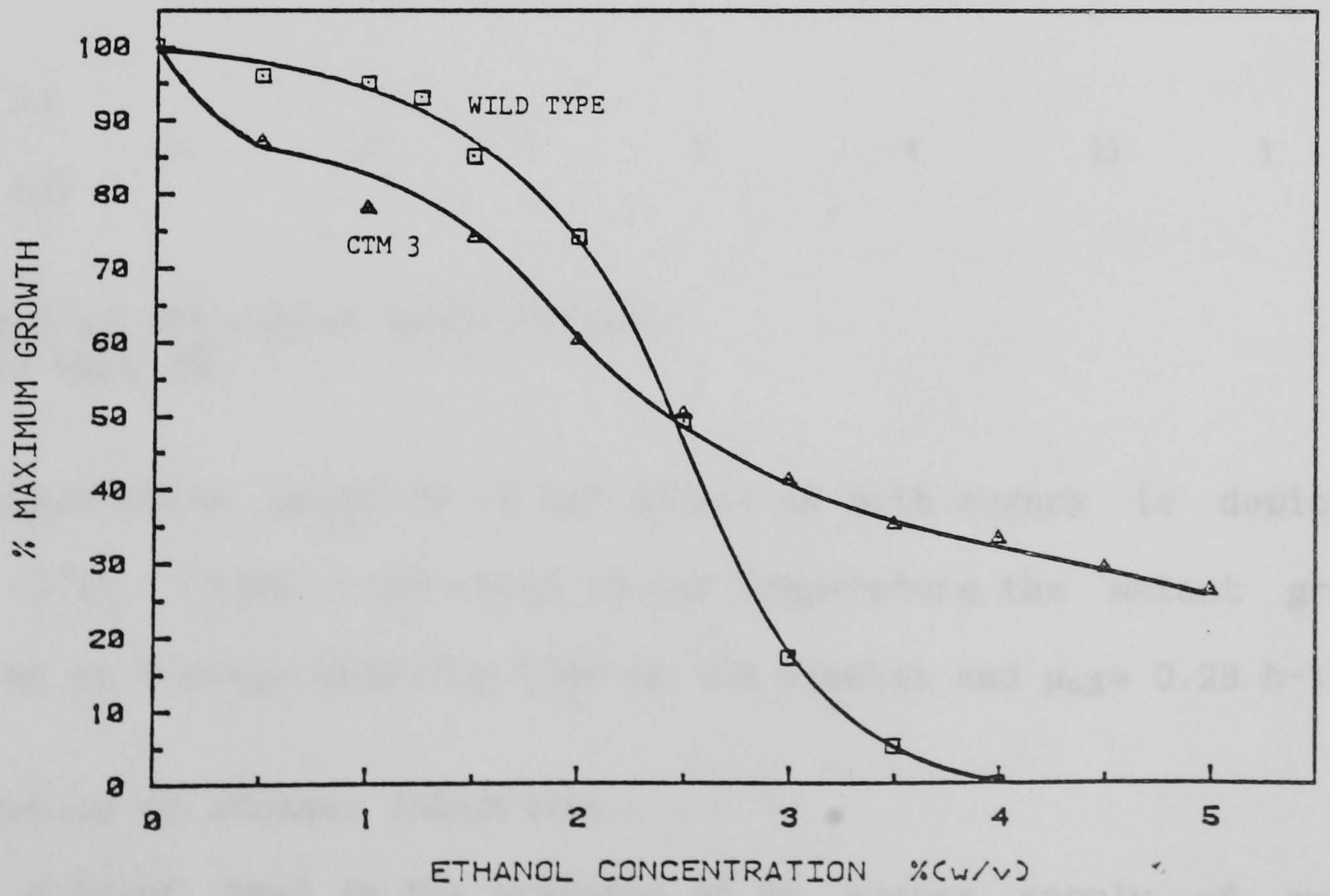

Figure 2.23 Maximum growth of wild type and mutant strain (CTM 3) of C.thermosaccharolyticum at different exogenous ethanol concentrations. (Batch growth after 24 hours).

Maximum optical density observed; Wild type : A 650 = 0.86; Mutant : A 650 = 0.66

slower growth was anticipated. The growth of the wild type strain after a further 24 hours of incubation shows an overall reduction in the cell number.

B : Carbon Balance of CTM 3

The respective yields for glucose and xylose fermentation by the CTM 3 strain are shown in Table 2.11. The ethanol yields are marginally higher than those observed with the wild type. Also like the wild type growth in the presence of glucose shows a higher cell mass production.

Table 2.11 Carbon balance of the 3% ethanol tolernat mutant, CTM 3

Carbon Source		End-Product Break-Down							
Type	Amount Consumed g/l	Bthanol Y_E %	Acetic Acid Y_{AA} %	Lactic Acid Y_L %	n-Butanol Y_{nB} %	Butyric Acid Y_{BA} %	Carbon Dioxide Y_{CO_2} %	Dry Cell Y_C[1] %	Total Yield %
Glucose	2.2	44	25	9	-	4	28	8	118
Xylose	1.37	54	17	-	3	-	19	5	98
Glucose + Xylose	2.4 } 1.25	31	22	7	3	4	23	5	95

1 : Based on 30% carbon contribution.
2 : Less than 1%.

The fermentation profiles of the mutant on both sugars is depicted in Figure 2.24. Under controlled pH and temperature the mutant grows on xylose at an average doubling time of 150 minutes and μ_{oX}= 0.28 h^{-1}.

C : Kinetics of Ethanol Inhibition

It is evident that in the presence of an excess supply of substrate neither the wild type nor the mutant CTM 3 is able to ferment sugars to ethanol concentrations above 2 g/l. This quantity is far less than the

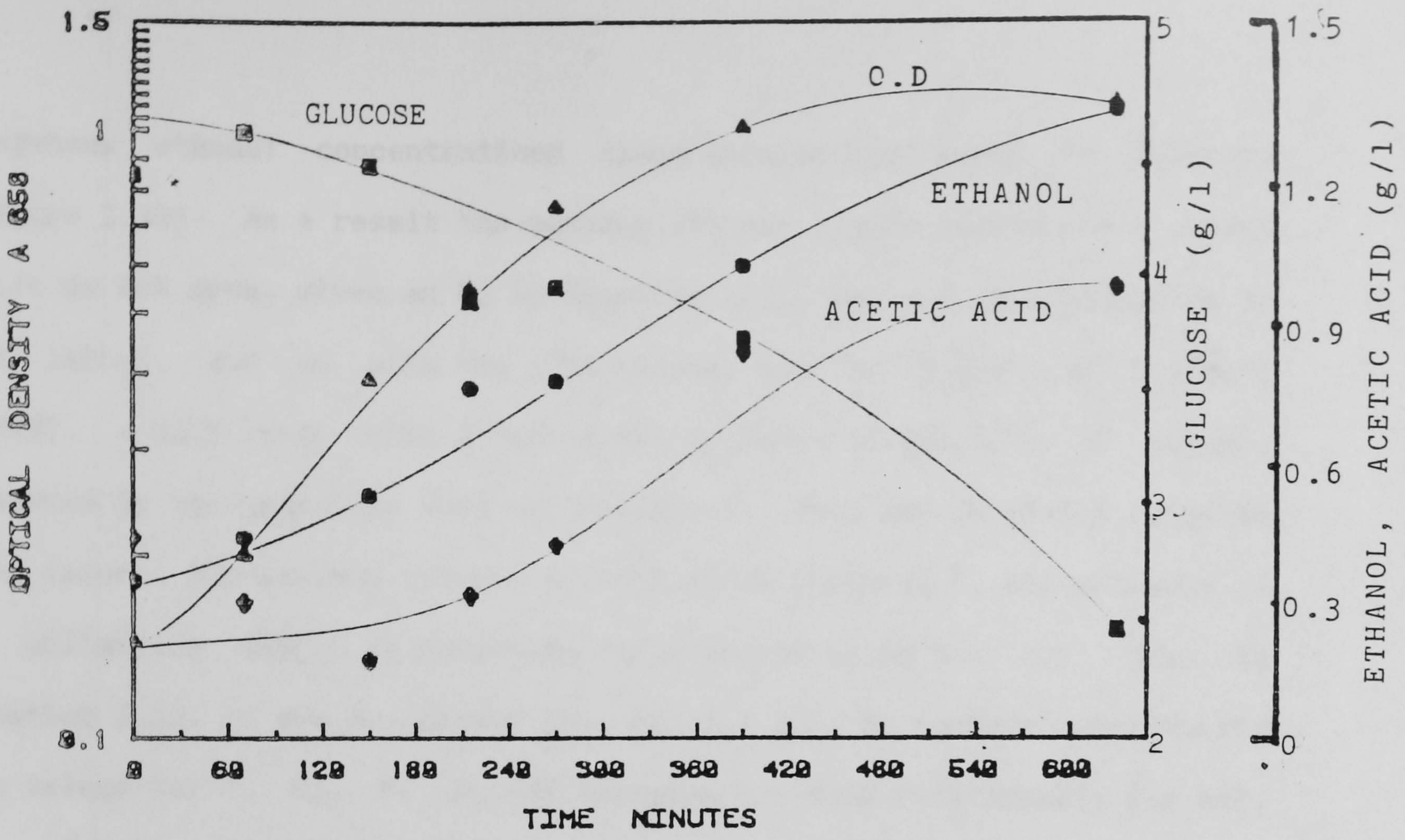

Figure 2.24 Batch fermentation profile of CTM 3 cells grown (a) on glucose.

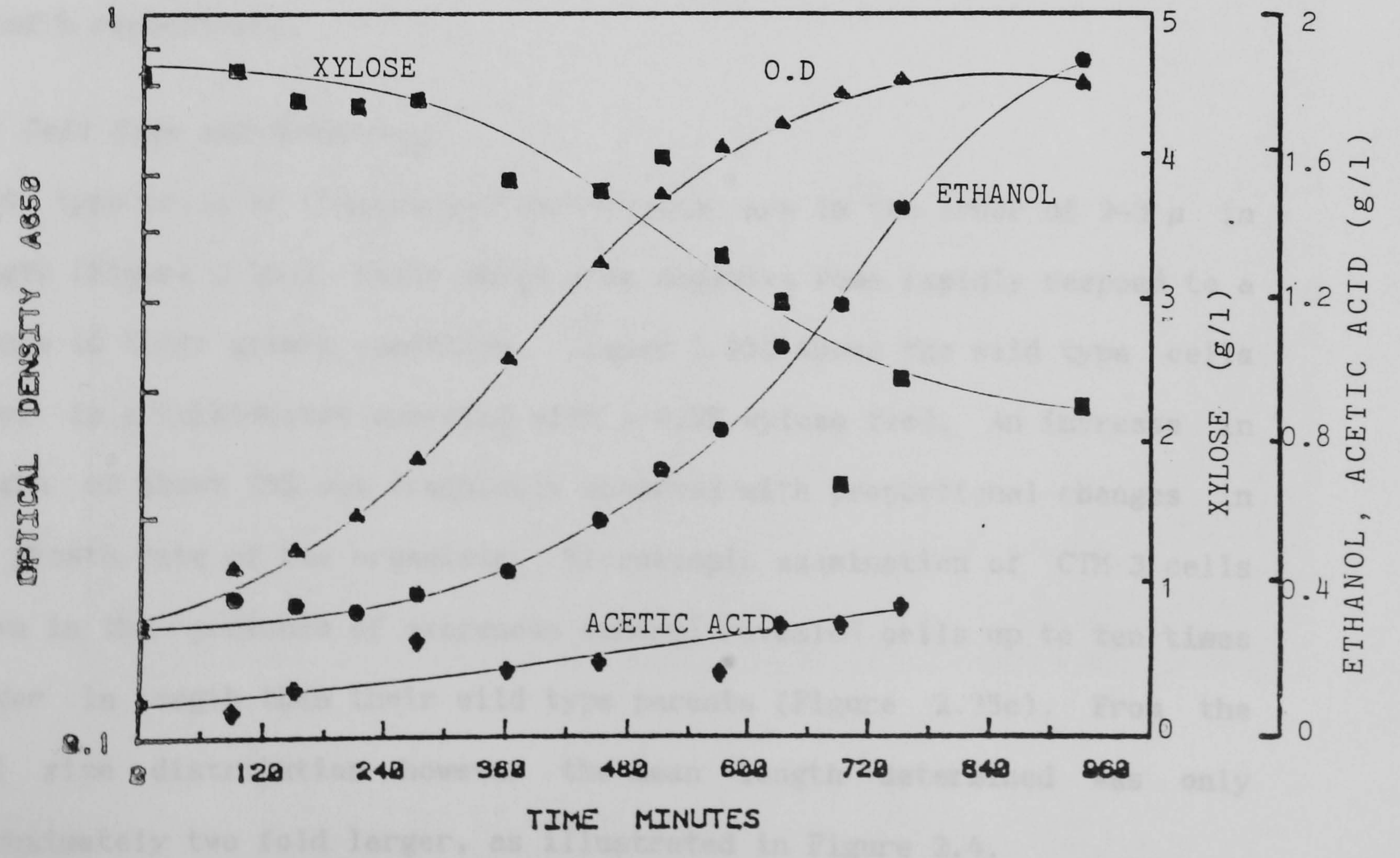

Figure 2.24 Batch fermentation profile of CTM 3 cells grown (b)

exogenous ethanol concentrations these strains are known to tolerate (Figure 2.23). As a result the maximum ethanol concentration above which cells do not grow, given as P_m in Equation 2.23, may not be represented by the latter, and as with the observations made by Hoppe and Hansford (1983), a much lower value given as the maximum concentration of ethanol produced by the organisms need be considered. From the fed-batch studies (see later), the maximum ethanol concentration produced in the presence of an unlimiting supply of substrate was observed to be 2.4 g/l. Thus in Equation 2.23, it may be assumed that P_m= 2.5 g/l. By further substituting the values for C, C_o, P, P_o and assuming a linear relationship i.e n=1, the estimated batch time can be determined. The dotted lines in Figures 2.21a and 2.21b refer to the variation of cell density with the estimated time according to Equation 2.23. The statistics determination (Unistat, Computer Package) of the goodness of fit indicate that the model is not an exact fit, however it correlates well with the observed data with the Pearson's coefficient of correlation of 0.9783 and 0.9811 for Figures 2.21 a and b repectively.

D : Cell Size and Morphology

Wild type cells of *C.thermosaccharolyticum* are in the order of 2-3 μ in length (Figure 2.25a). These short gram negative rods rapidly respond to a change in their growth condition. Figure 2.25b shows the wild type cells grown in a turbidostat operated with a 0.5% xylose feed. An increase in length of about 35% was frequently observed with proportional changes in the growth rate of the organisms. Microscopic examination of CTM 3 cells grown in the presence of exogenous ethanol revealed cells up to ten times longer in length than their wild type parents (Figure 2.25c). From the cell size distribution however the mean length determined was only approximately two fold larger, as illustrated in Figure 2.4.

(a)

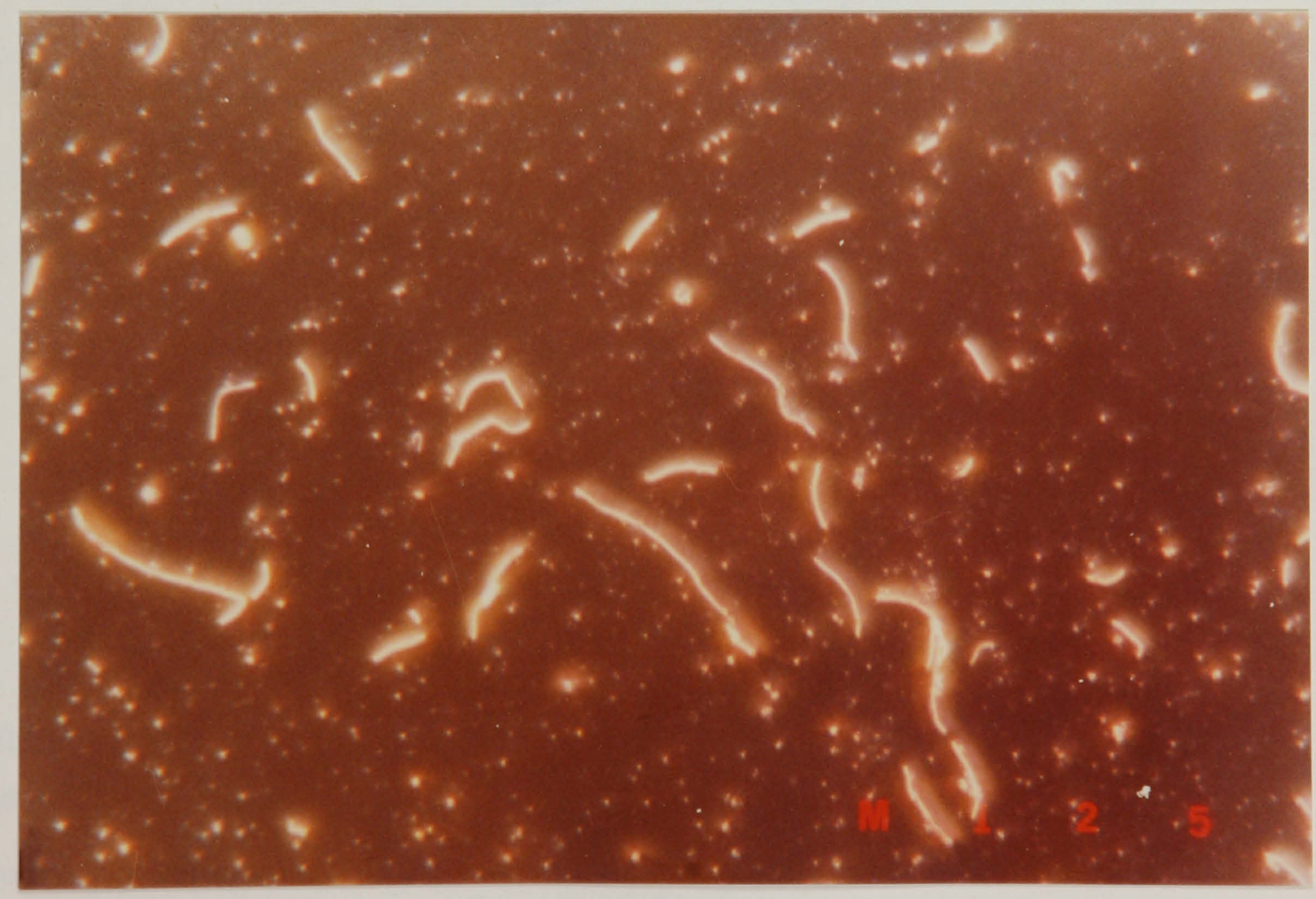

(b)

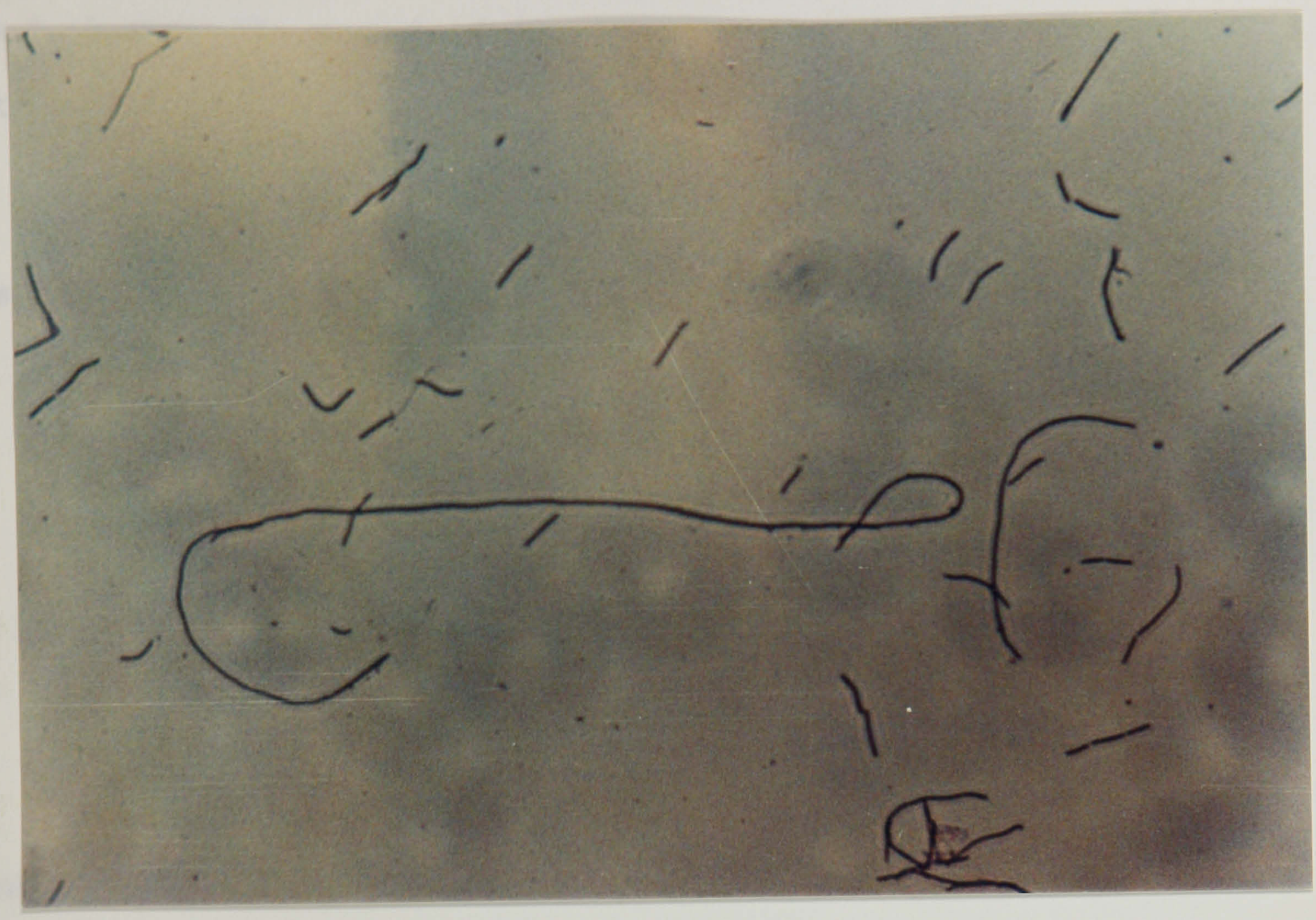

(c)

Figure 2.25 Influence of environmental factors on the morphology of C. thermosaccharolyticum

(a) : Wild type cells grown on 0.5% xylose; Magnification x40, phase contrast

(b) : CTM 3 cells grown in the absence of exogenous ethanol; Magnification x40, dark field

(c) : CTM 3 cells grown in the presence of 3% (w/v) ethanol; Magnification x40, phase contrast

Table 2.12 shows the summary of the cell size distributions of cells grown in the presence of varying amounts of exogenous ethanol. It is evident that increasing stress has a direct effect on the cell size.

Table 2.12 Effect of exogenous ethanol on the size distribution of wild type *C.thermosaccharolyticum* .

Ethanol concentration % (w/v)	Mean cell length (μm)	Range (μm)
0	2.17	0.66 - 5.7
0.5	2.13	0.8 - 5.3
1	2.57	1.26 - 7.8
2	4.4	1.34 - 12
3	5.03	1.27 - 12.29
5	5.86	0.88 - 26.77

Microscopic observations of cells grown at different pH or in the absence of medium components such as carbon source, phosphor buffer and ammonia revealed similar trends, although these observations were not photographed for further analysis.

2.3.3 Fermentation Studies

The carbon balances shown in Tables 2.9 and 2.11 were obtained by carrying out simple batch fermentations in a small 0.8 litre fermenter. Further studies were carried out in order to investigate end-product formation under different growth conditions by batch fermentation, and optimal growth and productivity by continuous operation.

A : Growth in the Presence of Glucose and Xylose

Batch growth of wild type and CTM 3 in the presence of both xylose and glucose showed preferential for glucose. Xylose uptake normally follows after complete glucose utilisation by the organisms. Figure 2.26a and b show the prefernetial growth of wild type and CTM 3 respectively. In both cases glucose is introduced to the culture after having grown on xylose, and taken up without any apparent lag. Preferential growth of the mutant

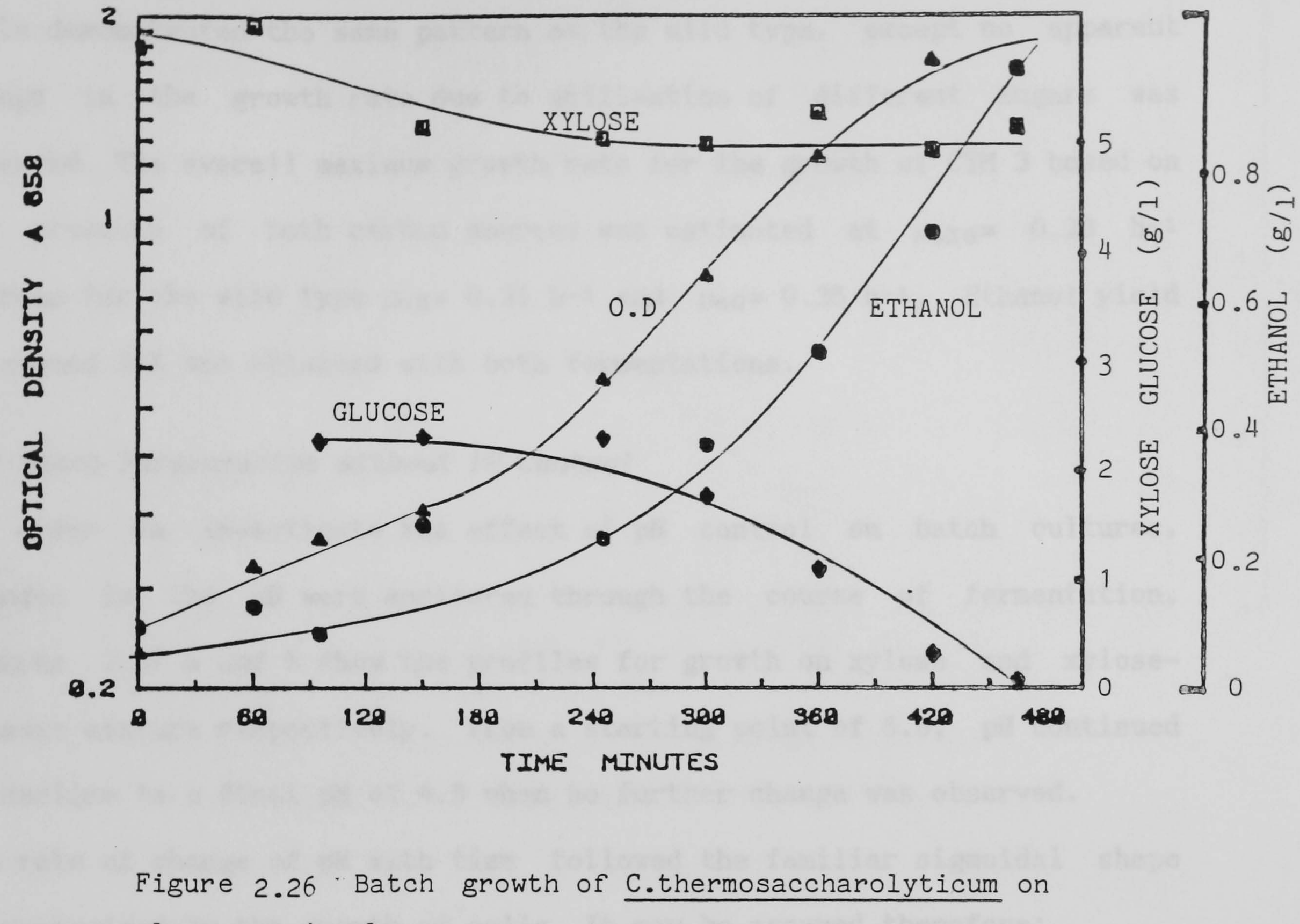

Figure 2.26 Batch growth of C.thermosaccharolyticum on glucose and xylose.

(a) : Growth of the wild type

(b) : Growth of the CTM 3 mutant strain

cells demonstrated the same pattern as the wild type, except no apparent change in the growth rate due to utilisation of different sugars was observed. The overall maximum growth rate for the growth of CTM 3 based on the presence of both carbon sources was estimated at μ_{oXG}= 0.28 h^{-1} whereas for the wild type μ_{oX}= 0.21 h^{-1} and μ_{oG}= 0.35 h^{-1}. Ethanol yield of around 31% was obtained with both fermentations.

B : Batch Fermentation without PH Control

In order to investigate the effect of pH control on batch cultures, changes in the pH were monitored through the course of fermentation. Figures 2.27 a and b show the profiles for growth on xylose and xylose-glucose mixture respectively. From a starting point of 6.8, pH continued to decline to a final pH of 4.5 when no further change was observed.

The rate of change of pH with time followed the familiar sigmoidal shape characterised by the growth of cells. It may be assumed therefore;

$$-\frac{d[pH]}{dt} \alpha \mu_o$$

The above gradient was determined from semi-log plots of pH against time.

Thus for xylose;

$$\frac{d[pH]}{dt} = -0.46 \qquad 6.2 \leq pH \leq 4.8$$

for glucose;

$$\frac{d[pH]}{dt} = -0.60 \qquad 6.2 \leq pH \leq 4.8$$

and for xylose-glucose;

$$\frac{d[pH]}{dt} = -0.55 \qquad 6.2 \leq pH \leq 4.8$$

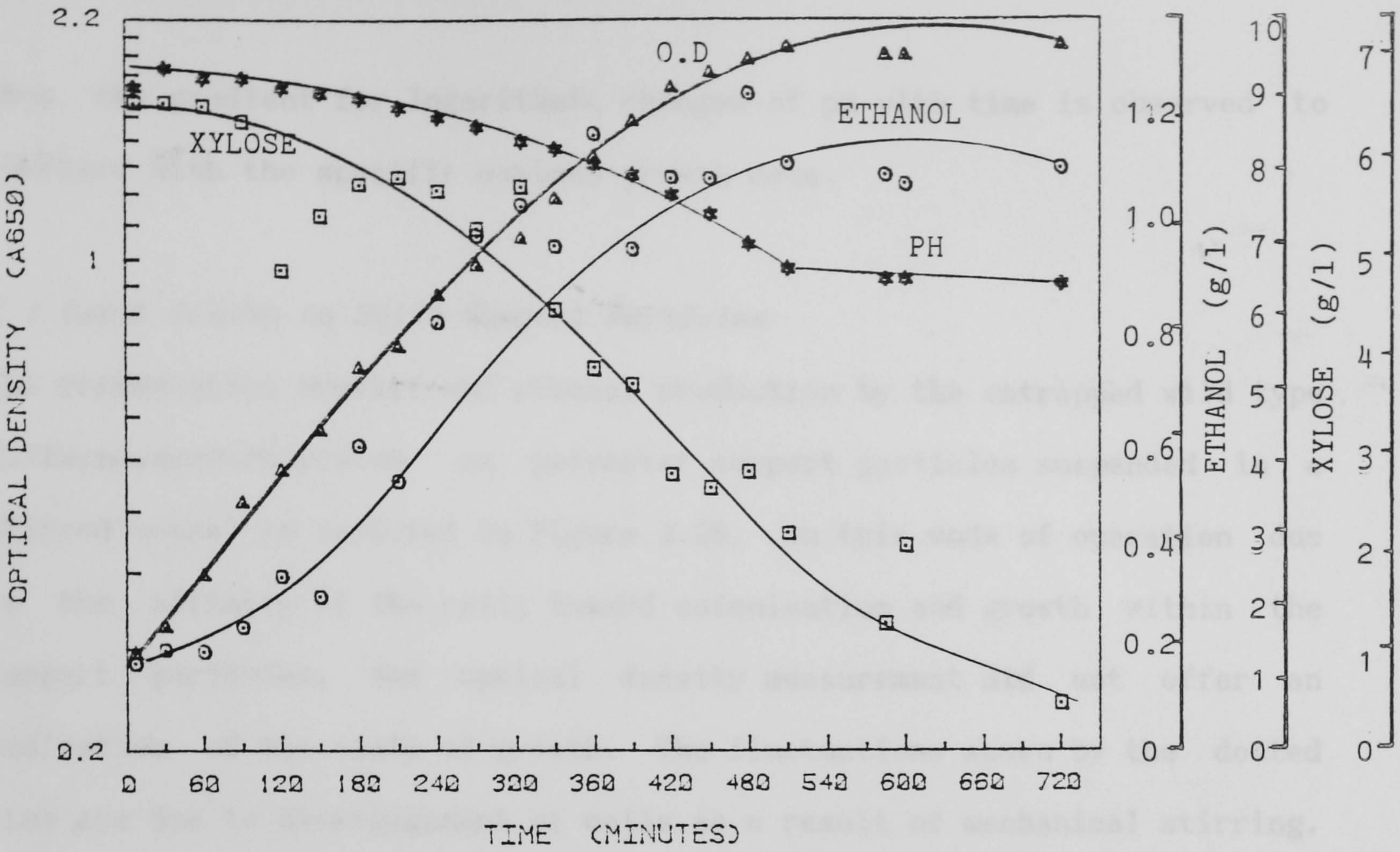

Figure 2.27a Variations of pH in batch fermentation of wild type C.thermosaccharolyticum grown on xylose.

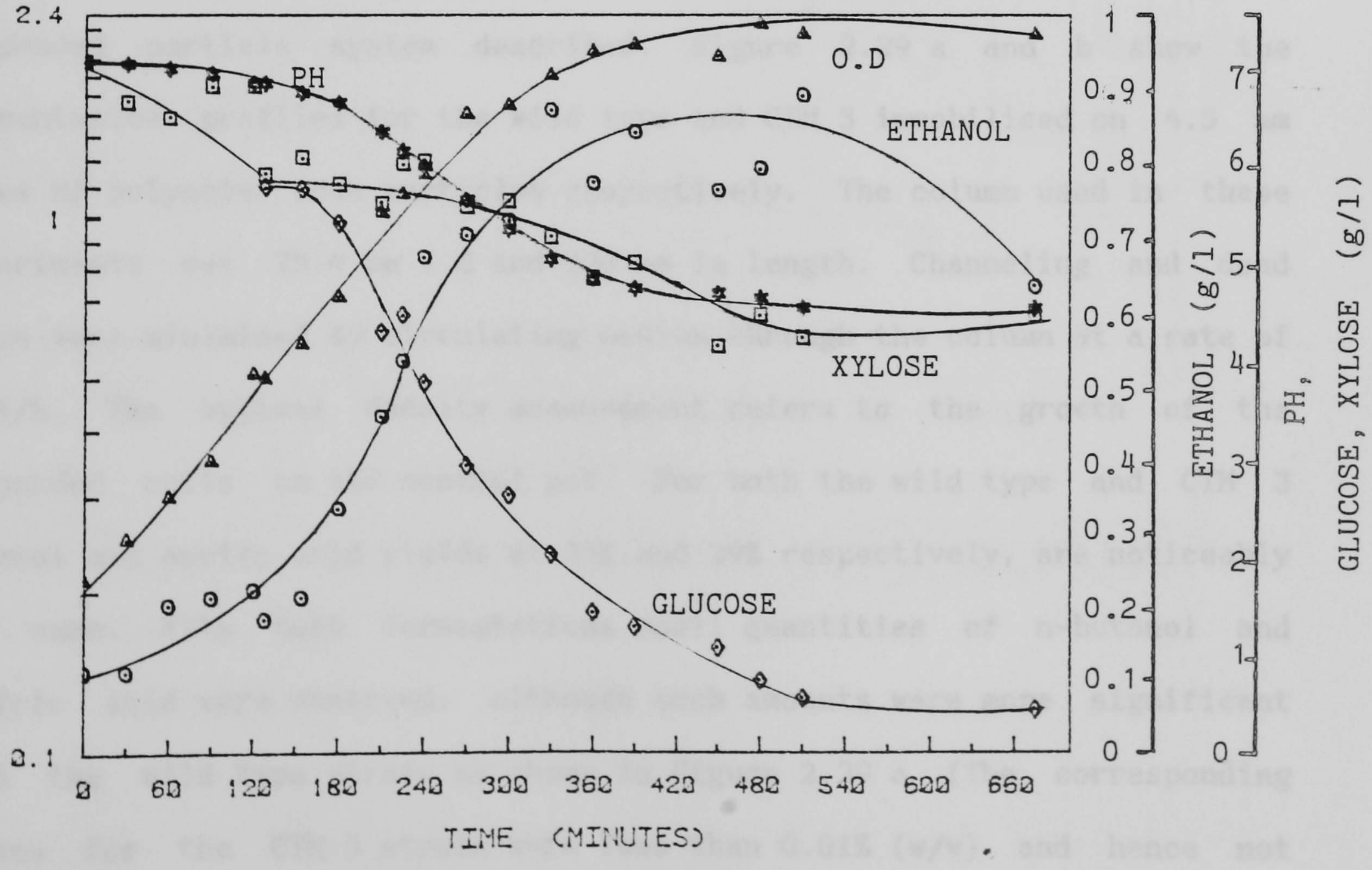

Figure 2.27b Variations of pH in batch fermentation of wild type C.thermosaccharolyticum grown on glucose and xylose.

Thus the gradient for logarithmic changes of pH with time is observed to increase with the specific maximum growth rate.

C : Batch Growth on Solid Support Particles

The fermentation profile and ethanol production by the entrapped wild type *C.thermosaccharolyticum* on polyester support particles suspended in a stirred vessel is depicted in Figure 2.28. In this mode of operation due to the affinity of the cells toward colonisation and growth within the support particles, the optical density measurement did not offer an indication of the state of growth. The fluctuations shown by the dotted line are due to disengagement of cells as a result of mechanical stirring. In the course of fermentation all support particles rose to the surface of the broth. The fermentation was carried out for six hours with ethanol yield at 46%. Operation of a side column packed with biomass support particles, overcame the buoyancy problems encountered with the free suspended particle system described. Figure 2.29 a and b show the fermentation profiles for the wild type and CTM 3 immobilised on 4.5 mm cubes of polyester foam particles respectively. The column used in these experiments was 25.4 mm i.d and 300 mm in length. Channeling and dead space were minimised by circulating medium through the column at a rate of 3 l/h. The optical density measurement refers to the growth of the suspended cells in the control pot. For both the wild type and CTM 3 ethanol and acetic acid yields at 35% and 29% respectively, are noticeably the same. With both fermentations small quantities of n-butanol and butyric acid were observed, although such amounts were more significant with the wild type strain as shown in Figure 2.29 a (The corresponding values for the CTM 3 strain were less than 0.01% (w/v) and hence not shown).

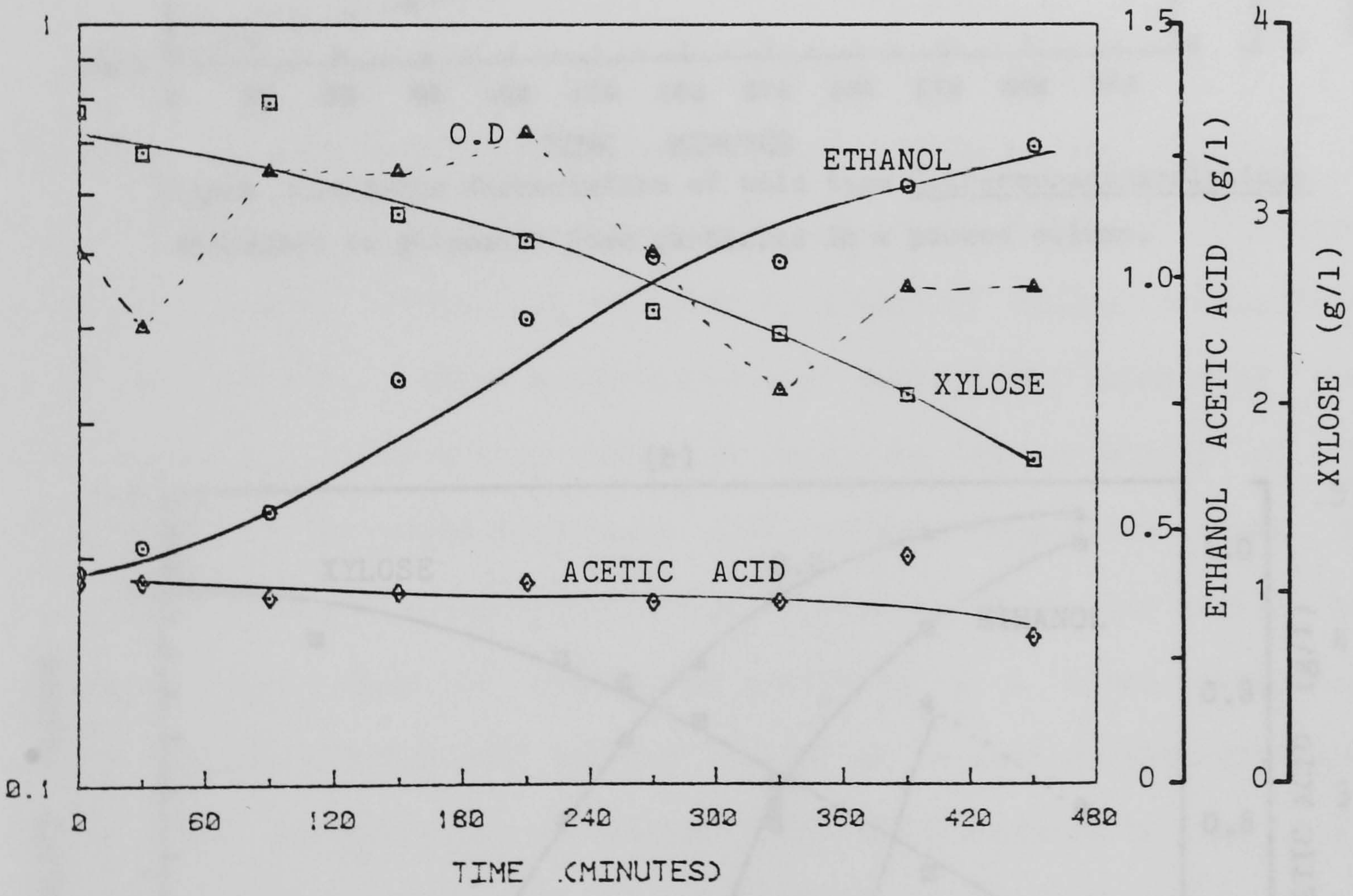

Figure 2.28 Batch fermentation of wild type C.thermosaccharolyticum in a 1 litre stirred fermenter containing 100 ml polyester support particles.

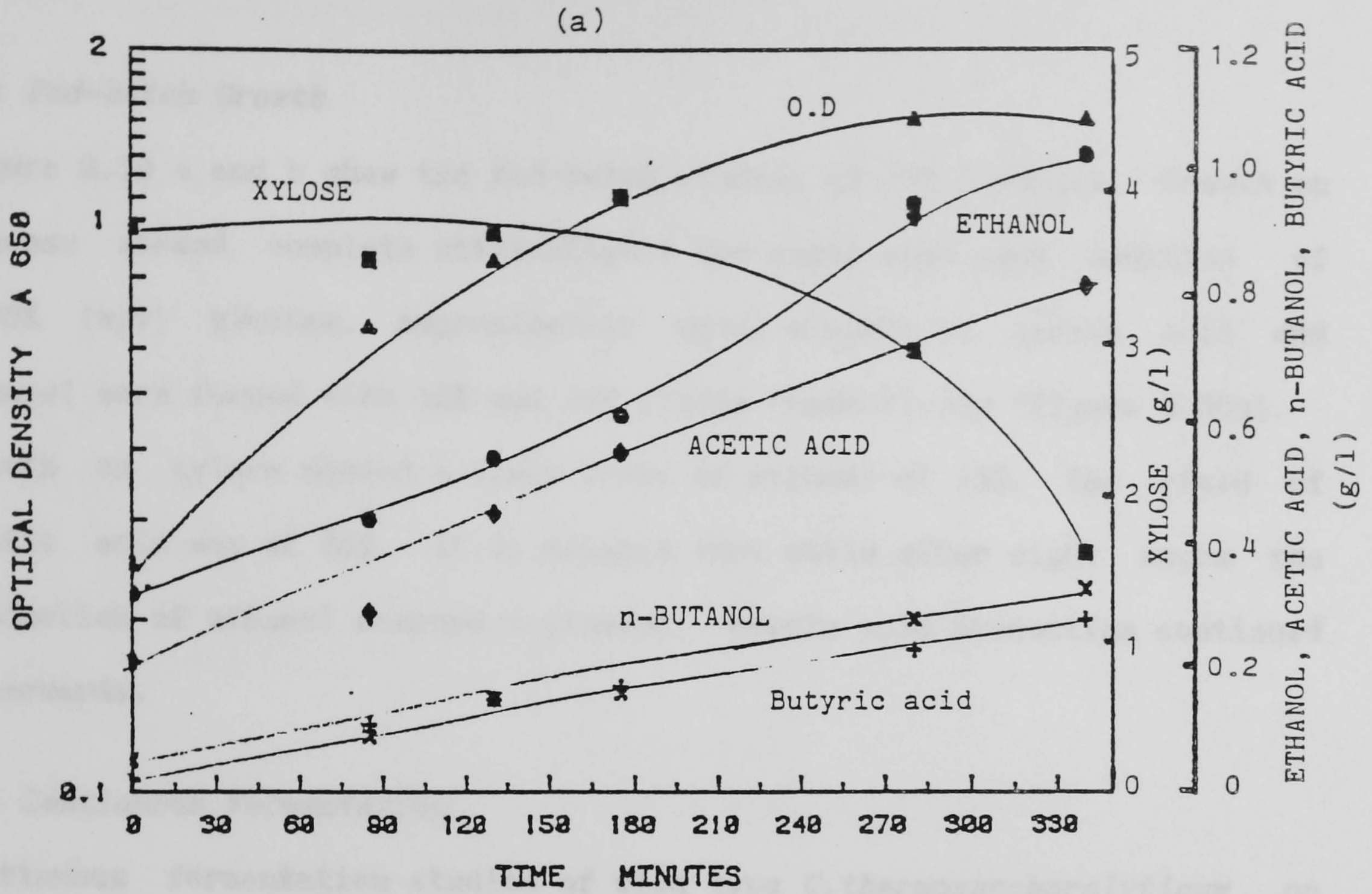

Figure 2.29 Batch fermentation of wild type C.thermosaccharolyticum entrapped in polyester foam particles in a packed column.

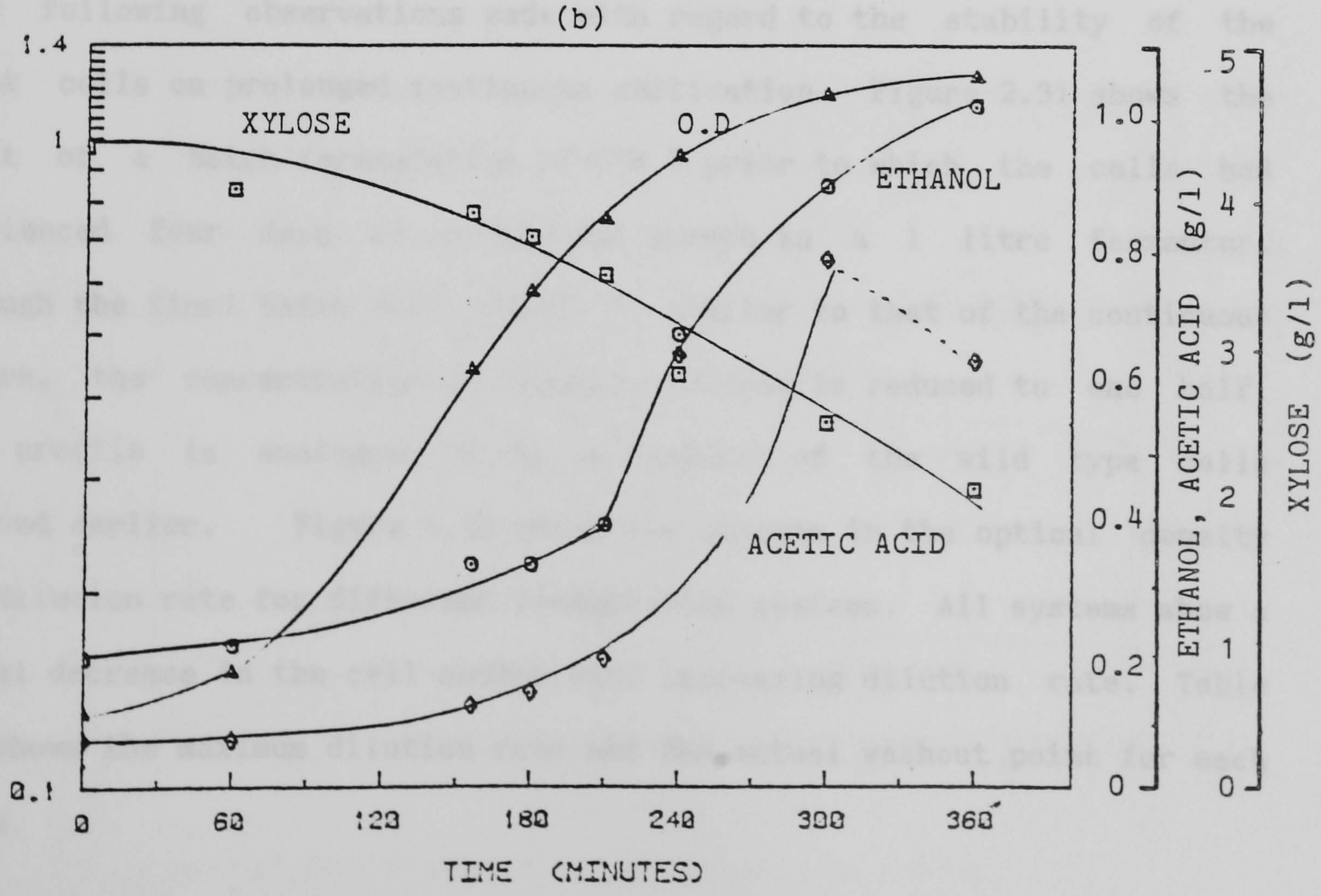

Figure 2.29 Batch fermentation of mutant CTM 3 entrapped in polyester foam particles in a packed column.

D : Fed-batch Growth

Figure 2.30 a and b show the fed-batch studies of CTM 3 strain. Growth on glucose showed complete utilisationof the sugar upon each addition of 0.25% (w/v) glucose. Approximately equal amounts of acetic acid and ethanol were formed with 22% and 24% yields respectively (Figure 2.30a). Growth on xylose showed a lower yield of ethanol at 15%. The yield of acetic acid was at 26%. It is notable that while after eight hours the production of ethanol reached a plateau, acetic acid production continued afterwards.

E : Continuous Fermentation

Continuous fermentation studies of wild type *C.thermosaccharolyticum* on immobilised support particles or as free suspended cells at different dilution rates were carried out in order to determine optimum productivity of the end-products. These experiments were carried out using wild type cells following observations made with regard to the stability of the mutant cells on prolonged continuous cultivation. Figure 2.31 shows the result of a batch fermentation of CTM 3 prior to which the cells had experienced four days of continuous growth in a 1 litre fermenter. Although the final batch cell density is similar to that of the continuous culture, the concentration of ethanol produced is reduced to one half. This profile is analogous to the performance of the wild type cells observed earlier. Figure 2.32 shows the changes in the optical density with dilution rate for different fermentation systems. All systems show a general decrease in the cell number with increasing dilution rate. Table 2.13 shows the maximum dilution rate and the actual washout point for each system.

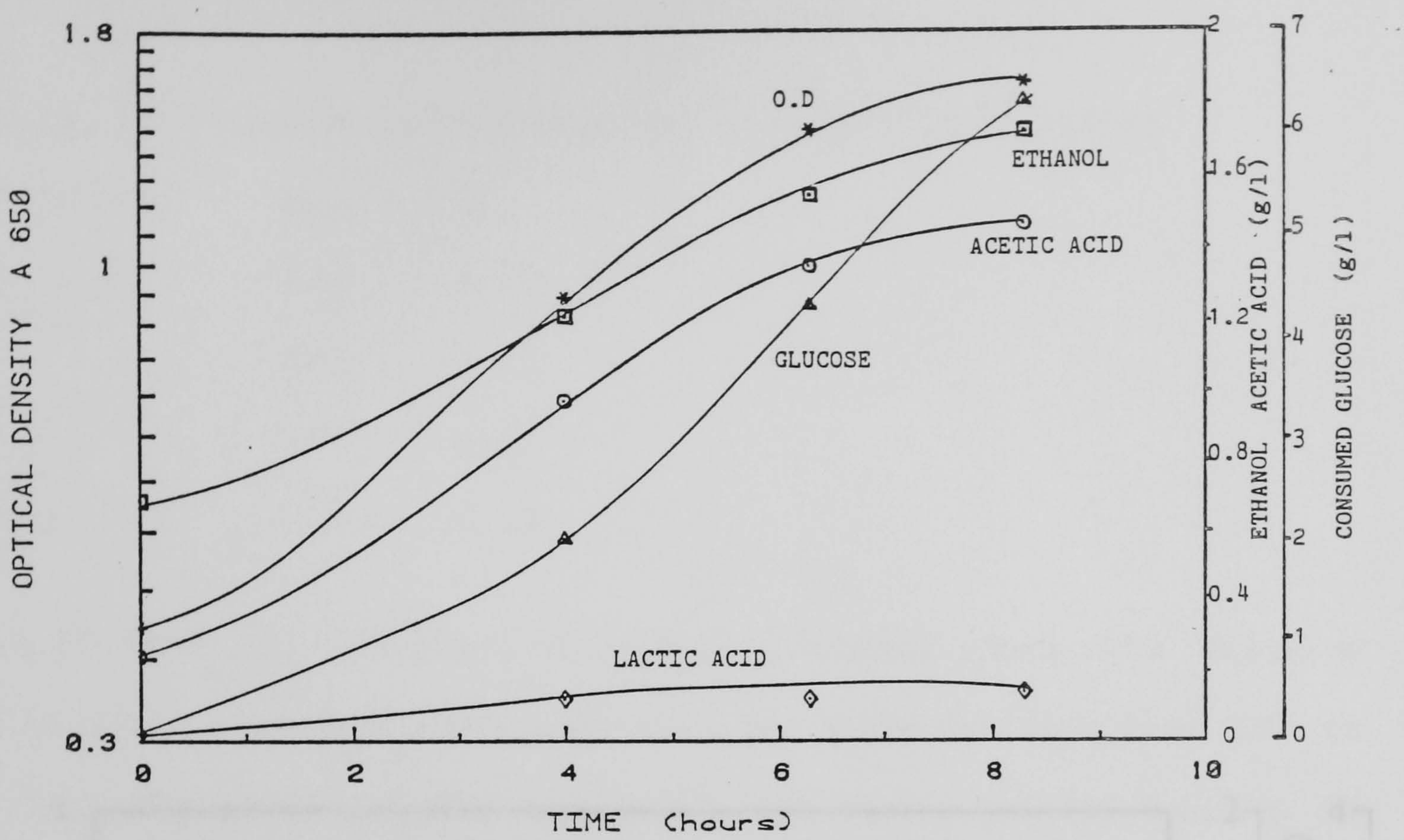

Figure 2.30 Fed-batch growth of C.thermosaccharolyticum on glucose.
(a)

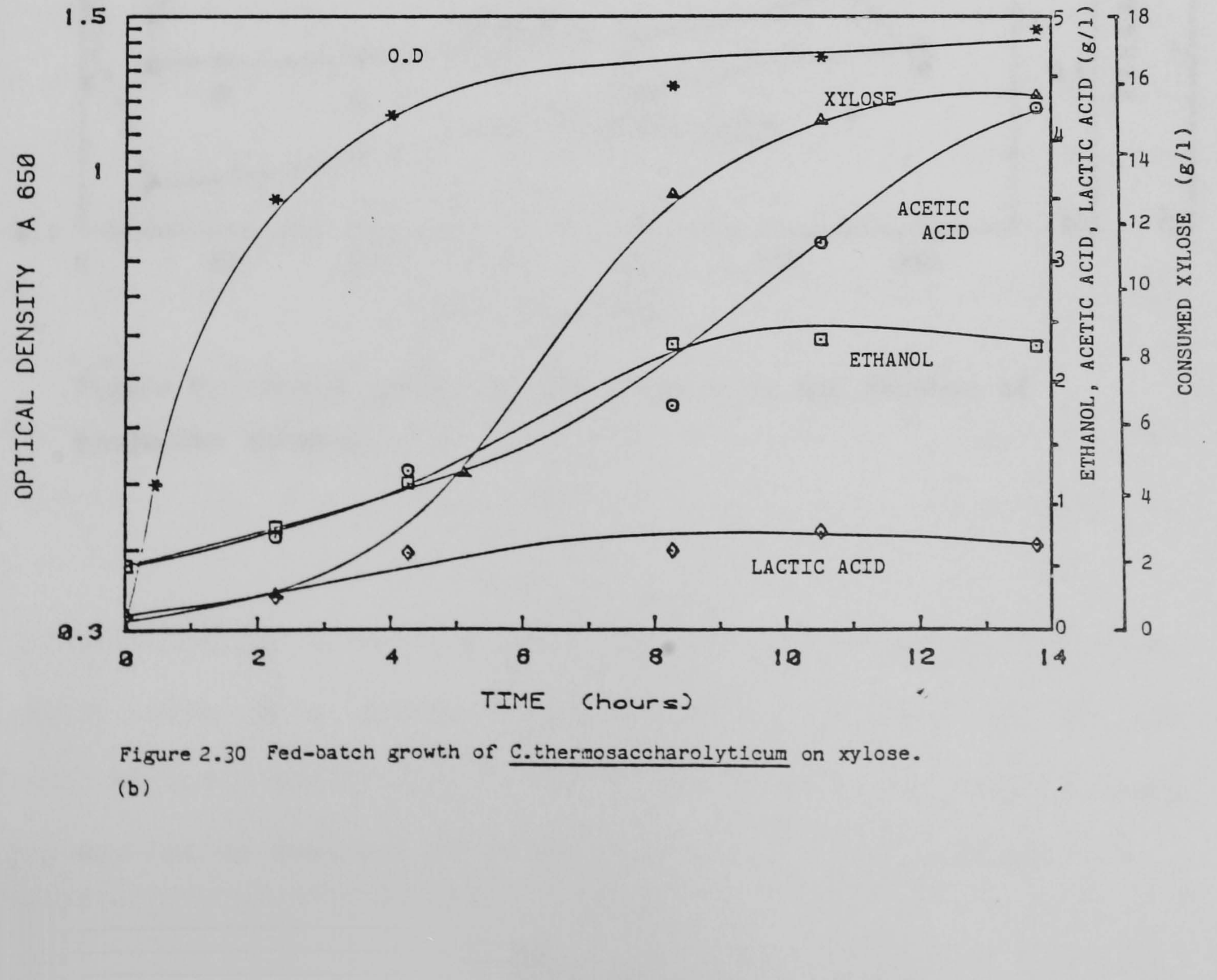

Figure 2.30 Fed-batch growth of C.thermosaccharolyticum on xylose.
(b)

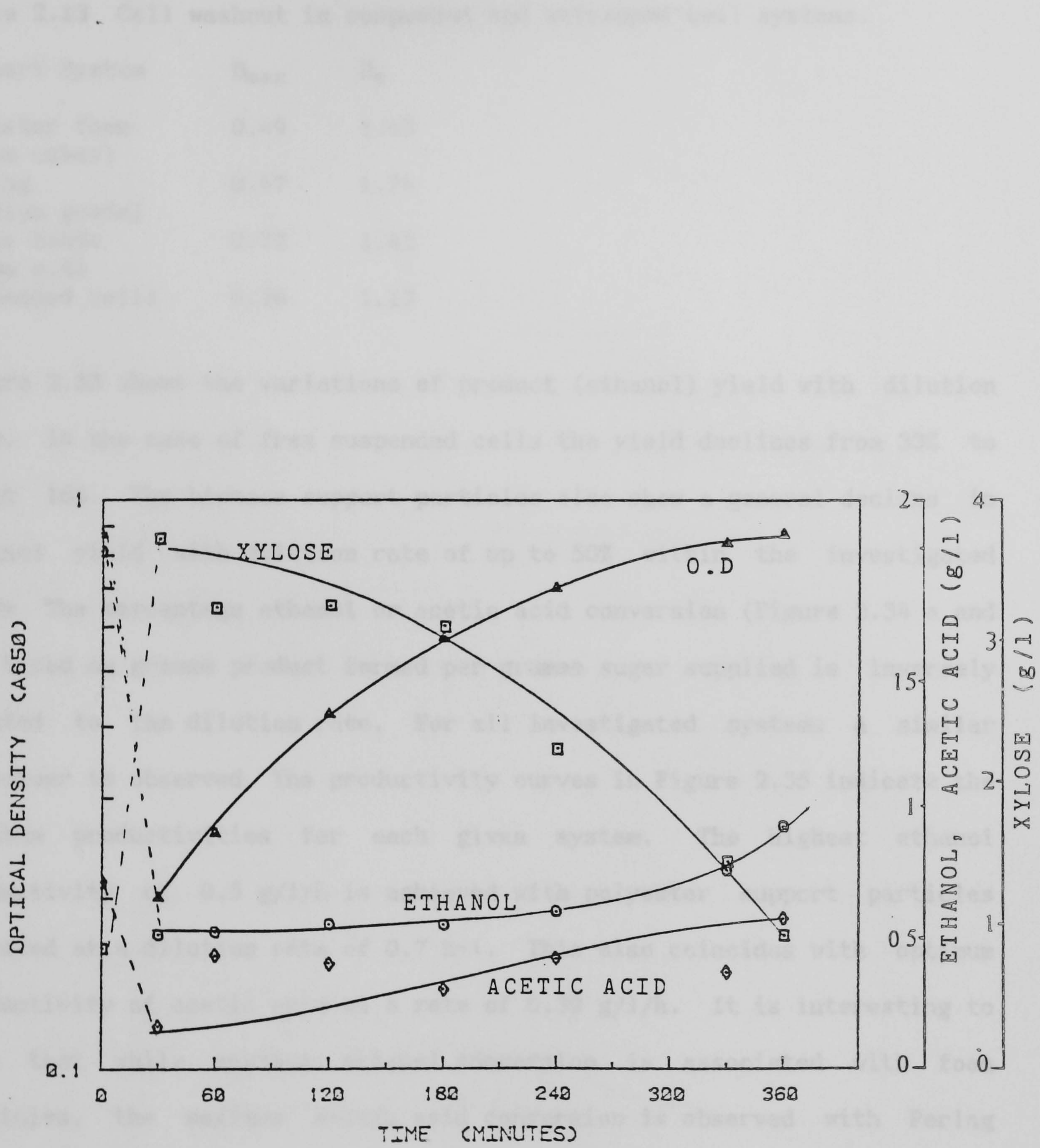

Figure 2.31 Batch growth of CTM 3 cells in the absence of exogenous ethanol.

Table 2.13 Cell washout in suspended and entrapped cell systems.

Support System	D_{max}	D_w
Polester foam (5 mm cubes)	0.49	1.63
Perlag (medium grade)	0.47	1.74
Glass beads (3 mm o.d)	0.35	1.83
Suspended cells	0.28	1.13

Figure 2.33 shows the variations of product (ethanol) yield with dilution rate. In the case of free suspended cells the yield declines from 33% to about 16%. The biomass support particles also show a general decline in ethanol yield with dilution rate of up to 50% within the investigated range. The percentage ethanol or acetic acid conversion (Figure 2.34 a and b) based on gramme product formed per gramme sugar supplied is inversely related to the dilution rate. For all investigated systems a similar behaviour is observed. The productivity curves in Figure 2.35 indicate the optimum productivities for each given system. The highest ethanol productivity of 0.5 g/l/h is achieved with polyester support particles operated at a dilution rate of 0.7 h^{-1}. This also coincides with optimum productivity of acetic acid at a rate of 0.39 g/l/h. It is interesting to note that while maximum ethanol conversion is associated with foam particles, the maximum acetic acid conversion is observed with Perlag support particles at 0.47 g/l/h.

The continuous culture experiments concluded the microbiological studies of the project. The main features of these results may be summarised as follows;

- In *C.thermosaccharolyticum* , production of ethanol and acetic acid occur concomitantly with cell growth. Under optimum conditions of pH and temperature ethanol constitutes the major end-product but acetic acid production may become dominant if ethanol production is suppressed.

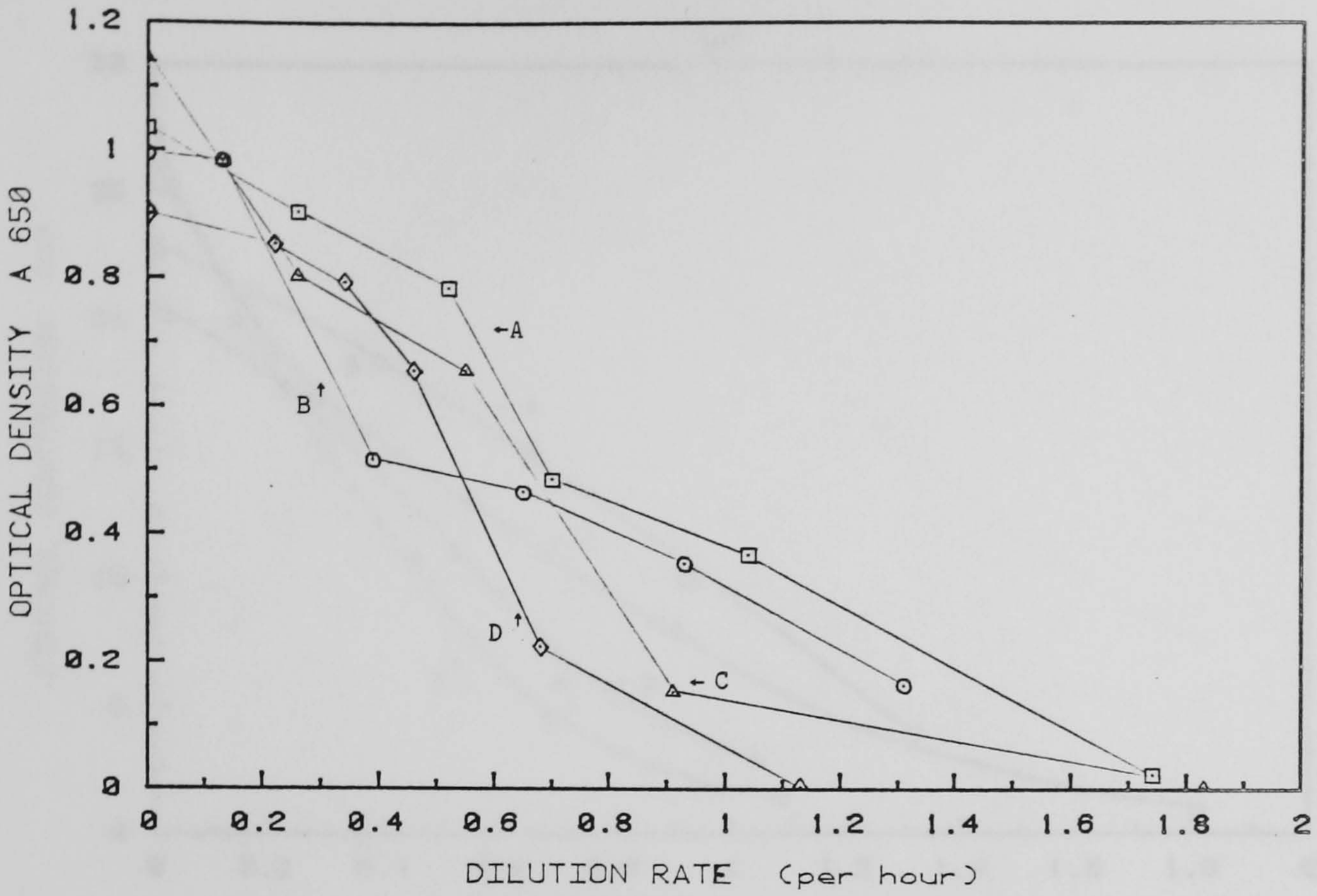

Figure 2.32 Continuous growth of wild type C.thermosaccharolyticum.
Variation of the cell density with the dilution rate.
A : Polyester foam particles; B : Perlag particles; C : Glass beads;
D : Free suspended cells.

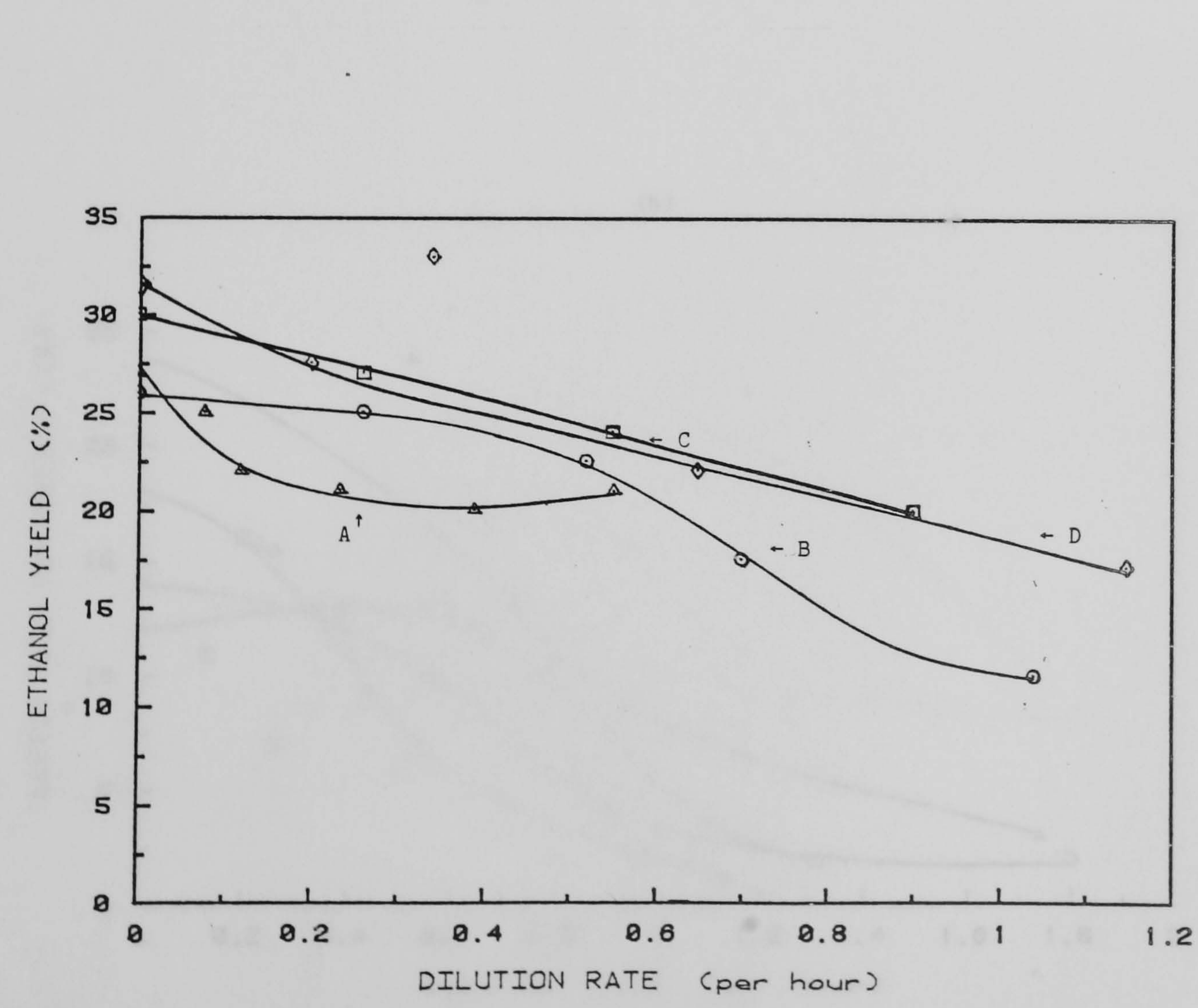

Figure 2.33 Continuous growth of wild type C.thermosaccharolyticum .
Variations of ethanol yield (g ethanol produced/ g xylose consumed) with dilution rate.
A : Polyester foam particles; B : Perlag particles; C : Glass beads;
D : Free suspended cells.

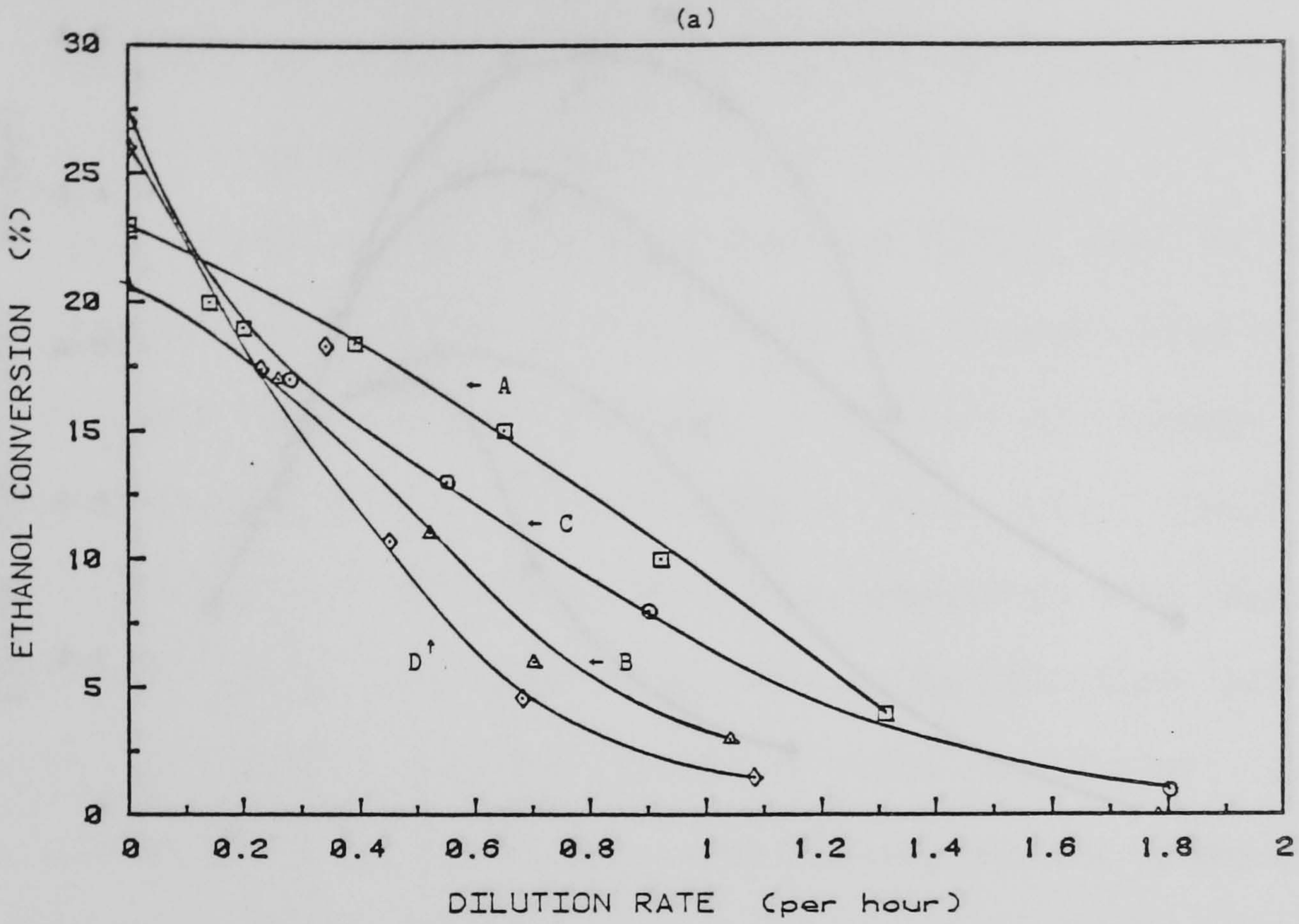

Figure 2.34a Continuous growth of wild type C.thermosaccharolyticum.
Variation of ethanol conversion (g ethanol/g feed xylose) with dilution rate.
A : Polyester foam particles; B : Perlag particles; C : Glass beads;
D : Free suspended cells.

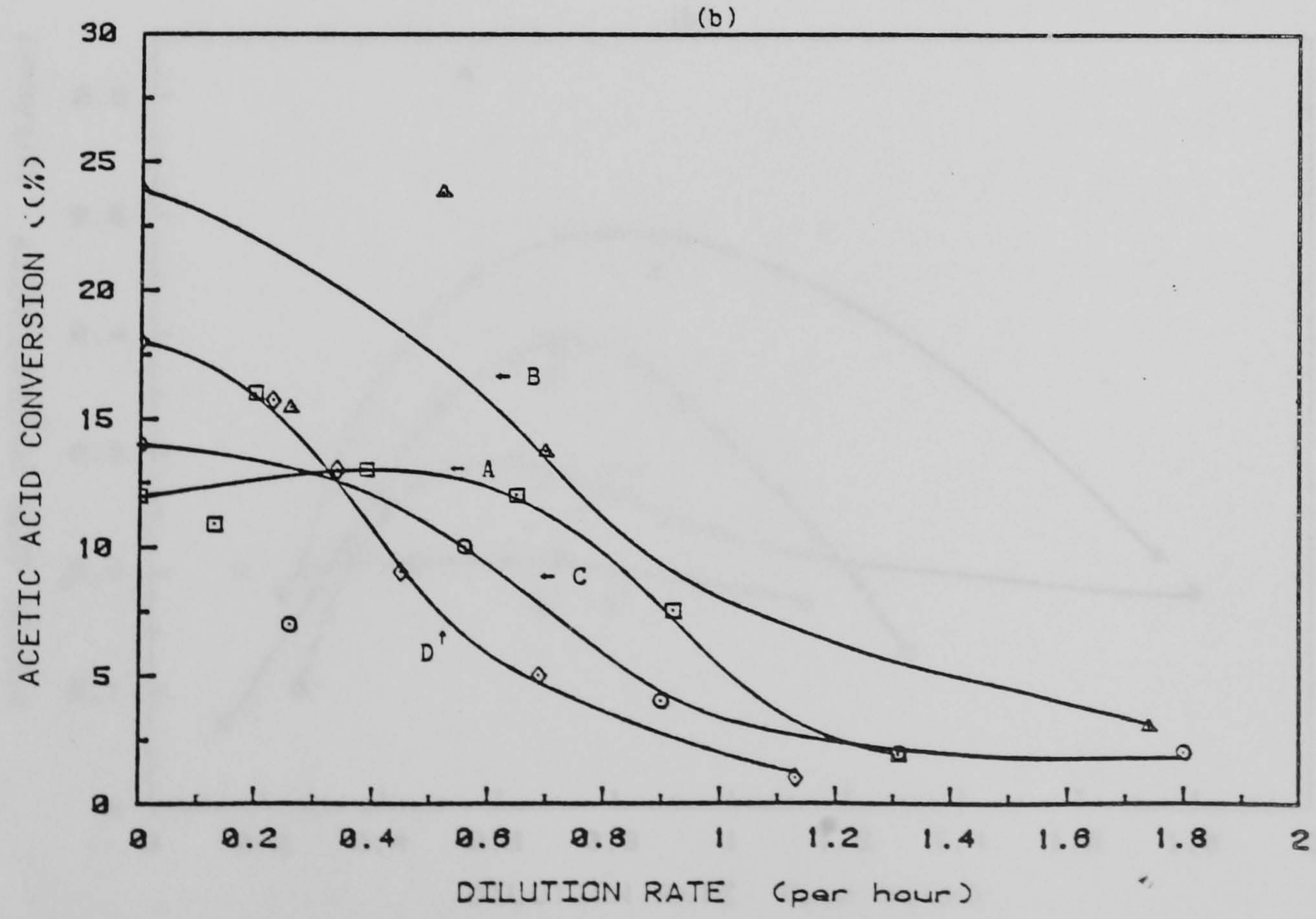

Figure 2.34b Continuous growth of wild type C.thermosaccharolyticum.
Variations of acetic acid conversion (g acetic acid/g feed xylose) with dilution rate.
A : Polyester foam particles; B : Perlag particles; C : Glass beads;
D : Free suspended cells.

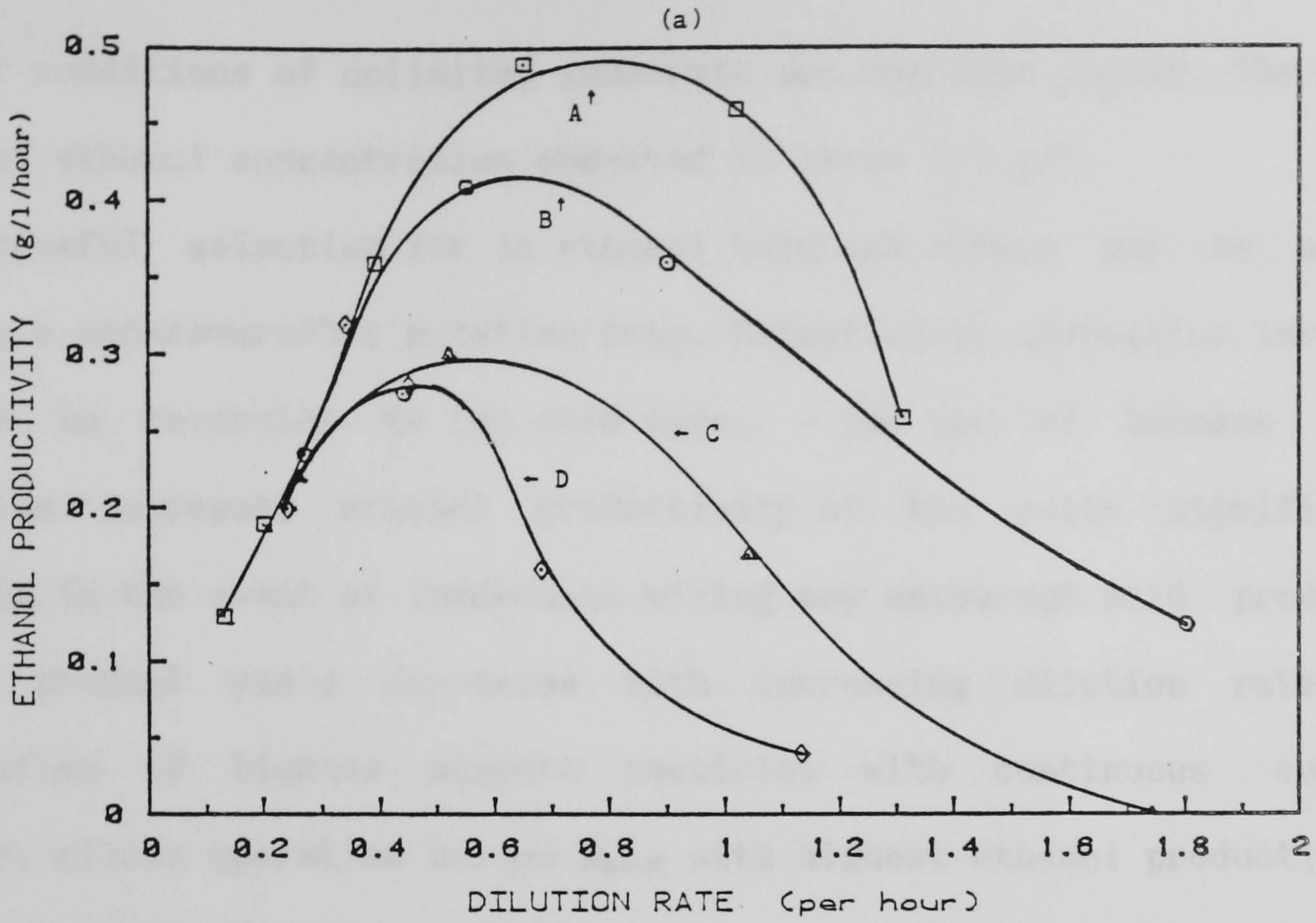

Figure 2.35a Continuous growth of wild type C.thermosaccharolyticum.
Determination of maximum ethanol productivity
A : Polyester foam particles; B : Perlag particles; C : Glass beads;
D : Free suspended cells.

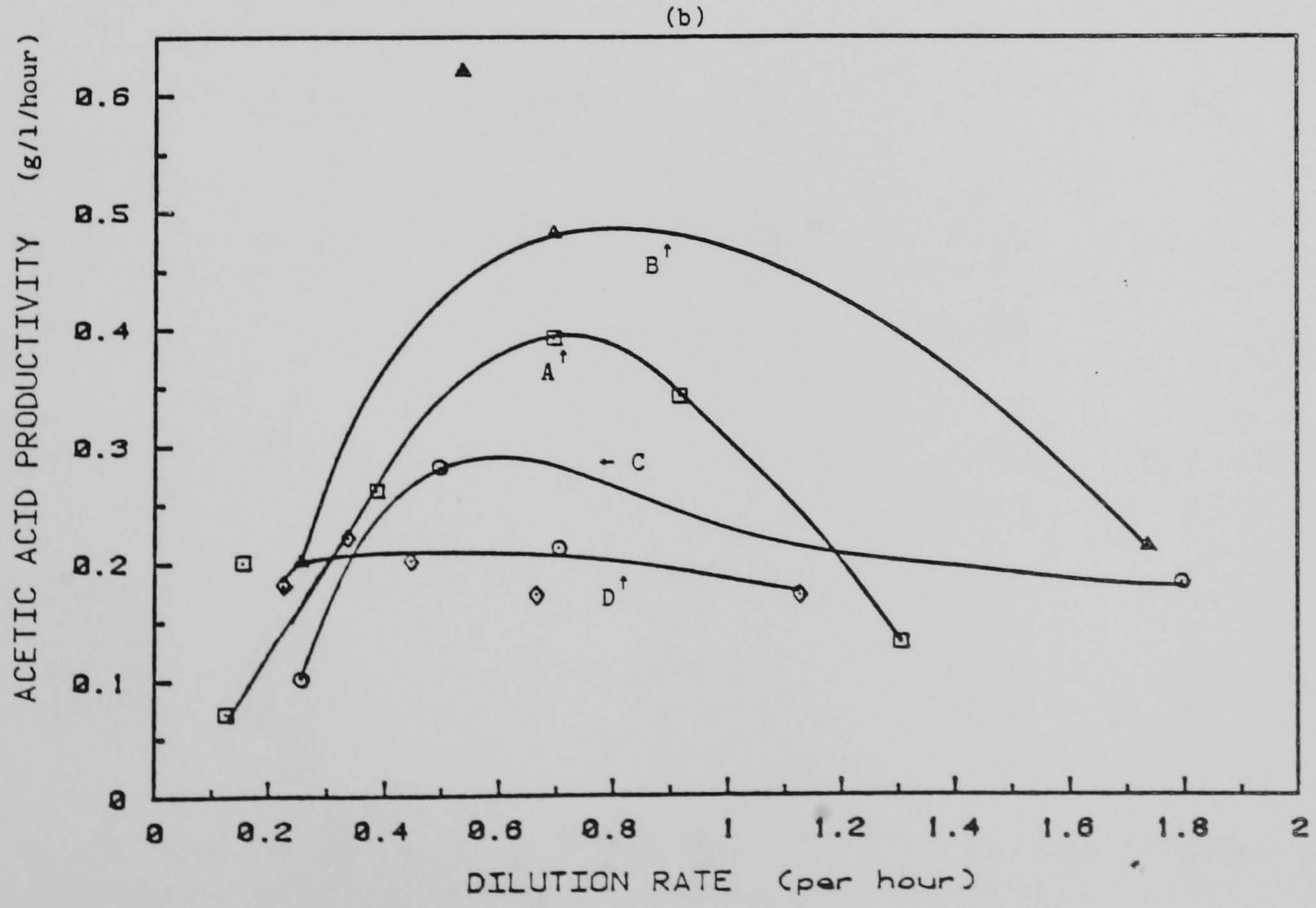

Figure 2.35b Continuous growth of wild type C.thermosaccharolyticum.
Determination of maximum acetic acid productivity.
A : Polyester foam particles; B : Perlag particles; C : Glass beads;
D : Free suspended cells.

- Under conditions of unlimited substrate and nutrient supply, the maximum level of ethanol concentration observed is below 2.5 g/l.

- Successful selection for an ethanol tolerant strain may be achieved through a non-reversible mutation step. Selection by adaptation invariably results in reversion to the wild type. - The use of biomass support particles increases ethanol productivity of the cells significantly, although in the event of inadequate mixing may encourage acid production.

- The product yield decreases with increasing dilution rate. The combination of biomass support particles with continuous cultures, however, allows operation beyond D_{max} with highest ethanol productivity of 0.5 g/l/h observed at D = 0.7 h^{-1}.

2.4 Discussion

2.4.1 Growth Studies

Basic phsyiological studies of *C.thermosaccharolyticum* revealed the optimum growth conditions for this organisms as observed elsewhere (Hsu and Ordal 1970, Fang 1980, Landuyt *et al* 1983, Aduse-Opoku and Mitchell 1988). Considerable variation of the reported data on growth and fermentation behaviour is primarily due to employment of different strains of the organism or various growth media. Table 2.14 presents a summary of some of the growth observations made in the past few years. Early experiments of Hsu and Ordal (1969 a) showed the ability of *C. thermosaccharolyticum* to grow on a variety of carbon sources with different maximum specific growth rates.

Table 2.14 Growth of *C.thermosaccharolyticum* with different carbon source[1].

Reference	Maximum specific growth rate h^{-1}					
	Glucose	Fructose	Galactose	Xylose	Cellobiose	Starch
Hsu and Ordal (1969a)[2]	0.578	0.501	0.55	-	0.26	0.147
Fang (1980)[3]	0.25	0.25	0.25	0.25	0.15	-
Landuyt *et al* (1983)[2]	-	-	-	0.33	-	-
Aduse-Opoku and Mitchell (1988)[2]	0.6	-	-	0.46	0.2	-
Present Study						
(RCM)[2]	0.6	-	-	0.46	-	-
(MCR)[2]	0.45	-	-	0.33	-	-
(MCR)[3]	0.6	-	-	0.46	-	-

Notes : 1- Based on media containing 0.5-1% (w/v) carbon source.
2- Batch cultures without automatic pH control.
3- Batch cultures with automatic pH control (≈pH 7).

From the studies of Hsu and Ordal (1969a) it may be observed that the growth rate is strongly dependent on the carbon supply. The rate of transport across the membrane and the path for metabolism may vary for different sugars (Rogers, 1986). The simple growth medium employed by Fang (1980) could account for the slow growth rates observed irrespective of the carbon supply. However this is contrary to the observations made in this study with a similar medium. Although only growth on xylose and glucose was investigated, under all conditions a higher growth rate with glucose was observed. Studies of Aduse-Opoku (1987) with the same organism and the medium employed by Hsu and Ordal (1969a) also showed a similar observation. Similar to the wild type, the growth of the mutant CTM 3 showed faster growth in presence of glucose than with xylose. The selection procedure did not affect the sugar uptake of the organism and preference for glucose was still observed with the mutant.

Growth at high sugar concentration (Figure 2.16) indicated a low tolerance for osmotic changes. The optimal sugar concentration at 1% (w/v) is typical for many fermentative bacteria. Studies of Fang (1980) revealed similar observations with xylose as the carbon source. It is however encouraging to note that even 10% (w/v) sugar concentration does not completely inhibit growth and some degree of survival is maintained. The low sugar tolerance is normally overcome by fed-batch cultures which will be discussed later.

Optimum growth of *C.thermosaccharolyticum* near neutral pH was reported by Hsu and Ordal (1969a) and Fang (1980). This was investigated by observing batch cultures at different pH (Figure 2.18) within the range of 4.5-8. The optimum pH of 6.8 for the cellular growth was confirmed. The ability of the organism for better growth under acidic conditions could be explained in terms of physiological behaviour and metabolism.

Coupling of ATP-forming and ATP-utilising reactions is a center piece of

anaerobic metabolism. For *C.thermosaccharolyticum* most of the carbon energy source is utilised to supply ATP rather than cell mass (Rothstein 1986). As shown in section 2.1 the overall pathway of alcohol fermentation generates one molecules of ATP per molecule of pyruvate formed. However formation of acetate from acetyl Co~A by phosphotransacetylase and acetokinase generates an additional molecule of ATP for every acetate molecule made. This mode of metabolism is concomitant with reduction of acetaldehyde to ethanol to regenerate NAD^+. The evidence for this pathway in *E.coli* was offered by Brown (1977) and later examined for *C.thermosaccharolyticum* by Rothstein (1986). Although equimolar quantities of ethanol and acetic acid are anticipated, it has been shown that under optimum growth conditions larger amounts of ethanol are produced in the ratio of 1.5-2 : 1 (Rothstein, 1986). Studies of Landuyt and Hsu (1984) also indicate that ethanol concentration exceeded acetate concentration and yet was not preceded by acetate production. These results correlate well with the former report and the observations made in the present study.

2.4.2 Influence of PH

As well as acetic acid, small quantities of lactic and butyric acid are also produced, thus rendering the natural intracellular condition of the cell acidic. Due to low solubilitiy of carbon dioxide at 60°C, any pH change as a result of hydration of dissolved CO_2 is thought minimal. In the course of fermentation, end-products accumulate inside the cell and form a concentration gradient directed towards the extracellular environment. The cell secretes the accumulated end-products down this concentration gradient. The free protons further contribute in facilitating transport of nutrients across the membrane. Hence any exogenous pH manipulation would require to allow for normal cellular functions. Over exposure to an alkali gradient would act as a proton sink

and thus interfere with membrane functions. An acidic gradient on other hand suppresses the transport of the acid end-products from the cells and may cause toxic accumulations. It has been shown however that similar fermentative neutrophiles show better survival under acidic conditions (Rogers, 1986).

From the batch culture studies it is evident that maximum specific growth rate is strongly influenced by pH. Cells grow best at pH 6.8 and any reduction in pH is accompanied by a slower growth rate until complete cessation at pH 4.5. Landuyt and Hsu (1984) observed complete cell death at pH 4.2. This is perhaps due to loss of enzymatic activity and/or membrane disorders. It is further observed that at around pH 6.3 an exponential decline in the pH in direct relationship to the maximum specific growth rate takes place (Figure 2.27a). At approximately pH 5.7 cellular growth enters the declining phase, whereas the rate of change of pH remains constant until pH 4.8. At this point both cell growth and pH reach a plateau with only slight changes until the terminal point of pH 4.5. These observations support the contention that a proton concentration gradient can influence the end-product formation in two ways, firstly by effecting μ_o and secondly by influencing mass transfer across the membrane. Batch fermentation studies at different pH were anticipated to indicate maximum yields at near neutral pH. The maximum yield of ethanol around 55% was obtanied at pH 6.8. This result however did not coincide with the acetic acid yield where a maximum yield at pH 6.5 was observed. This is unlike the observations made elsewhere. Landuyt and Hsu (1984) reported that in the pH range of 5-7, the final concentration of ethanol produced in batch cultures was effected only minimally by any change in pH. In contrast Fang (1980) showed that between pH 6 and 7 the ethanol concentration was maximum at pH 6.5 and the acetic acid concentration remained constant at all pH values within the

anaerobic metabolism. For *C.thermosaccharolyticum* most of the carbon energy source is utilised to supply ATP rather than cell mass (Rothstein 1986). As shown in section 2.1 the overall pathway of alcohol fermentation generates one molecules of ATP per molecule of pyruvate formed. However formation of acetate from acetyl Co~A by phosphotransacetylase and acetokinase generates an additional molecule of ATP for every acetate molecule made. This mode of metabolism is concomitant with reduction of acetaldehyde to ethanol to regenerate NAD^+. The evidence for this pathway in *E.coli* was offered by Brown (1977) and later examined in *C.thermosaccharolyticum* by Rothstein (1986). Although equimolar quantities of ethanol and acetic acid are anticipated, it has been shown that under optimum growth conditions larger amounts of ethanol are produced in the ratio of 1.5-2 : 1 (Rothstein, 1986). Studies of Landuyt and Hsu (1984) also indicate that ethanol concentration exceeded acetate concentration and yet was not preceded by acetate production. These results correlate well with the former report and the observations made in the present study.

2.4.2 Influence of PH

As well as acetic acid, small quantities of lactic and butyric acid are also produced, thus rendering the natural intracellular condition of the cell acidic. Due to low solubility of carbon dioxide at 60°C, any pH change as a result of hydration of dissolved CO_2 is thought minimal. In the course of fermentation, end-products accumulate inside the cell and form a concentration gradient directed towards the extracellular environment. The cell secretes the accumulated end-products down this concentration gradient. The free protons further contribute in facilitating transport of nutrients across the membrane. Hence any exogenous pH manipulation would require to allow for normal cellular functions. Over exposure to an alkali gradient would act as a proton sink

and thus interfere with membrane functions. An acidic gradient on other hand suppresses the transport of the acid end-products from the cells and may cause toxic accumulations. It has been shown however that similar fermentative neutrophiles show better survival under acidic conditions (Rogers, 1986).

From the batch culture studies it is evident that maximum specific growth rate is strongly influenced by pH. Cells grow best at pH 6.8 and any reduction in pH is accompanied by a slower growth rate until complete cessation at pH 4.5. Landuyt and Hsu (1984) observed complete cell death at pH 4.2. This is perhaps due to loss of enzymatic activity and/or membrane disorders. It is further observed that at around pH 6.3 an exponential decline in the pH in direct relationship to the maximum specific growth rate takes place (Figure 2.27a). At approximately pH 5.7 cellular growth enters the declining phase, whereas the rate of change of pH remains constant until pH 4.8. At this point both cell growth and pH reach a plateau with only slight changes until the terminal point of pH 4.5. These observations support the contention that a proton concentration gradient can influence the end-product formation in two ways, firstly by effecting μ_o and secondly by influencing mass transfer across the membrane. Batch fermentation studies at different pH were anticipated to indicate maximum yields at near neutral pH. The maximum yield of ethanol around 55% was obtained at pH 6.8. This result however did not coincide with the acetic acid yield where a maximum yield at pH 6.5 was observed. This is unlike the observations made elsewhere. Landuyt and Hsu (1984) reported that in the pH range of 5-7, the final concentration of ethanol produced in batch cultures was effected only minimally by any change in pH. In contrast Fang (1980) showed that between pH 6 and 7 the ethanol concentration was maximum at pH 6.5 and the acetic acid concentration remained constant at all pH values within the

investigated range. It is thought that variation in results stems from different culture conditions. The reported data in both studies indicate maximum specific growth rates of around 0.25 h^{-1}. The comparatively slower growth (cf $\mu_{ox} \approx 0.46\ h^{-1}$) is further complicated by the inconsistencies frequently encountered by batch cultivation. From these observations it is fair to assume that maximum ethanol yield lies in the pH range of 6.5-6.8.

2.4.3 Selection for the Ethanol Tolerant Strain, CTM 3

Selection for the 3% (w/v) ethanol tolerant strain CTM 3, was successfully carried out by the method described in section 2.2.3. The CTM 3 cells appeared very different from their wild type parents; they were longer and grew slower. Size distribution analysis of these cells indicated that an increase in cell size was related to the solvent concentration in the medium. Hsu and Ordal (1970) observed such changes prior to sporulation of *C. thermosaccharolyticum* and suggested that rapid growth rates observed with readily utilisable carbon sources such as glucose exerted a catabolic repression of the NADPH generating system, and that this repression was sufficient to prevent sporulation. In a later study Landuyt and Hsu (1984) reported on similar morphological observations regarding ethanol fermentation and cells up to 40-50 times their wild type size were observed. The ethanol tolerant mutant SD105 employed by Landuyt and Hsu (1984) was obtained in the same way as CTM 3 reported in the present work. The stability of these selected strains was examined in both batch and continuous cultures. It was observed that by subculturing these cells into a rich medium such as RCM, without any exogenous ethanol, a reversion of cells to their wild type state was achieved. Such back mutation however, was reversible and a further subculture from the rich medium into MCR containing exogenous ethanol resulted in a return to the CTM 3 cells. Similarly a continuous culture of CTM 3 cells was maintained for 4 days

without any apparent reversion to the wild type characteristics. However a batch growth of these cells achieved by diluting the cells with fresh medium, immediately caused reversion to wild type state with lower final ethanol concentration (Figure 2.31). These observations correlate well with growth studies of SD 105. Continuous elongated cell growth on xylan was maintained for 26 hours until hexose as carbon source was introduced to the medium and normal vegetative growth similar to wild type resumed (Landuyt and Hsu, 1983). Although similar morphological changes have been observed with a number of *clostridia* (Rogers, 1986) there are no explanations provided for its mechanism and regulation. It may be suggested that a malfunction in the normal binary fission brought about by environmental changes leads to elongated growth. Such conditions normally trigger sporulation in spore forming organisms (Pheil and Ordal 1967). Thus the elongated intermediate stage could provide for a storage function of the cell prior to the dormant phase.

The growth of the wild type was completely inhibited by supplementing the growth medium with 4% (w/v) ethanol (Figure 2.23). It is thought that like the findings of Herrero and Gomez (1982) with *C. thermocellum* , the ability of CTM 3 to tolerate high solvent concentrations is due to selection for cells able to maintain the homoviscosity of their membrane at reduced fluidity. Thus it may be suggested that adaptation and selection beyond tolerance at 3% (w/v) may be possible although not necessarily stable under ambient conditions of wild type growth. The product tolerance of the mutant strain CTM 3 was shown to have a marked improvement over the wild type cells (Figure 2.23). Although tolerance to the exogenous ethanol was never matched with the actual amount of alcohol produced, higher ethanol concentrations with batch fermentations were observed (Figure 2.24 a and b). This was however achieved at the expense of reduced growth rate. Table 2.10 shows the increased growth of the

mutant after a further 24 hours incubation compared with a decline for the wild type cells. The mutant strains HG-3 and HG-6 isolated in a similar fashion by Fang (1980) were able to grow in the presence of 3.5% and 4.0% (w/v) ethanol respectively. At 3% (w/v) ethanol, HG-3 was reported to grow only marginally better than the wild type strain (by about 25%), whereas HG-6 showed around 70% improvement. The latter compares favourably with the performance of CTM 3 where at the same ethanol concentration a 60% improvement was observed (Figure 2.23). The ethanol productivities of HG-3 and HG-6 were astonishingly higher and under fed-batch cultivation, HG-6 produced almost same amount of ethanol (about 37.5 g/l) as it could tolerate exogenously. These observations could not be repeated in our labarotory. The highest ethanol concentration observed did not exceed 2.5 g/l which was similar to the reported data by Landuyt *et al* (1983) where a maximum concentration of 2.16 g/l ethanol was reported.

The effect of ethanol inhibition was observed in almost all fermentation studies. In the presence of excess substrate supply the growth ceased prematurely at ethanol concentrations around 1.5 g/l. The growth kinetics were found to be adequately described by Levenspiel's general relationship in which the effect of end-product inhibition was taken into account. It was found that the linear relationship best fitted the data and provided a good correlation with the experimental data in the order 0.98. Undoubtedly this indicates an imperfect fit , but in view of the scatter of the experimental data the model is thought reasonably accurate.

2.4.4. Ethanol Fermentation with the Immobilised Cell Systems

Growth of yeast and bacteria on inert biomass support particles (BSPs) such as the samples used in this study is well documented elsewhere (Atkinson and Mavituna, 1986). Study of porous BSPs indicated high affinity for local colonisation by cells. Both biological and physico-

hydrogen yields of around Y_H= 0.6% (Rogers, 1986). It has been shown that by increasing the partial pressure of hydrogen in the head space of a *C.thermocellum* culture, a slight increase in ethanol concentration may be obtained (Ziekus *et al* , 1981). Increased solvent productivity may be alternatively achieved by inhibition of hydrogenase activity by carbon monoxide (Datta and Zeikus, 1985). Thermophilic operation minimises the solubility of gaseous end-products in the fermentation broth. It is therefore unlikely that suppression of CO_2 or H_2 will be of practical use. Moreover accumulation of carbon dioxide may inhibit conversion of pyruvate to acetyl Co~A and thus lead to formation of lactate.

Growth studies using both glucose and xylose showed preferential growth on glucose (Figure 2.26). Extensive studies of Hsu and Ordal (1970) indicated that such catabolic repression is extended to the pentoses and carbon sources containing a glycosidic linkage. The utilisation of these carbon sources would require activation of normally non-operating metabolic systems. Aduse Opoku and Mitchell (1988) showed that the activity of xylose isomerase and xylulokinase is only induced when xylose uptake commences. It is expected that the phosphorylated xylulose would follow the oxidative phosphate pathway generating ATP, NADPH and NADH. It is interesting to observe that unlike the wild type, the CTM 3 mutant did not exhibit a change in the rate of growth related to the uptake of different carbon sources. The evidence for the catabolic repression however is revealed by analysis of carbon uptake (Figure 2.26b). It therefore appears that for cells growing under stress such as the selected mutant cells, intrinsic factors other than the sugar transport system regulate the rate of metabolism.

The fed-batch growth of the mutant strain of *C.thermosaccharolyticum* CTM 3, is depicted in Figure 2.30. Stepwise addition of carbon source did not allow any increase in overall concentration or yield of end-products for a

glucose grown culture. The results for xylose are considerably different. Despite complete utilisation of xylose, the ethanol concentration did not increase in proportion and consequently a very poor ethanol yield with fed-batch cultures was observed. The acetic acid yield on other hand was maintained at 27% with a final concentration at new levels not previously observed. These results indicate that solvent fermentation precedes acid fermentation up to a point where no further ethanol is produced. Fermentation is then dominated by acid production. The ethanol concentration at this point is in the order of 0.2-0.3% (w/v) and does not compare with observations made by Fang (1980) for a similar experiment where ethanol concentrations of upto 4% (w/v) were reported.

Continuous culture experiments highlight the advantages of immobilised cell systems over free suspension of cells. Experiments employing BSPs were carried out with the tank/column arrangement. Batch studies showed that BSPs are best contained in a packed column rather than a stirred tank system (Figures 2.28 and 2.29).

2.4.6 Continuous Culture

Fermentation studies carried out at optimum growth conditions revealed the percentage conversion, productivity and yield at different dilution rates. Moreover the washout points associated with the maximum specific growth rate were also obtained.

In a continuous culture the dilution rate takes the value of the specific growth rate (Atkinson and Mavituna, 1986). In a non-limiting medium, cells grow at maximum rate at all dilution rates not exceeding the maximum and when cells are removed faster than they can grow. From Figure 2.32 it is observed that none of the fermentation systems behave in the ideal fashion. The concentration of free suspended cells decrease steadily with increasing dilution rate until complete washout at three times D_{max}. The

results for the entrapped cell systems closely follow the former. All the free cells growing in the bulk medium and those sloughed off the support particles are gradually washed away from the system. It may be assumed that in an active culture the number of new cells formed within the particle is proportional to the number of older cells removed hence an approximate estimate of cell retention may be achieved. Larger particles with higher porosity such as the foam particles have higher cell retention than smaller solid particles such as the glass beads (Figure 2.32). Unlike the suspended cell system, BSPs maintain a permanent presence of cells independent of the dilution rate. The cell concentration in the broth however remains related to the dilution rate.

As the cell density inside the fermenter declines the concentration of end-product in the effluent stream becomes more dilute. Figure 2.34 a and b show the percentage conversion of xylose to ethanol and acetic acid respectively. The conversion is proportional to the net amount of biomass in the fermenter, and thus in relation to the dilution rate it follows a similar trend. An interesting result is the evidence of acid fermentation brought about by the Perlag particles which is further supported by the data obtained for the productivity of ethanol and acetic acid (see below). Perlag particles are essentially volcanic agglomerates with high mineral content. This may influence the redox potential of the system towards acid fermentation although no clear evidence for this phenomenon is presented. The productivity values defined as gramme product per litre of broth per hour show maxima in their relation with the dilution rate. Evidently from Figures 3.35 a and b, the trend closely follows the former results for conversion. The maximum productivity P°, of 0.27 g/l/h for free suspended cells occurs at around D_{max} (0.4-0.5 h^{-1}). This is almost half the value observed with the polyester foam particles where P°= 0.50 g/l/h at D = 0.65-0.75 h^{-1}. The highest productivity for acetic acid of 0.48 g/l/h was

observed with Perlag support particles at D = 0.7-0.8 h^{-1}. Due to the lack of data in the literature, these studies can not be compared with any other work. The continuous cultures studies reported by Fang (1980) and Landuyt and Hsu (1984) were carried out with free suspended cells at dilution rates not exceeding the maximum. They found the highest ethanol productivity of 2.2 g/l/h at D = 0.3 h^{-1}, and 0.30 g/l/h at D = 0.14 h^{-1} respectively. The latter corresponds well with results obtained in this study.

In comparison with other organisms able to ferment xylose these results are equally impressive. In Table 2.15 the highest ethanol productivity of 1 g/l/h is observed with enzyme supplemented yeast system. The enzyme xylose isomerase, allows the pentose to be metabolised by the yeast. This system however increase the process costs by invloving a further fermentation step in order to prepare the enzyme supplement. Moreover the xylose isomerase reaction is an equilibrium reaction and at most, 20% of xylose is converted to xylulose. The bacterial systems offer the advantage of higher growth rates and despite lower maximum ethanol concentrations, show reasonable productivities.

The data given for *C. saccharolyticum* in Table 2.15 indicate much lower productivity of ethanol. The effect of incubation temperature on the fermentation end-products of *C. thermosaccharolyticum* IMG 6544, and IMG 6564, has demonstrated considerable variation between the two strains. (Vancanneyt *et al* , 1987). In the absence of evidence for such variation no conclusion may be drawn for the strain employed in this study and further work in this field is recommended.

The estimation of yield of ethanol at different dilution rates as shown in Figure 2.33 indicates that the assumption for a constant yield is not rigorously true for the microbial system investigated in this study. In all cases batch cultures show the highest yields which thereafter decrease

Table 2.15 Fermentation of xylose with yeast, fungi and bacteria.

Source : Skoog and Hahn-Hägerdal (1988)

Microrganism	Xylose (gl^{-1})	Maximum ethanol (gl^{-1})	Yield (gg^{-1})	Productivity ($gl^{-1}h^{-1}$)	Cultivation time (h)	By-product (gl^{-1})	Substrate consumption (%)
Yeast							
S.cerevisiae + Novo sweetzyme	120	34.6	0.29	0.74	47	16.7	
S.cerevisiae + MKC Optisweet P	48	24	0.5	1.0	24	4	100
Fungi							
Monila sp	50	10	0.2	0.06	168		
Fusarium oxysporum VTT D-80134	50	25	0.5	0.17	144		100
Bacteria							
Thermoanaero-bacter ethanolicus	10	4.8	0.48	0.12	40		100
Zymomonas anaerobia	26	37.3	0.29	0.78	48		59
Clostridium sacc-harolyticum ATCC 35040	26	8.5	0.07	0.05	168		29

with increasing dilution rate. This is most likely accounted for by the intrinsic changes within *C.thermosaccharolyticum* brought about by the environmental factors indicated earlier. Thus in this case it is incorrect to assume constant product yield at all dilution rates although such values may be interpolated by fitting a curve to the experimental results. The results for continuous culture indicate that with the view of xylose fermentation, *C.thermosaccharolyticum* can certainly produce a relatively high amount of ethanol. Together with the ability to grow at high temperature and metabolise pentoses other than xylose, the organism projects great industrial potential. At present however such applications are limited due to high pretreatment cost of the substrate and relatively cheap price of petroleum.

Chapter Three

Design and Operation of Gas-Lift Fermenters

Design and Operation of Gas-Lift Fermenters

3.1 Background

Large scale batch or continuous fermentation of ethanol is mostly carried out in large mechanically agitated tanks (Atkinson, 1974). Indeed stirred tanks remain the most widely used type of reactor vessels in both chemical and biochemical industry (Figure 3.1 a). Many laboratary scale fermentation and cell culture experiments are carried out relatively successfully in small mechanically stirred vessels. Such experience in operation has led to good technical expertise and helped to provide successful models to simulate the process system. Good mixing is achieved by the mechanical action of the impellers which can be of various designs and configurations depending upon the process requirements and the flow behaviour of the fermentation fluids. Theoretically there is no concentration gradient with such a system and in practical terms, it generally provides a satisfactory mixing of low solubility substrates (e.g oxygen) in the liquid phase.

As indicated in Chapter 2 applications of stirred tanks are no longer universal to all fermentation systems and in the case of immobilised cell systems it is often replaced by packed or fluidised bed reactors. Other pertinent limitations are difficulties frequently encountered in scale-up of the stirred tanks and high attrition and shear rate as a result of the impeller action. Aseptic design of large scale stirred tanks has been shown to be particularly difficult due to the moving parts involved. Moreover because of variations in hydrodynamics, power dissipation, and heat and mass transfer rates many empirical design equations derived for laboratary scale fermenters do not translate into large scale systems. It is, therefore, often necessary to study and design intermediate pilot scale vessels.

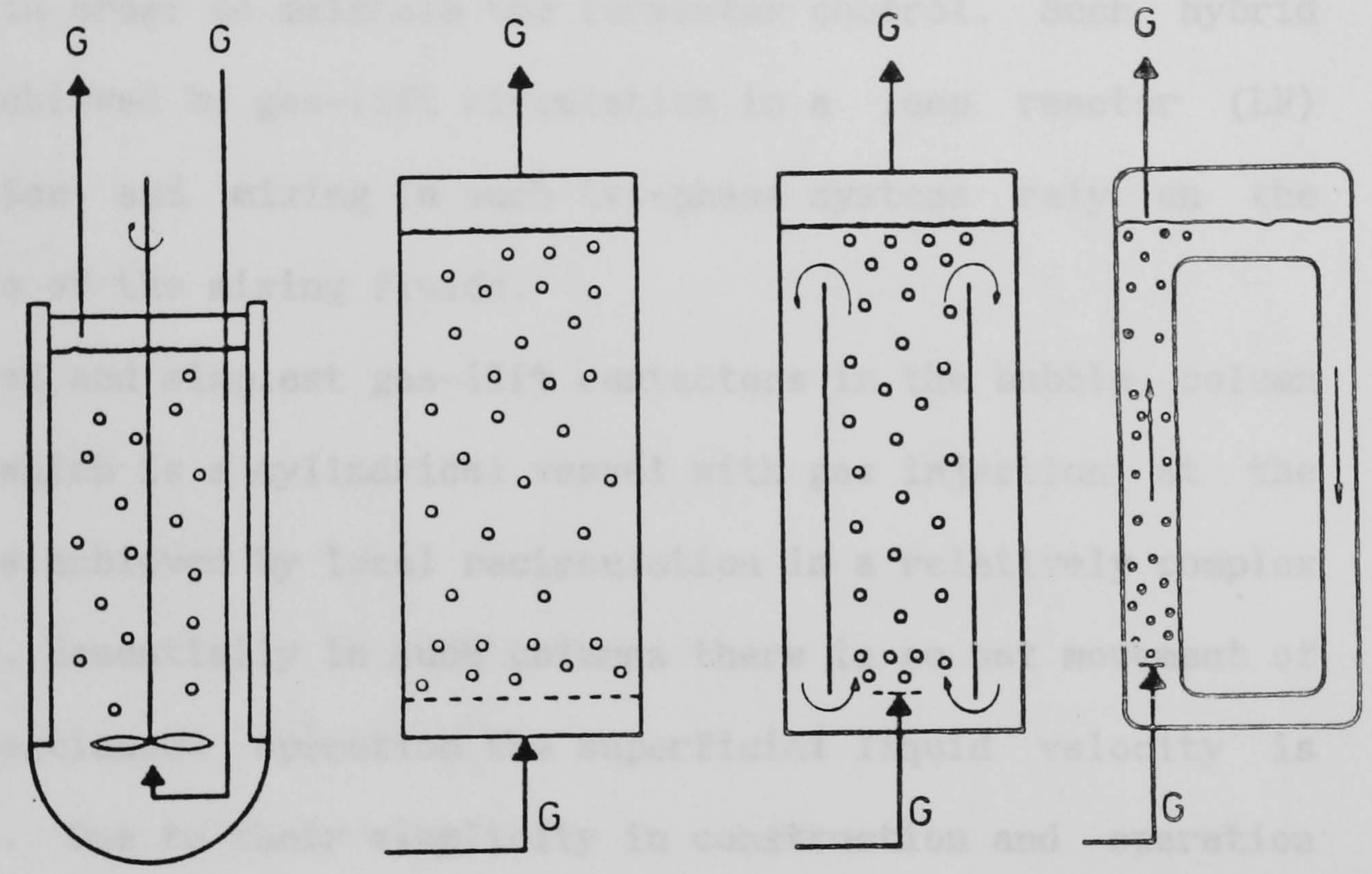

Figure 3.1 Types of gas-liquid contactors for submersed fermentations

Onken and Weiland,(1983)

Design improvements on both stirred and plug flow systems by incorporating baffles or recycle lines have increased reactor performance (Levenspiel, 1972). Ideally the necessary mixing , dispersing, and cooling effects should be achieved at the lowest power input. It is therefore desirable to combine the advantages of plug flow concentration gradients for a better mass transfer and a smaller fermenter volume with the stirred tank mixing characteristics in order to maintain the fermenter control. Such hybrid design may be achieved by gas-lift circulation in a loop reactor (LR) system. Circulation and mixing in such two-phase systems rely on the density difference of the mixing fluids.

One of the earliest and simplest gas-lift contactors is the bubble column (Figure 3.1 b) which is a cylindrical vessel with gas injection at the bottom. Mixing is achieved by local recirculation in a relatively complex and random manner. Essentially in such columns there is no net movement of liquid. Under continuous operation the superficial liquid velocity is almost negligible. Due to their simplicity in construction and operation bubble columns are widely used in the industry as absorbers, strippers, gas-liquid reactors etc.. The flow behaviour of fluids in bubble columns has been extensively studied in the past and recently reviewed by Viswanathan (1986). In a comparative study Weiland and Onken (1981) investigated the hydrodynamic behaviour and bubble flow in the response to a number of influencing parameters such as liquid properties and reactor geometry. Godbole and Shah (1986) have also examined the design and operation of bubble column reactors. Circulation in bubble columns is enhanced by introduction of baffles or a concentric draught tube (CDT) in order to create defined flow zones or loops (Hatch, 1973). A number of different baffle arrangement has been designed and some of them are shown in Figures 3.1 and 3.2 In contrast to the random liquid motion in bubble columns, loop reactors show a directed, well defined circulation flow

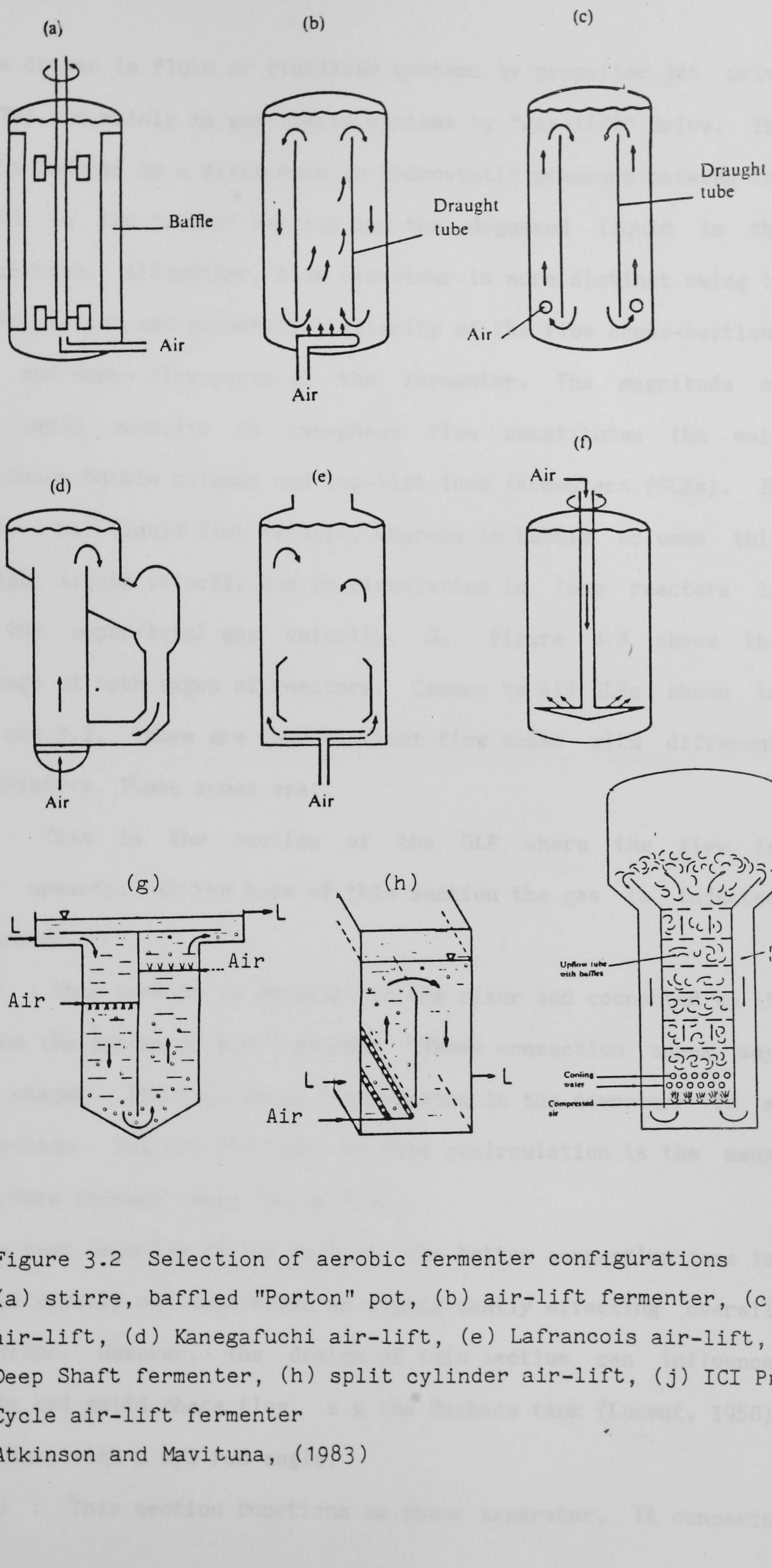

Figure 3.2 Selection of aerobic fermenter configurations
(a) stirre, baffled "Porton" pot, (b) air-lift fermenter, (c) Wasco air-lift, (d) Kanegafuchi air-lift, (e) Lafrancois air-lift, (g) ICI Deep Shaft fermenter, (h) split cylinder air-lift, (j) ICI Pressure Cycle air-lift fermenter
Atkinson and Mavituna, (1983)

which can be driven in fluid or fluidised systems by propeller jet drive (Blenke, 1979) and mainly in gas-liquid systems by "gas-lift" drive. The circulation is induced by a difference in hydrostatic pressure between the gassed liquid in the "riser" section and the degassed liquid in the "downcomer" section. Altogether, flow behaviour is more distinct owing to predictive circulation and geometric similarity of the flow cross-sections in the up- and down- flow parts of the fermenter. The magnitude of superficial liquid velocity in two-phase flow constitutes the main difference between bubble columns and gas-lift loop fermenters (GLFs). In GLF there is a net liquid flow velocity whereas in bubble columns this is zero. High liquid velocity due to circulation in loop reactors is related to the superficial gas velocity, J_G. Figure 3.3 shows the operation range of both types of reactors. Common to all GLFs shown in Figures 3.1 and 3.2, there are four distinct flow zones with different flow characteristics. These zones are;

The riser : This is the section of the GLF where the flow is predominantly upwards. At the base of this section the gas is injected into the fermenter.

The Downcomer : This section is parallel to the riser and connected to it at the top and the bottom of the fermenter. These connection zones may take diverse shapes. The dispersion recirculates in the downcomer in a downward direction. The driving force of this recirculation is the mean density difference between these two sections.

The base : In vast majority of GLF designs, the bottom connection zone is very simple and usually not considered as significantly affecting overall reactor behaviour. However, the design of this section can influence liquid velocity and solid phase flow, e.g the Pachuca tank (Lamont, 1958) has a conical base with a $\pi/3$ rad angle.

The head space : This section functions as phase separator. It connects

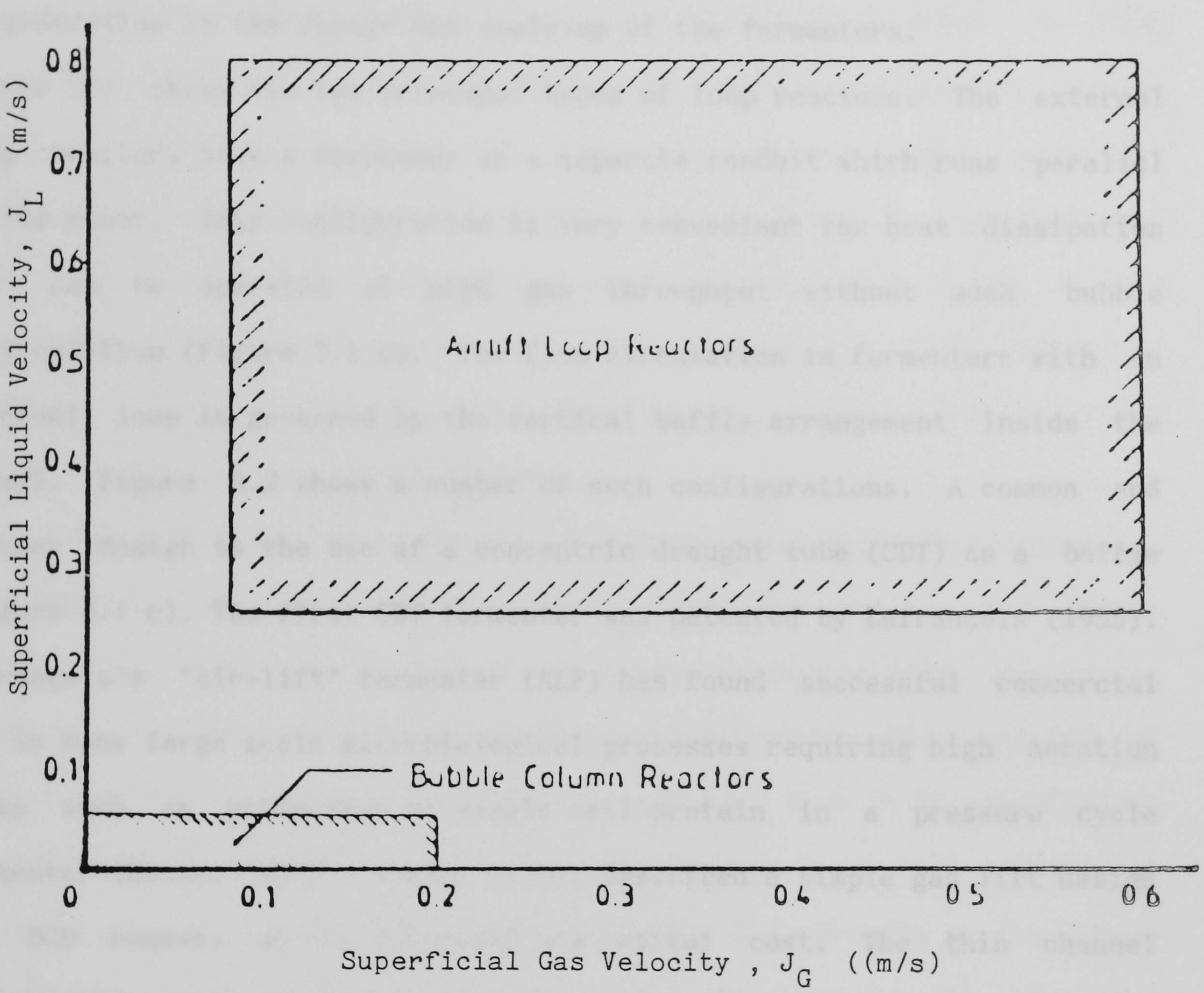

Figure 3.3 Operating ranges of bubble columns and air-lift loop reactors

Weiland and Onken (1981)

the riser to the downcomer at the top of the fermenter. The degree of gas disengagement is related to the design of this section.

In general behaviour of any GLF is related to the interaction of these parts. The specific characteristics of each section should be taken into consideration in the design and scale-up of the fermenters.

Figure 3.1 shows the two principal types of loop reactors. The external loop reactors have a downcomer as a separate conduit which runs parallel to the riser. This configuration is very convenient for heat dissipation and can be operated at high gas throughput without much bubble recirculation (Figure 3.1 d). The flow circulation in fermenters with an internal loop is governed by the vertical baffle arrangement inside the vessel. Figure 3.2 shows a number of such configurations. A common and popular design is the use of a concentric draught tube (CDT) as a baffle (Figure 3.1 c). The first CDT fermenter was patented by Lefrançois (1955). Lefrançois's "air-lift" fermenter (ALF) has found successful commercial use in many large scale microbiological processes requiring high aeration rates such as production of single cell protein in a pressure cycle fermenter (Hines, 1978). Gasner (1974) described a simple gas lift design for BOD removal at low operating and capital cost. The thin channel rectangular ALF (Figure 3.2) offers an attractive alternative to conventional waste water treatmnet reactors. Its low degree of coalescence in the upflow and enhanced entrainment in the downflow is even more efficient than other internal loop configurations. Based on the same principle an aeration system employing a long vertical shaft of 100 m was developed by the ICI for waste water treatment (Kubota, 1978). The interior of the shaft is split into two parts (Figure 3.2) with air bubbles sparged in one side of the interior flow down to the bottom and then up through the other side of the shaft to the surface as liquid circulates through both sides. Depending on the design, the riser could be

chosen to be the draught tube for normal flow, or the annulus for the inverse flow. Lefrançois's original ALF was designed as an inverse flow reactor for a better heat transfer from the column wall and a reduction in foam formation. The normal flow CDT however is favoured for its simplicity in construction and scale-up. Currently normal flow ALFs are being manufactured by a number of U.K companies such as LH fermentation. Blenke (1979) described the hydrodynamics of a variety of GLFs with particular interest in the jet loop reactor (JLR) (Figure 3.2). A cocurrent gas liquid injection through at least one nozzle at the bottom of the reactor ensures a very high dispersion and liquid circulation. These types of reactors are considered extremely effective in dealing with insoluble liquid substrates such as n-paraffins.

The loop circulation offers several advantages over the radial mixing in the stirred tank system. Some of these advantages have so far become apparent in terms of manufacturing, costs, and scale-up. Biological reactions involve population kinetics which respond to a number of influencing factors brought about by poor mixing . Thus it is essential to maintain the homogeneity of broth components without any cell damage or minimum loss of viability. Characteristically GLFs provide a low shear mixing which minimises the attrition level. Moreover due to the flow pattern of GLFs, the culture suspension will pass through individual zones of the fermenter periodically in a regular manner. Thus any inhomogeneity, especially existing in larger reactors, will act on all micro-organisms in the same way. Wase *et al* (1985) studied cellulase production by *Aspergillus fumigatus* in two disc turbine agitated vessels of 5 and 10 l working volume, and in a 10 l ALF. It was observed that in the stirred vessels the yield of cellulase was reduced when the agitation rate was increased with strong evidence of damage to mycelial mass due to shear effects. The use of ALF reduced the shear effects and improved yields of

enzyme by about 20%. In a comparative study Euzen *et al* (1978) investigated the performance of mechanically stirred tank and loop fermenters. Their criteria of choice were based on biomass productivity (weight of biomass per unit volume and time) and energy consumption per per kg of dry material produced. Both internal (CDT) and external loop fermenters were examined for their productivity, power requirements and compared with a stirred tank at different gas throughputs. A summary of their observations is shown in Table 3.1 . From their observations it was generally concluded that as ALFs show a higher dispersion (interfacial area) at lower power inputs their overall energy consumption is significantly lower than the mechanically agitated vessels. In GLF all the mechanical energy is supplied by the gas. This energy is delivered by the compressor and subsequently transferred to the liquid as kinetic energy and energy of expansion. Dussap and Gros (1982) applied Bernoulli's theorem and the principle of conservation of momentum to derive an energy consumption expression for GLF given by;

$$E = Q_v\{M_g/2RT(T_o/T)^2P^3/[P_h+\rho_L g(H_r-H_i)]^2(Q_G/A_o)$$

$$+ P \ln [\frac{\rho_L g (H_r - h_i) + P_h}{P_h}]\} \qquad \textbf{(3.1)}$$

For definitions see the nomenclature.

For air in small fermenters where $(H_r - h_i) < 1.5$ m, Dussap and Gros (1982) proposed the following reduced equation;

$$E/V_L = (7.98 \times 10^8 Q_G + 203) \quad vvm \qquad \textbf{(3.2)}$$

where vvm is volume of gas per liquid volume per minute.

Interfacial area is directly linked to the energy dissipated per unit volume , which is always lower than that required in stirred tanks.

Table 3.1 Performance of stirred tanks fermenters and ALFs

Source : Euzen *et al* (1978)

Volume V_L l	J_G cm/s	$Z=P/V_L$ kW/m3	Mechanical energy fraction %	Interfacial area $m^2/m3$	Productivity kg O2/m3h	Energy consumption kWh/kgO2	1-ε
A- Mechanical Stirring (1000 rpm)							
450	1.45	3.6	86	236	2.6	1.38	-
450	1.95	3.4	79	220	2.4	1.42	-
450	2.90	2.6	55	280	3.0	0.87	-
B- Air Lift							
Type A [1]							
60	5	0.4	-	287	1.55	.26	-
	8	0.7	-	315	1.70	0.41	-
160	12	1.0	-	287	1.55	0.65	0.09
	15	1.33	-	333	1.8	0.74	0.17
235	9	0.75	-	250	1.35	0.56	-
	13.5	1.15	-	278	1.50	0.77	-
	18	1.50	-	370	2.00	0.75	-
850	8	0.89	-	590	3.2	0.28	-
	12.5	1.40	-	800	4.30	0.33	0.29
1900	19	1.5	-	590	3.20	0.47	0.13
Type B [2]							
3300	26	2.75	-	780	4.2	0.65	0.58
C. External Loop Fermenter							
	3.5	-	-		0.5	-	

1 : Type A airlift is normal flow
2 : Type B airlift is inversed flow

3.1.1 Parameter Identification

The three areas of concern in modelling of a GLF are mixing, mass transfer, and kinetics. All these areas interact with each other via a number of key parameters. Luttmann *et al* , (1982) and (1983) developed a distributed parameter model to predict the performance of a tower loop fermenter. They recognised four operation parameters that can be used to control a GLF. These are;

- Gas flowrate at inlet: determines the superficial gas velocity, and hence all related parameters,
- Circulation ratio: indicates the mixing efficiency,

- Dilution ratio: determines the maximum throughput,
- Substrate concentration: under limited supply acts as a control parameter.

While the system mean residence time is dependent on the dilution rate defined by the kinetics of the biological process, the fermenter's mean residence time is further dependent upon the circulation ratio controlled by the gas flowrate, and other system parameters namely;

- Mean gas hold-up, ϵ
- Superficial liquid velocity, J_L
- Longitudinal dispersion coefficient, D_T
- Volumetric mass transfer coefficient, K_v
- Hydrostatic pressure, P_T

The system parameters are defined by the reactor design and geometry, and moreover by the physical properties of the mixed phases. Gas hold-up or the voidage presents the most important system parameter and directly influences all other system parameters.

Blenke (1979) identified a number of especially important parameters for optimal fluid dynamic design of a GLF. These are listed in Table 3.2.

Detailed explanation and significance of paramters shown in Table 3.2 will become apparent in due course.

As well as Reynolds number already mentioned a number of other dimensionless groups are frequently encountered in the two-phase flow and mass transfer analysis. These are given in Table 3.3 .

Table 3.2 Fluid dynamic parameters of GLF.

Source : Blenke (1979)

Parameter	**Relationship**	**Nomenclature**
Slenderness, S	H/D_c	H: Reactor Height D_c: Reactor Diameter
Effective reactor volume, V_R	$\pi/4\ D_c^2 H$	
Reaction mass, M_R	$\rho_{em} V_R$	ρ_{em}: Mean liquid density
Circulation number, n_c	$M_3/M_1 = 1 + (M_2/M_1)$	M_1: Mass through flow M_2: Circulation Mass flow M_3: Total mass flow
Mean circulation velocity, u_m	$\frac{8Q_L}{\pi D_c^2} = \frac{8M_1}{\rho_{em}\pi D_c^2} n_c$	Q_L: Volumetric liquid flow
Circulation rate, r_c	$M_3/M_R = u_m/2H$	M_R: Reaction mass
Mean circulation time, t_c	$M_R/M_3 = 1/r_c$	μ_m: Mean viscosity of liquid
Mean residence time, τ	$M_R/M_1 = n_c/r_c = n_c t_c$	
Mean circulation Reynold number, Re_m	$u_m D_c/\mu_m = 8M_1 n_c/\pi D_c \mu_m \rho_{em}$	

Table 3.3 Common dimensionless groups for GLF parameters.

Source : Various

Bubble behaviour	**Fluid dynamics**	**Mass transfer**
N.Eotvos $g\delta\rho d_e^2/\sigma$	N.Reynold $\rho u_L D/\mu$	N.Bodenstein $u_L L/De$
N.Morton $g\delta\rho\mu^4/r^2\sigma^3$	N.Bond $D_d \rho_L g/\sigma$	N.Sherwood $K_L a D_d/De$
N.Weber $Lu_m^2 \rho/\sigma g$	N.Euler $\delta P_c/\rho_m u_m$	N.Schmidt $\mu/\rho De$
N.Galileo $gD_d \rho^2/\mu^2$	N.Froude $J_d/(gD_d)^{1/2}$	N.Peclet Re Sc

For definitions see nomenclature.

3.1.2 Hydrodynamics of GLF

The fluid dynamic processes in GLF such as liquid circulation, distribution and dispersion of the gas phase and also the resulting mass, momentum and heat transfer rates are determined by a complex interaction between buoyancy, inertia, friction and hydrostatic pressure. Although such interactions differ in various types of loop reactors described earlier, the fundamental transport processes show similar relationships with respect to operating conditions in all types of GLF. This is due to the presence of loop circulation which allows the liquid to flow successively through the individual zones of the reactor loop. Blenke (1979) and Onken and Weiland (1981) studied the fluid dynamics of a variety of GLFs based on two-phase flow; although their observations could be extended to describe multiphase biological systems such as cell growth. Most observations are examined for their influence on the expansion of the fluid bed. Thus the voidage or gas hold-up plays a key role in characterising the performance of the fermenter.

Two-phase flow studies of gas liquid systems such as air/water invariably relate to bubble behaviour and dynamics. Generally speaking bubbles are closely approximated to spheres if interfacial tension and/or viscous forces are much more important than inertia forces. Bubble formation depends upon a number of parameters which are shown in Equation 3.3.

$$V_b = f\ (Q_{Gm},\ d_{or},\ p,\ \mu,\ \sigma,\ p_p,\ K_{or},\ V_c,\ g,\ H) \qquad \textbf{(3.3)}$$

for definitions refer to nomenclature.

Thus for a given reactor system containing a liquid with defined properties, bubble volume V_b, becomes only function of gas time-mean flowrate, Q_{Gm}. Bubble size is often characterised by its equivalent diameter which generally increases with gas flow. Under laminar conditions bubbles show a uniform distribution in size (typically 1-3 mm in

equivalent diameter), and from the moment of formation rise in the column in a homogeneous swarm. With increasing Reynolds number inertia forces dominate and influence drag and terminal velocities as well as bubble shape (Clift *et al* 1978). Ellipsoidal and hemispherical (spherical caps) bubbles unlike spherical bubbles do not have a rigid structure and are frequently formed under moderate turbulent conditions of gas flow. In contrast to the homogeneous flow of rigid bubbles these larger bubbles (about 2-15 mm in equivalent diameter) coalesce more readily to form a heterogeneous size distribution. If the bubble is sufficiently large to fill most of the container cross section "slug flow" results (Figure 3.4). In a non-coalescing system, an increase in the gas throughput directly affects the bubble population in the vessel and as result entrainment in the downcomer is observed (Figure 3.5).

Bubble size distribution can be predicted by several empirical correlations found in literature. It has been suggested (Hinze, 1955) that in turbulent liquid the maximum stable bubble diameter is determined by Weber number, We (see Table 3.3). This dimensionless group is proportional to the ratio of the inertia force deforming the bubble to the surface tension force which maintains its shape. Thus there exists a critical Weber number, We_c, above which the inertial forces dominate and bubbles break up. Calderbank (1958) showed that in general, for gas-liquid or liquid-liquid dispersion in turbulent systems, the critical Weber number, We_c, is 4.7 and proposed a relationship by which the equivalent bubble diameter can be predicted. More recently Lewis and Davidson (1982) studied the influence of shear rate on bubble break-up in a turbulent two-phase column system. Their reults were in good agreement with former study and confirmed We_c=4.7. Thus for a turbulent fluid system that may be considered as homogeneous and isotropic we have;

$$d_e = k\ \sigma^{.6}/(E^{.4} p^{.2}) \qquad (3.4)$$

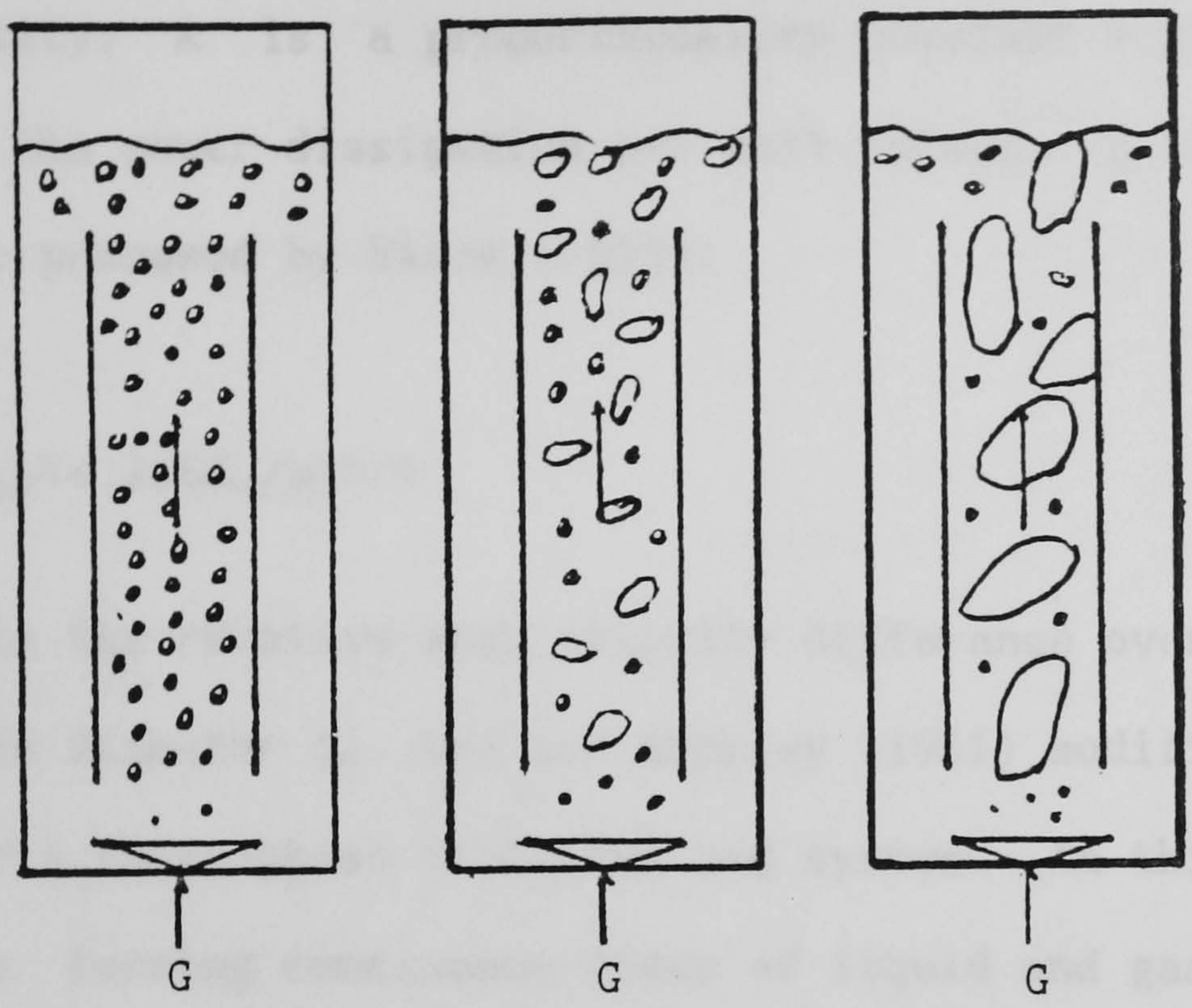

Figure 3.4 Bubble flow behaviour in a gas-lift fermenter
(a) homogeneous bubble flow, (b) Ellipsoidal bubble flow,
(c) slug flow

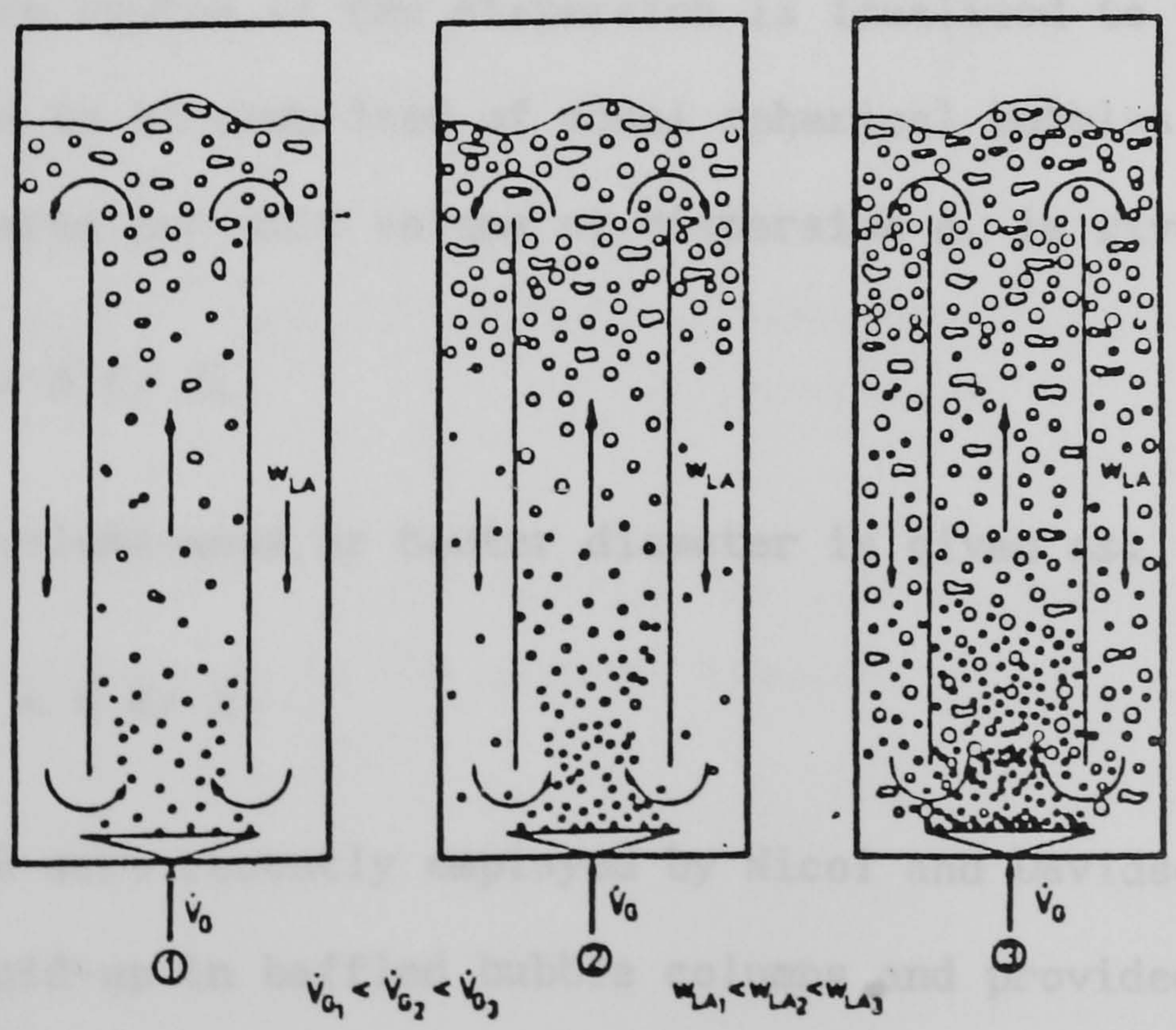

Figure 3.5 Change in the pattern of gas-phase distribution in a gas-lift fermenter, with increasing gas throughput
Weiland (1984)

where d_e is the equivalent diameter of a sphere of equal volume; p is the liquid density, k is a proportionality constant = $\frac{1}{2}(We_c)^{.6}$ and E is defined as the power dissipation per unit volume. E is determined by a relationship proposed by Hinze (1955);

$$U_{mr}^2 = 2(Ed_e/p)^{2/3} \qquad (3.5)$$

Where U_{mr} is the relative mean velocity difference over a distance equal to the bubble diameter d_e. Lee and Buckley (1981) modified Equation 3.5 to account for a three-phase fluidised bed system. In this system power is expended in forcing continuous flows of liquid and gas through the bed against the pressure drop created by the weight of the suspended particles. Thus;

$$E = [p_s \epsilon_s (J_L+J_G) - p_L J_L (1 - \epsilon_L) + p_L J_G \epsilon_L] g / \epsilon_L \qquad (3.6)$$

where ϵ_s, ϵ_L are the volume fractions of solid and liquid respectively. In a two-phase system if the dispersion is idealised to the extent that it is considered to be comprised of equal spherical bubbles of size d_e, the interfacial area per unit volume of dispersion a, is given by;

$$a = 6 \epsilon / d_e \qquad (3.7a)$$

and surface-volume-mean or Sauter diameter is given as;

$$d_s = 6 \epsilon / a \qquad (3.7b)$$

Equations 3.8 were recently employed by Nicol and Davidson (1988) in their studies of hold-up in baffled bubble columns and provided good correlation with experimental observations in an external loop column.

Maximum Bubble Diameter; $d_{max} = 1.67\sigma^{-.6}E^{.4}p^{-.2}$ **(3.8 a)**
(Lewis and Davidson, 1982)

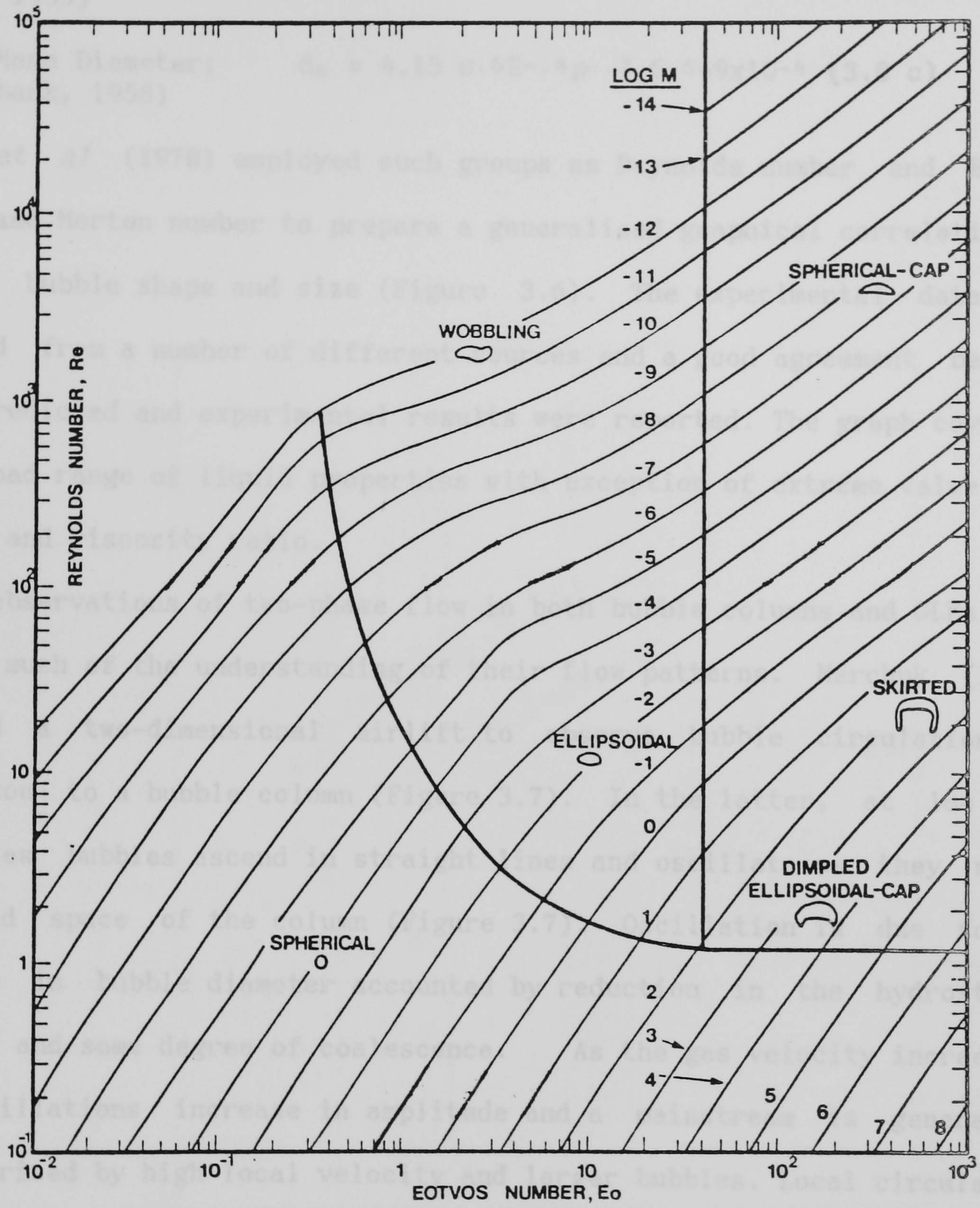

Figure 3.6 Shape regimes for bubbles and drops in unhindered gravitational motion through liquids

Clift et al (1978)

Mean Bubble Diameter; $d_m = 0.725\sigma^{.6}E^{-.4}p^{-.2}$ **(3.8 b)**
(Hinze, 1955)

Sauter Mean Diameter; $d_s = 4.15\ \sigma^{.6}E^{-.4}p^{-.2}\ \epsilon^{.5}+9x10^{-4}$ **(3.8 c)**
(Calderbank, 1958)

Clift *et al* (1978) employed such groups as Reynolds number and Eotvos number and Morton number to prepare a generalised graphical correlation to predict bubble shape and size (Figure 3.6). The experimental data was compiled from a number of different sources and a good agreement between their predicted and experimental results were reported. The graph covers a very broad range of liquid properties with exception of extreme values of density and viscosity ratio.

Visual observations of two-phase flow in both bubble columns and GLFs have led to much of the understanding of their flow patterns. Merchuk (1986) employed a two-dimensional airlift to observe bubble circulation in comparison to a bubble column (Figure 3.7). In the latter, at low gas velocities bubbles ascend in straight lines and oscillate as they reach the head space of the column (Figure 3.7). Oscillation is due to an increase in bubble diameter accounted by reduction in the hydrostatic pressure and some degree of coalescence. As the gas velocity increases, the oscillations increase in amplitude and a mainstream is generated, characterised by high local velocity and larger bubbles. Local circulation patterns in the axial direction trap the smaller bubbles near to the wall of the column allowing the larger bubbles to pass through the central path (Figure 3.7). Such flow patterns are significantly different from those of an airlift fermenter (Figure 3.7) especially at high gas velocities. In general, the bubbles ascend in straight lines and only oscillate at high gas throughputs. There is smaller degree of coalescence and the movement of liquid appears less turbulent. Only at high gas velocities the bubble swarm begin to meander, and still without any local recirculation. Such defined flow patterns explained in terms of superficial liquid velocity

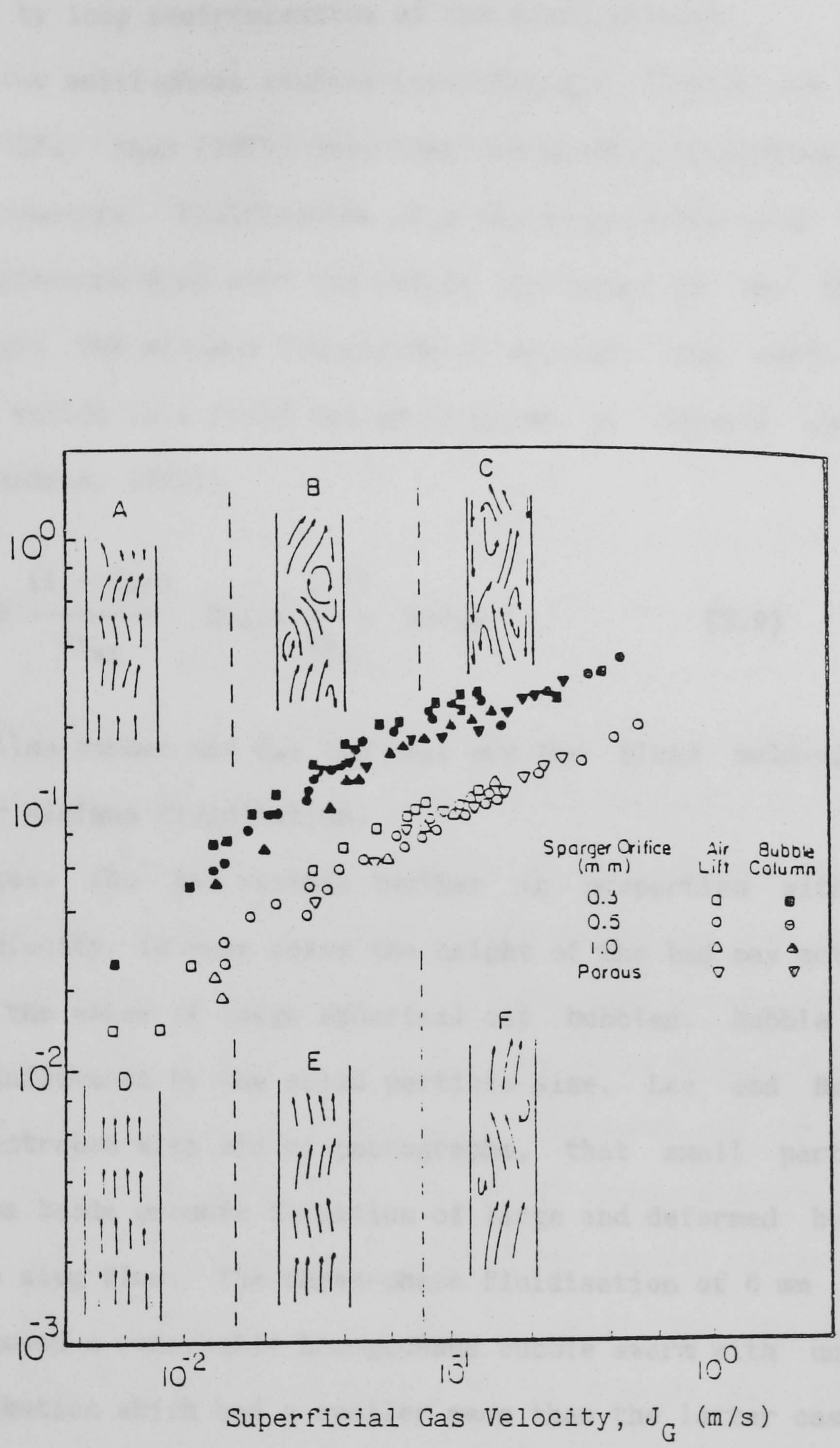

Figure 3.7 Gas hold-up in a two-dimensional bubble column with and without external recirculation and the flow patterns observed Merchuk (1986)

are brought about by loop recirculaution of the fluid mixture.

There are only a few multi-phase studies involving gas, liquid, and solids carried out with GLFs. Shah (1979) described the general hydrodynamics of gas-liquid-solid reactors. Fluidisation of a particulate bed by a liquid occurs when the pressure drop over the bed is just equal to the buoyant weight of the bed. The minimum fluidisation velocity for particulate fluidisation of solids in a fluid medium is given by Ergun's equation (Coulson and Richardson, 1978);

$$Ga = 150 \frac{(1 - \epsilon_{mf})}{\epsilon^3_{mf}} Re_{mf} + \frac{1.75}{\epsilon^3_{mf}} Re^2_{mf} \qquad (3.9)$$

where Ga is Galileo number and ϵ_{mf} and Re_{mf} are the fluid hold-up and Reynold number for minimum fluidisation.

By introducing gas, the bed expands further in proportion with the superficial gas velocity. In some cases the height of the bed may actually decrease due to the wakes of large spherical cap bubbles. Bubble size distribution is influenced by the solid particle size. Lee and Buckley (1981) have demonstrated with aid of photographs, that small particles such as 2 mm glass beads promote formation of large and deformed bubbles as encountered in slug flow. The three-phase fluidisation of 6 mm glass beads, however showed a remarkable homogeneous bubble swarm with uniform bubble size distribution which had a smaller mean than the latter case. At low J_G large particles (>6 mm in diameter) with high inertia are able to deform and split any large gas bubble entering the bed. The result is dispersion of relatively small gas bubbles of diameter 2 mm or less. These gas bubbles add to the total flow of fluid between the particles and therefore the bed expands a little further. Smaller particle are apparently unable to penetrate large bubbles due to surface tension forces.

The multiphase fluidised bed reactors have found wide applications in the waste water treatment industry (Cooper and Atkinson, 1981). Owing to the high dispersion associated with fluidisation, such systems are particularly beneficial as slurry reactors (Koide *et al* ,1985) and fluidised biomass support particle reactor described by Atkinson (1980).

Recently Fan *et al* (1984) described the hydrodynamic behaviour of a gas-liquid-solid system in a 1.22 m high CDT vessel with $D_d:D_c$= 0.67. The vessel was designed with a conical bottom (with a cone angle of 90°) in order to enhance particle recirculation. 3 and 4 mm glass beads of similar density, and 2.2 mm alumina particles were used to observe the flow behaviour in the vessel. Depending on the superficial gas and/or liquid velocity, three flow modes were observed; packed bed mode, fluidised bed mode, and circulated bed mode. These observations are outlined as follows:

At low values of J_G and J_L, the bed is in the packed bed mode where all particles are packed at the bottom of the draught tube and annular region of the column. As fluid velocity increases the solid particles under the draught tube become fluidised to form a spout. The onset of the fluidised bed mode is defined as the point where the global downward movement of the solid particles occurs around the wall area of the conical section of the bed. With further increases in velocity, the solid particles under the annular region begin to massively migrate to the draught tube region to form a fluidised bed. As a result, considerable liquid circulation occurs and some bubbles are circulated into the annular region. With increasing J_G the height of the fluidised bed eventually reaches the top of the draught tube. When it exceeds this height, the solid particles are carried over into the annular region and thus circulate back to the draught tube. An intensive solid particle circulation thus commences with an apparent velocity relative to the fluid velocities. This flow pattern characterises the circulated bed mode. In this flow mode large number of bubbles are

observed in the annular region. Koide *et al* (1985) described a slurry vessel based on a CDT design similar to Pachuca tank used in the minning industry (Lamont, 1958). They observed that gas hold-up decreases with increase in the concentration of suspended glass or bronze spheres (mesh: range 60-200). This was primarily due to flow restrictions created in the vessel resulting in bubble coalescence. Moreover solids may settle on the sparger surface and disturb the uniform gas distribution otherwise achieved. Larger or denser solids would require higher gas velocities in order to become fluidised.

3.1.2.1 Gas Hold-Up

Owing to its simplicity of measurement and dependence upon variable design parameters such as superficial gas velocity, gas hold-up is widely reported in the literature as the characteristic parameter of gas-lift fermenters. Gas hold-up determines the mean residence time of the gas phase and influences decisively the interfacial area per unit volume, the mass transfer efficiency from gas to liquid , and the circulation velocity of the liquid phase (or the fluid mixture depending on the design). At a constant gas throughput the gas hold-up is only a function of the mean rise velocity of the bubble swarm. It is inversley proportional to the drift velocity of the system (Merchuk, 1986). Drift velocity is the difference between the velocity of the gas and the superficial velocity of the liquid. It is positive in the riser and negative in the downcomer. Since the gas flowrate in the downcomer is only a fraction of the gas flowrate in the riser, the hold-up in the downcomer will always remain lower which is necessary condition for circulation.

Gas hold-up is influenced by the bubble size distribution, mobility of bubble interface, density ratio of the two phases, the liquid velocity surrounding the bubbles, and reactor geometry. The former parameters are

of course related to fluid properties of the the mixture. In a comparative study of bubble columns and GLFs, Weiland and Onken (1983) indicated that the largest gas hold-up occurs in bubble columns. The overall hold-up in GLFs decrease with increasing superficial liquid velocity. The effect of liquid velocity on gas hold-up increases with increasing gas throughput as a result of stronger influences on the mutual hinderance of the bubbles in the swarm.

Similar trends of gas hold-up behaviour are observed in a three-phase system (Shah, 1979). In contrast to observations made by Onken and Weiland (1981), Fan *et al* (1984) observed that in a three-phase system, increasing liquid velocity would result in an increase in gas hold-up. This is because in a three-phase system, the flow mode of the bed could influence the type of bubbles and gas hold-up. Solid particles restrict the bubble flow and promote coalescence, and a flow profile similar to slug flow is observed. Thus an increase in the concentration of solids is expected to decrease the overall gas hold-up of the system (Figure 3.8). Unlike a fluidised bed, a circulated bed resulting from high superficial gas and liquid velocities, offers less resistance to bubble flow. The inertial force of the particles in a circulated bed breaks up the bubbles and show a comparitively higher gas hold-up. This important behaviour allows operation at high liquid throughputs while maintaining high contacting efficiency between the gas and the liquid phases.

A : Local Gas Hold-Up

Distribution of gas is not uniform throughout the liquid. Determination of gas hold-up in riser, head and downcomer regions for both internal loop (e.g, Merchuk and Stein, 1981) and external loop (Weiland and Onken, 1981) have led to a better understanding of the hydrodynamics of the fermenter. Chakravarty *et al* (1973) investigated the influence of superficial gas velocity, sparger type, draught tube geometry, and fluid properties on

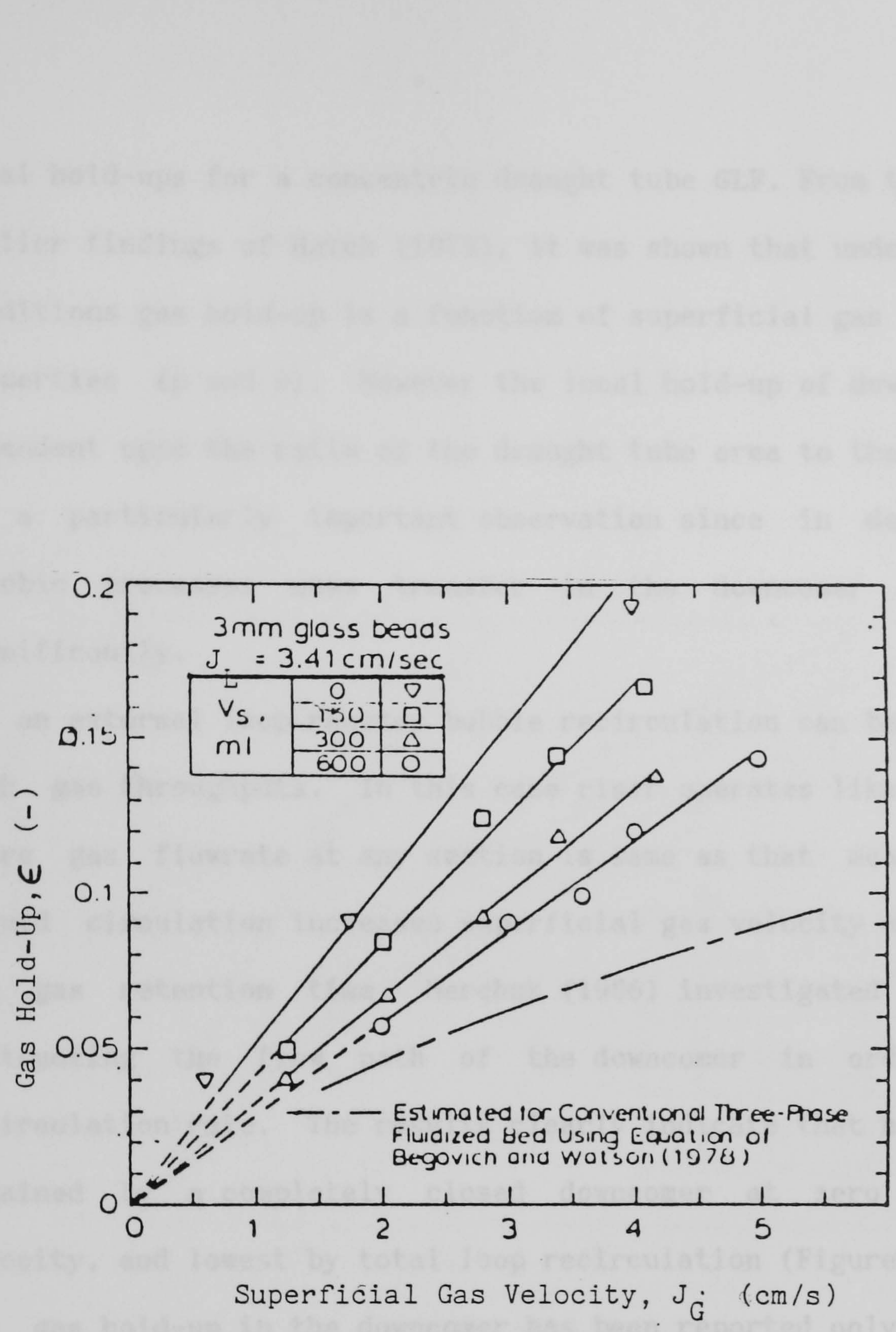

Figure 3.8 Effect of solids loading on the gas hold-up

Fan et al , (1984)

local hold-ups for a concentric draught tube GLF. From this study based on earlier findings of Hatch (1973), it was shown that under all experimental conditions gas hold-up is a function of superficial gas velocity and fluid properties (μ and σ). However the local hold-up of downcomer is further dependent upon the ratio of the draught tube area to the column area. This is a particularly important observation since in designing GLFs for aerobic processes mass transfer in the downcomer could contribute significantly.

In an external loop reactor bubble recirculation can be avoided even at high gas throughputs. In this case riser operates like a bubble column where gas flowrate at any section is same as that measured externally. Liquid circulation increases superficial gas velocity and thus influence the gas retention time. Merchuk (1986) investigated such effects by obstructing the flow path of the downcomer in order to alter the recirculation rate. The results clearly indicate that highest hold-up is obtained by a completely closed downcomer at zero superficial liquid velocity, and lowest by total loop recirculation (Figure 3.9).

The gas hold-up in the downcomer has been reported only for a few cases (Hsu and Dudukovic, 1980, Fields and Slater, 1983, and Merchuk, 1986). The gas hold up in the annular region is mainly determined by the liquid downflow velocity and bubble size distribution. At low gas throughputs bubbles disengage in the head space to allow the bulk liquid circulate in the downcomer. As the gas flowrate increases some bubbles are trapped at the inlet of the downcomer. The front of the bubbly liquid consists of bubbles of almost equal size. With further increase in gas flowrate the front moves progressively downwards until it eventually reaches the bottom and gas recirculation begins. Chakravarty *et al* (1973) showed that the behaviour of the hold-up in the downcomer is similar to that in the riser with lower absolute values as expected. If the gas hold-up in the

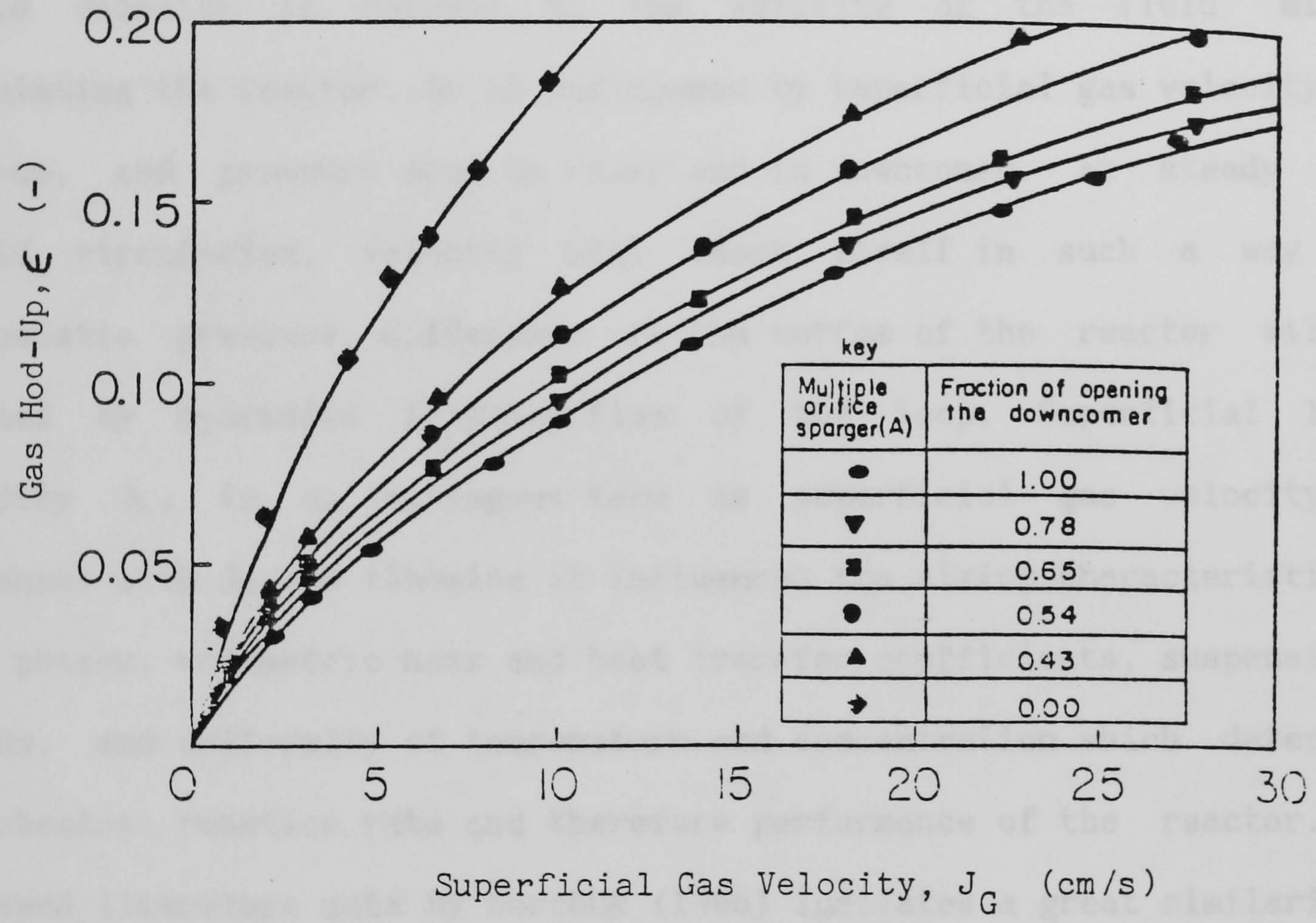

Figure 3.9 Gas hold-up in the riser of an external loop air-lift fermenter for several different openings of the downcomer section, multiorifice sparger
Merchuk, (1986)

downcomer rises above a critical value, the direction of flow may be reversed. This depends on the reactor configuration, sparger location and the physical properties of the system. An increase in the hold-up in the downcomer may be due to enhanced coalescence which increases the upward velocity of the swarm and therefore reduces the gas velocity.

3.1.2.2 Liquid Velocity

Liquid velocity is defined as the velocity of the fluid mixture circulating the reactor. It is influenced by superficial gas velocity, gas hold-up, and pressure drop in riser and in downcomer. At steady state liquid circulation, velocity will adapt itself in such a way that hydrostatic pressure difference at the bottom of the reactor will be matched by hydraulic friction flow of the loop. Superficial liquid velocity J_L, is an analogous term as superficial gas velocity. J_L increases with J_G and likewise it influences the mixing characteristic of both phases, volumetric mass and heat transfer coefficients, suspension of solids, and uniformity of temperature and concentration which determines the chemical reaction rate and therefore performance of the reactor. The reviewed literature data by Merchuk (1986) indicates a great similarity in the rate of change of J_L with J_G for both external and internal loop with an approximate gradient of 0.4. Merchuk (1986) proposed the following relationship based on a number of independent observations;

$$u_L = bJ_G^{.4} \qquad (3.10)$$

where b is a constant and u_L is the liquid velocity.

For a three-phase system Fan *et al* (1984) have characterised liquid velocity by an observed parameter known as the apparent liquid circulation rate Q_L, given by;

$$Q_L = V_L/t_c \qquad (3.11)$$

where V_L is the liquid volume of the bed and t_c is the time taken for one complete circulation of the fluid element round the reactor loop. Figure 3.10 shows the changes of Q_L with superficial liquid velocity in the draught tube (the riser) region. At the extreme ends of the liquid velocity scale, there is a sharp increase in the apparent circulation rate due to the presence of large bubbles brought about by coalescence. It is notable that in the two-phase system indicated in Figure 3.10, the apparent circulation rate increases linearly with the liquid velocity.

3.1.2.3 Factors Influencing Gas hold-up and Liquid Velocity

A : Geometric Factors

Liquid circulation depends upon the difference in the hydrostatic pressure and hence on the height of the fermenter. Gas-lift fermenters are usually of a slender design resulting in more uniform flow and higher liquid velocities. Weiland (1984) has decribed the effect of draught tube size on the flow behaviour and the gas hold-up on CDT vessels of various sizes and volumes. The ratio of draught tube diameter D_d, to the column diameter D_c, was varied between 0.59 and 0.88. Their observations indicate more bubble entrainment in the downcomer and higher gas hold-up values with increasing draught tube diameter (Figure 3.11) with an optimum ratio of 0.74. Bello *et al* (1981) employed the ratio of cross-sectional area of the downcomer A_d, to the riser A_r as the main geometric parameter to characterise their CDT reactor. Their results indicate that the ratio of liquid flow velocities in the draught tube and annular region can be determined by the ratio of the cross-sectional area of the two reactor zones which is given by;

$$u_L = 0.66\ (A_d/A_r)^{0.078}\ J_G^{1/3} \qquad \textbf{(3.12)}$$

For non-aerated conditions, the liquid velocities in the draught tube and

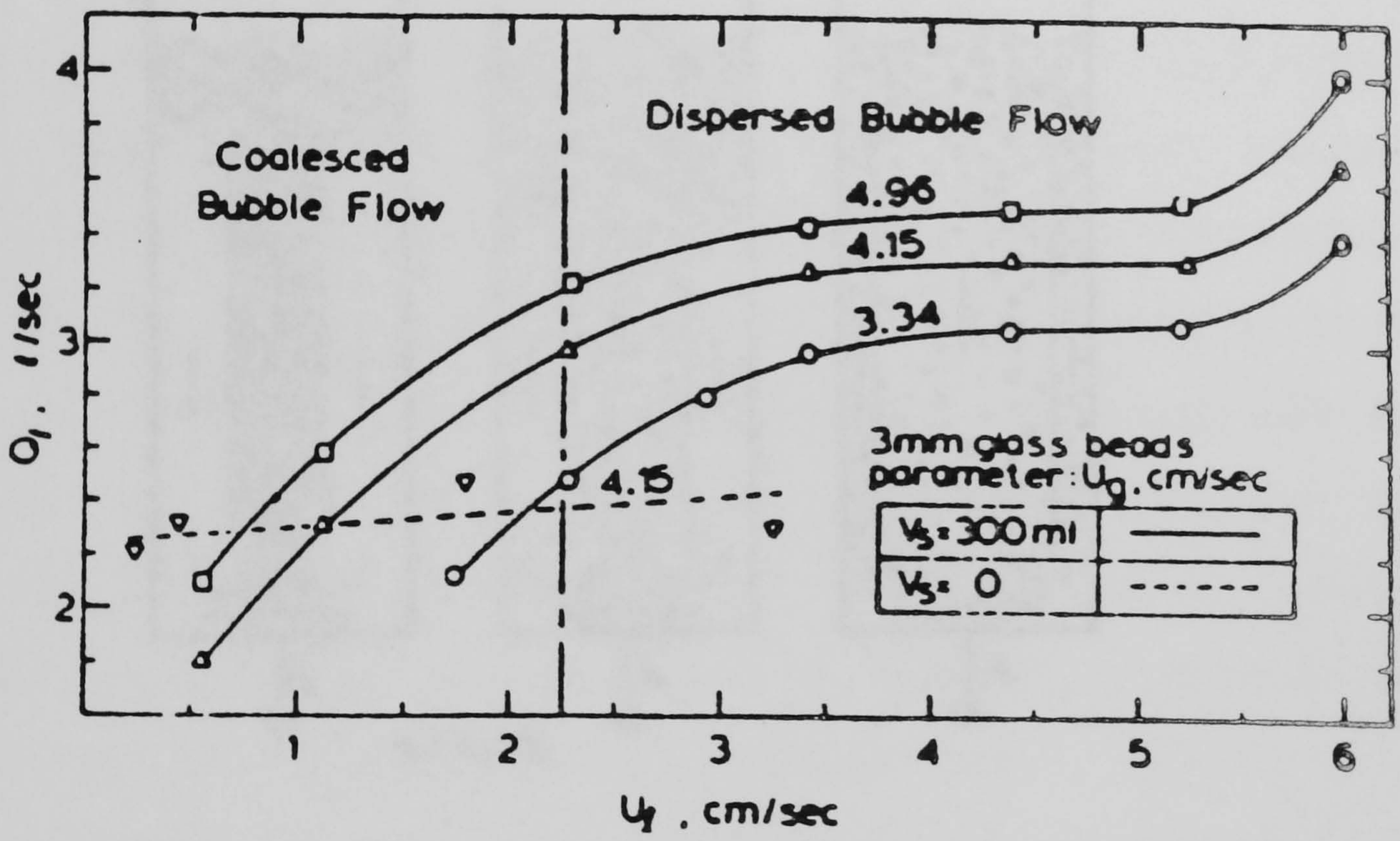

Figure 3.10 Effect of the liquid velocity on the liquid circulation rate as a function of the gas velocity
Fan et al, (1984)

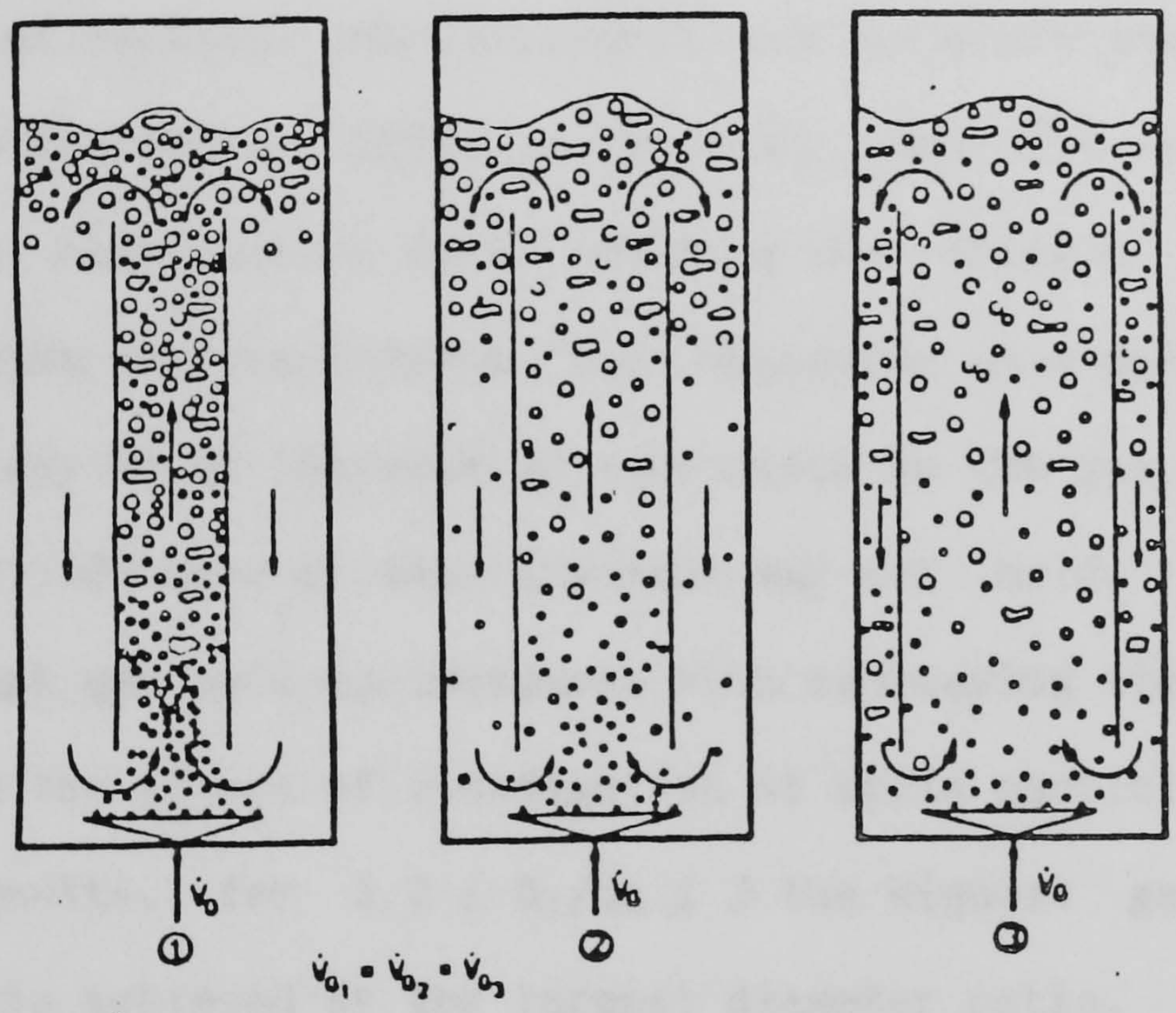

Figure 3.11 Influence of draught tube diameter on gas-phase distribution at a given gas throughput
Weiland (1984)

in the annular space are the same only at a diameter ratio of $D_d/D_c \approx 0.7$ (Weiland, 1984). Under aerated conditions the ratio of effective liquid velocities is a function of gas hold-up in the draught tube ϵ_d and in the annular section ϵ_a. Thus;

$$u_{Ld}/u_{La} = (D_c^2/D_d^2-1)\ (1-\epsilon_a)/(1-\epsilon_d) \qquad \textbf{(3.13)}$$

A decreasing ratio of draught tube to reactor diameter leads to two different effects. On one hand superficial gas velocity in the draught tube increases at constant gas throuhgput and therefore the gas hold-up in the region also increases. While on the other hand, the increasing liquid velocity which also results from reducing the draught tube diameter, tends to decrease the gas hold-up. Thus depending on a particular design, the net effect may be an increase or a decrease in the gas hold-up. In the presence of solids however this argument may not hold. Hwang and Fan (1986) found that gas hold-up increases with increasing liquid and/or gas velocity due to the effect of fluidisation of solid particles on hold-up. From their results, for $1.2 \leq D_c/D_d \leq 2$ the highest gas hold-up and optimum mixing is achieved at the largest diameter ratio.

The volume of head space was found to have negligible effect on the gas hold-up (Chakravarty *et al* 1973), but it was shown to play an important part in the mixing of the internal loop vessels (Fields and Slater, 1983). The bottom section of the loop reactors is frequently ignored in most of its hydrodynamic studies. Hwang and Fan (1986) designed a conical bottom section with a cone angle 90° for a three-phase CDT system. The conical design allowed a better recirculation of solids. It was further observed that the distance between the gas distributor and the bottom of the draught tube influenced the overall gas hold-up.

B : Rheological factors

Dependence of bubble formation upon liquid properties of the continuous

phase has already been mentioned. Fermentation broth is a complex mixture of nutrients and secreted products of living cells. The rheological behaviour of such a fluid system is frequently approximated to that of the base fluid, water. This assumption however, is not justified when broth contains filamentous micro-organisms or a high cell density (Kemblowski and Kristiansen, 1986). Increase in cell density influences both the viscosity and the surface tension of the broth. Various studies reviewed by Metz *et al* (1979) indicate a pseudoplastic flow behaviour associated with an increase in liquid viscosity. This is mainly due to the presence of polysaccharides and proteinaceous material either as nutrients or as cellular components.

Similarly at high cell concentrations, formation of organic end-products (e.g alcohols) can dramatically lower the surface tension. In a two phase gas-liquid system, the physical propeties of the fluid mixture are essentially governed by the liquid properties. Generally three distinct types of compounds affect the flow characteristics, viz. those affecting viscosity, coalescence, and coalescence inhibition. The latter two are affected by the surface activity of the fluid. Addition of alcohols and salts for instance increases the interfacial area by inhibiting bubble coalescence. Although inhibition is by two completely different mechanisms the effect is brought about by the changes in the surface activity of the media.

Fermentation studies of airlift fermenters have revealed the influence of viscosity on the oxygen mass transfer rates (Barker and Worgan, 1981). Viscosity influences the diffusion rate due to a decrease in the interfacial area per unit volume of dispersion. Consequently the volumetric mass transfer coefficient may also decrease (Erickson *et al*, 1983). The terminal velocity of bubbles determine the gas retention time and hence the voidage of the vessel. At low Re (< 2), bubbles in viscous

solutions rise very slowly with a terminal velocity given by the Stoke's equation (Coulson *et al* , 1978). Under turbulent bubble flow, the effect of inertial forces dominates the flow and the larger bubbles rise more rapidly to the surface.

The combined effect of reactor geometry and liquid properties was investigated by Weiland (1984). In the case of glycerol which at ambient temperature has a viscosity fourteen times that of pure water, Weiland (1984) reports on an increase in ϵ of upto 60% if the ratio of draught tube to reactor diameter is increased from 0.59 to 0.74. For larger diameter ratios the influence is only slight.

Table 3.4 Literature Guide on Liquid Properties and Gas Hold-Up in GLFs.

Reference	**Type**	**D_c** cm	**D_d** cm	**System**
Barker and Worgan (1981)	Concentric tubes	10	7	Starch Soln.
Barker and Worgan (1981)	Concentric tubes	30	21	Starch soln.
Fields and Slater (1983)	Concentric tubes	152	95	Water
Fields and Slater (1983)	Concentric tubes	152	95	1% Ethanol
Fields and Slater (1983)	Concentric tubes	152	95	Antifoam agent
Koide *et al* (1983)	Concentric tubes	140	94	Water
Koide *et al* (1983)	Concentric tubes	140	82	270 mol/m² BaCl
Koide *et al* (1983)	Concentric tubes	140	82	50% Glycerol
Chakravarty *et al* (1973)	Concentric tubes	10	7.4	Water
Chakravarty *et al* (1973)	Concentric tubes	10	4.5	Water
Onken and Weiland (1980)	External loop	10	5	Water
Onken and Weiland (1980)	External loop	10	5	51% Saccharose
Akita and Kawasaki (1983)	External loop	33	5.2	Water (riser)
Akita and Kawasaki (1983)	External loop	33	5.2	Water (annulus)
Hills (1976)	External loop	149	149	Water
Shah (1982)	Bubble columns	Reviewed Literature		

Many studies (Table 3.4) have observed a more significant effect on the two-phase flow behaviour of GLFs when the surface tension of liquid is altered. Figure 3.12 shows the effect of different additives on the gas hold-up as observed by Weiland (1984). Hydrodynamic studies of GLFs have often ignored measuring the surface activity of the system and this has

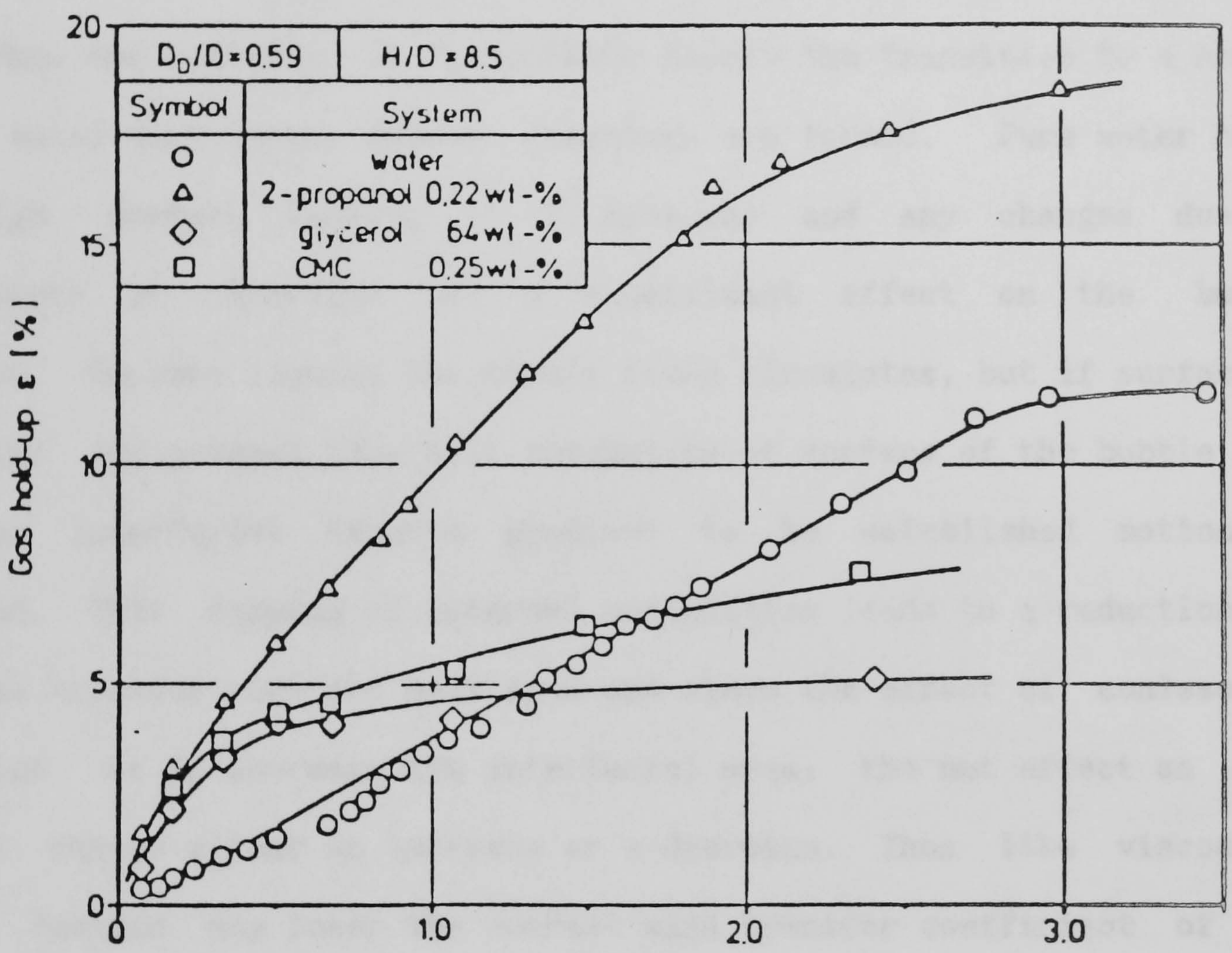

Figure 3.12 Gas hold-ups in different liquids as functions of superficial gas velocity in a 54 l air-lift fermenter
Weiland, (1984)

led to difficulty in analysing reported data. In real systems even trace amounts of impurities tend to restrict surface mobility of smaller bubbles. Both terminal and drag velocities are sensitive to the presence of surfactants. Studies on terminal velocity of bubbles showed a marked decrease for bubbles rising in contaminated media (Clift *et al* , 1978). Surfactants tend to damp out internal motion by rendering the interface rigid. Thus the activity of surfactants delays the transition to a mobile surface until much larger bubble diameters are formed. Pure water has a very high surface tension (~ 74 dyne/cm) and any changes due to contaminants or otherwise has a significant effect on the bubble formation. In pure liquids the bubble fluid circulates, but if surfactant impurities are present they will accumulate at surface of the bubble and cause an interfacial tension gradient to be established motion is inhibited. This damping of internal circulation leads to a reduction in the mass transfer rate per unit area and since the effect of coalescence inhibition is to increase the interfacial area, the net effect on mass transfer can be either an increase or a decrease. Thus like viscosity, surface tension may lower the overall mass transfer coefficient of the system. This argument applies to those additives which are surface active, that is, which preferentially adsorb in the interface and tend to reduce the surface tension. A wide range of substances fall into this catagory, with a notable exeption of inorganic electolytes (e.g NaCl) which increase the surface tension of water. This is due to the "salt-effect" where the ionic strenght of media could inhibit coalescence (Benedek and Heideger, 1971). In Figure 3.12 CMC and glycerol show similar flow properties. Higher gas hold-up with CMC is attributed to the presence of coalescence inhibiting electrolytes. An increase in interfacial area does not always promote mass transfer although it is certain to increase the gas hold-up. Addition of antifoaming agents reduces the mass transfer coefficient

(Fields and Slater, 1983 and Benedek and Heideger, 1971). Antifoams appear to operate by replacing the foam producing surface film by an entirely different type of film often insoluble in the bulk medium. To do this they must displace any foam stabiliser, such as surfactants present in the film. They must, therefore, have a surface tension low enough in the pure state so that they can spread spontenously over the existing film. Studies of Fields and Slater (1983) on a small CDT fermenter showed that addition of alcohols (1% ethanol, 1% methanol and 1% iso-propanol) decreased the mean bubble size distribution and enhanced entrainment. Their observations revealed that inhibition of coalescence led to higher bubble recirculation higher hold-up and lower longitudinal dispersion. These results were in agreement with the observations of Onken and Weiland (1980) in an external loop fermenter. They observed that longitudinal dispersion is smaller in alcoholic solutions because of more uniform liquid flow and a reduction in the formation of eddies by the narrower wakes resulting from smaller bubbles. In the same study Onken and Weiland (1980) reported increases in the gas hold-up with increases in the ionic concentration of the solution (using NaCl) upto an ionic strength of I=0.4.

It may be generally concluded that the rate of mass transfer is decreased by the addition of antifoaming agents and increased by surfactants and salts. Moreover, the effect of broth viscosity may become significant at high cell densities or low Reynolds number circulation. In all cases an increase in the interfacial area may result due to inhibition of coalescence which has a direct effect on the gas hold-up.

3.3.4 Measurement and Prediction of Gas Hold-Up and Liquid Velocity

Gas hold-up and liquid velocity can both be measured by simple direct techniques. Essentially in a two-phase flow system the gas hold up ϵ_G, is given by;

$$\epsilon_G = 1 - \epsilon_L \qquad (3.14)$$

where ϵ_L is the liquid hold-up.

Thus a simple technique based on the displacement of liquid by gas would directly determine the gas hold-up (see section 3.2.3).

Predictions are made by use of models involving both parameters. Hatch (1973) applied the drift-flux model of Zuber and Findley (1965), supplemented with empirical correlations for an internal loop GLF in order to calculate liquid velocities and the voidage in both the riser and the downcomer. The semi-empirical model which did not take into account the pressure effects, predicted the hydrodynamic parameters to within 10%. Merchuk and Stein (1981) employed the two-phase flow momentum balance equations given by Wallis (1969) to derive an equation for hold-up in both internal and external loop GLF. The model based on the pressure drop in the vessel was considered in terms of frictional, gravitational, and accelerational components. Calculations of this study indicated that the latter component only contributed less than 1% towards the hold-up determination and thus ignored in the final analysis. According to Merchuk and Stein (1981) the overall gas hold-up is given by;

$$\epsilon_G = \frac{2J_L}{gD_r}\left[(1 + J_{Gr}/J_L)\, C_{fM} + C_{fL}\,(1 + L_E/L)\delta\right] \qquad (3.15)$$

where $C_{fM} = 0.046\ Re^{-0.2}$

$C_{fL} = 0.079\ Re^{-0.25}$

refer to nomenclature for definitions.

Jones (1985) introduced a simple model on the basis of an energy balance in the upflow region, ignoring the hold-up in the down flow region. In this model it was assumed that the work performed by the ascending air bubbles is equal to the work performed in accomplishing liquid circulation. Nevertheless discrepancy occured between the model and the experiments in a CDT, and especially for large draught diameters where gas

hold-up in the downcomer was promoted. More recently Verlaans *et al* (1986) described a general analytical model for a GLF with an external loop where there is negligible hold up in the downcomer. This model is based on a force balance relating the local hold-ups in the riser and the downcomer to frictional losses (and hence J_L).

Hold-up determination in a three-phase suspended solid system is achieved by extending Equation 3.14. Thus;

$$\epsilon_G = 1 - (\epsilon_L + \epsilon_S) \qquad \textbf{(3.16)}$$

where ϵ_S is the solid hold-up.

Shah (1979) has reviewed hold-up determinations in three-phase fluidised beds. As with two-phase systems, many correlations developed are empirical. Kim *et al* (1972) studied the effects of air and water velocity, and particle sizes ranging from 1 - 6 mm on the gas and liquid hold-ups in a two-dimensional column. They developed an empirical correlation which accounts for the physical properties of the liquid phase adequately described by the liquid's Weber number, We_L. Thus;

$$(\epsilon_L + \epsilon_G) = 1.4\ (Fr_L)^{.17}(We_L)^{.078} \qquad \textbf{(3.17 a)}$$

and

$$\epsilon_L = 1.504(Fr_L)^{.234}(Fr_G)^{-.086}(We_L)^{.092}(Re_L)^{-.082} \qquad \textbf{(3.17 b)}$$

where $Fr_L = J_L^2/d_p g$; $Fr_G = J_G^2/d_p g$
$We_L = J_G \mu_L/\sigma_L$; $Re_L = \rho_L J_L d_p/\mu_L$
$1 < \mu_L < 70$ Pas ; $40 < \sigma_L < 75$ dyne/cm.

The standard error for Equation 3.17 was 0.04.

Kim *et al* (1972) showed that $(\epsilon_L + \epsilon_G)$ increased with μ_L for all particle sizes, and the effect of surface tension of liquid depended on the particle size. For 2.6 mm gravel and 6mm glass beads, hold-up remained essentially independent of surface tension.

Fan *et al* (1984) studied three-phase dynamics and circulation in a CDT

reactor. They related the gas hold-up to the circulation Reynold number , Re_C, by curve fitting. This is given by;

$$\epsilon_G = -0.115 + 1.045 \times 10^{-5} Re_C \qquad (3.18)$$

Equation 3.18 satisfied a wide range of solid concentrations with a correlation coefficient of 0.85.

Koide *et al* (1985) studies on a slurry reactor revealed that the presence of suspended solid particles in a CDT reactor reduces the values of gas hold-up. From their experiments involving different reactor geometry, liquid properties, and solid concentrations they proposed the following empirical relationship;

$$\frac{\epsilon}{(1-\epsilon)^4} = 0.127 \left(\frac{J_G \mu_L}{\sigma_L}\right)^{0.934} \left(\frac{\rho_L \sigma_L}{g \mu_L}\right)^{0.292} \left(\frac{D_d}{D_c}\right)^{0.3}$$

$$\times \left(1-0.196\left(1-\exp(-0.135\, Crk^2/\sigma_L)\right)^{-1}\right)$$

$$\times \left(1+0.17\left(\frac{C_s}{\rho_s}\right)^{0.091}\left(\frac{\rho_L \sigma_L}{g \mu_L}\right)^{0.043}\left(\frac{U_t}{J_G}\right)^{0.067}\right) \qquad (3.19)$$

The average error in estimating ϵ was within 12% in the experimental ranges of;

$3.59 \times 10^{-4} \leq (J_G \mu_L/\sigma_L) \leq 3.70 \times 10^{-2}$, $0.471 \leq (D_d/D_c) \leq 0.743$,

$1.69 \times 10^{-11} \leq (g\mu_L/\rho_L\sigma_L) \leq 2.55 \times 10^{-6}$, $0 \leq (Crk^2/\sigma_L) \leq 95.9$,

$0 \leq (C_s/\rho_s) \leq 8.00 \times 10^{-2}$ and $1.17 \times 10^{-2} \leq (V_t/J_G) \leq 0.844$.

3.1.3 Mixing Behaviour of GLFs

Biological reactions are often sensitive to the homogeneity of their fluid environment. Inadequate mixing of substrate or control factors such as pH or anti-foaming agents with micro-organisms could lead to low conversion and yield. For a stirred tank system, scale-up is accompanied by an economic balance between the mixing quality and the power requirements.

This is frequently met by operation of tank in series or forced power input to improve mixing. In bubble columns the mixing is achieved by local recirculation of liquid and it is strongly dependent upon the liquid volume in the reactor . For GLF systems the mixing time only slightly increases with scale-up (Table 3.5) because the liquid circulation rate does not significantly increase with increase in the reactor volume. This is due to an increase in the driving pressure difference with height, and a decrease in wall friction with enlargement of diameter. Moreover, for aerobic cultures, oxygen solubility in the broth grows in proportion to the liquid depth.

Table 3.5 Mixing Data for Bubble Columns and GLFs

Source : Sittig and Faust (1982)

Reactor Type	Reactor Volume (m^3)	Circulation Time (s)	Mixing[1] Time (s)
Bubble	2	-	18
Column	28	-	80
GLF	0.4	10	65
	2	14	80
	27	17	101

1 : Mixing time for 95% homogeneity after acidic pulse at 60^{-1} aeration.

In continuous reactors, the mixing characteristics are usually expressed as residence-time distributions (RTD). This is a statistical measure of the history of a fluid element in the vessel. In tubular reactors it is customary to adopt the axial or longitudinal dispersion model, which has the advantage of being a single parameter model. This parameter is the axial dispersion coefficient, D_T, which can be described in dimensionless form as Péclet or Bodenstein numbers (Table 3.3). In a batch system it is usual to report the mixing characteristics as the mixing time, which is defined as the time required to achieve a definite degree of homogeneity

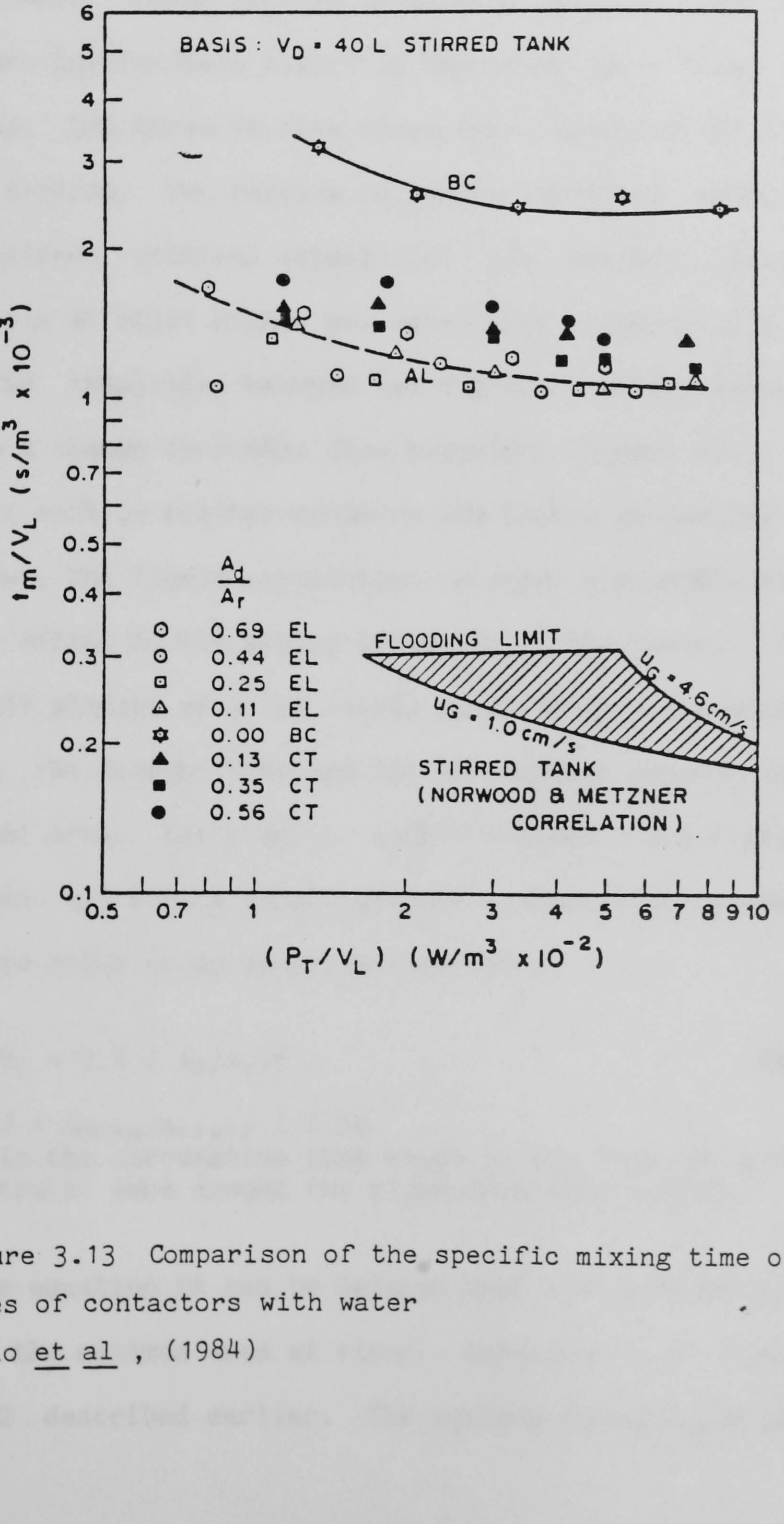

Figure 3.13 Comparison of the specific mixing time of various types of contactors with water

Bello et al , (1984)

(usually 90% or 95%) after the injection of a pulse tracer.

The mixing behaviour of GLFs has been investigated by a number of workers (e.g Onken and Weiland, 1983 and Blenke, 1979). It has been generally observed that mixing time decreases with increasing gas flow rate. Figure 3.13 refers to the variation of specific mixing time (t_m/V_L) with total power due to isothermal gas expansion, for water in GLFs, bubble columns and stirred tanks. These results in general indicate that the gas-lift contactors are intermediate mixers of the order three times better than bubble columns, but three to five times worse than stirred tanks. In all investigated devices, two regimes of mixing behaviour could be observed. Up to a distinct critical superficial gas velocity mixing improves rapidly, whereas at still higher gas velocities liquid mixing becomes less efficient. The transition between two different mixing regimes seems to correspond to a change in bubble flow behaviour (Figure 3.4). As a result, all parameters such as reactor geometry and liquid properties that affect the gas hold-up, the liquid circulation velocity and bubble flow behaviour have a direct effect on the mixing behaviour of the vessel. Rousseau and Bu'lock (1980) studies on a CDT vessel revealed that the mixing time is minimal when the draught tube and the surrounding annulus are of equal cross-sectional area. Bello *et al* (1984) derived a correlation relating the mixing time, t_m, with a single geometric ratio of cross-sectional area of downcomer to riser in an inversed flow CDT ;

$$t_m/t_c = 3.5 \left(A_d/A_r \right)^{\frac{1}{3}} \qquad (3.20)$$

where $0.13 < A_{down}/A_{riser} < 0.56$
t_c is the circulation time which is the time for a liquid volume to travel once around the riser-downcomer circuit.

From the above equation it can be deduced that the shortest mixing time is achieved at the maximum area of riser. Equation 3.20 closely follows Equation 3.12 described earlier. The optimum operating liquid velocity

and hence gas flowrate is thus adjusted for the degree of homogeneity required in the vessel.

Due to liquid recirculation the mixing behaviour in a CDT vessel shares some characteristics of tubular reactors and backmixed batch reactors. The mixing process in the loop consists of combined effects occuring in the draught tube, annular space and in the top and bottom deflection zones. Mixing in the riser and downcomer zones is produced by axial dispersion which mainly results from the difference in the velocities of gas and liquid phases. Unlike the bubble columns, there is little local recirculation or random mixing in the riser. Such random behaviour in bubble columns results in mixing times shorter than those in GLFs (Table 3.5).

The axial mixing fraction of the overall mixing process increases with the start of gas recirculation since bubbles which coalesce in the downcomer rise against the liquid flow and, therefore, considerably speed up the mixing process. The intensive mixing at the deflection zones is caused by the differences in flow velocities in the riser and the downcomer (end effects). In the head space mixing is intensified by the formation of a ring vortex above the draught tube. At low recirculation velocities plug flow prevails with minimum backmixing. As the recirculation velocity becomes faster, so does the concentration change along the tubes. In other words, as the superficial gas velocity increases, a flatter concentration profile, characterising a stirred vessel is achieved. In fact under all operating flow conditions axial dispersion always occurs. Weiland and Onken (1981) measured D_T in the riser of a CDT and showed that the superficial liquid velocity only slightly lowers the value of D_T within their investigated range (0.05 m/s < J_L < 0.28 m/s). Because of this mixed behaviour of GLFs, data on mixing have been reported both as mixing time and as axial dispersion coefficient. The tracer technique has been

widely employed in mixing studies and has led to an understanding of the mixing pattern of fluids in the vessel. This useful technique will be discussed later in this chapter. Figure 3.14 shows a typical tracer response data from pulse experiment in a CDT.

Blenke (1979) developed a solution for the response of a cyclic reactor to a pulse injection of tracer, by superimposing the responses expected in each successive cycle of the tracer in a single phase (i.e non-aerated) jet-loop CDT vessel. By curve fitting, a single parameter known as Bodenstein number Bo, is obtained that characterises the mixing behaviour of the whole reactor. Bo is the ratio of convective to diffusive transport rates which decreases with enhanced backmixing. It was assumed that a single loop circulation is equivalent to flow through a pipe with uniform liquid velocity, u_L, and axial dispersion, D_T, so that the tracer concentration c, at a point x in the at time t is given by;

$$\frac{\delta c}{\delta t} = D_T \frac{\delta^2 c}{\delta x^2} - u_L \frac{\delta c}{\delta x} \qquad (3.21)$$

Fields and Slater (1983) showed that D_T can be determined for a CDT by applying the correlation given by Baird and Rice (1975) for the eddy diffusivity in a bubble column;

$$D_T = k l^{4/3} P_m^{1/3} \qquad (3.22)$$

where k is a dimensionless constant given as 0.35
l is a length parameter chosen as the column diameter
P_m is power dissipated by turbulance by unit mass of liquid given by;

$$P_m = g[J_G - \epsilon J_m/(1-\epsilon)] \qquad (3.23)$$

The effective Bo is $u_L L/D_T$ where L is the mean length of the loop. Blenke (1979) showed that the solution of Equation 3.21 for the open vessel boundary conditions appropriate to a loop reactor is the summation of

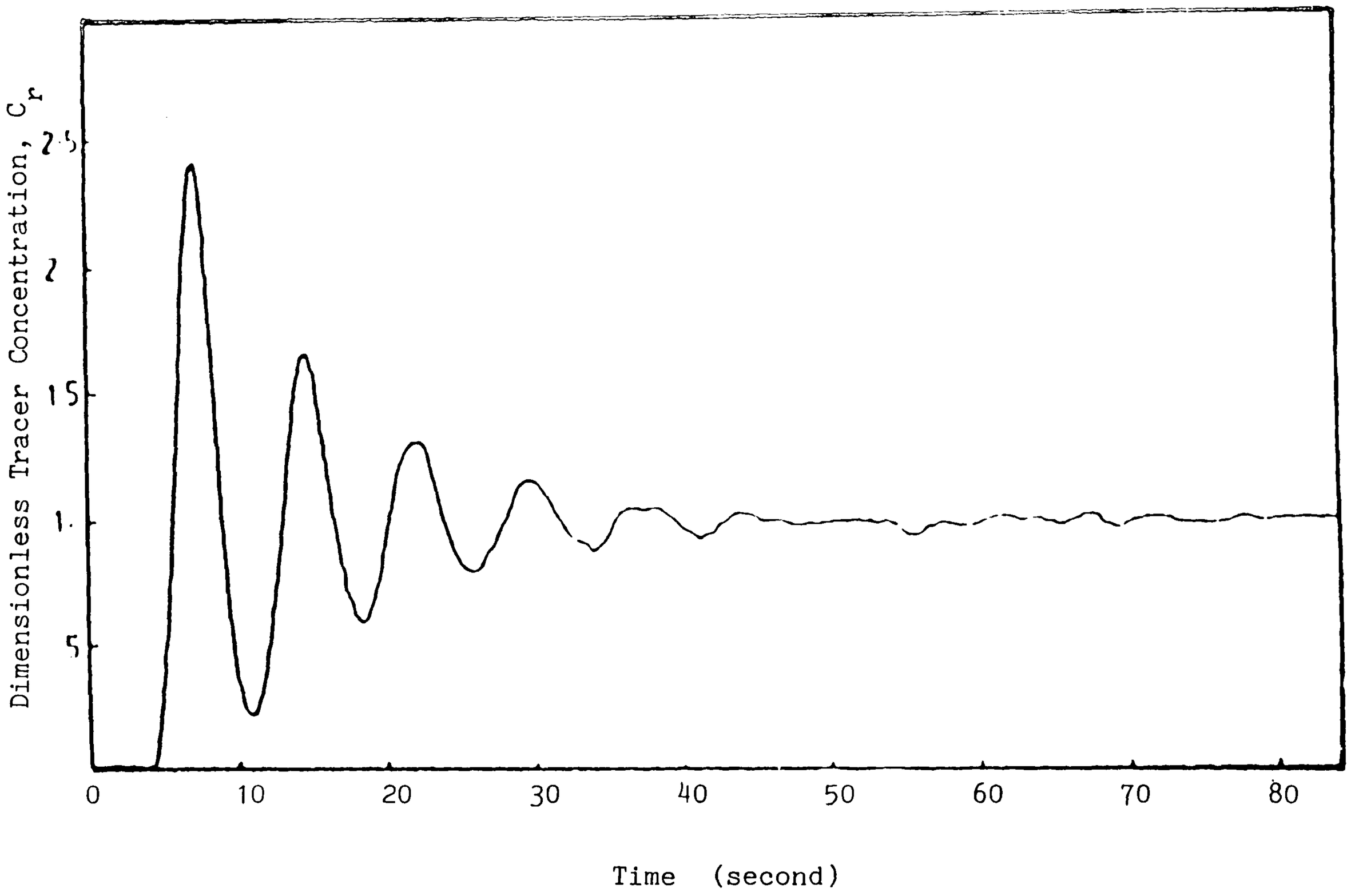

Figure 3.14 Time variation of the dimensionless tracer concentration (C_r) at the top of the riser subsequent to the injection of a pulse NaCl into the head section of an airlift fermenter. Liquid volume = 28.9 l, J_G= 16 cm/s
Fields and Slater, (1983)

dispersion traces for n complete circulations around the loop,

$$C_r = \sum_{n=0}^{\infty} (Bot_c/4\pi t)^{½} \exp\ [\ -\ (x+nL-tu_L)^2 Bo/4tu_L L] \qquad \textbf{(3.24)}$$

where t_c is the mean circulation time
C_r is the ratio of tracer concentration c/c_∞.

This method is especially suitable for systems with mean circulation time that is short with respect to the mixing time. If the circulation time is much shorter than the mixing time, the response to a pulse will be the sum of the effects of successive passages of the traces in front of the detector. This will be essentially the case of shorter reactors and much of the reported data on GLFs are included in this category. Since the gas-liquid separation zone can be approximately considered as perfectly mixed, and the riser and downcomer as plug flow regions, it follows that an increase in the length of the latter zones will lead to a system whose response to a pulse injection will be peaks that can be easily separated, while a short device will yield peaks that are superimposed. Fields and Slater (1983) studied the dispersion in a CDT with two-phase fluid circulation. They fitted their experimental data obtained from a 1.5 m high CDT vessel with various diameter ratios, to Equation 3.24. Estimated values of Bo were obtained by relating the changes in variance of a tracer due to its passage through a mixing region to the local Bo. This is given by;

$$\frac{\sigma^2}{t_c^2} = \frac{2}{Bo} + \frac{8}{Bo^2} \qquad \textbf{(3.25)}$$

Their results also indicate the importance of the head space mixing towards the overall mixing of the fermenter. The volume of head was maintained constant by operating the vessel under a constant aerated volume. With increasing J_G, for a system with constant liquid volume, Bo

decreased to a constant value which was independent of draught tube length at high gas flowrates. Whereas such observations with a constant aerated volume showed substantial changes in Bo with the draught tube height. This data shows that at high J_G the head space reaches a state of complete mixing while at low J_G little dispersion occurs. Blenke (1979) related the tank-in-series model to the dispersion model by the following equation;

$$N_{eq} = 1 + 0.5(Bo^2+1)^{½} \approx 1 + Bo/2 \qquad \textbf{(3.26)}$$

where N_{eq} is the number of equivalent ideal stirred tand reactors of equal volume, and Bo > 8.

There is no information available in the literature concerning the effect of suspended solid particles on the axial dispersion in a three-phase CDT system. Studies involving suspended solids in a bubble column (Schügerl, 1967) indicate that unlike the gas-liquid system, the liquid phase axial dispersion coefficient in a three-phase system depends upon the liquid velocity. The nature of the effect is however, dependent upon the superficial gas velocity and solid particle size.

3.5 End-product recovery from fermentation broth

Conventionally volatile organic end-products such as ethanol are separated from fermentation broth by distillation. Distillation of ethanol from the broth is hindered by its inherent dilute nature and formation of an azeotrope with water. The latter effect is further enhanced by the presence of other organic end-product which could also form azeotropes with ethanol or with water such as acetic acid. In a binary ethanol-water mixture only 96% (w/v) ethanol is recovered and 100 % (w/v) concentration is achieved by azeotropic distillation. Much research has been carried out to economise the high energy requirements of this operation and also to develop more efficient means of azeotropic separation for systems such as ethanol-water. The one-column distillation process is uneconomical because

of its high energy consumption and large size (Kosaric *et al* ,1986). Maiorella *et al* (1981) described 2,3 and 4-column systems incorporating vapour recompression and vapour re-use to reduce the energy cost of the conventional systems.

The most used technique to break the azeotrope, and hence produce anhydrous ethanol, is by the addition of a chemical agent which is able to enhance the volatility of water or ethanol. When the additive is more volatile than water, e.g benzene, the separation is called azeotropic distillation, and when it is less volatile than water it is termed extractive distillation. As an example for the latter gasoline can be mentioned which allows the process to produce gasohol directly form fermentation (Black, 1980).

The energy costs of distillation has led to development of less energy intensive processes. In a recent literature survey, Serra *et al* (1987) have reported on a number of conventional separation systems developed for ethanol recovery from fermentation broth. Table 3.6 shows a summary of some of these processes and compares them with the distillation operations.

Generally all non-conventional systems are less energy intensive than the distillation operations. However many operation still rely on a rectification step by distillation (Table 3.6). Water adsorption on adsorbent agents in vapour phase has shown to have the least energy usage. In this process ethanol is concentrated from 10% (w/v) to 85-90% (w/v) followed by an adsorption step in the vapour phase to obtain anhydrous ethanol.

Table 3.6 Methods for recovery of anhydrous (99.9% w/v) ethanol from fermentation broth.

Source : Serra *et al* (1987)

Conventional Systems				*Non-conventional Systems*			
Bthanol conc. %(w/v) P_0	P_F	Process	Energy KJ/l ethanol	Bthanol conc. %(w/v) P_0	P_F	Process	Energy KJ/l ethanol
6.4-10	99.9	2-column conventional distillation. Second vacuum distillation	10300	10	99.9	Near critical fluid extraction with propane	2700
6.4	99.9	Conventional distillation + azeotropic distillation with benzene	9650	15	99.9	Bthanol adsorption in carbon+water adsorption in a molecular sieve	6960
6.4	99.9	Conventional+azeotropic distillation with pentane	8100	10	99.9	Conventional distillation + water adsorption in cornmeal	3340
10	99.9	Conventional distillation + azeotropic distillation with ether	5570	10	99.9	Conventional distillation with vapour recompression +water adsorption in cornmeal	2170
10	99.9	Conventional distillation with vapour recompression + azeotropic distillation with benzene	4400	8	99	Liquid-phase ethanol sorption/desorption in polymeric compounds (resins)	7850
6.25-10	99.9	Conventional distillation + benzene azeotropic distillation with vaour re-use	5000	8	99.5	Conventional distillation +membrane-prevaporation system (GKSS)	3680
10	99.9	Conventional distillation + benzene azeotropic distillation with vapour recompression and vapour re-use	4230[1]	10	gasohol	Conventional distillation to 80% ethanol+solvent extraction with gasoline	5500[2]
6.4	gasohol	Conventional distillation +extractive distillation gasoline	8100	10	gasoline	Conventional distillation with vapour re-use + catalytic conversion to gasoline	550

1 : Assuming 33% heat to work conversion efficiency
2 : 500 KJ/l of gasohol

With many ethanol fermentations based on xylose, the final concentration does not exceed 1% (w/v). In GLFs, the gas-liquid contact could provide for a rectification step prior to complete separation by one of the methods described above. This is accomplished by a desorptive process whereby the volatile component(s) of the bulk liquid diffuse into the gas phase and thus removed from the bulk liquid. Frequently the gas supplied from the compressor, enters the vessel at a low relative humidity. Thus desorption is often coupled with gas humidification.

The removal rate of water vapour and its volatile component(s) would depend upon temperature, liquid properties, gas flowrate, vapour pressure and concentration of solute and reactor design. The background theory and complete details of these type of diffusional processes are well documented elsewhere (Perry, 1986; Treybal, 1980) and only the relevant results will be referred in this text. For an adiabatic process where no heat is gained or lost from the system the rate of water removal from the system is governed by (Charm, 1978);

$$\frac{dw}{dt} = \frac{h_c a(T_a - T_s)}{L_H} \qquad (3.27)$$

where T_s is surface or equilibrium temperature; T_a is the gas temperature; L_H is the latent heat of vapourisation, and a is a function of the size and the number of the gas bubbles = $6\ \epsilon/d_b$.

The heat may come from either the continuous phase or the the dipersed phase. If the liquid is initially at a temperature higher than the gas dew point, the vapour pressure of the liquid will be higher at the surface than the partial pressure of vapour in the gas, and the liquid will evaporate and diffuse into the gas. The gas is thus humidified and it will reach an equilibrium temperature with the bulk liquid. On the other hand if the heat comes from the gas, the surface temperature T_s, at the gas-

liquid interface assumes the wet bulb temperature of the gas approximately. The gas is adiabatically cooled and it actually assumes the adiabatic saturation temperature.

The heat transfer coefficient for a bubble may be considered from the point of view of evaporation from a drop. The heat transfer coefficient from a drop is;

$$h_c = 2\ K_f/d_b \qquad (3.28)$$

where K_f is the thermal conductivity of gas film and d_b is the diameter of the gas bubble (Perry and Green, 1984).

The rate at which the volatile components are removed from the liquid by desorption is dependent upon the diffusivity of the component in the bulk liquid. Under conditions of turbulent flow, the mass transfer is dominated by eddy diffusion, and for desorption without a chemical reaction, the penetration theory can be applied (Treybal, 1980). Thus;

$$D_B \frac{d^2B}{dx^2} = \frac{dB}{dt} \qquad (3.29)$$

where B is the component desorbed from the liquid into the gas phase and t is the time required for the bubble to rise a distance equal to its diameter while the liquid particle slips along the surface of the wall.

By considering the following boundary conditions;

$B = B_0$ $\quad t = 0$ $\quad$ for $x > 0$

$B = B_i$ $\quad x = 0$ $\quad$ for $t > 0$

$B = B_0$ $\quad x \to \phi$ $\quad$ for $t > 0$

in the absence of gas phase resistance to the transfer. The solution of Equation 3.29 is given by (Shah and Sharma, 1976);

$$R_B = D_B \left(\frac{dB}{dx}\right)_{x=0} = (B_0 - B_i)\ (D_B/\pi t)^{1/2} \qquad (3.30)$$

where R_B is the instantenous desorption rate, and B_0 and B_i are the bulk and interfacial concentrations of component B in the liquid.

It sholud be noted that $(D_B/\pi t)^{\frac{1}{2}} = k_L$, and the overall desorption rate is obtained by determination of the overall mass transfer coefficient k_La.

In comparison to the Film Theory (Treybal, 1980), Shah and Sharma (1976) have found the above model to be a more realistic model for a desorptive process as it accounts for transient mass transfer conditions.

3.2 Materials and Methods

3.2.1 Design and Construction of a 50 l Pilot GLF

A schematic diagram of the experimental apparatus is shown in Figure 3.15. All materials of construction were made from 316 stainless steel unless otherwise stated. A concentric draught tube GLF was constructed similar to that described by Fan *et al* (1984). In order to facilitate flexibility for different geometric specifications or possible future use, the vessel was designed in three sections. For the purpose of this study all these sections were 300 mm in height and in internal diameter leading to an aspect ratio (or slenderness) of 3 and a working volume of 44 litres.

The bottom conical section with a cone angle of 62° was fabricated at Alval Engineering (Fife, U.K). Appendix 2 outlines the detailed drawings of the stainless steel parts of the vessel. The base section provided support for the draught tube, QVF glass 500 mm in height and 100 mm i.d, 180 mm above the bottom plate. It housed a lever type sampling valve (Life Science Labarotories, U.K) and an industrial pH probe unit (Ingold, Switzerland). Six further connection ports, three near the gas distribution level and three near the bottom of the draught tube were designed for probe connections, side outlets, and an injection port. When not in use, all ports were capped. Gas was distributed from the centre of the bottom plate either through a nozzle (3mm i.d) or a stainless steel sintered disc (150μ mesh). The bottom plate had two further outlet used for drainage (¼" needle valve; Swagelok, U.K) and hydrostatic pressure measurement (2 bar pressure transducer; Druck, U.K).

The middle and top sections of the vessel were constructed from QVF glass (Corning, U.K). The size of the middle section could be easily altered in order to vary the aspect ratio of the vessel. A height of 1.5 m would result in an aspect ratio of 7 which is similar to the designs employed by

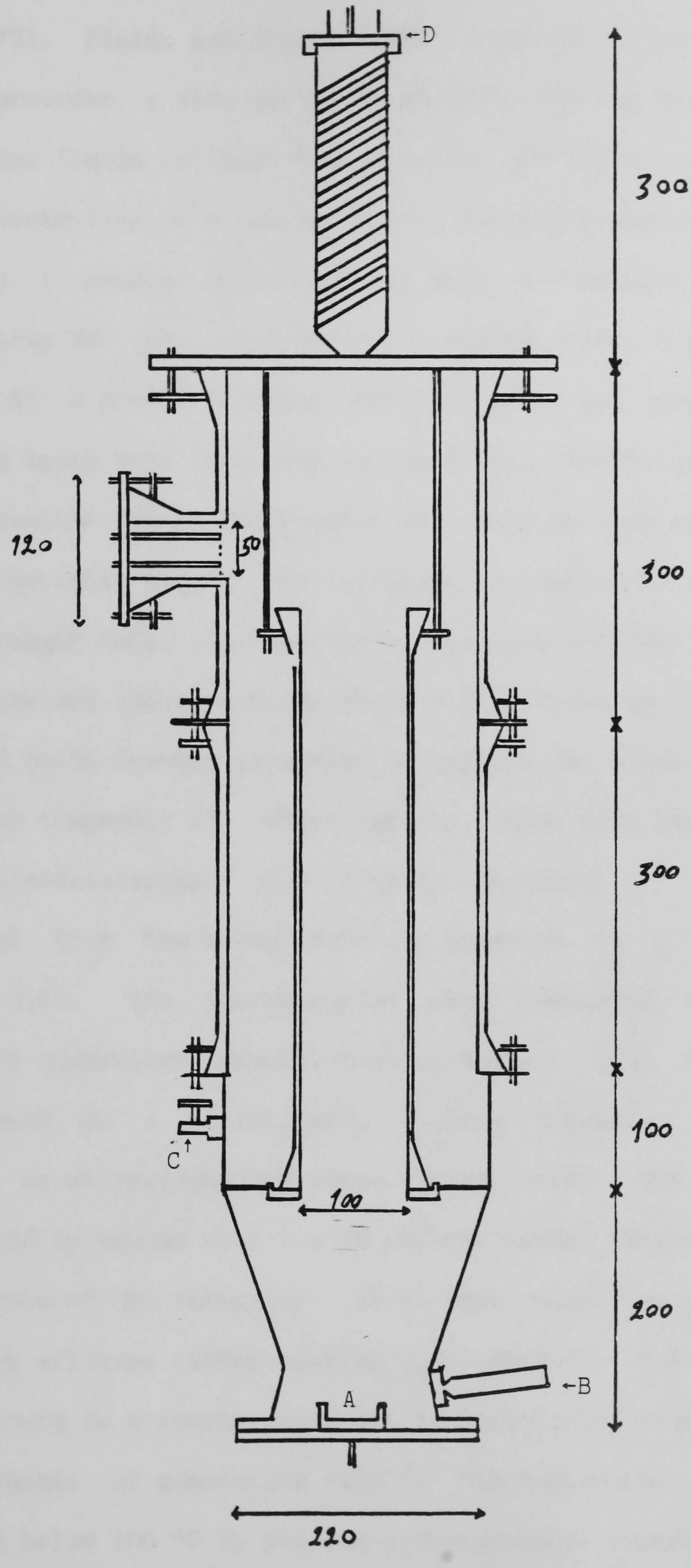

Figure 3.15 Scale diagram of the concentric draught tube gas-lift fermenter

A : Sintered disc gas distributor, B : PH probe holder, C : Sampling valve, D : Condensor

Hatch (1973), Fields and Slater (1983), and Fan *et al* (1984). The top section provided a side outlet 40 mm above the top of the draught tube allowing for liquid collection by overflow and probe connection either for a level controller or a thermocouple. The top plate housed 8 connection ports and a double coil condensor with a transfer surface area of approximately 250 cm^2. A thermocouple (Watlow, U.K), a pressure transducer (Druck, U.K), a pressure relief valve set at 16 psi gauge (Swagelok, U.K), and medium inlet were connected to the plate. Provisions for draught tube support from the top of the reactor were made by welding eight equispaced bolts to the inner side of the top plate to connect to a flange at the top of the draught tube. In practice it was realised that the weight of the draught tube was adequate to maintain a firm stand on the bottom support. The welded bolts however were used to support the experimental baffles in the annulus (Appendix 2). These baffles, made from perspex, reduced the annulus cross-sectional flow area by one-half.

The signal from the transducers was measured by a digital indicator (Druck, U.K). The thermocouples were connected to a multichannel temperature controller (Raytel Control Master, U.K). The medium flowrate was measured by a sterilisable turbine flowmeter (Titan, U.K) and indicated on an analogue indicator (Titan, U.K). For sterilisation the vessel would be heated by a 2.4 KW Firerod heater (Watlow, U.K) situated at the bottom of the fermenter. 60 °C test conditions were alternatively achieved by silicone rubber heating tape (Hotfoil, U.K). The 7.5 m long tape was wound in a spiral round the the bottom and middle section of the vessel capable of generating 1100 W. The temperature of the tape was maintained below 100 °C by placing a thermocouple control. The vessel was lagged by one inch glass wool ropes. Distilled water was used throughout this work. The air supply was available on line from a compressor at 7 bar pressure. A pressure reduction valve was installed to reduce this pressure

to a working pressure of 1.5 bar. Solid particles used were medium and coarse grade "Perlag" (Silvaperl Products Ltd, U.K). The use of these volcanic agglomerates follows the favourable experimental observations made in the microbiological section of this work. Their porous structure allows a high biomass hold up at a relatively low density. Some of their physical properties are indicated in Table 3.7 (see also Table 1.7).

Table 3.7 Liquid hold up and density of different grades of Perlag

Source : Silvaperl Products Ltd. (U.K)

Properties	PERLAG		
	Fine	Medium	Coarse
Bulk density Kg/m^3	500-550	450-500	400-500
Water holding capacity Kg/m^3	300-350	200-250	150-200

A : Sizing of the Draught Tube

The cross-sectional area of the draught tube determines the superficial fluid velocities of the reactor. Therefore its size becomes a key design parameter which would influence the hydrodynamics of the reactor. In the three-phase systems it also plays an important part in determining the minimum velocity necessary to achieve particulate fluidisation of solid particles.

Consider a three-phase loop fermenter system containing biomass support particles, BSPs, which are required to circulate in its liquid volume. In such systems fluidisation is readily achieved owing to the very small density difference between the solid and the liquid phase. This is due to the highly porous structure of the BSPs which is prerequisite for their use as biological support matrices. Typically, for BSPs in the size range of d_e= 3-10 mm, and density of $\rho_s \approx$ 1100 kg/m^3, fluidised in a liquid system with physical properties similar to water, the Galileo number Ga,

defined as;

$$Ga = p(p_s-p)gd_e^3/\mu \qquad (3.31)$$

is in the order of 25000-10^6.

The minimum fluidisation velocity u_{mf}, is given by Ergun's equation (see Coulson *et al*, 1978) which relates Ga with the Reynold number for the minimum fluidisation, Re_{mf}. By assuming that for a three-phase system with a dilute solid concentration ca 5% (v/v), and d_e= 5 mm the minimum fluidisation liquid hold up ϵ_{mf} may be taken as 0.9. By substituting for the constants in Ergun's equation, Re_{mf}=223 and hence J_{mf}= 4 cm/s are obtained. Merchuk and Siegel (1986) reported that for most observed data with loop reactors a linear relationship between the superficial gas and superficial liquid velocities exists which is generally given as J_G= 0.4 J_L. Thus the minimum superficial gas velocity required to achieve the minimum fluidisation is J_{Gf}= 1.6 cm/s.

The value of J_{Gf} may be alternatively estimated by the method outlined by Shah (1979). By substituting for the above constants and a static slurry height of 11 cm, J_{Gf}= 1.9 cm/s is obtained.

Thus for the of gas flowrates in the operating range of 2 - 10 l/min the maximum diameter of the draught tube to ensure fluidisation is in the range of 51.5 - 115.2 mm. For the purpose of this design a draught tube 500 mm in height and 100 mm in diameter was chosen. These dimensions proved adequate for fluidising 2.5% (v/v) medium grade Perlag particles at J_{Gf} = 0.64 cm/s.

3.2.2 Trace Analysis

A : Fluid Mixing

In this classical technique employed for studying the residence time distribution and the mixing behaviour of a reactor vessel, the flow of a

tracer substance is followed by a suitable detector. The tracer response data is then used to provide a statistical measure of the history of a fluid element in the vessel (Levenspiel, 1972; Nauman, 1987).

Mixing studies of GLFs by trace analysis could be easily accomplished by measuring the conductivity of a pulsed electrolyte (Fields and Slater, 1983; Weiland, 1984). In this work the tracer used was a salt solution. The effect of salt on the bubble size distribution was minimised by using only a small volume of concentrated tracer (0.5 ml of 2M KCl). For a two-phase batch system the mixing data were obtained by recording the liquid conductivity (Corning 220 conductivity meter and probes, U.K) at three different locations in the tank subsequent to the addition of a pulse of KCl by a hyperdermic syringe just above the gas distributor. The electrodes were situated at the injection point in place of the pH probe, at the top of the draught tube via the side plate, and finally at the bottom of the draught tube in place of the sampling valve. The electrodes only projected about 2 cm inside the vessel and their effect on the flow was assumed negligible. The signal from each conductivity meter was recorded by a multi-channel data logger (Data Harvest, U.K). 1032 data points per channel were simulatanously recorded at rate of 10^{-6}- 10^{3} seconds per input. The data were stored on 5¼" floppy discs and processed on a BBC microcomputer.

Figure 3.16 shows a typical tracer output from the conductivity meters. Trace P1 follows the tracer from the point of injection and is the reference point for the curves. Trace P2 refers to the next sighting of the tracer at the top of the draught tube, and trace P3 completes the cycle at the bottom of the draught tube. The distance AB on the time-axis is taken to be the rising time of the tracer. The distance BC is therefore the settling or the dowcomer time of the fluid element and the distance AC the circulation time. The mixing time is taken to be the point at which

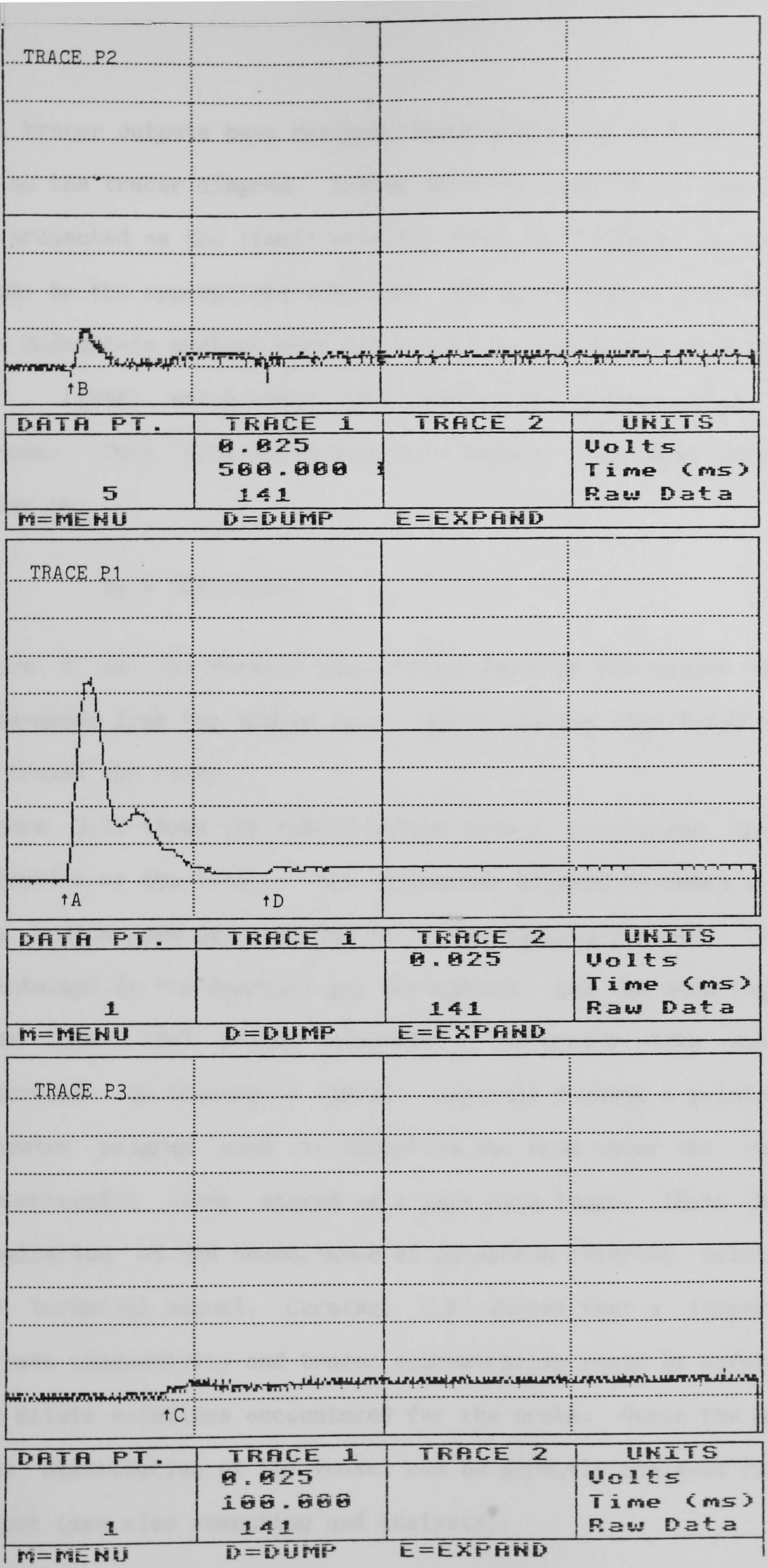

Figure 3.16 Time variation of the conductivity signal received from the electrodes in different regions of the gas-lift fermenter, subsequent to the injection of a pulse KCl into the base section.
Trace P1 : Base section, Trace P2 : Head section, Trace P3 : Downcomer (annular) section

all tracer outputs have reached steady-state and is given by the distance AD on the tracer diagram. Rather than the time data, the tracer analysis is presented as the liquid velocity data, by dividing the time between the peaks by the appropriate distance. The axial dispersion coefficients and the Bodenstein numbers were determined by the method described by Kamp *et al* , (1986) which treats the longitudinal dispersion as a diffusional process. Thus from the penetration theory, the axial dispersion D_T is given by;

$$D_T = (\delta^2)/(\pi t_r) \qquad \textbf{(3.32)}$$

where δ is the forward penetration depth of the tracer in the riser, determined from the tracer data, and t_r is the time taken for the tracer to travel the riser.

Figure 3.17 shows the tracer output from a continuous operation. After injection of the tracer, the system was allowed to reach steady-state and the medium pump was switched on at the desired flowrate. The mixing was maintained by the constant gas throughput, and the data logger was set at slow input (2-5 second intervals). The tracer data was analysed as described by Levenspiel (1972). Appendix 3 shows a printout of a short computer program used to integrate the area under the curve from the concentration curve stored on a Vela data logger (Data Harvest, U.K). Examination of the conductance of potassium chloride solutions (Corning 220 technical manual, Corning, U.K) showed that a linear relationship between conductivity and tracer concentration could be safely assumed for the dilute solutions encountered for the probe. Hence the mean residence time distribution of the vessel can be directly achieved from the tracer output (see also computing and analysis).

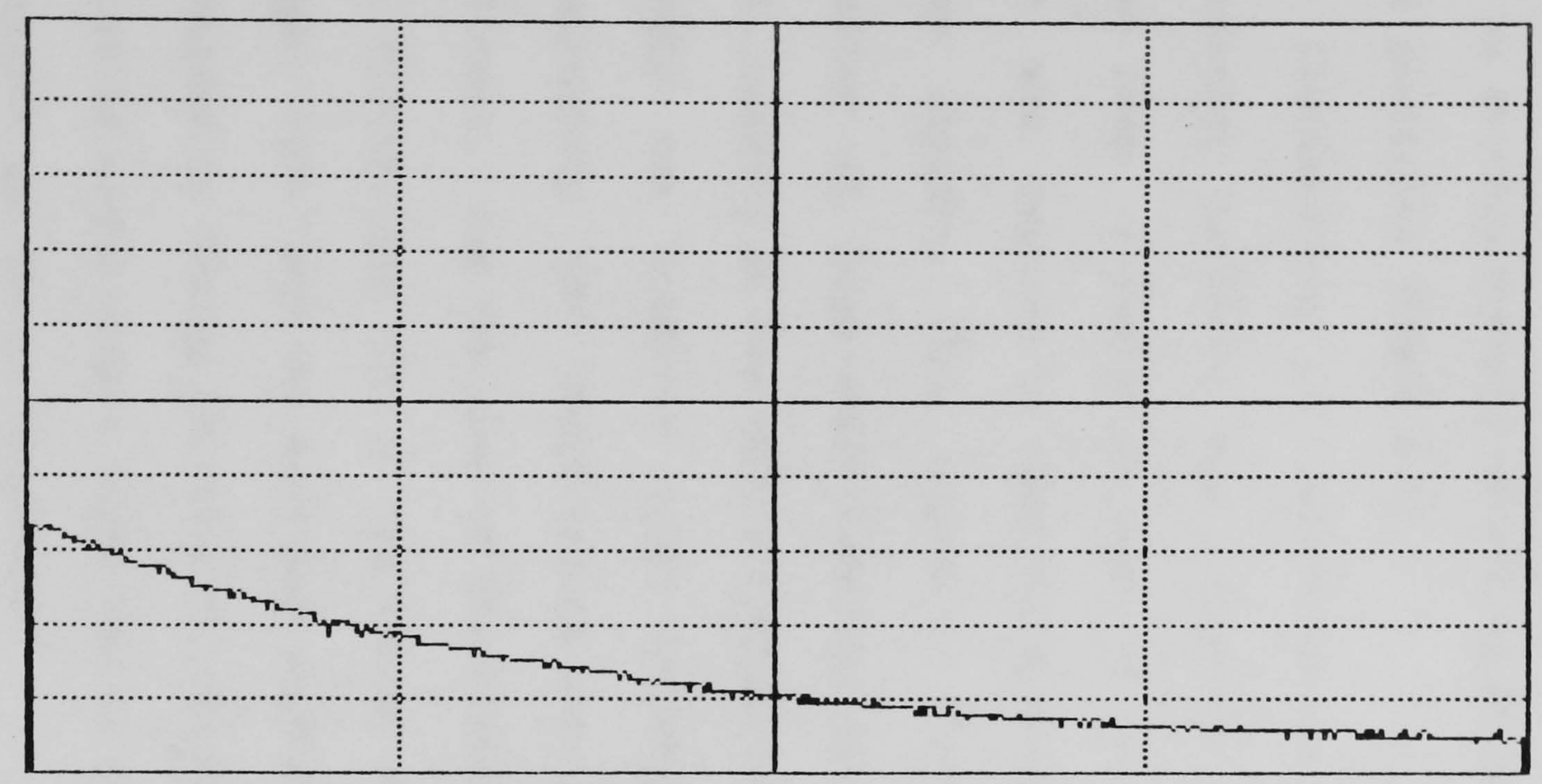

DATA PT.	TRACE 1	TRACE 2	UNITS
	0.082		Volts
	5.000		Time (ms)
5	170		Raw Data
M=MENU	D=DUMP	E=EXPAND	

Figure 3.17 Time variation of the conductivity signal received from the electrode in the head section of the GLF, operated at a constant flow of 22.8 l (dist water)/h.
Area under the curve (Appendix 3) = 158664

B : Three Phase Mixing

The mixing of the solid particles relative to the fluid phases was studied by visual observation of their flow behaviour. A tracer was made by covering a solid particle with a coat of fluorescent paint. The particle had an average density of 670 kg/m^3 which was similar to that of wetted solid particles (Table 3.7).

Upon fluidisation of the particles by the gas stream the flow of the fluorescent particle was obsereved under the illumination of an ultra violet lamp, situated in place of the top plate of the vessel. Background light was reduced to complete darkness and as a result only the tracer became visible. This approach proved to be particularly useful when operating at high solid loadings (ca > 1.5% w/v). From an arbitrary point, usually at top of the draught tube, the time taken for the particle to make one complete cycle was measured with a digital stop watch. Approximately 100 observations were made for each set of experimental conditions, and the mean of the distribution was estimated to reflect the mean circulation time of the tracer particle. The rise velocity in the draught tube and the settling velocity in the downcomer were similarly determined by timing the flow of the tracer between two arbitrary points. The use of ultra violet light was in accordance to the recommendations of the Health and Safety Executive.

3.6.3 Gas Hold-Up Measurement

Over all gas hold-up was measured by weighing out the quantity of water displaced as a result of bed expansion. This was accomplished by shutting off the overflow valve on the side plate of the vessel and filling the reactor to the overflow level. The gas supply was turned on at the desired flowrate and after a few seconds allowing for the system to stabilise the overflow valve was opened and the displaced liquid was drained into a measuring cylinder. The gas supply was then turned off and the drop in the

static liquid height δH, was recorded. More water was added to the vessel and the experiment was repeated for a range of gas flowrates. The voidage ϵ was claculated as follows;

$$\epsilon = \frac{\text{volume of water displaced}}{\text{total volume of water}} = \frac{\text{Static height of liquid}}{\text{Height of liquid + gas}}$$

where height of liquid + gas = Static height of liquid + δH.

Both methods of calculation are linked and gave rise to the same result. The pressure transducers also indicated the changes in the pressure due to bed expansion. Their signal however fluctuated and was not as accurate in measurement as the previous method.

3.2.4 Determination of Desorption Rate of Ethanol

The rate of removal of water from the vessel by the gas stream was measured by observing the change in volume of water level with time at a constant gas flowrate. This was repeated at different gas flowrates and temperatures.

For the vessel containing approximately 1% (w/v) ethanol, the concentration of ethanol in the effluent vapours was measured by taking 500 μl samples by a microsyringe and assaying by gas chromotography as described in section 2.2.6.

3.2.5 Bubble size distribution

The bubble size distribution was determined by photographic techniques described earlier in section 1.5.8. The photographs were analysed by an image analyser (Bild analyser, Kontron, W.Germany). The chosen parameters for analysis were the volume, the equivalent diameter, and the maximum diameter of the bubbles. The data were inputed by drawing round the bubbles using a digital pen. The results were analysed by a statistical package used with the analyser. Figure 3.18 a & b show typical

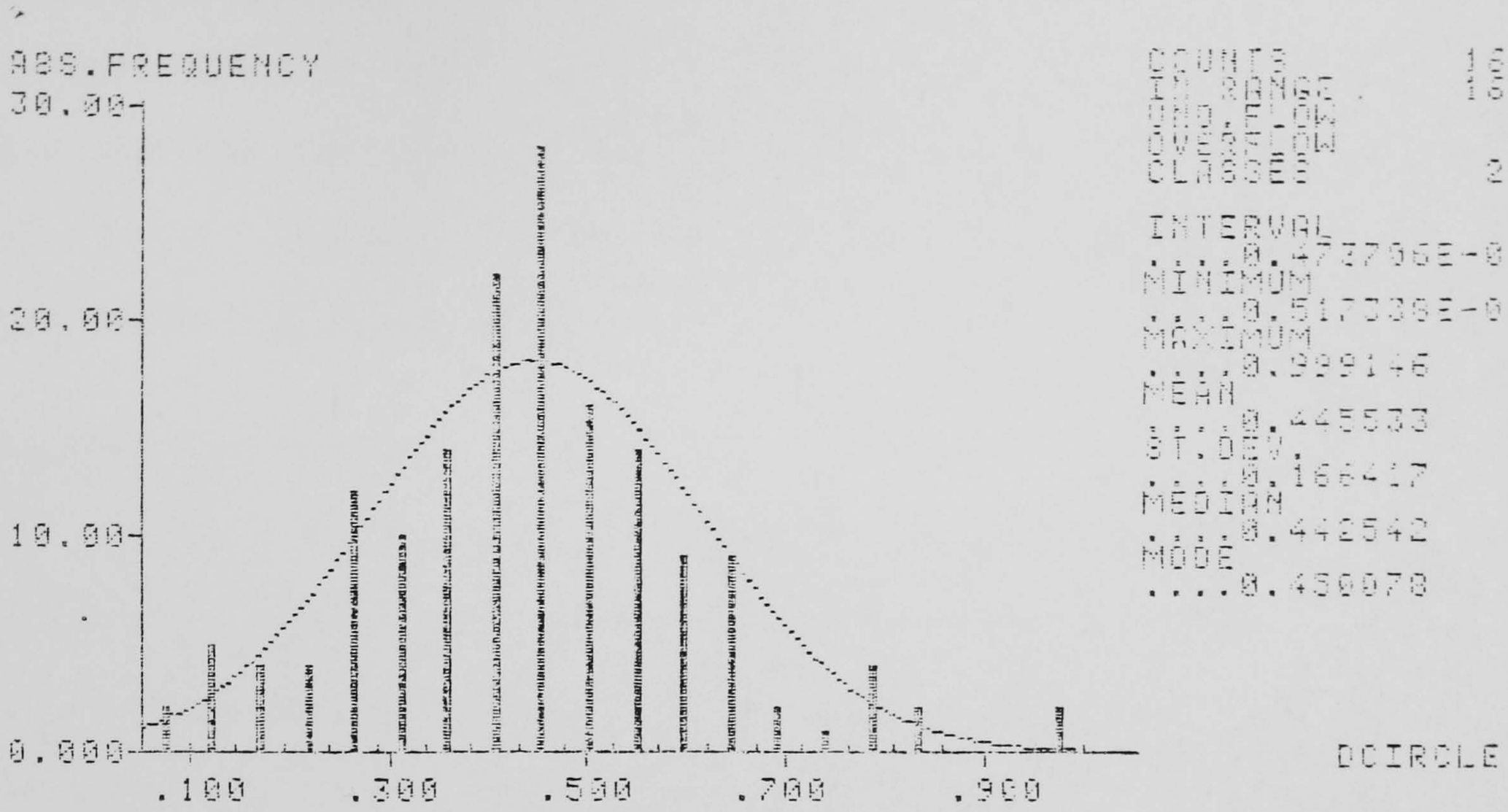

(a) Bubble size parameter d_{circle} (mm)

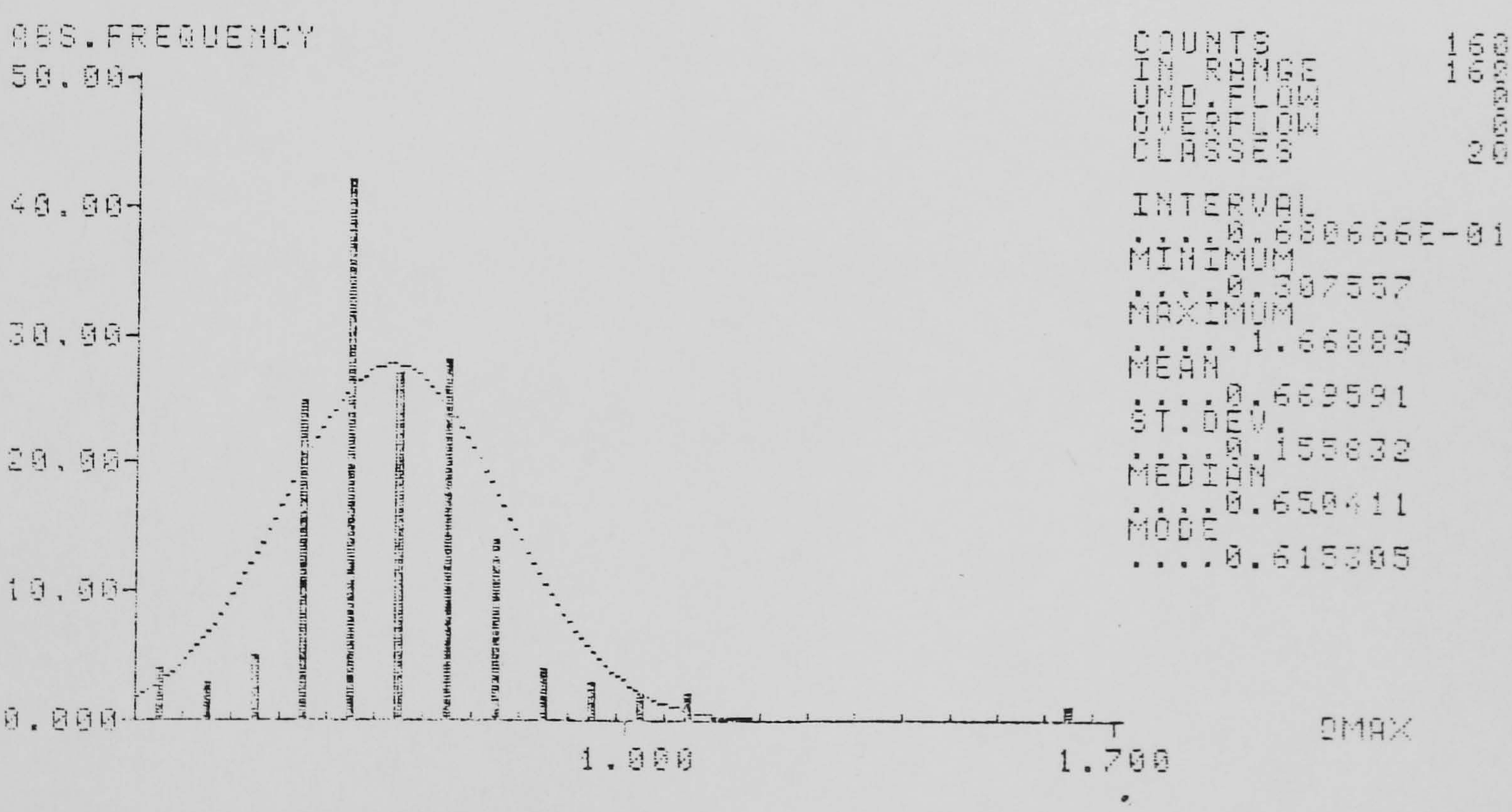

(b) Bubble size parameter d_{max} (mm)

Figure 3.18 Example of bubble size distributions obtained by Image Analysis
Liquid-phase : 1% (w/v) ethanol, Gas-phase : Air at 0.64 cm/s

distributions obtained by this procedure.

3.3 Results and Observations

The following sections outline the results and observations of hydrodynamic and mass transfer experiments on a 50 litre pilot gas-lift fermenter. Unless otherwise stated the fluid system employed is air/distilled water at room temperature.

3.3.1 Rheological Observations

The results for the measurement of viscosity of fermentation media is shown in Table 3.8. The extremes are represented by solid free MCR at μ = 1.08 mPa.s and uncontaminated RCM at μ = 1.71 mPa.s. While the results with MCR media indicate a Newtonian flow behaviour (Figure 3.19), the RCM media indicates a pseudoplastic trend. In Figure 3.20, at room temperature, viscosity is shown to increase linearly with cell concentration before reaching a plateau at 0.5 g/l (dry cell weight). At 60°C, the change observed was linear over the investigated range, notably significantly smaller.

Table 3.8 Results of the regression analysis for Figure 3.19

Liquid system	Gradient	Std error	Regression coefficient	Std error of regression	Viscosity mPa.s
Solid free MCR (supernatant)	37.078	1.465	0.9907	103.74	1.08
Uncontaminated MCR	36.154	1.132	0.9940	82.372	1.11
Contaminated CMR (C=2 g/l)	34.745	1.197	0.9929	90.523	1.15
Uncontaminated RCM	23.437	0.710	0.9945	79.707	1.71
Contaminated RCM (C=0.5 g/l)	24.880	0.293	0.9992	30.997	1.61

The surface tension measurements of fermentation broth showed that for the bacterial suspension investigated changes in the cell concentration have little effect on its surface activity. For measurements both at room

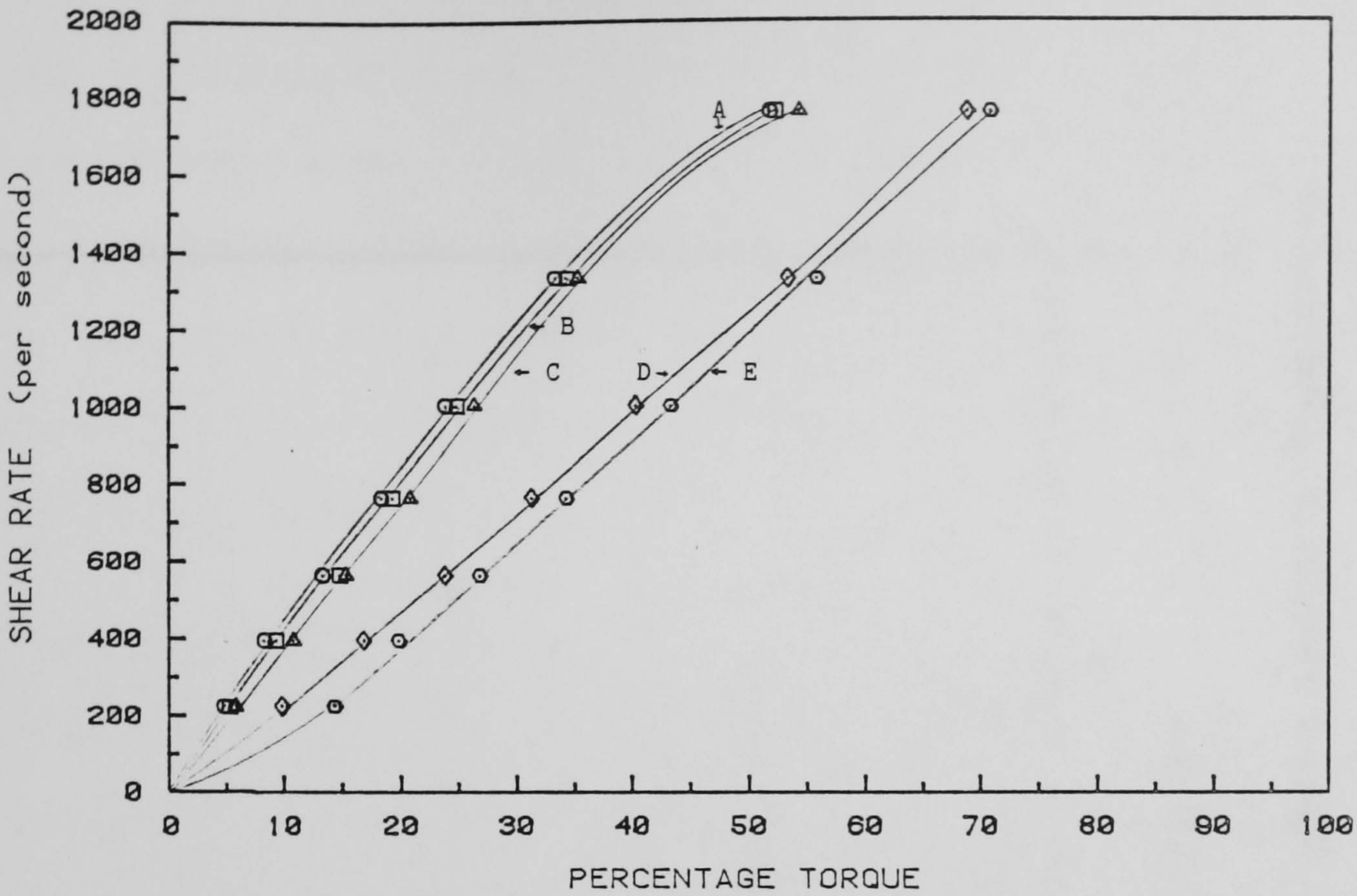

Figure 3.19 Flow characteristics of different fermentation broths.
A : Solid free broth (supernatant); B : Uncontaminated MCR medium; C : contaminated MCR medium (C=2 g/l); D : Contaminated RCM medium (C=0.5 g/l); E : Uncontaminated RCM medium.

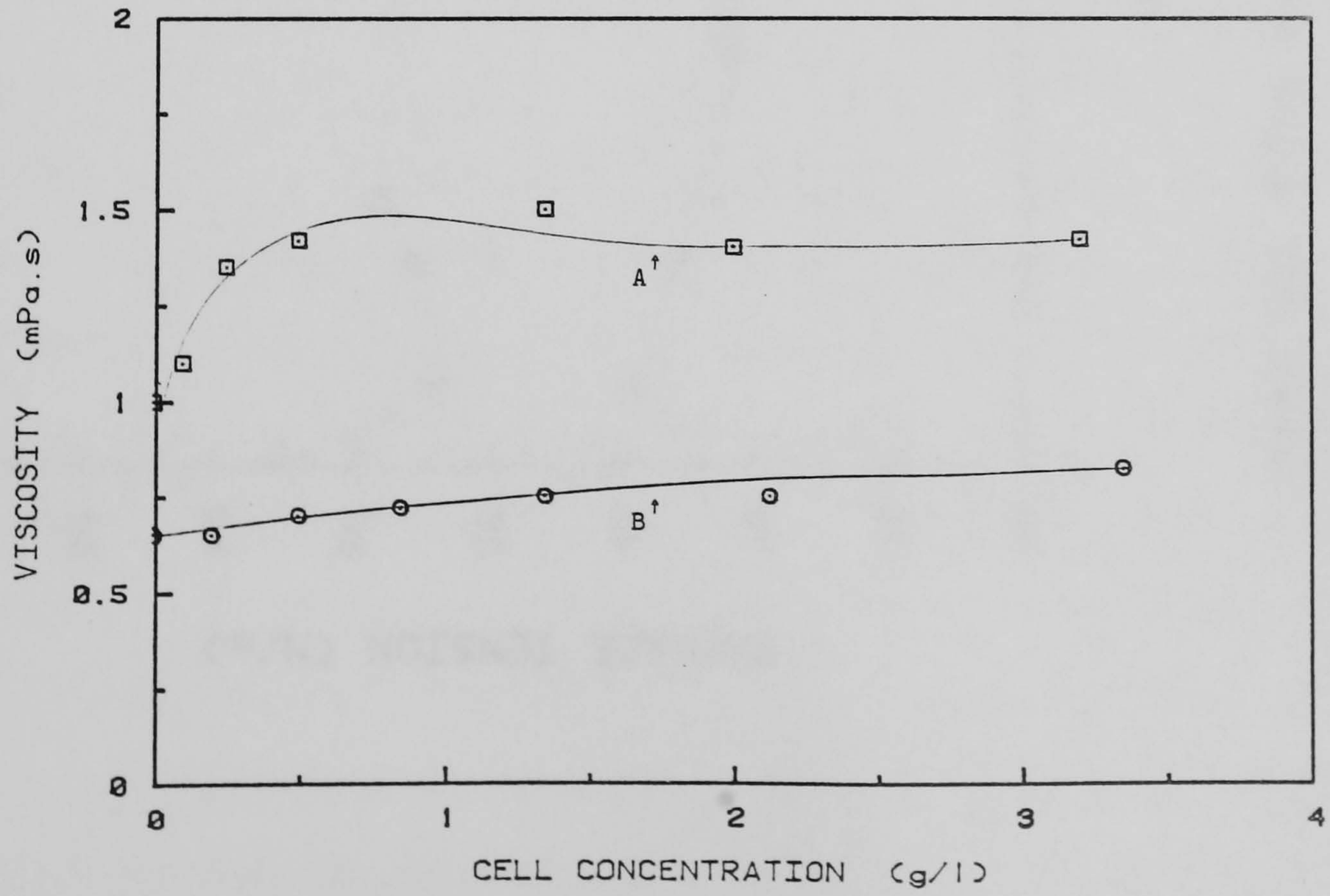

Figure 3.20 Effect of cell concentration on the viscosity of fermentation broth.
A : MCR medium at room temperature; B : MCR medium at 60'C.

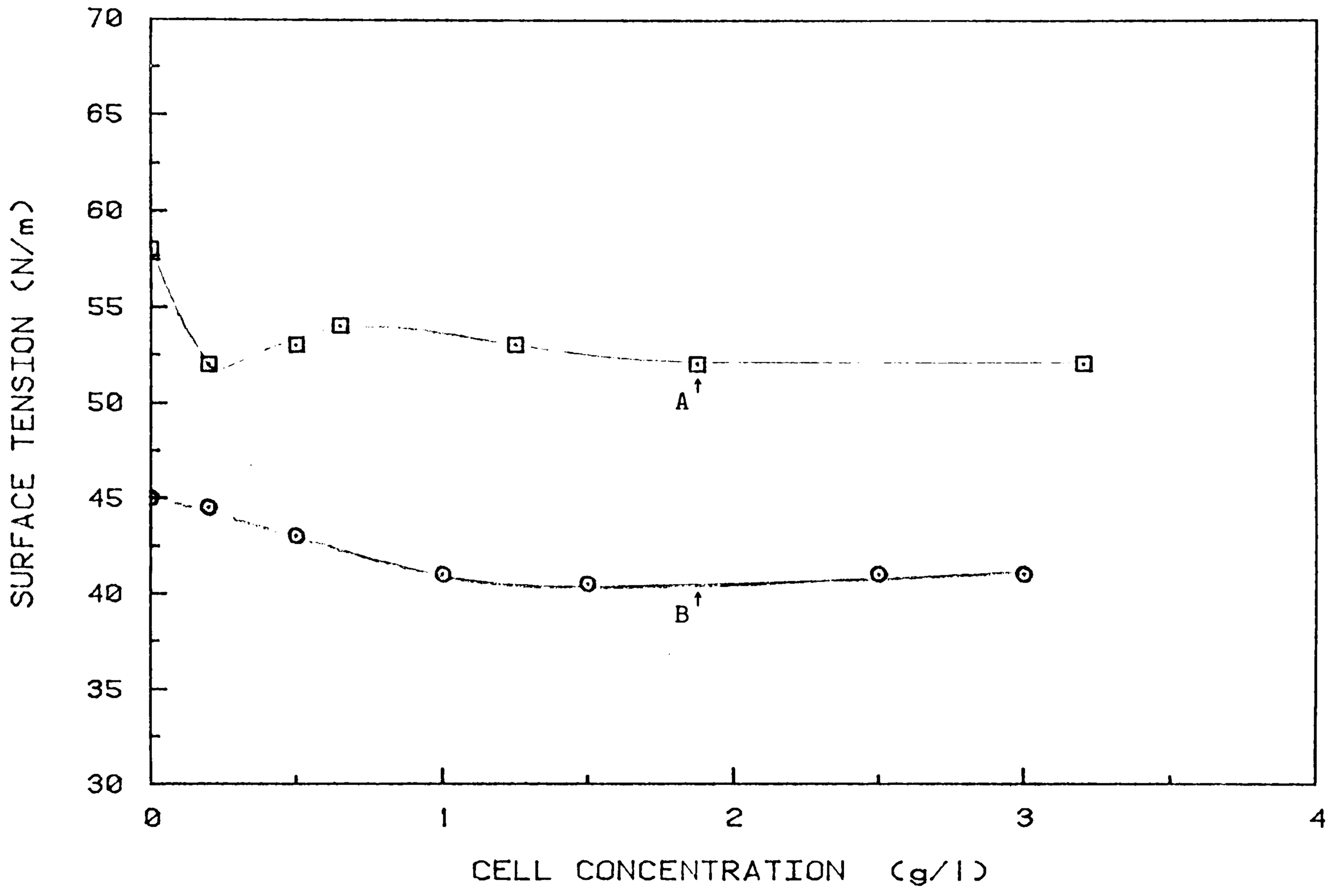

Figure 3.21 Effect of cell concentration on the surface tension of fermentation broth.

A : MCR medium at room temperature; B : MCR medium at 60'C.

temperature and 60°C, an initial decline was observed prior to curves reaching a plateau at around 1.0 g/l dry cell weight (Figure 3.21). The effect of increasing temperature from approximately 20°C to 60°C resulted in an overall 22% reduction in surface tension values. However, the results for contaminated medium show lower surface tension values in comparison to sterile medium, indicating the influence of organic end-products on the surface tension

3.3.2 Bubble Size Distribution

The bubble size distributions of various fluid systems and gas velocities were obtained according to the method described in section 3.2.5. Unlike the single orifice nozzle, the use of a stainless steel sintered disc was preferred on the account of a more uniform gas distribution in the vessel and the results presented here are based on the use of this device.

Figures 3.22 and 3.24 show the effect of additives in distilled water on bubble size at a constant gas flowrate. The results of the image analysis of the photographs taken allowed determination of size distributions for each set of conditions. Two parameters, namely, the maximum and equivalent diameters of a circle were selected to indicate the the general trends in the bubble size with the changing variables. The mean of equivalent diameter was found to be a more representative parameter to describe the mean bubble diameter of the bubbles . Generally, the mean bubble diameter increases with increasing J_G. With the distilled water system, the homogeneity of bubble swarm was observed to deteriorate with increasing gas velocity. At low values of J_G, mainly spherical bubbles were observed in all liquid systems. These bubbles rose to the surface with the same velocity and disengaged at the head space. No bubbles were observed to recirculate through the downcomer, although due to the local recirculation in the head space some experienced a short residence time before disengagement. With increasing J_G bubbles became more ellipsoidal and

irregular in shape (Figure 3.22). At this stage, an increasing concentration of bubbles at the top of the downcomer was observed. The slug flow regime occured in the region J_G = 1.27-1.38 cm/s. Notably at around these gas velocities the bubble size distributions of distilled water and 0.05% (w/v) starch systems are at maximum before a rapid decline (Figure 3.23), whereas 0.05% (w/v) CMC and 1% (w/v) ethanol systems show continuous increases over the investigated range (Figure 3.23). During the slug flow the bubble swarm became very heterogeneous and random in flow pattern. Breakdown products of larger bubbles together with faster liquid velocities allowed recirculation of smaller bubbles (less than 1.5 mm) through the downcomer (Figure 3.24), thus permitting a permanent presence of small bubbles in the vessel. Variations in bubble size, indicated by the range and the standard deviation in Table 3.9, resulted in random velocity profiles with such effect as local recirculations in the riser.

From Table 3.9 the following observations are made;

- Under all experimental conditions, the mean bubble size increases with increasing J_G. Exceptions are observed at high values of J_G with a liquid system of relatively high surface tension, in which slug flow prevails (Figure 3.23).

- The range, standard deviation and the difference between d_{max} and d_{circle} increase with J_G.

- The effect of all additives examined in the tabulated data, have resulted in a smaller bubble size distribution than the pure water system. Notably ethanol has shown the greatest effect (Figure 3.25).

The data in Table 3.9 are processed to obtain some characteristic features of the bubble flow in the system (Table 3.10). The relationship between Morton number M, Eotvos number Eo, and Reynold number Re, in predicting bubble shape and size has already been discussed (section 3.1.2).

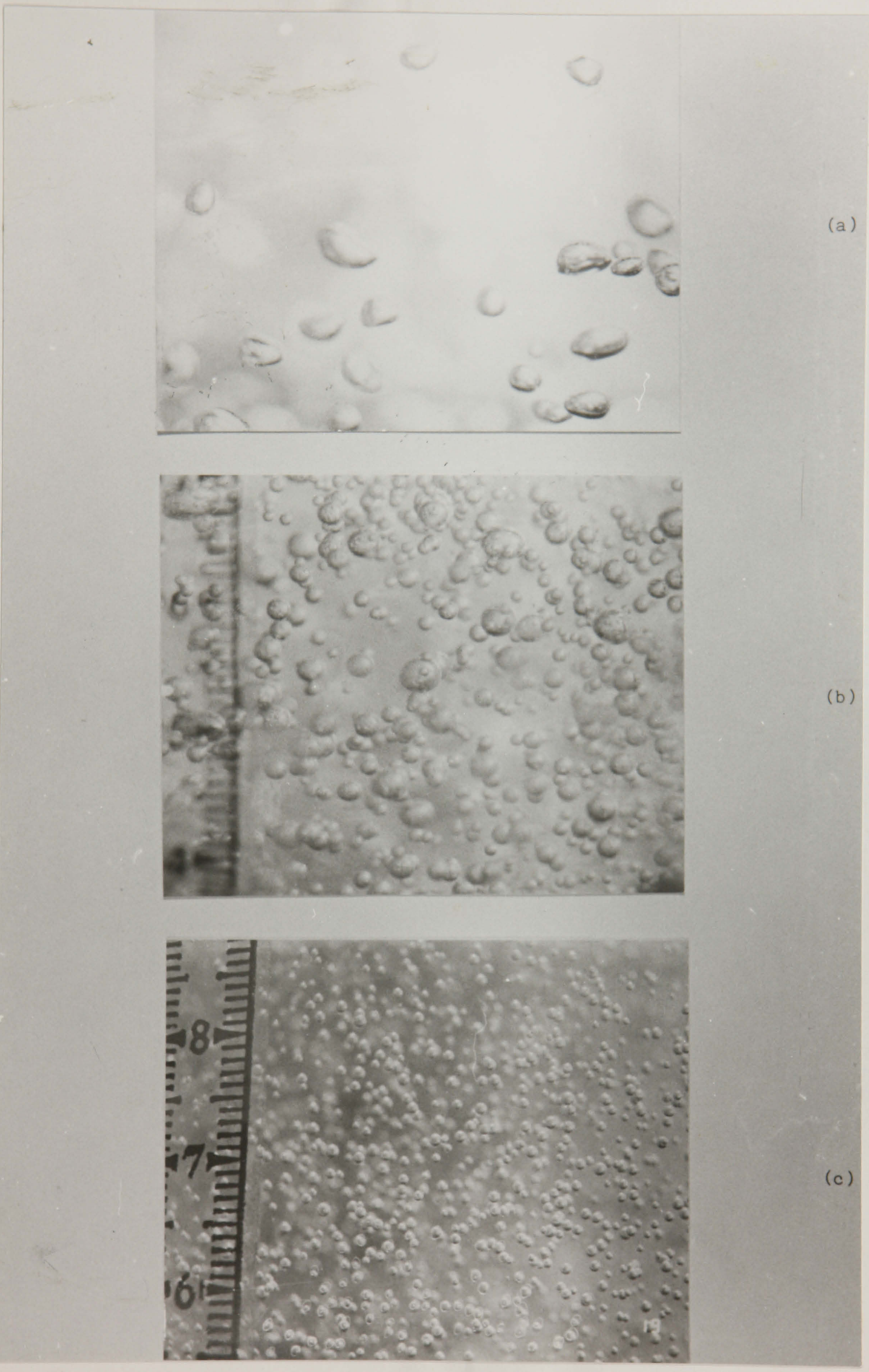

Figure 3.22 Bubble shapes in different liquids

(a) : Distilled water, J_G= 1.06 cm/s; (b) : 0.05% (w/v) CMC, J_G= 0.85 cm/s

(c) : 1% (w/v) ethanol, J_G= 0.64 cm/s

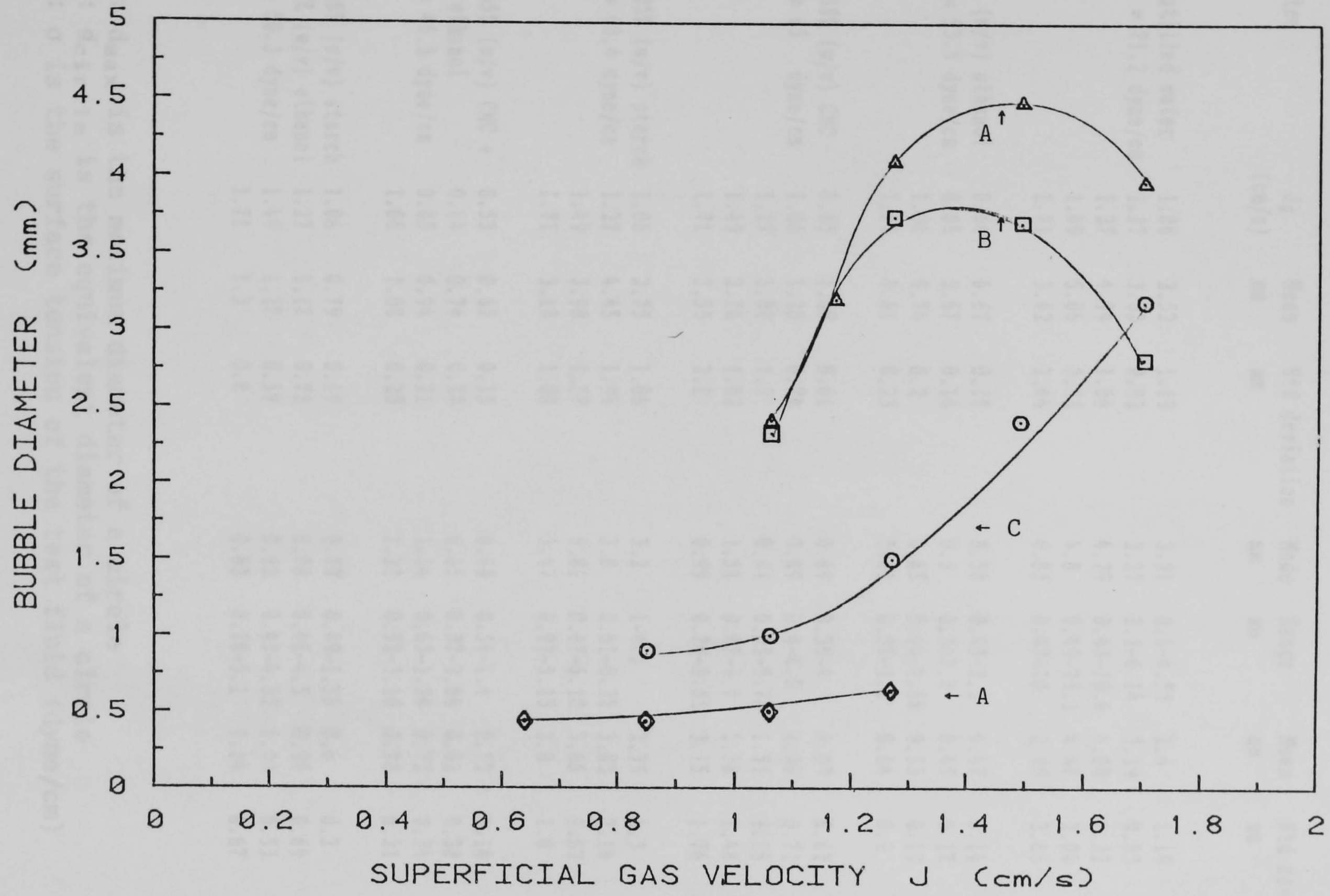

Figure 3.23 Variations of mean bubble diameter with superficial gas velocity in two-phase fluid systems.

A : Distilled water; B : 0.05% (w/v) starch; C : 0.05% (w/v) CMC; D : 1% (w/v) ethanol.

Table 3.9 Bubble size distribution of various fluid systems in a 50 l GLF

Sytem	J_G (cm/s)	d_{max}[1] Mean mm	Std deviation mm	Mode mm	Range mm	d_{circle}[2] Mean mm	Std deviation mm	Mode mm	Range mm
Distilled water	1.06	2.52	1.19	3.91	0.6-4.53	2.4	1.19	2.12	0.43-4.3
[3]σ = 71.2 dyne/cm	1.17	3.62	0.82	3.27	2.1-6.14	3.19	0.83	3.16	1.27-5.19
	1.27	4.94	1.84	4.79	0.43-10.6	4.08	1.32	4.7	1.9-7.2
	1.49	5.06	3.53	4.8	0.49-25.1	4.47	2.04	4.97	0.39-8.45
	1.71	3.42	2.44	0.85	0.47-10	2.96	2.06	0.67	0.45-8.9
1% (w/v) ethanol	0.64	0.67	0.17	0.58	0.43-2.1	0.47	0.14	0.52	0.16-1.02
σ = 53.5 dyne/cm	0.85	0.67	0.16	0.6	0.3-1.7	0.45	0.17	0.45	0.05-1
	1.06	0.74	0.2	0.65	0.44-1.66	0.53	0.19	0.44	0.27-1.41
	1.27	0.81	0.23	0.61	0.35-2.2	0.64	0.2	0.48	0.21-1.88
0.05% (w/v) CMC	0.85	1.07	0.61	0.69	0.38-4	0.89	0.62	0.73	0.19-3.8
σ = 65 dyne/cm	1.06	1.25	0.74	0.89	0.4-4.5	1.00	0.71	0.85	0.86-3.66
	1.27	1.81	1.3	0.81	0.55-5.76	1.51	1.16	0.80	0.23-4.56
	1.49	2.76	1.82	1.51	0.47-9.8	2.38	1.48	1.2	0.37-7.6
	1.71	3.55	2.1	0.99	0.76-9.81	3.15	1.76	3.1	0.48-7.6
0.05% (w/v) starch	1.06	2.75	1.06	3.2	1-4.5	2.35	1.3	2.21	0.5-4.51
σ = 68.4 dyne/cm	1.27	4.45	1.94	3.8	0.61-8.35	3.83	2.14	3.37	0.38-6.74
	1.49	3.98	1.77	0.81	0.67-6.18	3.65	1.62	0.68	0.4-5.13
	1.71	3.18	1.05	3.47	0.92-5.13	2.8	1.0	1.44	0.33-4.20
0.05% (w/v) CMC +	0.53	0.65	0.15	0.68	0.34-1.4	0.52	0.18	0.56	0.085-1.4
1% ethanol	0.64	0.74	0.27	0.65	0.37-2.64	0.62	0.28	0.58	0.11-2.8
σ = 46.2 dyne/cm	0.85	0.94	0.21	1.04	0.63-1.39	0.72	0.34	0.96	0.21-1.22
	1.06	1.08	0.23	1.21	0.52-3.16	0.78	0.21	1.04	0.39-2.67
0.05% (w/v) starch	1.06	0.79	0.19	0.79	0.49-1.58	0.6	0.2	0.62	0.18-1.56
+ 1% (w/v) ethanol	1.27	1.17	0.73	0.78	0.46-4.5	0.99	0.69	0.65	0.15-4.13
σ = 50.3 dyne/cm	1.49	1.27	0.59	0.92	0.43-4.33	1.09	0.53	0.71	0.99-3.4
	1.71	1.3	0.8	0.83	0.28-5.1	1.14	0.67	0.62	0.18-4.55

1 : d_{max} is the maximum diameter of a circle
2 : d_{circle} is the equivalent diameter of a circle
3 : σ is the surface tension of the test fluid (dyne/cm)

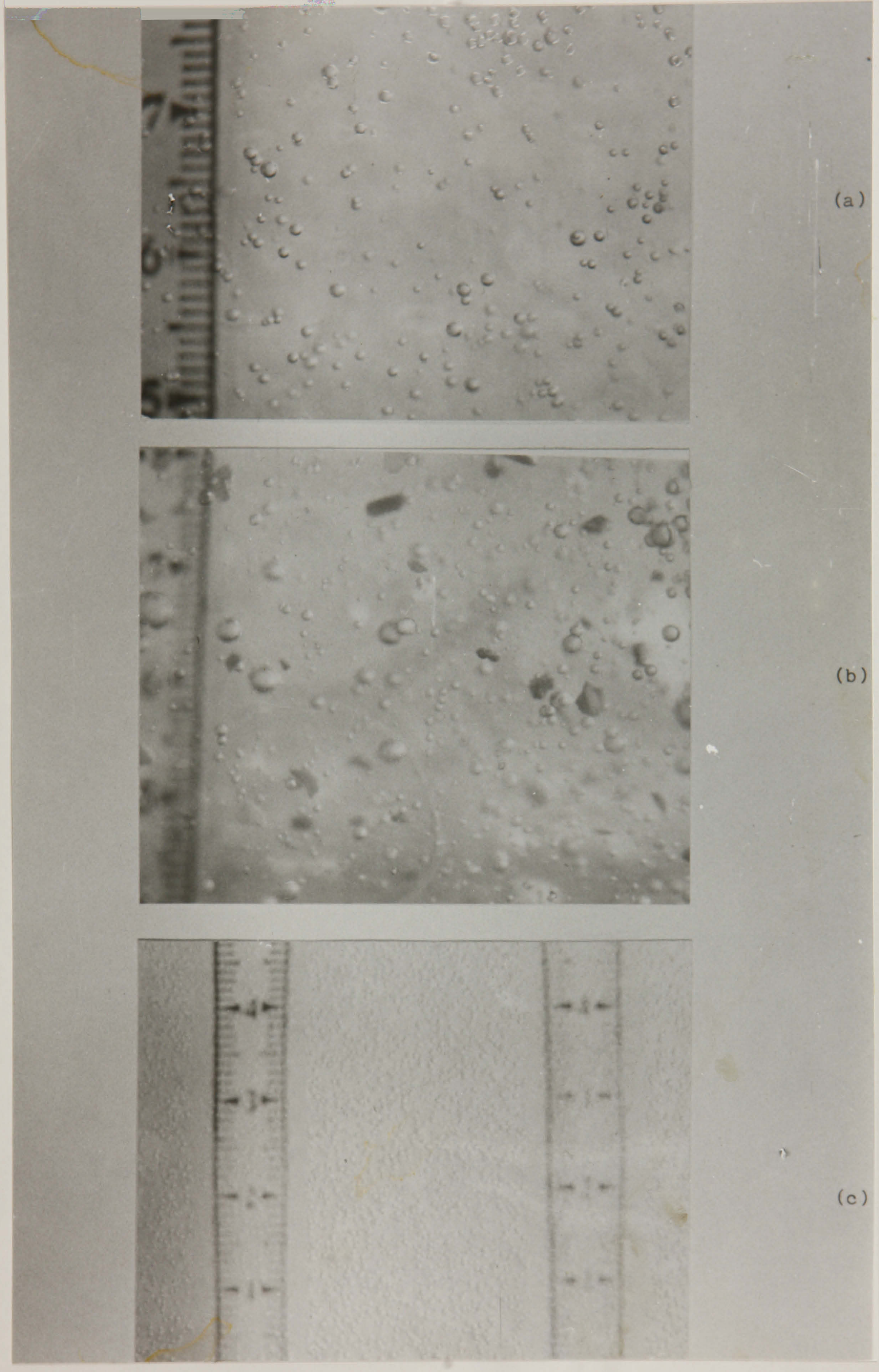

Figure 3.24 Bubble characteristics in the simulated fermentation broth (a) : 1% (w/v) ethanol + 0.05% (w/v) CMC, J_G=0.64 cm/s; (b) : as (a) + 2.5% (v/v) solids, J_G=1.06 cm/s; (c) : As (a),bubbles in the downcomer

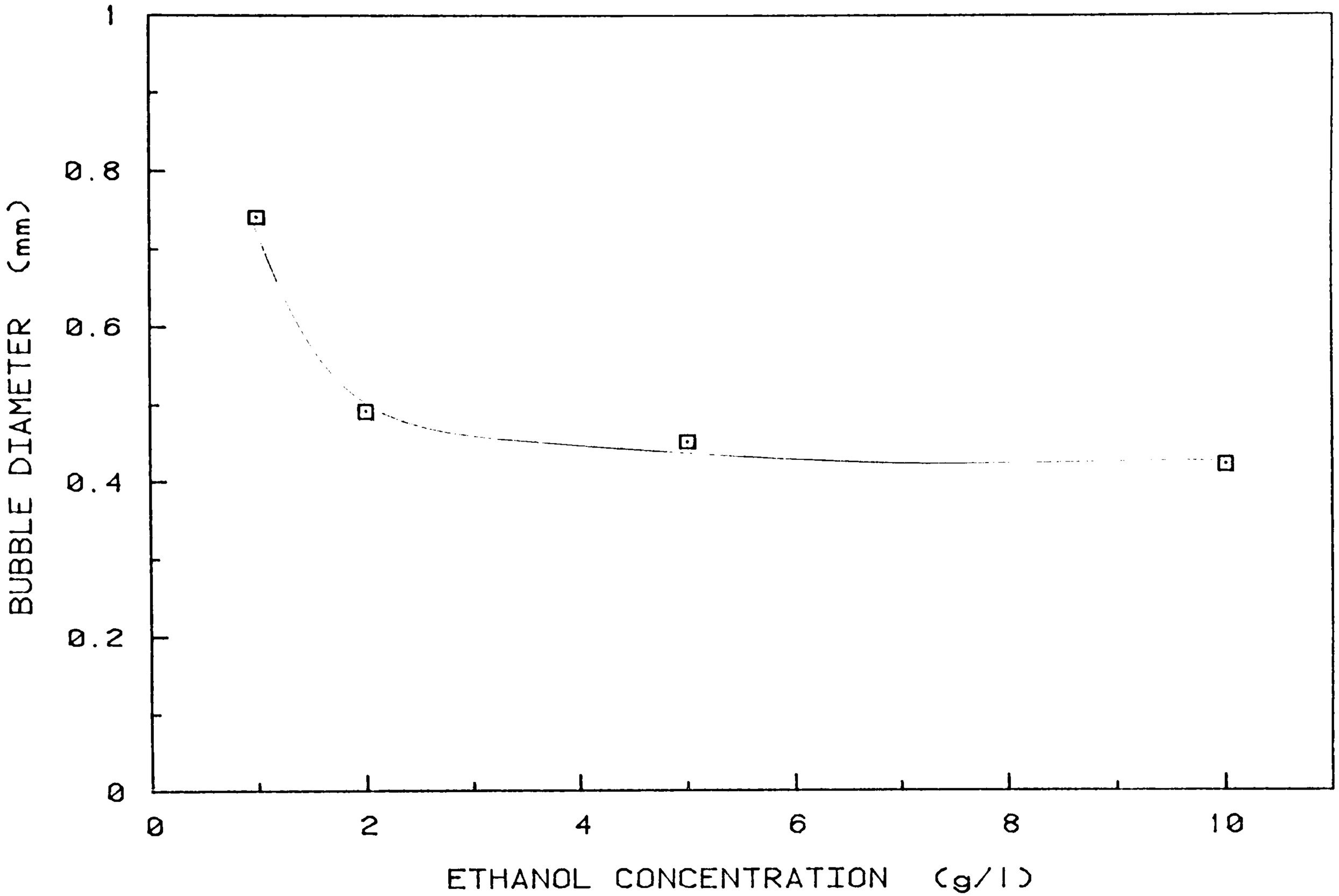

Figure 3.25 Variations of mean bubble diameter with ethanol concentration in a 50 l GLF.

Superficial gas velocity = 0.64 cm/s; Gas distributer : sintered disc

Table 3.10 Characteristic parameters for the bubble size distribution of various fluid systems in a 50 l GLF

Sytem	J_G cm/s	Eo	Re	U_{mt} m/s	We	E W/m^3	d_s mm	a m^2
Distilled water	1.06	0.79	700	0.29	2.83	101	2.75	6.53
σ^3= 71.2 dyne/cm	1.17	1.4	810	0.25	2.8	111	2.79	7.28
Log M = -10.57	1.26	2.29	970	0.24	3.3	120	2.83	7.97
	1.49	2.75	1020	0.23	3.32	140	2.9	9.44
	1.71	1.21	780	0.26	2.81	158	2.96	10.82
1% (w/v) ethanol	0.64	0.04	30	0.06	0.03	60	3.26	8.40
σ = 53.5 dyne/cm	0.85	0.04	33	0.07	0.04	77	3.86	15.53
Log M = -10.2	1.06	0.05	39	0.07	0.05	91	4.25	18.14
	1.27	0.08	73	0.11	0.14	105	4.55	22.4
0.05% (w/v) CMC	0.85	0.12	110	0.12	0.2	80	3.34	8.64
σ = 65 dyne/cm	1.06	0.15	150	0.15	0.35	97	3.64	11.87
Log M = -10.15	1.27	0.34	370	0.25	1.45	113	3.91	14.9
	1.49	0.85	600	0.25	2.28	129	4.11	17.93
	1.71	1.5	710	0.23	2.56	143	4.27	20.7
0.05% (w/v) starch	1.06	0.79	460	0.2	1.37	98	3.38	9.86
σ = 68.4 dyne/cm	1.27	2.1	650	0.17	1.62	116	3.5	11.95
Log M = -9.91	1.49	1.91	700	0.19	1.93	135	3.6	14.09
	1.71	1.12	515	0.18	1.33	151	3.68	16.08
0.05% (w/v) CMC +	0.53	0.06	34	0.07	0.06	51	2.58	5.58
1% ethanol	0.64	0.08	49	0.08	0.09	60	3.06	8.94
σ = 46.2 dyne/cm	0.85	0.11	71	0.1	0.16	77	3.61	14.47
Log M = -9.7	1.06	0.13	92	0.12	0.24	91	3.97	19.43
0.05% (w/v) starch	1.06	0.07	40	0.07	0.06	91	4.13	18.67
+ 1% (w/v) ethanol	1.27	0.19	110	0.11	0.24	104	4.42	23.07
σ = 50.3 dyne/cm	1.49	0.23	155	0.14	0.42	117	4.68	27.39
Log M = -9.51	1.71	0.25	170	0.15	0.51	127	4.89	31.25

In this section the graphical correlation (Figure 3.6) given by Clift *et al* (1978) is employed in determining the mean terminal velocity of bubbles U_{mt}. Weber number We, indicates a measure of bubble integrity against inertial force and it is determined from it's definition given in Table 3.3. The power E, is calculated from Equation 3.6. The Sauter mean diameter d_s, and interfacial area a, are calculated from Equations 3.7a and 3.7b. The following observations from Table 3.10 are made;

- All calculated parameters increase with increasing J_G. Exception is observed with the distilled water system (high surface tension) at very

high J_G due to reasons previously described.

- The increase in the interfacial area is associated with increase in J_G, and the relative decrease in the surface tension of the bulk liquid (Figure 3.26)

- The mean terminal velocity of the bubbles sharply decreases with decreasing bubble size brought about by lower surface tension of the bulk liquid.

- The values of Sauter mean diameter do not increase at the rate similar to the other mean diameter values experimentally measured.

- The power dissipation is highest (marginally) with the systems of high surface tension value

Table 3.11 Bubble size distribution of three-phase systems in a 50 l GLF

		d_{max}				d_{circle}			
Sytem	J_G (cm/s)	Mean mm	Std deviation mm	Mode mm	Range mm	Mean mm	Std deviation mm	Mode mm	Range mm
0.05% (w/v) CMC +	1.06	1.72	0.81	1.31	0.45-5.01	1.52	0.71	1.14	0.29-4.47
2.5% (v/v) solids	1.27	2.32	0.95	1.74	0.53-6.21	1.89	0.83	1.43	0.4-5.25
σ = 63.4 dyne/cm	1.49	2.04	0.92	1.66	0.34-7.3	1.7	0.81	1.26	0.29-5.68
	1.71	2.28	1.12	1.78	0.3-6.78	1.77	1.02	1.55	0.26-6.1
0.05% (w/v) starch	1.06	1.8	0.51	1.45	0.6-6.54	1.27	0.44	1.11	0.41-4.83
+2.5% (v/v) solids	1.27	1.92	0.61	2.78	0.65-7.66	1.58	0.54	2.39	0.32-5.58
σ = 67.7 dyne/cm	1.49	2.4	0.78	1.18	0.4-9.36	1.73	0.82	2.09	0.23-6.08
	1.71	3.28	1.57	0.81	0.67-6.2	2.65	1.31	0.68	0.4-5.13
0.05% (w/v) CMC +	1.06	0.93	0.47	0.7	0.47-9.63	0.7	0.38	0.46	0.18-2.3
1% (w/v) ethanol +	1.27	1.19	0.64	0.88	0.52-5.41	1.0	0.6	0.73	0.27-4.18
2.5% (v/v) solids	1.49	1.22	0.66	0.74	0.34-6.3	1.08	0.6	0.59	0.21-4.7
σ = 51.2 dyne/cm	1.71	1.54	0.72	1.03	0.41-7.88	1.37	0.63	0.97	0.33-6.1
0.05% (w/v) starch	1.06	0.73	0.28	0.64	0.42-2.3	0.52	0.29	0.37	0.11-1.97
+ 1% (w/v) ethanol	1.27	0.84	0.49	0.58	0.36-3.1	0.67	0.48	0.4	0.18-2.91
+ 2.5% (v/v) solids	1.49	1.05	0.55	0.66	0.44-3.16	0.87	0.53	0.54	0.21-2.89
σ = 56.9 dyne/cm	1.71	1.44	0.64	0.8	0.31-4.1	1.13	0.6	0.55	0.16-3.22

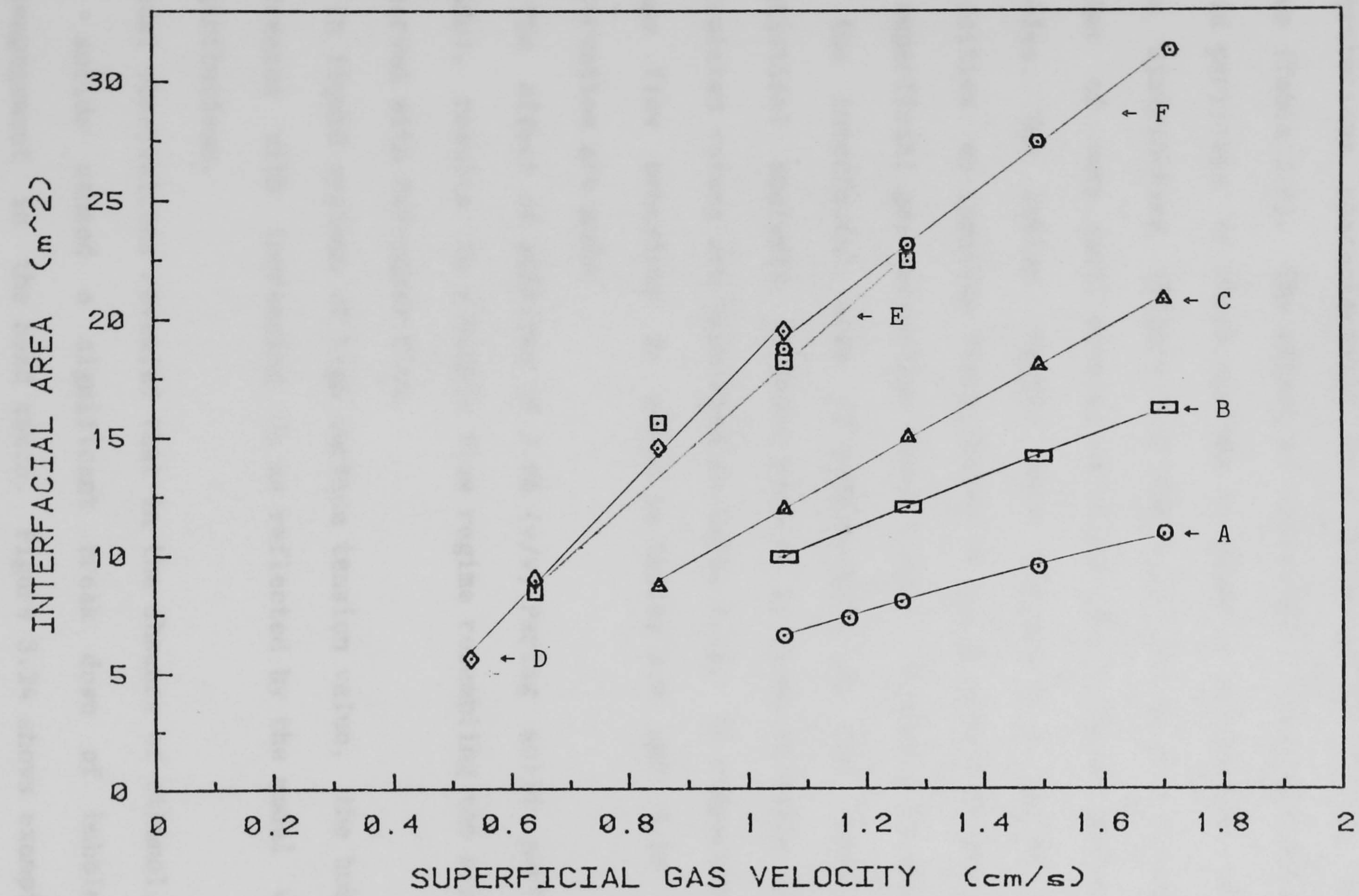

Figure 3.26 Variation of interfacial area of bubbles in a two-phase gas-lift fermenter

A : Distilled water; B : 0.05% (w/v) starch; C : 0.05% (w/v) CMC; D : 0.05% (w/v) CMC + 1% (w/v) ethanol; E : 1% (w/v) ethanol; F : 0.05% (w/v) starch + 1% (w/v) ethanol

Figures 3.27 and 3.28 refer to two simulated broth conditions; a- by liquid systems of similar viscosity and surface tension, and b- by three-phase broth system. Both starch/ethanol and CMC/ethanol mixtures show size distributions characteristic to a liquid system of low surface tension value (Table 3.9). The effect of addition of 2.5-4 mm medium grade Perlag solid particles to these systems is shown by an overall reduction in the size distribution (Figure 3.27 and 3.28) due to the presence of large number of very small bubbles which are the break up products of larger bubbles. The latter results were limited to a narrow range of gas velocities as complete fluidisation of soild particles was only achieved at superficial gas velocities above 1 cm/s. Figure 3.29 shows the changes in the interfacial area of bubbles with J_G for these systems. The statistical analysis of these results is shown in Table 3.11 and their calculated values are tabulated in Table 3.12. In comparison to the two-phase flow behaviour as shown in Tables 3.9 and 3.10 the following observation are made;

- The effect of addition of 2.5% (v/v) Perlag solid particles (medium grade), results in a bubble flow regime resembling the slug flow regime observed with two-phase flow.
- In liquid systems of high surface tension value, the bubble break up increases with increasing J_G as reflected by the modal values of the distributions.

Visual observations revealed that in the absence of ethanol, the addition of solids caused a significant break down of bubbles prior to disengagement in the head space. Figure 3.24 shows examples of bubble sizes in the simulated conditions. It is notable that in the presence of ethanol, there is a presence of large number of small bubbles, less than 1 mm in diameter, which are observed to recirculate in the downcomer of the fermenter (Figure 3.24).

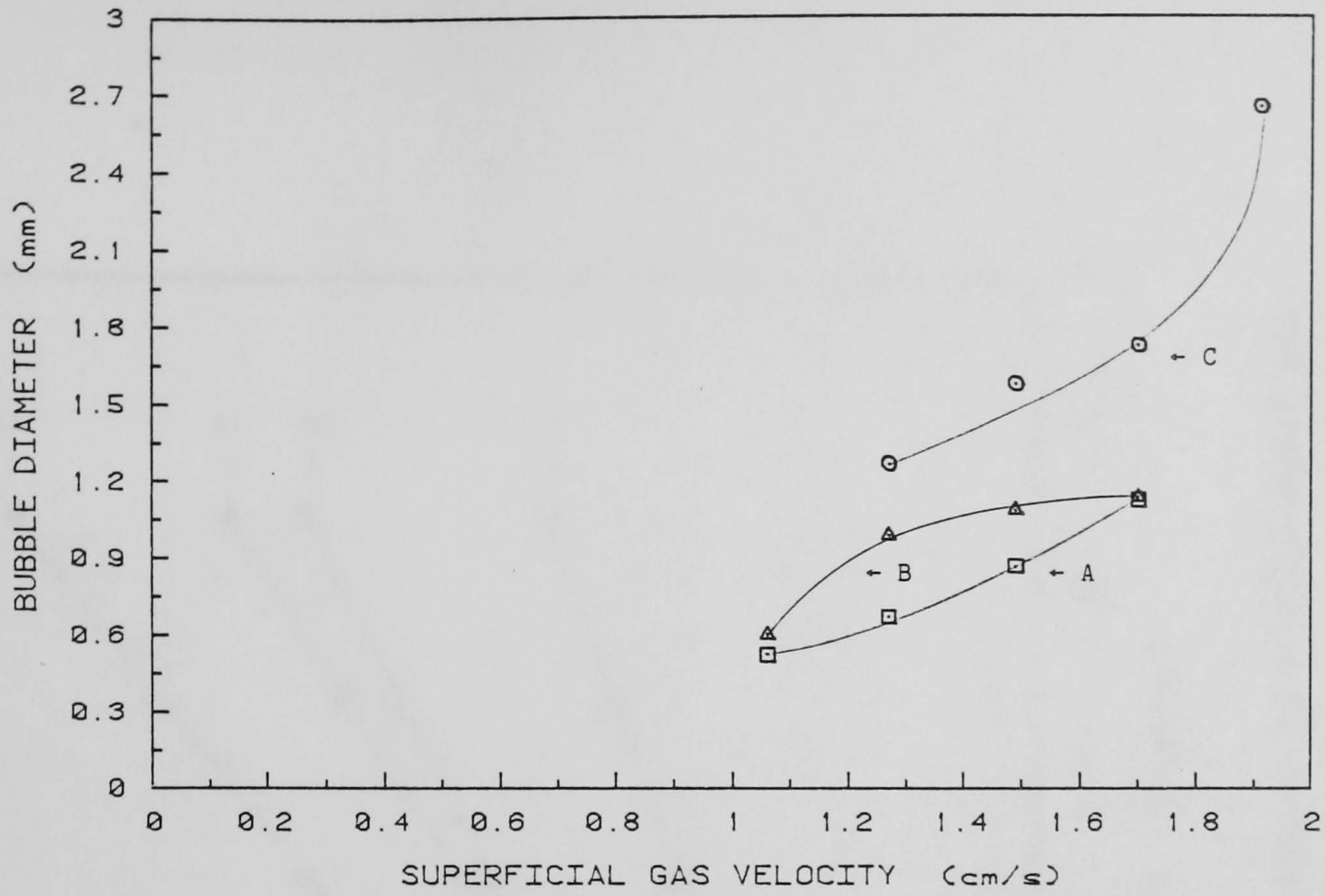

Figure 3.27 Variations of mean bubble diameter with superficial gas velocity in multi-phase systems containing 0.05% (w/v) starch

A : 2.5% (v/v) solids + 1% (w/v) ethanol; B : 1% (w/v) ethanol; C : 2.5% (w/v) solids

Solids : Medium grade Perlag

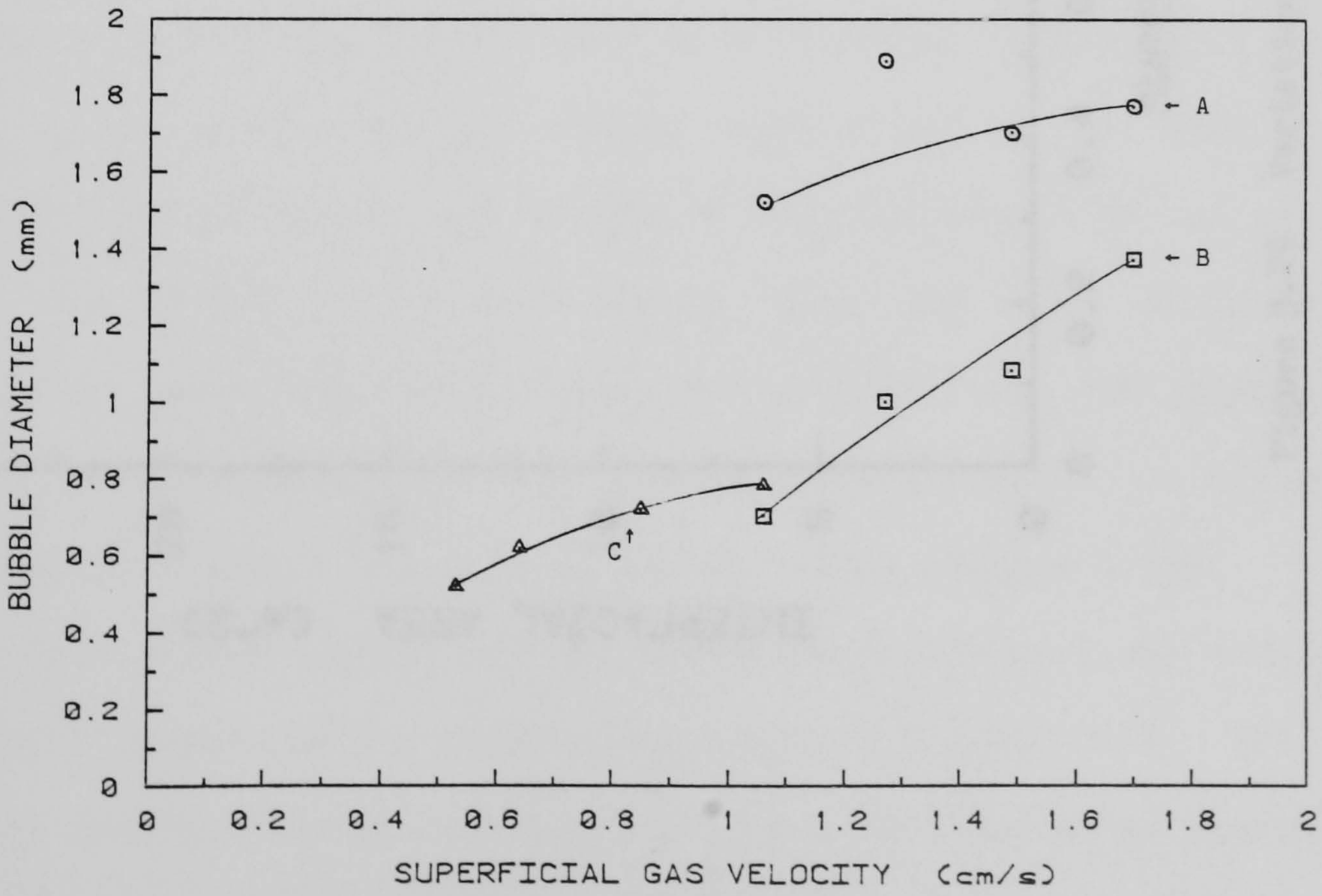

Figure 3.28 Variations of mean bubble diameter with superficial gas velocity in multi-phase systems containing 0.05% (w/v) CMC

A : 2.5% (v/v) solids; B : 2.5% solids + 1% (w/v) ethanol; C : 1% (w/v) ethanol

Solids : Medium grade Perlag

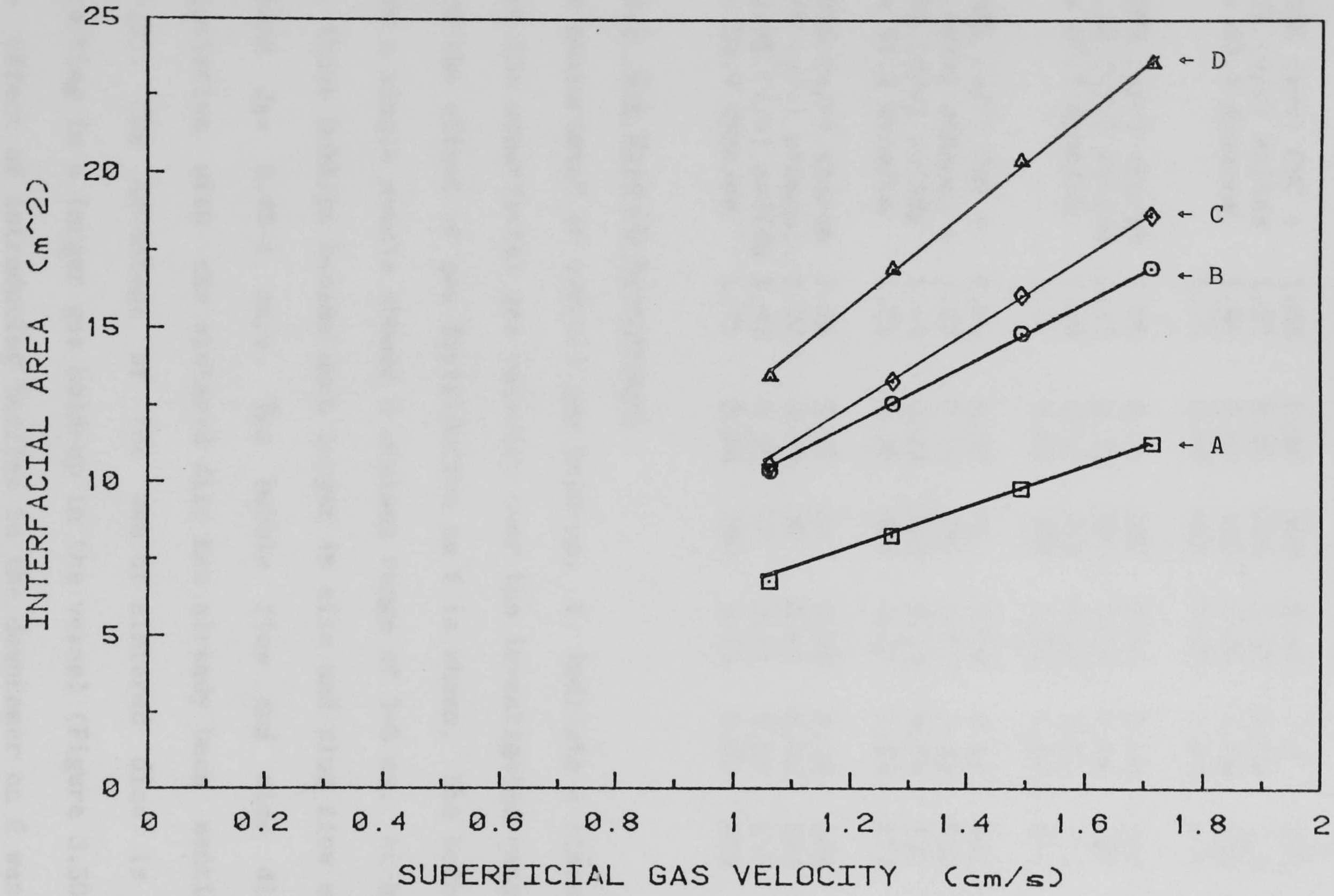

Figure 3.29 Variations of interfacial area of bubbles in a multi-phase gas-lift fermenter with 2.5% (v/v) Perlag solid particles.

A : 0.05% (w/v) starch; B : 0.05% (w/v) CMC; C : 0.05% starch + 1% (w/v) ethanol

D : 0.05% (w/v) CMC + 1% (w/v) ethanol

Table 3.12 Characteristic parameters for the bubble size distribution of three-phase systems in a 50 l GLF

Sytem	J_G cm/s	Eo	Re	U_{mr} m/s	We	E W/m^3	d_s mm	a m^2
0.05% (w/v) CMC +	1.06	0.36	380	0.25	1.5	103	3.23	10.4
2.5% (v/v) solids	1.27	0.55	500	0.26	2.02	123	334	12.6
σ = 63.4 dyne/cm	1.49	0.45	410	0.24	1.54	142	3.42	14.8
	1.71	0.48	440	0.25	1.74	160	3.50	16.9
0.05% (w/v) starch	1.06	0.23	200	0.16	0.48	106	2.65	6.75
+2.5% (v/v) solids	1.27	0.36	300	0.19	0.84	127	2.73	8.25
σ = 67.7 dyne/cm	1.49	0.43	343	0.20	1.02	147	2.8	9.78
	1.71	1.02	520	0.20	1.57	167	2.85	11.2
0.05% (w/v) CMC +	1.06	0.09	60	0.09	0.11	102	3.24	13.4
1% (w/v) ethanol +	1.27	0.19	130	0.13	0.33	120	3.45	16.9
2.5% (v/v) solids	1.49	0.22	170	0.16	0.54	137	3.62	20.4
σ = 51.2 dyne/cm	1.71	0.36	290	0.21	1.18	152	3.75	23.6
0.05% (w/v) starch	1.06	0.05	24	0.05	0.02	104	3.01	10.5
+ 1% (w/v) ethanol	1.27	0.09	50	0.07	0.06	123	3.19	13.3
+ 2.5% (v/v) solids	1.49	0.15	93	0.11	0.19	141	3.33	16.0
σ = 56.9 dyne/cm	1.71	0.24	180	0.16	0.51	159	3.44	18.6

3.3.3 Gas Hold-Up Measurement

The measurement of overall gas hold-up, ϵ, indicate a linear relationship with the superficial gas velocity over the investigated range. In Figure 3.30 the effect of gas distribution on ϵ is shown. The bubbles generated from a single nozzle showed a minimum range of 3-5 mm. At high values of J_G, these bubbles became much larger in size and slug flow was observed at around J_G= 0.85-1 cm/s. The bubble flow and size distribution in association with the sintered disc has already been mentioned (section 3.3.2). The advantage of the use of sintered disc is reflected by resulting in a larger gas hold-up in the vessel (Figure 3.30).

The effect of introducing baffles in the downcomer on ϵ was studied with air water system and the results are shown in Figure 3.31. The results indicate that baffles reduce the overall gas hold-up of the system. There is an overall decrease of around 12% compared to the system without the baffles.

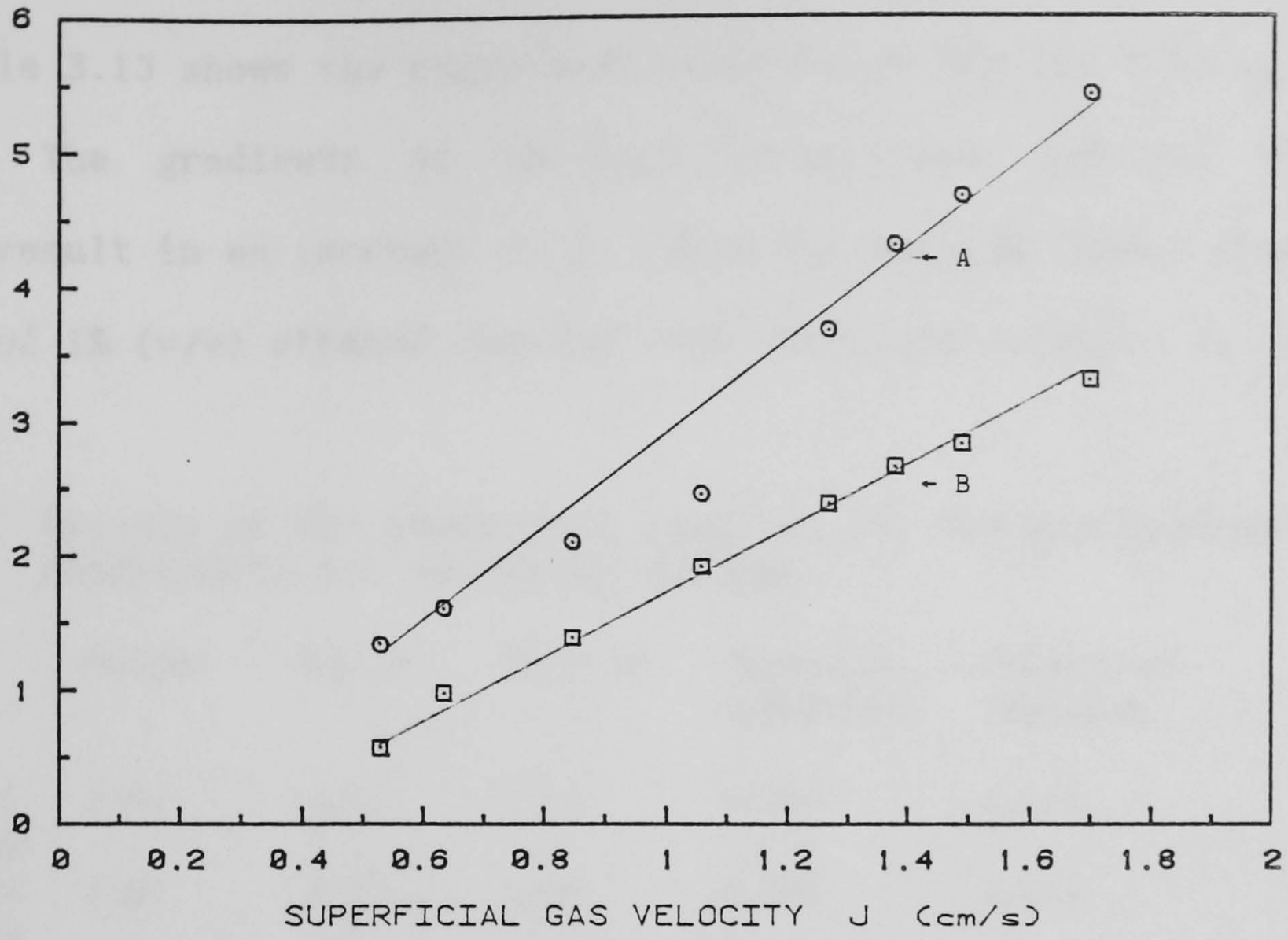

Figure 3.30 Variations of gas hold-up with superficial gas velocity for two different gas distributors in the reactor.
A : Sintered disc; B : Single nozzle.

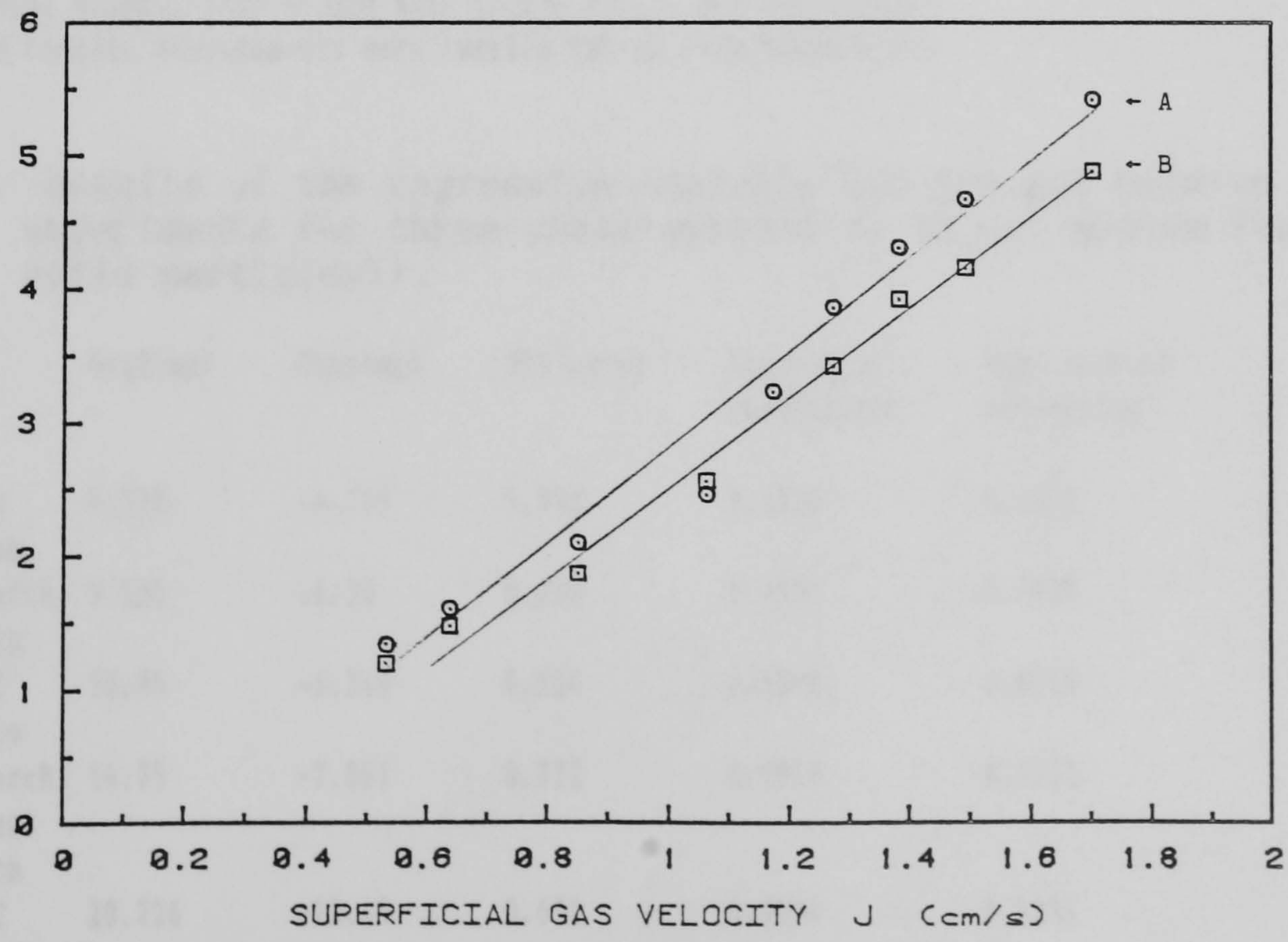

Figure 3.31 Variations of gas hold-up with superficial gas velocity for different downcomer arrangement.
A : Without baffles; B ; With baffles.

The influence of additives on the overall gas hold-up is shown in Figure 3.32. Table 3.13 shows the regression analysis of the gas hold-up studies described. The gradients of the best fitted lines indicate that all additives result in an increase in ϵ, with the maximum effect observed by addition of 1% (w/v) ethanol causing over five fold increase in the gas hold-up.

Table 3.13 Results of the regression analysis for the gas hold-up experiments for two-phase systems.

Liquid system	Gradient	Constant	Std error	Regression coefficient	Std error of regression
Distilled water[1] σ = 71.1 dyne/cm[4]	3.679	-0.919	0.244	0.9743	0.2695
Distilled water[2] σ = 71.1 dyne/cm	3.252	-0.716	0.130	0.9905	0.1439
Distilled water[3] σ = 70.3 dyne/cm	2.27	-0.565	0.072	0.9941	0.0789
0.05% (w/v) starch[1] σ = 68.4 dyne/cm	6.76	-1.621	0.461	0.9726	0.5112
0.05% (w/v) CMC[1] σ = 65 dyne/cm	11.684	-5.13	0.392	0.9923	0.4295
1% (w/v) ethanol[1] σ = 53.5 dyne/cm	19.735	-8.065	1.738	0.9556	1.5621

1 : Reactor vessel without baffles and with sintered disc gas distributor
2 : Reactor vessel with baffles and sintered disc gas distributor
3 : Reactor vessel without baffles and with single nozzle gas distributor
4 : All surface tension measurements were carried out at room temperature

Table 3.14 Results of the regression analysis for the gas hold-up experiments for three-phase systems (2.5% w/v medium Perlag soild particles)[1].

Liquid system	Gradient	Constant	Std error	Regression coefficient	Std error of regression
Distilled water σ = 70.4 dyne/cm	6.529	-4.195	0.593	0.9525	0.2695
0.05% (w/v) starch σ = 67.7 dyne/cm	9.331	-6.30	0.823	0.9551	0.1439
0.05% (w/v) CMC σ = 63.4 dyne/cm	10.95	-6.518	0.559	0.9846	0.0789
0.05% (w/v) starch +1% (w/v) ethanol σ = 56.9 dyne/cm	14.75	-7.861	0.722	0.9858	0.5112
0.05% (w/v) CMC +1% (w/v) ethanol σ = 51.2 dyne/cm	20.726	-12.18	0.630	0.9954	0.4295

1: Experiments were carried out in the reactor vessel without baffles at room temperature.

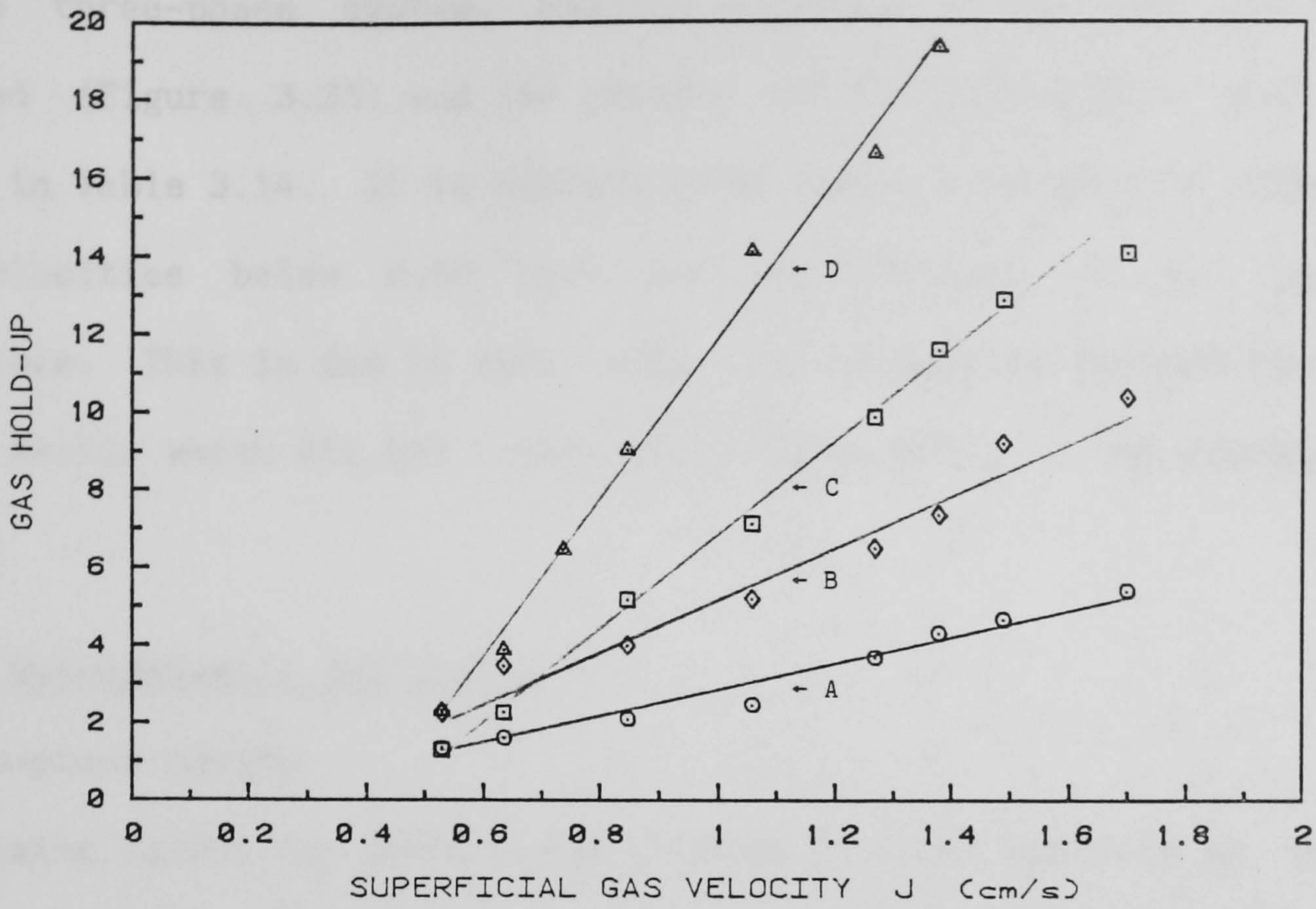

Figure 3.32 Variations of gas hold-up with superficial gas velocity for various fluid systems.

A : Distilled water; B : 0.05% Starch; C : 0.05% CMC; D : 1% Ethanol.

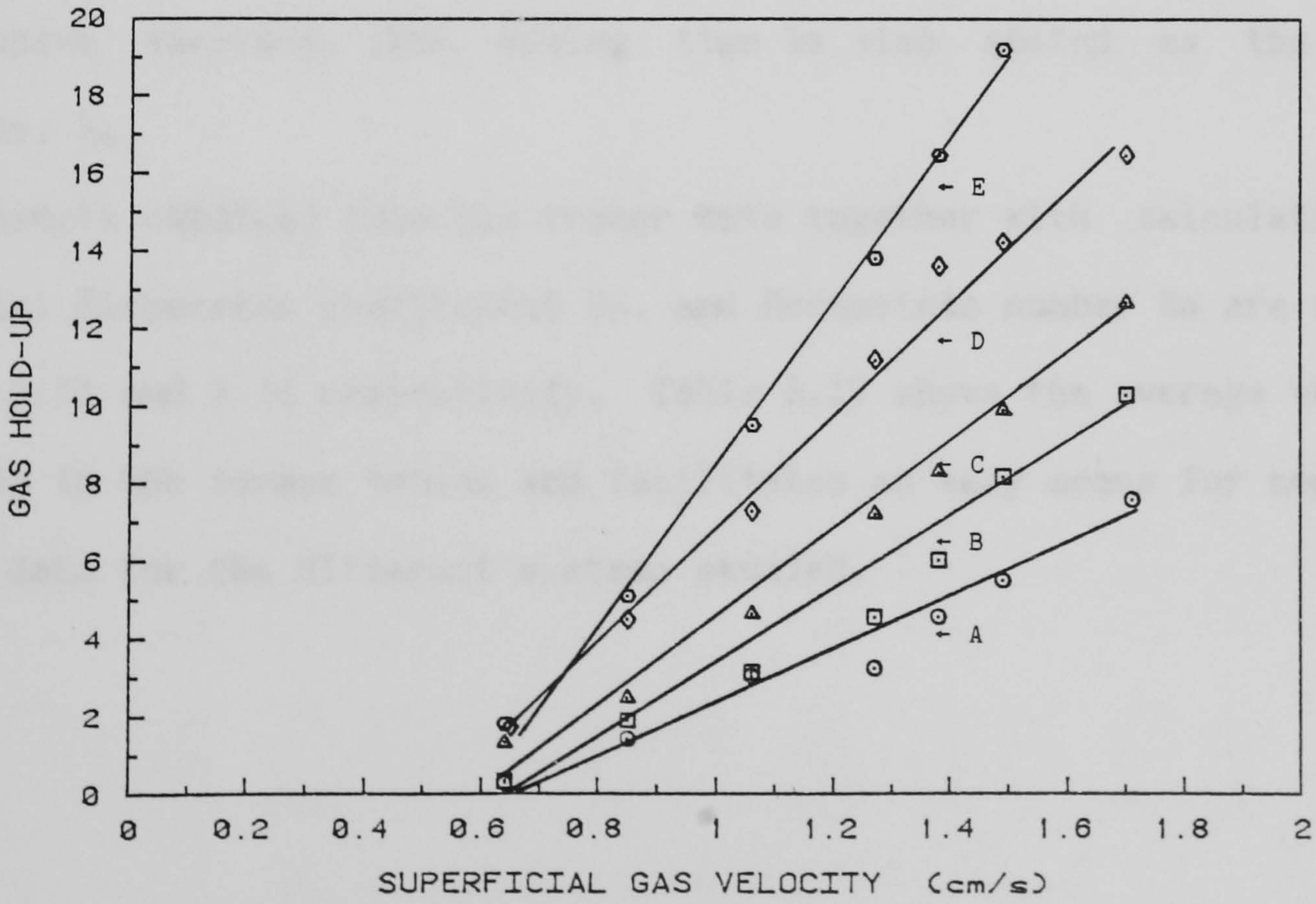

Figure 3.33 Gas hold-up in a multi-phase gas-lift fermenter containing 2.5% (v/v) medium Perlag solid particles

A : Distilled water; B : 0.05% (w/v) starch; C : 0.05% (w/v) CMC; D : 0.05% (w/v) starch + 1% (w/v) ethanol; E : 0.05% (w/v) CMC + 1% (w/v) ethanol

In the three-phase system, similar increases in the gas hold-up are observed (Figure 3.33) and the results for the statistical analysis is shown in Table 3.14. It is notable from Figure 3.33 that at superficial gas velocities below 0.63 cm/s the gas hold-up in the system is negligible. This is due to very large slug formations through the static bed of solids which did not contribute significantly to the voidage of the system.

3.3.4 Hydrodynamics and mixing

A : Two-phase mixing

The mixing inside the reactor was studied by trace analysis as described in section 3.2.2. This technique proved very powerful in determining the the liquid velocity in various sections of the reactor, and residence time distribution of a liquid element travelling through the reactor. The velocity at which a liquid element travels the riser section of the reactor is referred to as the rising velocity, V_r, and one complete cycle as the circulation velocity, V_c. In order to maintain consistency for comparative analysis, the mixing time is also stated as the mixing velocity, V_m.

The results obtained from the tracer data together with calculation for the axial dispersion coefficient D_T, and Bodenstein number Bo are shown in Tables 3.15 and 3.16 respectively. Table 3.17 shows the average values of the data in the former tables and facilitates an easy means for comparison of the data for the different systems studied.

Table 3.15 Liquid velocity profiles for loop circulation in pilot GLF
(a) Single nozzle gas distributor

Reactor Without baffles							*Reactor with baffles*						
J_G (cm/s)	V_r (cm/s)	V_c (cm/s)	V_a (cm/s)	δ (cm)	D_T (cm²/s)	Bo	J_G (cm/s)	V_r (cm/s)	V_c (cm/s)	V_a (cm/s)	δ (cm)	D_T (cm²/s)	Bo
0.42	3.46	2.03	1.88	28.9	13.2	23.1	0.42	19.4	9.45	2.45	36	114	12.4
0.42	3.08	2.29	1.69	19.0	4.51	76.1	0.42	16.7	6.63	3.88	42.2	135	7.38
0.42	3.22	1.66	1.25	33.9	8.68	28.7	0.42	18.4	7.61	7.55	41.3	143	7.92
0.85	7.38	5.47	5.36	18.1	11.0	74.5	0.85	35.3	1.66	2.07	66.7	713	0.35
0.85	8.11	5.08	4.22	26.1	25.2	30.2	0.85	46.7	4.72	2.04	62.9	840	0.85
0.85	9.6	6.42	6.14	23.2	23.5	41.0	0.85	15.6	2.69	1.81	57.9	237	1.7
1.27	12.8	10.4	10.2	13.1	10.0	155	1.27	25.0	11.9	10.9	36.7	153	11.6
1.27	18.2	13.7	7.71	17.3	24.8	82.9	1.27	26.9	10.3	6.07	43.3	230	6.7
1.27	17.5	8.96	5.81	34.2	92.9	14.5	1.27	100	13.2	5.11	60.8	1679	1.18
1.71	63.6	9.38	7.50	59.7	1030	1.37	1.71	58.3	8.89	7.61	59.3	934	1.43
1.71	46.7	8.77	7.02	56.9	686	1.92	1.71	117	13.5	9.04	61.9	2033	0.99
1.71	41.2	8.28	6.03	55.9	586	2.12	1.71	38.9	13.2	12.6	46.3	378	5.23

Table 3.16 Liquid velocity profiles for loop circulation in pilot GLF
(b) Sintered disc gas distributor

Distilled Water System							*1% (w/v) Ethanol + 0.05% (w/v) CMC*						
J_G (cm/s)	V_r (cm/s)	V_c (cm/s)	V_a (cm/s)	δ (cm)	D_T (cm²/s)	Bo	J_G (cm/s)	V_r (cm/s)	V_c (cm/s)	V_a (cm/s)	δ (cm)	D_T (cm²/s)	Bo
0.42	17.1	8.11	7.74	36.8	105	11.6	0.63	12.1	4.65	5.32	43.0	102	6.86
0.42	15.6	9.32	7.55	28.2	56.3	24.8	0.63	9.59	7.64	6.33	14.2	8.83	130
0.42	16.3	8.52	8.28	33.4	82.7	15.5	0.63	10.9	8.25	7.17	16.8	13.9	89.1
0.85	17.9	11.6	9.3	24.6	49.4	35.2	0.85	17.7	9.00	9.52	34.5	95.8	14.1
0.85	22.2	12.9	10.5	29.3	86.8	22.3	0.85	17.7	7.25	9.06	41.4	138	7.89
0.85	15.7	11.5	10.9	18.7	25.0	68.9	0.85	13.1	6.88	8.60	33.2	65.5	15.8
1.06	17.1	14.1	12.6	12.1	11.4	186	1.06	23.7	10.9	10.7	38.0	155	10.5
1.06	24.1	19.3	11.1	6.19	3.69	784	1.06	26.4	9.80	12.2	44.0	233	6.31
1.06	18.4	15.6	11.9	10.8	9.76	239	1.06	25.3	9.16	10.0	44.6	229	6.00
1.27	17.1	13.4	8.77	15.1	17.7	114	1.27	26.7	21.7	17.2	13.0	20.5	159
1.27	22.6	15.8	9.65	21.1	45.6	52.0	1.27	18.5	12.7	10.2	21.9	40.5	47.0
1.27	13.3	12.5	4.55	4.22	1.07	1743	1.27	25.2	13.1	12.8	33.9	132	14.8
1.71	20.0	14.8	7.85	18.2	30.0	74.0	1.71	24.8	13.3	8.66	32.4	115	16.8
1.71	20.3	13.6	9.71	23.2	49.7	40.9	1.71	30.1	12.3	8.76	41.1	231	8.06
1.71	17.1	13.9	8.52	13.1	13.4	156	1.71	28.9	12.5	9.42	39.8	208	9.01

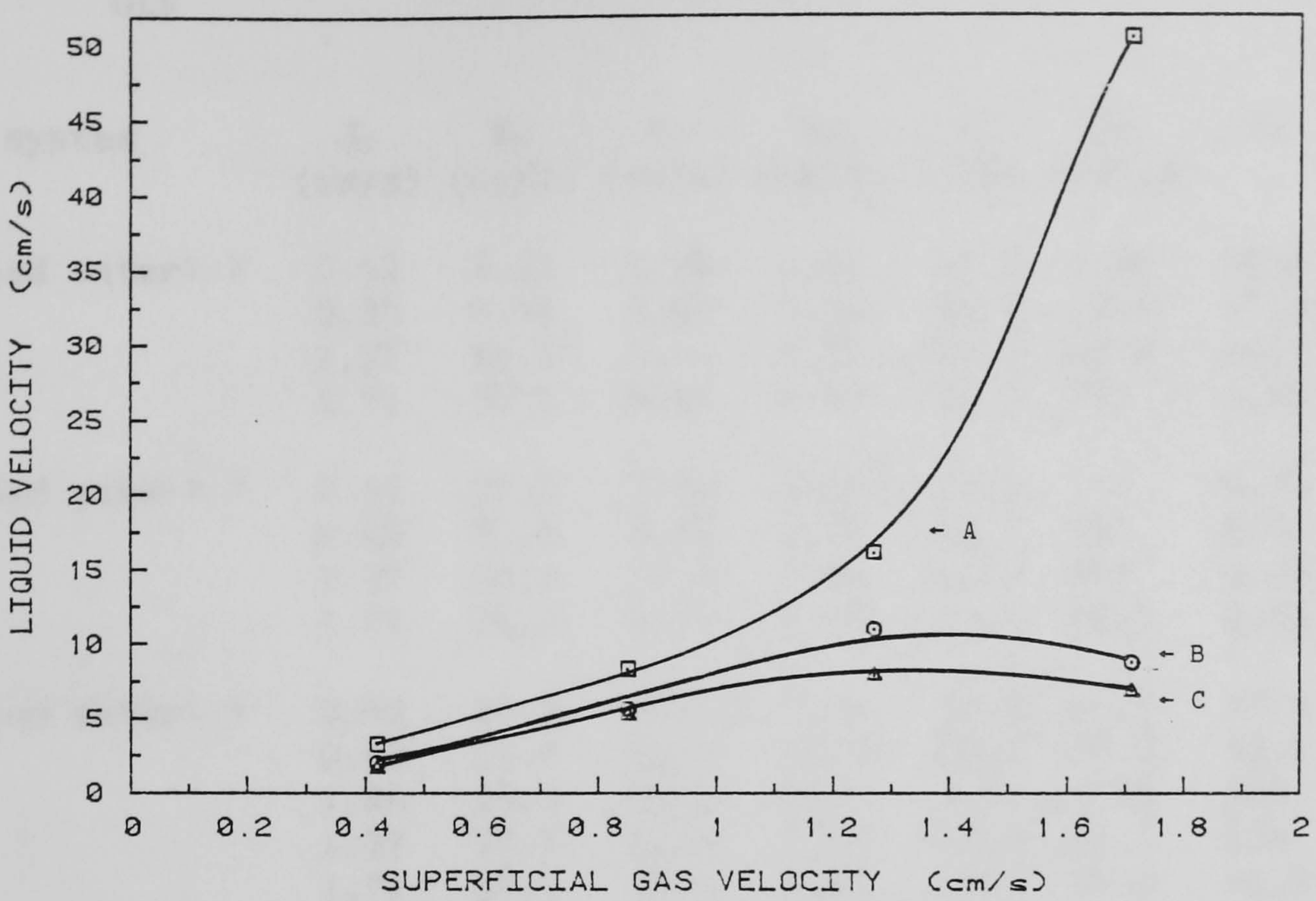

Figure 3.34 Liquid velocity characteristics in the gas-lift fermenter
A : Riser liquid velocity; B : Liquid circulation velocity; C : Liquid mixing velocity

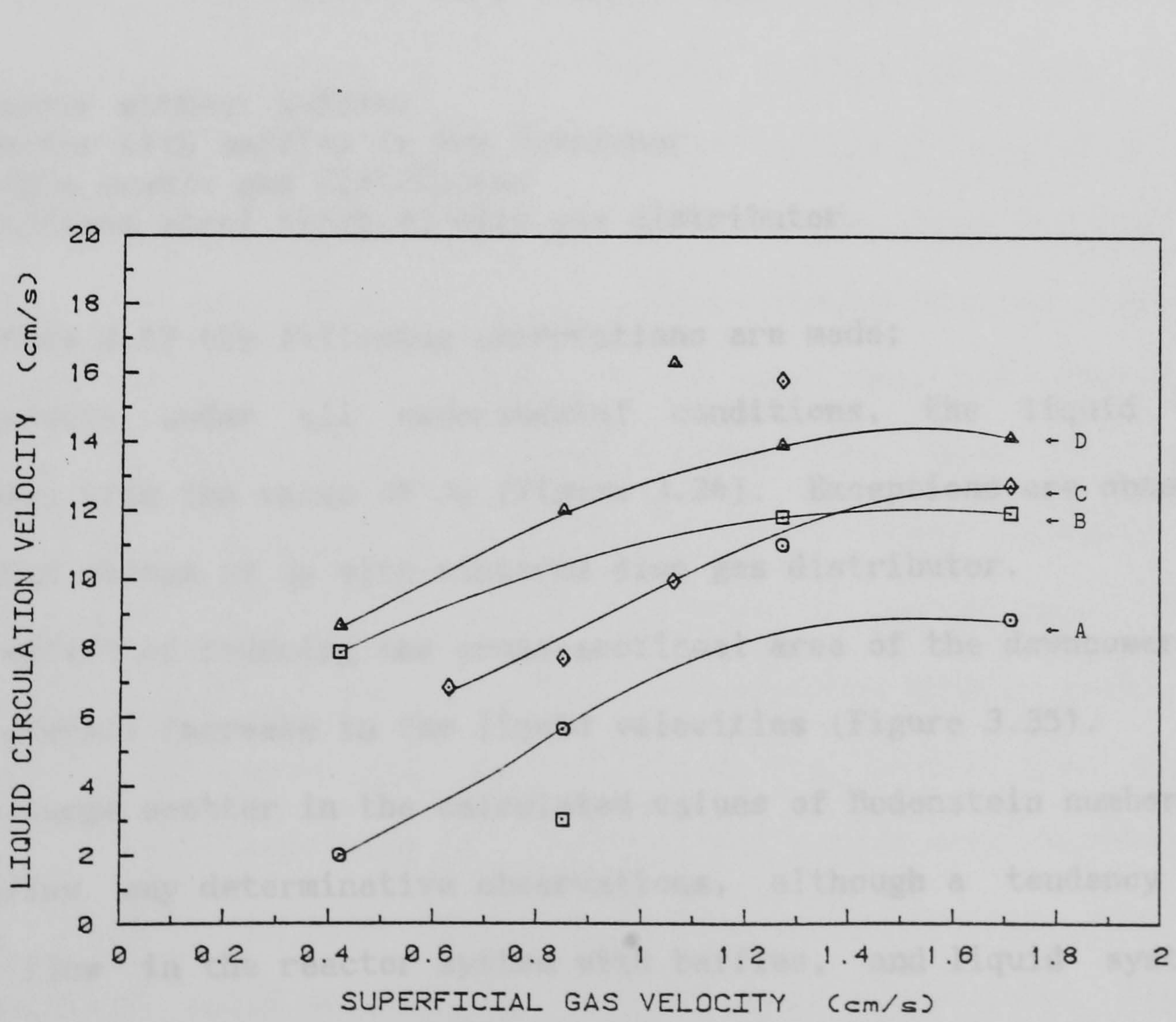

Figure 3.35 Variations of liquid circulation velocity with different systems in a gas-lift fermenter
A : Single nozzle gas distributor; B : Sintered disc gas distributor; C : S Single nozzle gas distributor with baffles in the downcomer; D : Sintered disc gas distributor. A,B,C : Distilled water; D : 0.05% (w/v) CMC + 1% (w/v) ethanol.

Table 3.17 Mean liquid velocity profiles for loop circulation in a 50 l GLF

Liquid system	J_G (cm/s)	V_r (cm/s)	V_c (cm/s)	V_m (cm/s)	δ (cm)	D_T (cm^2/s)	Bo
Distilled water[1,3]	0.42	3.25	1.99	1.61	27.3	8.80	42.6
	0.85	8.36	5.66	5.24	22.5	19.9	48.6
	1.27	16.2	11.0	7.91	21.5	42.6	84.1
	1.71	50.5	8.81	6.85	57.5	767	1.80
Distilled water[2,3]	0.42	18.2	7.90	4.63	39.8	131	9.23
	0.85	32.5	3.02	1.97	62.5	597	0.97
	1.27	50.6	11.8	7.36	46.9	687	6.49
	1.71	71.3	11.9	9.75	55.8	1115	2.55
Distilled water[1,4]	0.42	16.3	8.65	7.86	32.8	81.3	17.3
	0.85	18.6	12.0	10.2	24.2	53.7	42.1
	1.06	19.9	16.3	11.9	9.70	8.28	403
	1.27	17.7	13.9	7.66	13.5	21.5	636
	1.71	19.1	14.1	8.69	18.2	31.0	90.3
1% (w/v) ethanol + 0.05% (w/v) CMC[1,4]	0.63	10.9	6.85	6.28	24.7	41.6	75.3
	0.85	16.2	7.71	9.06	36.4	99.8	12.6
	1.06	25.1	9.95	11.0	42.2	206	7.60
	1.27	23.5	15.8	13.4	22.9	64.3	73.6
	1.71	27.9	12.7	8.95	37.8	185	11.3

1 : Reactor without baffles
2 : Reactor with baffles in the downcomer
3 : Single nozzle gas distributor
4 : Stainless steel sintered disc gas distributor

From Table 3.17 the following observations are made;

- Generally under all experimental conditions, the liquid velocity increases with the value of J_G (Figure 3.34). Exceptions are observed at very high values of J_G with sintered disc gas distributor.

- The effect of reducing the cross-sectional area of the downcomer results in an overall increase in the liquid velocities (Figure 3.35).

- The large scatter in the calculated values of Bodenstein numbers does not allow any determinative observations, although a tendency towards mixed flow in the reactor system with baffles, and liquid system with suraface tension reducing additives may be observed by inspection.

Table 3.18 shows the summary of results for the residence time

distribution of a salt tracer in the vessel. The percentage dead volume in the reactor was determined under continuous flow. The liquid flowrates are in the same order as the operating dilution rates in actual fermentation conditions.

Table 3.18 Analysis of the results of residence time distribution in 50 l GLF with a sintered disc distributor and without baffles.
System : Distilled water at constant J_G= 1.06
Liquid volume = 44 litres

Liquid flowrate Q_L (l/hour)	Integrated area (mVs)	Residence time Experimental (hour)	Residence time Theoretical (hour)	% Dead volume
4.8	797580	10.07	9.17	8.76
10.8	346370	4.34	4.07	6.13
22.8	167943	2.12	1.93	8.28

B . Multi-phase mixing

The mixing studies of the particulate solids in the reactor was investigated by studying a multi-phase system containing 2.5% (v/v) solid. At this concentration, the soild particles completely submerged the gas distributor and at low values of J_G very large bubbles, some in excess of 50 mm in diameter were generated through the bed. At this stage the gas hold-up at was observed to be lower than the distilled water system. No particle was fluidised at J_G less than 0.53 cm/s. With increasing J_G (above 0.64 cm/s) the particles became gradually fluidised and complete solid fluidisation was observed at J_G=0.85 cm/s. Even with a complete mixed multi-phase system, homogeneous bubble flow was never observed. The mean and the variance of the bubble size distribution increased with increasing J_G, although the values were considerably less than the distilled water system at similar gas velocities. The flow of a fluorescent solid particle was observed under ultra-violet illumination. At low gas velocities the particle was observed to take a random path in travelling the riser. It frequently recirculated and/or "slipped" off to

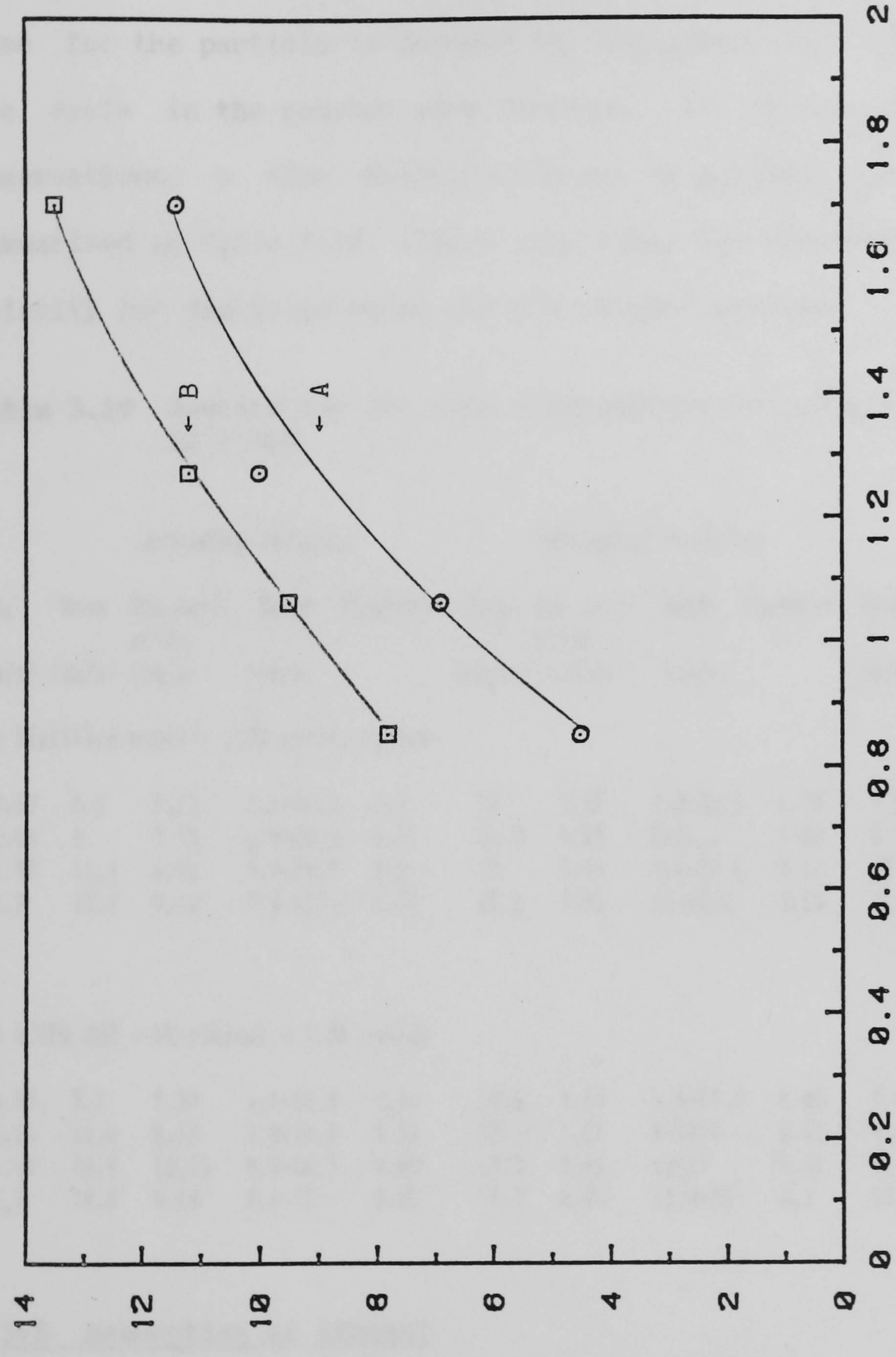

Figure 3.36 Observed solids circulation velocity in three-phase GLF.
Solids : 2.5 % (v/v) medium grade PERLAG (Silvaperl Ltd, U.K)
A : Distilled water; B : 0.05% (w/v) CMC + 1% (w/v) ethanol

the bottom before making its way up to the head space of the reactor. The rising time was recorded from the moment the particle was first observed in the draught tube until it reached the top. In a similar fashion the time for the particle to descend the downcomer, and finally to complete one cycle in the reactor were obtained. Due to the variations in the observations, a time distribution was established and the results are summarised in Table 3.19. Figure 3.36 shows the observed solid circulation velocity for distilled water and CMC/ethanol systems.

Table 3.19 Results for the time distribution of solid tracer particle in 50 l GLF

	Ascending velocity				*Descending velocity*				*Circulation velocity*			
J_G	Mean	Std deviation	Range	Skewness	Mean	Std deviation	Range	Skewness	Mean	Std deviation	Range	Skewness
(cm/s)	(cm/s)	(cm/s)	(cm/s)		(cm/s)	(cm/s)	(cm/s)		(cm/s)	(cm/s)	(cm/s)	
(a) Distilled water + 2.5% solids system												
0.85	5.1	5.75	1.1-56.3	0.7	15	3.88	9.8-25.3	0.55	4.5	2.98	0.4-21.4	0.59
1.06	8	7.70	1.8-36.9	0.51	14.8	4.25	8-28.3	0.09	6.9	4.12	2.1-21.4	0.52
1.27	11.3	8.00	3.7-52.3	0.6	17	3.96	8.8-23.8	0.31	10	4.01	3.1-37.5	0.45
1.7	17.1	9.10	7.9-112.5	0.31	17.1	3.93	11-40.2	0.58	11.4	3.49	5.6-24.2	0.52
(b) 0.05% CMC + 1% ethanol + 2.5% solids												
0.85	7.1	5.37	2.1-17.7	0.36	10.6	3.67	4.4-17.3	0.43	7.8	2.83	3.7-38.7	0.29
1.06	11.6	8.45	2.8-34.6	0.53	13.1	3.57	8-23.7	0.53	9.5	2.81	4.7-15	0.41
1.27	16.9	12.33	4.9-64.3	0.69	15.2	3.56	10-25	-0.24	11.2	2.31	7.4-19	0.31
1.7	19.8	9.48	9.4-75	0.05	18.2	4.05	12.9-30	0.3	13.5	3.41	7.5-21.4	-0.3

3.3.5 Desorption of Ethanol

The effect of gas-liquid contact in rectifying ethanol concentration in the effluent vapours was demonstrated by measuring ethanol concentration in the effluent gases at different values of J_G. The rate of evaporation of water was observed to increase with J_G and reached a maximum of 0.28 l/h at around J_G=1.5 cm/s (Figure 3.37). The normalised data accounting

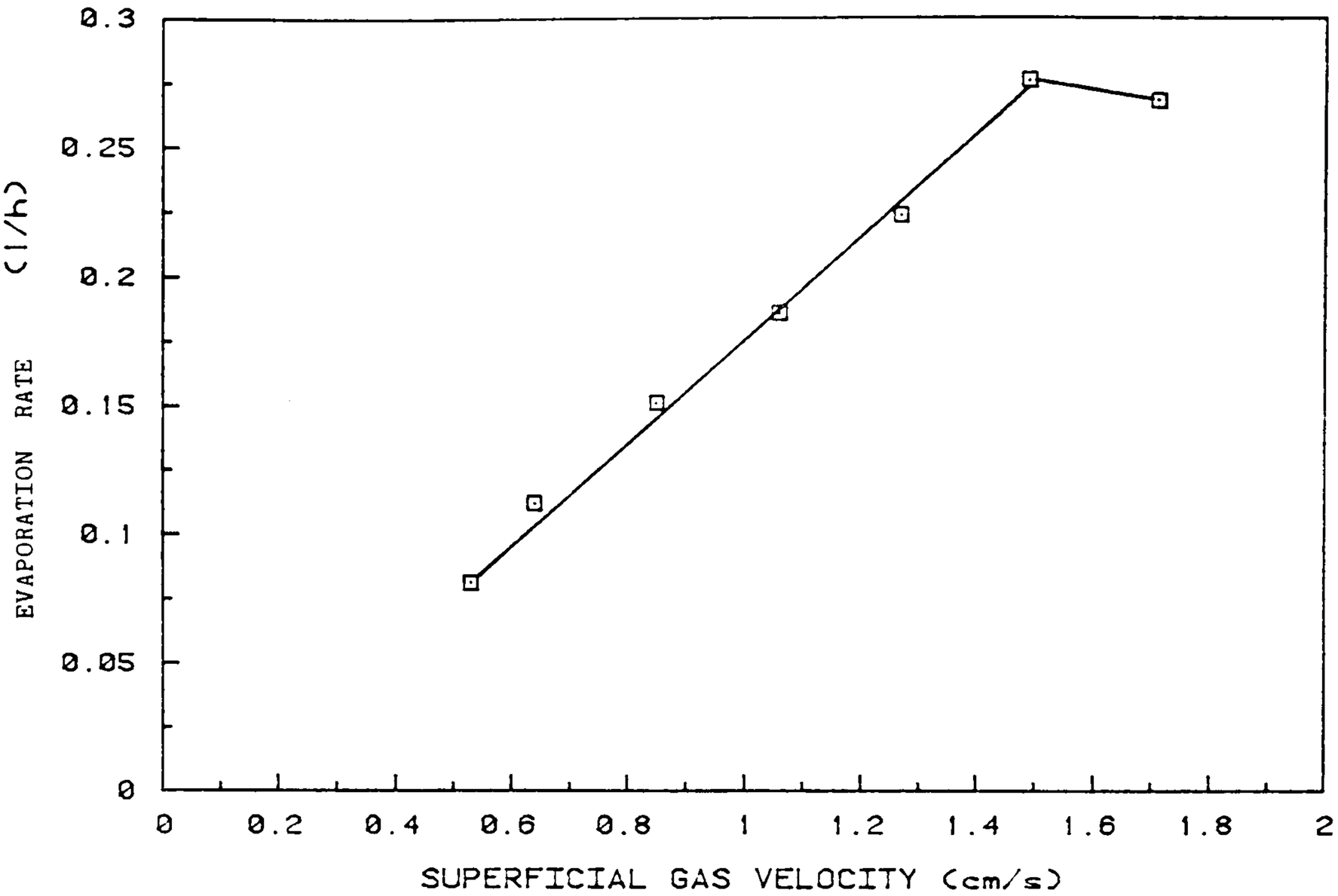

Figure 3.37 Evaporation rate of water at 60 'C in a two-phase GLF
Liquid system : 1% (w/v) ethanol; Liquid volume : 44 l

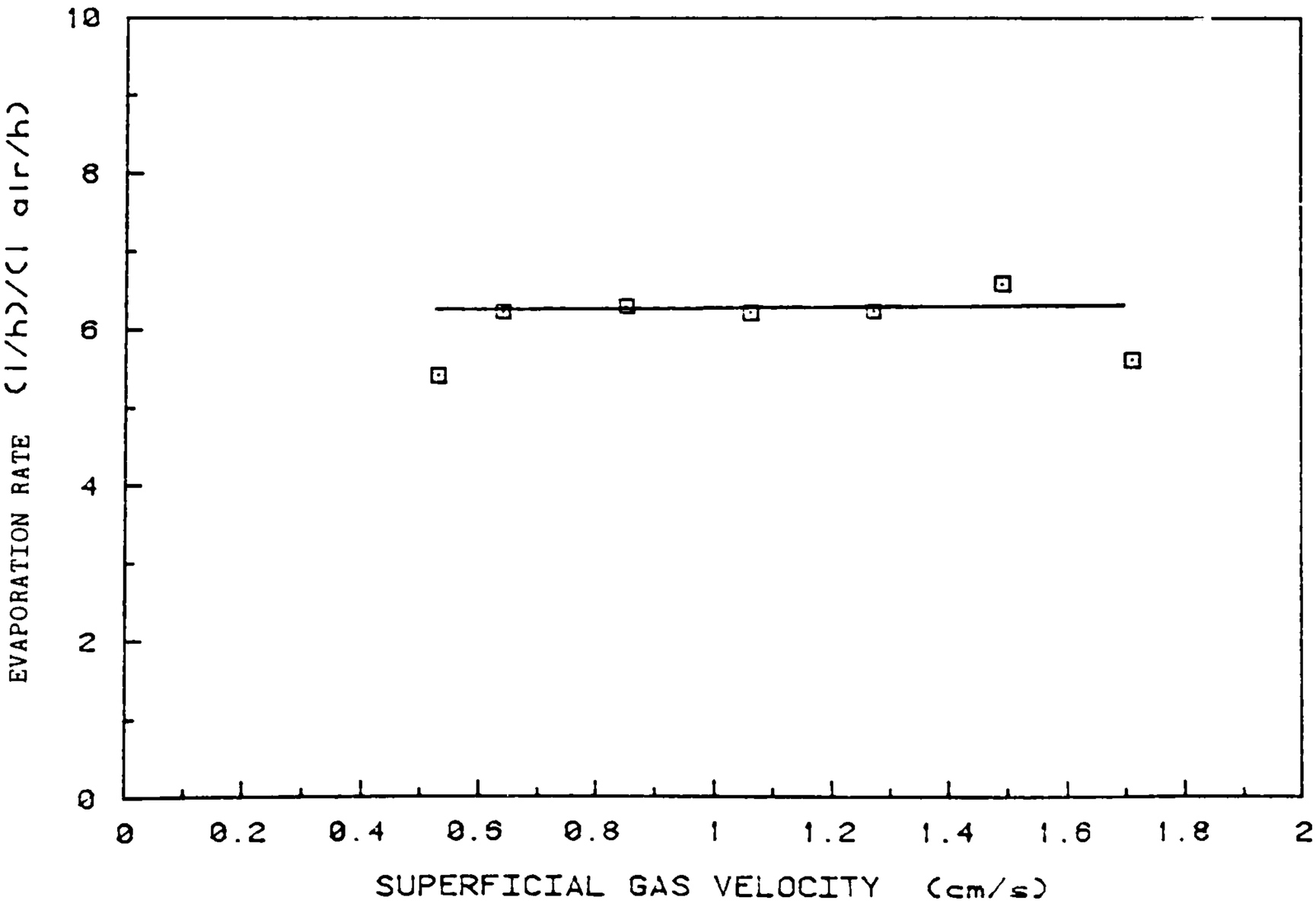

Figure 3.38 Evaporation rate of water at 60 'C in a two-phase GLF - Normalised data
Liquid system : 1% (w/v) ethanol; Liquid volume : 44 l

for the gas throughput (Figure 3.38) shows the humidity of the effluent vapour to be independent of superficial gas velocity.

The rate of desorption of ethanol into the vapour phase was determined by analysing the concentration of ethanol in the vessel at constant gas velocities. In Figure 3.39, it may be observed that the rate of removal of ethanol is constant at constant temperature and J_G. From the gradients of Figure 3.39, the ethanol desorption rate of 0.51 g/l/1 and 0.6 g/l/h at superficial gas velocities of 1.06 cm/s and 1.27 cm/s respectively are obtained. In Figure 3.40, the ethanol concentration in the effluent vapour shows the expected profile whereby an increase in the concentration with increasing velocity is observed. The normalised data as illustrated in Figure 3.41 clearly shows the maximum at J_G= 1.06 cm/s. In Table 3.20, the observed results are compared with the those calculated from the penetration theory from Equation 3.32. For dilute solutions, the diffusivity of ethanol in water D_E at 60 °C can be predicted from the Wilke-Chang method described by Treybal (1980). Thus D_E= 1.49 x 10^{-9} m^2/s. For pure air at a low relative humidity and room temperature (approx. 0.005 kg water/ kg dry air and 20 °C) entering a dilute binary liquid system such as ethanol/water, it may be assumed that there are no gas-phase resistance to the mass transfer and Equation 3.30 can be applied to predict the desorption rate.

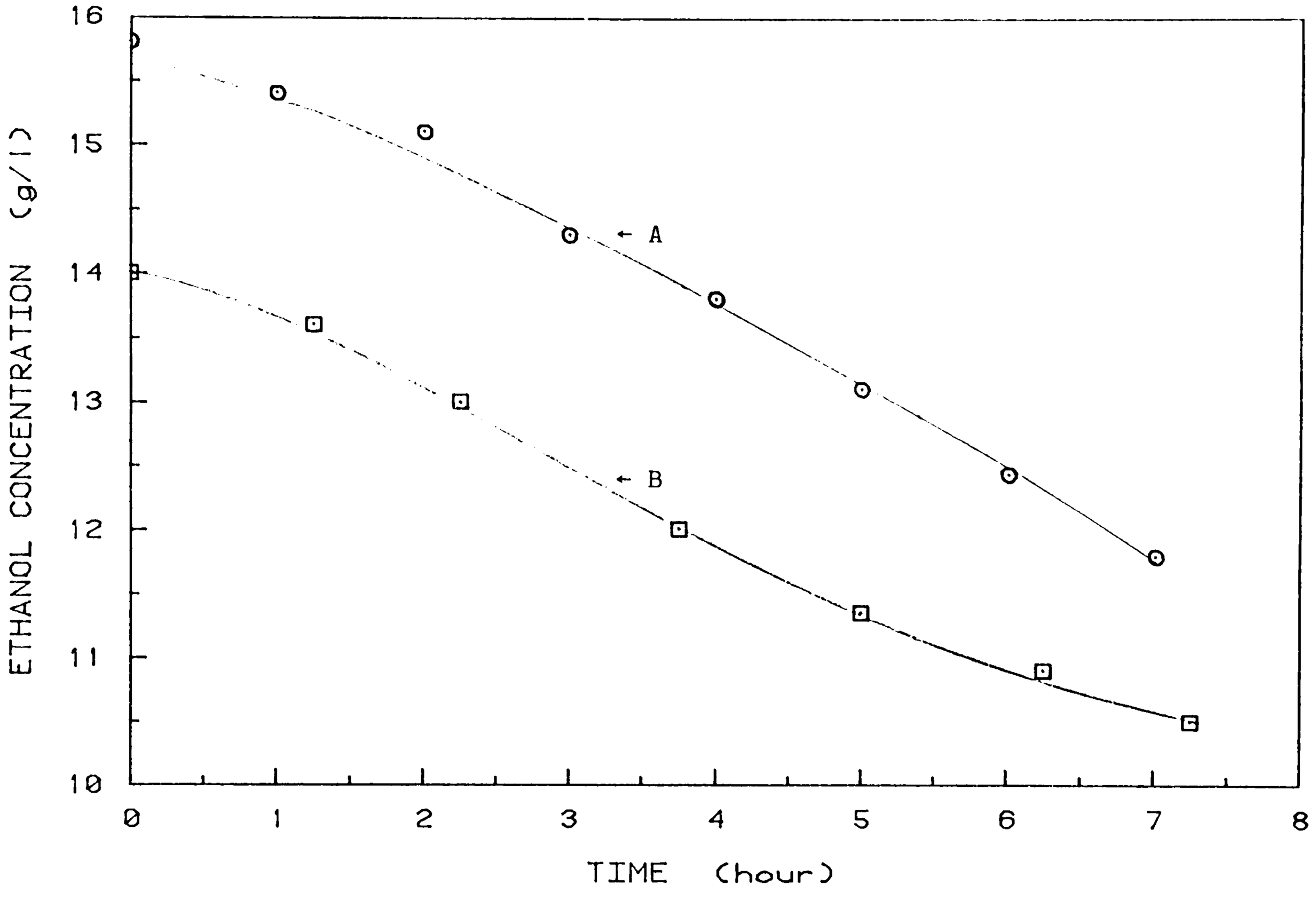

Figure 3.39 Residual concentration of ethanol in bulk liquid under batch desorption at 60 'C

A : Superficial gas velocity = 1.06 cm/s; B : Superficial gas velocity = 1.27 cm/s

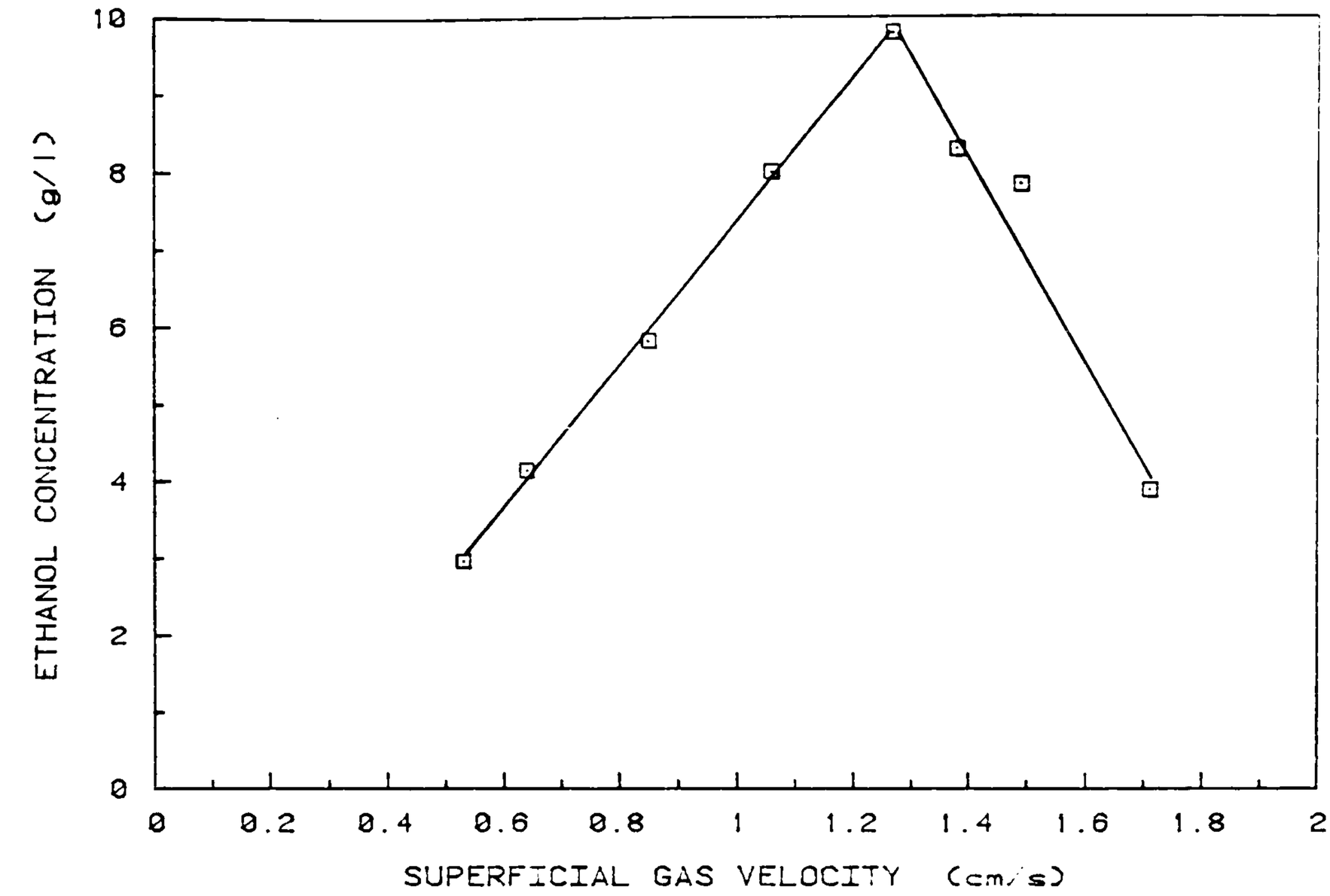

Figure 3.40 Concentration of ethanol in the effluent vapour of a two-phase GLF
Liquid system : 1% (w/v) ethanol; Liquid volume : 44 l

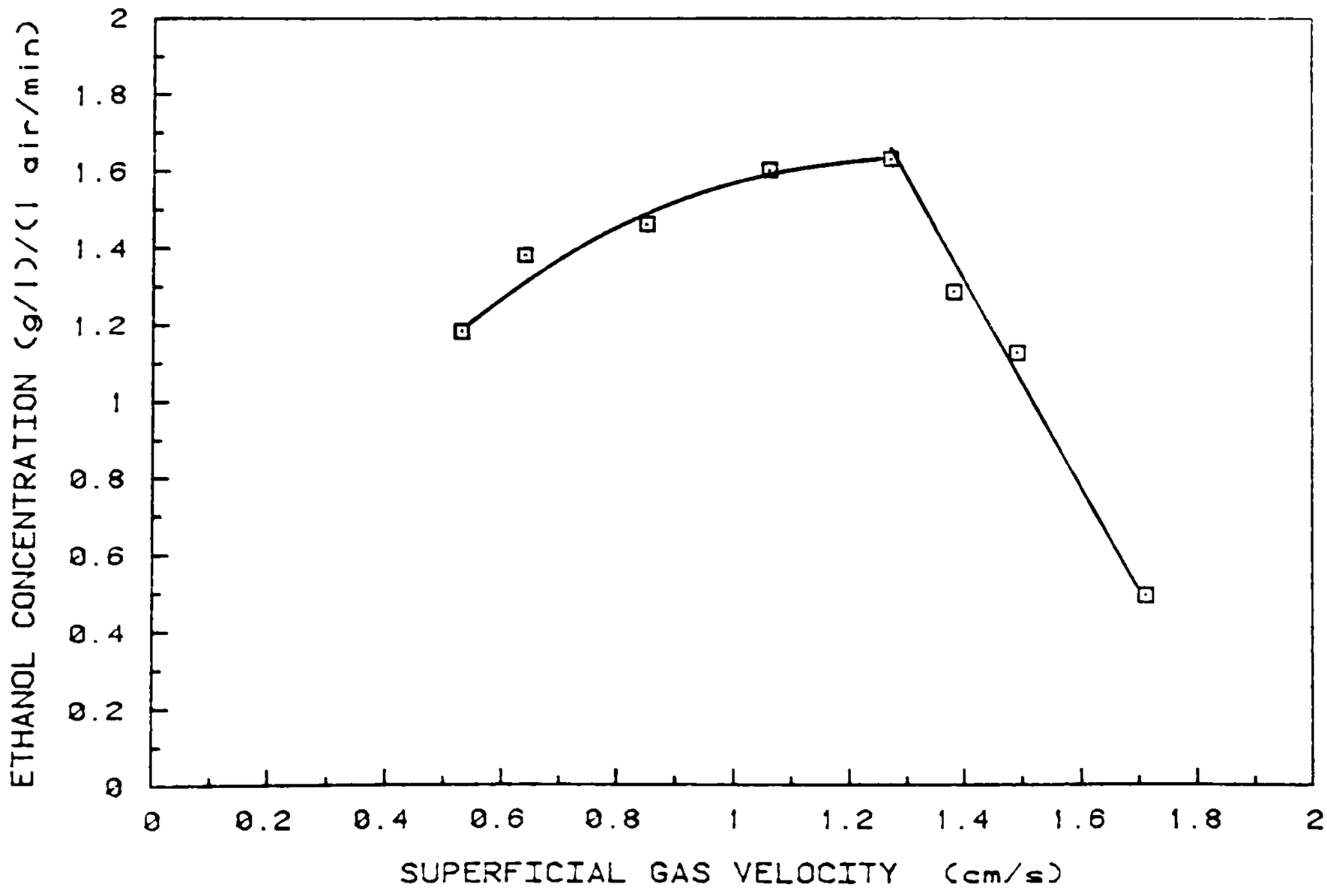

Figure 3.41 Desorption rate of ethanol in a two-phase GLF at 60 'C
Liquid system : 1% (w/v) ethanol; Liquid volume : 44 l

Table 3.20 Calculated and observed values of desorption rate of ethanol in GLF at 60 °C.
Initial ethanol concentration = 14 g/l = 304 mmol

J_G (cm/s)	a (m^2)	á[a] (m^2)	t[b] (s x10^3)	k_L (mmol/ m^2s)	R_Ea (mmol/s)	R_Eá (mmol/s)	$(R_E)_{obs}$ (mmol/s)
0.53	5.68	1.15	7.80	0.242	418	84.7	64.3
0.64	8.40	1.69	7.83	0.241	616	124	90.0
0.85	15.5	3.13	6.43	0.266	1257	253	127
1.06	18.1	3.66	8.57	0.230	1270	256	174
1.27	22.4	4.48	9.00	0.225	1568	314	213
1.38	22.9	4.63	8.08	0.237	1654	334	180
1.49	25.2	5.07	7.79	0.242	1853	373	171
1.71	29.6	5.98	7.6	0.245	2182	446	84.8

a : á is the interfacial area of the bubbles in the turbulent region of the fermenter. Thus R_Ea' is the corrected desorption rate for the system.

b : t is calculated from d_e/U_{mt}, the values of which are not given earlier are extrapolted form the data.

Figure 3.42 shows the plot of the desorption rates shown in Table 3.20.

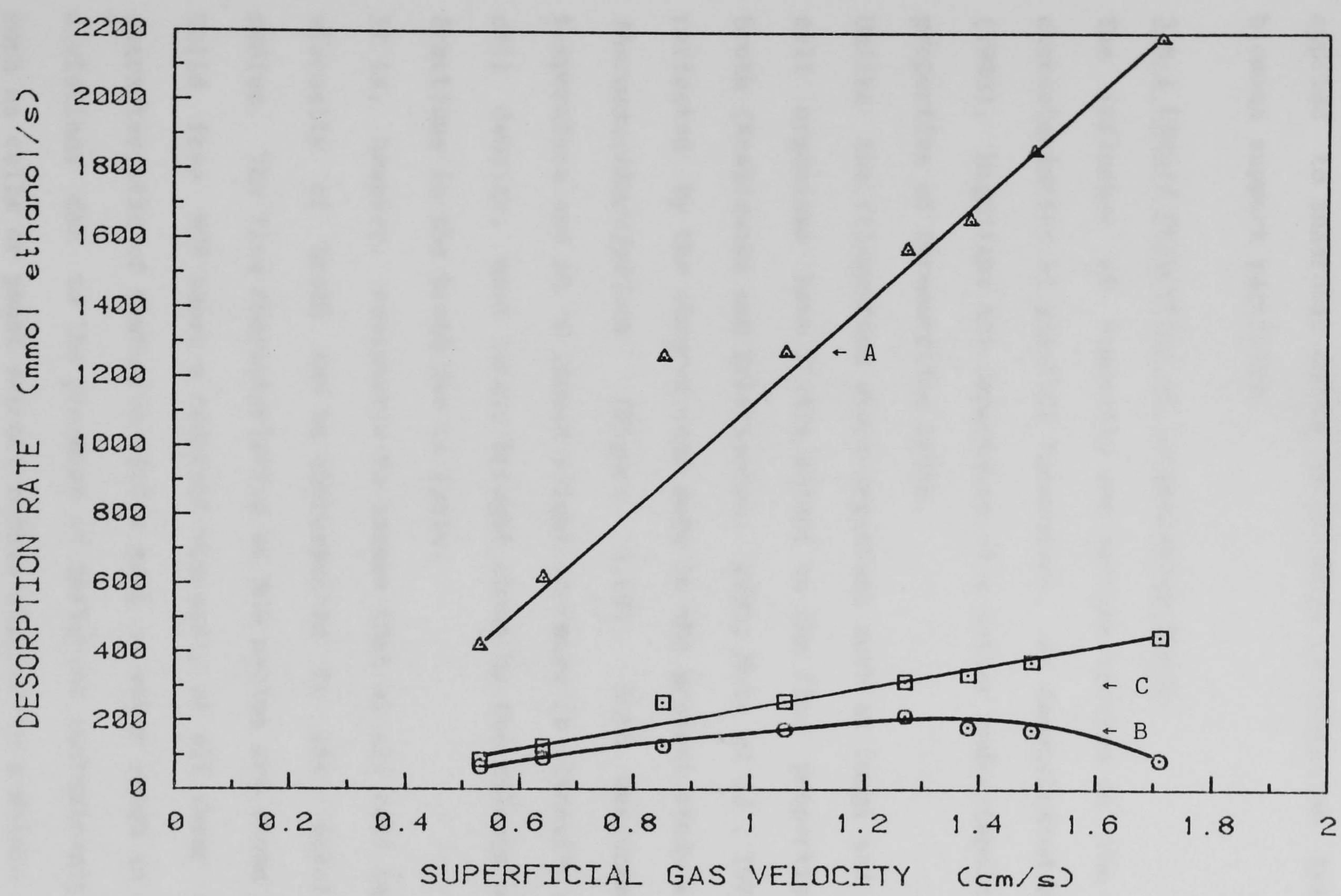

Figure 3.42 Theoretical and experimental desorption rate of ethanol in a two-phase GLF at 60 °C

Liquid system : 1% (w/v) ethanol; Liquid volume 44 l

A : Theoretical ethanol desorption rate, B : Observed ethanol desorption rate

C : Corrected theoretical ethanol desorption rate

3.4 Discussion

The discussion which follows analyses the results for a fundamental hydrodynamic study of a concentric draught tube gas-lift fermenter as applied to anaerobic and/or multi-phase fermentation systems containing biomass support particles.

3.4.1 Liquid Properties of Fermentation Broth

The influence of viscosity and surface tension on the two-phase flow characteristics of gas-lift fermenters, as demonstrated by Erickson *et al* (1983), highlight the importance of a better understanding of the liquid properties of fermentation broth.

Unlike the filamentous micro-organisms such as fungi and moulds, single cell organisms have little effect on the flow properties of fermenter broth (Kemblowski and Kristiansen, 1986; Metz *et al* , 1979). This is also reflected by the observations made in the present study with cells of *C. thermosaccharolyticum* (Figure 3.19). Both measurements at room temperature and 60 °C showed slight increase in viscosity with increasing cell density, most likely brought about by the release of intracellular fractions in the broth due to lysis.

It is, however, reasonable to assume that at all cell concentrations the viscosity of broth can be approximated to its basal uncontaminated medium. The flow characteristics of MCR medium are shown in Figure 3.19. Solid free MCR shows a constant viscosity at all shear rates which is characteristic of Newtonian fluids such as water shown in Figure 1.6. The deviations due to the presence of different contaminants in the medium such as cells or yeast extract behave similar to a dilute solution of CMC (Figure 1.6).

Indeed the effect of medium components is demonstrated by the difference in the flow characteristics of RCM and MCR. Unlike MCR, RCM behaves in a pseudoplastic manner which is thought to be due to the presence of

undefined protein extracts in its composition. This is supported by the observation made with contaminated RCM showing a lower apparent viscosity than sterile RCM as result of utilisation of medium components by the organisms.

The changes in solvent concentration and ionic strength do not affect the viscosity of the broth, but they may significantly change its surface activity. Although most hydrodynamic studies of GLFs have considered the influence of surface tension on two-phase flow, this parameter is not reported for the actual fermentation studies carried out. The effect of additives on the surface tension of water has been already mentioned (see section 3.1.2) and it can be observed from Figure 3.21 that the overall effect of ingradients of MCR results in an approximately 20% decrease in the surface tension of distilled water. As a result of fermentation, the accumulation of solvents causes a further decrease in the surface tension despite their dilute nature (< 0.5% w/v). Such behaviour is supported by observations made with different solution of ethanol shown in Figure 1.7 where the maximum change in surface tension was observed at the lowest concentrations of ethanol. The presence of cells however, has little effect on this parameter and from Figure 3.21 it can be observed that after the initial decline due to solvent fermentation, the surface tension of the broth remains constant with increasing cell density. The flow behaviour of the fermentation broth was adequately characterised by a liquid system of similar viscosity and surface tension. Hence from the characteristics of a fermentation broth based on MCR, the proposed simulated system contained 1% (w/v) ethanol and 0.05% (w/v) CMC.

3.4.2 Hydrodynamics and Mixing

The significance of two-phase flow behaviour in design of gas-lift contactors such as the proposed concentric draught tube gas-lift

fermenter, has already been discussed in an earlier section (see section 3.1.2). Basic hydrodynamic experiments carried out in the present study provide an indication for the potential use of GLFs for multi-phase fermentation systems. This was achieved by observing the hydrodynamic behaviour of three-phase flow in comparison to two-phase flow in a small 50 litre pilot vessel, under different conditions of fluid properties and fluid flow.

The role of bubble dynamics in a loop reactor, such as the GLF studied in this report, is central in describing the trends for the gas hold-ups and liquid velocities observed in the vessel for a given set of conditions.

In the absence of resources, the visual observation of the bubble flow with aid of photography and image analysis, was the only technique employed in the study of bubble behaviour in GLF, although more advanced and rapid techniques have been developed and successfully applied to bubble columns elsewhere (Lewis *et al* , 1984). The limitation of the photographic technique arose due to bubble motion in three dimensions. Bubbles were photographed in the head space near the column wall of the fermenter. For most measurements the bubble population in this region was representative of the bubbles throughout the vessel. In the extremes of superficial gas velocities employed in these experiments these results were less satisfactory. In the homogeneous bubble flow at very low gas velocities, the bubble population near the wall was too small or non-existent and sample photographs were taken from the riser section which encountered the problem of depth of field. In the other extreme, where slug flow prevailed, larger bubbles approximately greater than 10 mm (o.d), broke up in the riser or rapidly disengaged in the head space. Due to the large bubble density in the riser, high velocities and depth of field, photographing of the bubbles in the riser was completely unsatisfactory, and in this case the reported data only refers to those

bubbles captured near the wall. It should be noted however that despite the heterogeneous nature of the slug flow, the main fraction of the bubble population was less than 2 mm in size. These bubbles were formed as a result of the break up of the larger bubbles, and because of their smaller size, they experienced a longer residence time in the vessel which increased their chances of being captured on the snapshot.

Fortunately these observations were identified with only two of the fluid systems experimented with. From Table 3.9, at the highest value of superficial gas velocity, the mean bubble size of the distilled water and the starch systems are observed to decline after a steady increase with increasing J_G. Such behaviour was not observed with fluid systems notably with lower surface tension values. Characteristic of such non-coalescing systems, exemplified here by the 0.05% (w/v) CMC and 1% (w/v) ethanol, is symmetrical distribution of homogeneous equisize bubbles which enlarged linearly with increasing J_G over the investigated range. Even at the maximum value of J_G slug flow was not observed. The effect of liquid properties on bubble size and gas hold-up can be observed in Figures 3.23 and 3.26 respectively. All additives inhibited coalescence to varying degrees. In an uncontaminated distilled water system the surface mobility of the bubbles is unrestricted (Clift *et al* , 1978). In such a system, the increase in the inertial forces brought about by the increase in the gas flowrate overcomes the surface tension forces, thus allowing bubbles to increase in size until the point they break up. In Table 3.10, the calculated Weber number is also an indication of this phenomenon. Again the exception is observed at the highest value of J_G when Weber number greater than the critical value of 4.7 (Calderbank, 1958) was anticipated. The low value of Weber number predicted is due to the decrease in the mean bubble diameter as a result of the break up of the bubbles.

Similar observations were made with the vessel containing 0.05% (w/v)

starch. Addition of starch at the concentration examined, did not significantly alter the surface activity of the liquid system and it was mainly experimented for its viscous effect (Figure 1.6).

With the view that the bubbles rise more slowly in viscous solutions (Erickson *et al* , 1983), for similar non-coalescing systems a higher gas hold-up with the more viscous system is anticipated. The results in this study show that addition of starch reduces the mean bubble diameter (Figure 3.23) and as a consequence both the interfacial area (Figure 3.26) and the gas hold-up (Figure 3.32) are marginally higher than the distilled water system.

Addition of CMC and ethanol had an inhibitory effect on the bubble coalescence in the reactor and as a result, increased homogeneity of the bubble flow regime, recirculation of smaller bubbles in the downcomer and longer residence time of the bubbles inside the vessel were observed. The consequent increase in the gas hold-up of the liquid system containing these additives, as demonstrated by the reported data of Weiland and Onken (1981), Merchuk and Stein (1983), was anticipated and confirmed by the results shown in Figure 3.32.

The homogeneity of the bubble flow regime is also dependent on the gas distribution (see Equation 3.3) in the reactor. Fine bubble dispersion achieved by using a sintered disc distributor, maintained the homogeneous bubble regime over a wider range of superficial gas velocity than the single nozzle distributor. Chakravarty *et al* , (1973) found that increasing the number of 0.15 cm (o.d) holes from 1 to 18 on the distributor plate of a concentric draught tube GLF, did not have any significant influence in the measured parameters such as the gas hold-up. The results shown in Figure 3.30 and 3.35 clearly indicate an increase in the gas hold-up and liquid circulation velocity when sintered disc is employed. The dispersion of bubbles increases the interfacial area and

larger fluid displacement is observed as a result.

It has been demonstrated that the gas hold-up is at a maximum in the absence of loop circulation in an external loop fermenter (Weiland and Onken, 1981; Merchuk, 1986). Merchuk (1986) observed that by closing the downcomer of an external loop GLF, the overall gas hold-up increased. This was accounted by the relative decrease in the liquid circualtion velocity in the vessel. In an attempt to observe such effects on a CDT vessel the cross-sectional area of the downcomer was reduced by 50 percent by placing baffles (see appendix). The baffles covered the length of the downcomer and hence the active circulating liquid volume of the downcomer was also reduced by one-half. As illustrated in Figure 3.31 at low gas velocities, the gas hold-up is the same for both systems. However at J_G values above 1.2 cm/s the system without baffles shows marginally higher values of gas hold-up. This is thought to be due to the higher liquid velocities in the reactor system with the baffles (see below).

The results of the liquid mixing behaviour of the GLF are in good agreement with observations made in the literature (Fields and Slater,1983; Blenke, 1979). While the batch experiments show clear evidence for loop recirculation (Figure 3.16), the continuous flow experiments provide tracer data (Figure 3.17) which are characteristic of a mixed flow reactor (Levenspiel, 1972) with relatively small dead space (Table 3.18). Perhaps the best description of the flow in the reactor would be that of a tubular, plug flow reactor with significant back mixing due to end effects.

The liquid velocity profiles of the designed fermenter (Table 3.17 and Figure 3.34) show little difference between the circulation and the mixing velocities for all liquid systems investigated. Thus in relatively short time after liquid travels one complete loop, a homogeneous mixing in the vessel is achieved. High values of the liquid velocity in the riser are

due to the relatively small liquid volume in this section. In Table 3.17 the mixing performance of the reactor is shown by the mixing velocity and the Bodenstein number. Both parameters are determined from the tracer data although the latter is derived from the dispersion theory (Levenspiel, 1972) and provides a measure of the axial dispersion in the vessel. Thus as Bo tends to zero the flow becomes completely mixed and as Bo tends to infinity complete plug flow is observed.

Apart from the superficial gas velocity, which is an independent operational variable, the mixing characteristic of the fermenter is observed to be influenced by two important factors, namely the homogeneity of the bubble swarm and the ratio of the cross-sectional area of the riser A_r to that of the downcomer A_d.

The liquid velocity profiles for the reactor system containing baffles in the downcomer are illustrated in Table 3.15. The results indicate improved mixing performance of the vessel owing to the relatively high liquid velocities observed. Such behaviour was anticipated since the baffles in effect reduced the volume of the circulating liquid in the vessel. High liquid velocities increase the turbulence and hence eddy diffusion throughout vessel. Without the baffles, for all values of J_G within the investigated range, turbulent bubble flow regime was only observed in the riser and the head sections of the reactor which only contributed to 20% of the total liquid volume of the vessel. It is believed that (Fields and Slater, 1983) both mixing and mass transfer predominantly occur in these turbulent regions of the reactor and the contribution of the downcomer to the former is negligible. Hence by maximising the ratio of A_r to A_d, the turbulent volume of the system may be increased.

The homogeneity of bubbles depends upon the quality of gas dispersion in the liquid phase. As already indicated, improvements in gas distribution, achieved by employing sintered disc distributor and reducing the surface

tension of the liquid, have led to smaller and more symmetrical bubble size distributions and larger interfacial area. As anticipated from the theory of bubble dynamics (Clift *et al* , 1978) the terminal velocities and the Reynolds numbers for these systems indicate a less turbulent system (Table 3.10). In terms of mixing, the slow rise of bubbles is counter balanced by increased population density as illustrated by large interfacial area (Figure 3.26), which increases the net volume of liquid displaced in the reactor. Hence the overall effect on the mixng becomes unpredictable. The results from Table 3.17 in fact show an increase in the circulation and mixing velocities for the systems with smaller and more homogeneous bubbly flow regime. It is notable that in these systems the values of Bodenstein number are relatively higher, and the mixing is mainly due to the axial dispersion in the reactor. From the observations made so far, it may be deduced that for the proposed reactor system the highest gas hold-up is observed when a liquid with low surface tension value is circulated in a reactor in the absence of baffles, and when the gas is finely dispersed through a sintered disc distributor. The use of baffles in the three-phase studies was not employed due to their obstructive nature towards solid circulation. These above condition were adopted to observe the behaviour of three phase flow in the reactor. The vessel was charged with 2.5% (v/v) medium grade Perlag particles. Due to the difficulties observed earlier (see section 2.4.4) the Perlag particles were the only support particles found suitable for circulation in the proposed GLF. Similar to the observations made by Fan *et al* , (1986), the bubble size distribution in the three-phase system, shown in Figures 3.27 and 3.28 and Table 3.11, indicates that the presence of solids significantly reduces the bubble size in the system. This is accounted by increased bubble break of the larger bubbles by obstructing solid particles. Visual observations revealed that in three-phase mixing

homogeneous bubble flow was never completely achieved and a condition similar to the slug prevailed at all gas flow rates. Unlike the slug flow regime in the two-phase flow, however, the increased density of smaller bubbles due to break up in the presence of solids shows more favourable results in terms of gas hold-up of the system.

The effect of liquid properties in the three-phase systems on the bubble size distribution (Table 3.11) and the gas hold-up (Figure 3.29) follow the trends observed in the two-phase studies. However, with surface tension reducing systems a more homegeneous bubble flow was achieved. It is also notable that in Figure 3.29 the the gas hold-up is minimum until solids began to fluidise at around J_G= 0.65 cm/s.

Circulation of solids was observed under the illumination of UV light on a fluorescent solid tracer particle (see section 3.2.2). The increase in the circulation rate with J_G followed the expected behaviour, however unlike the two-phase flow the effect of liquid properties showed a direct effect by increasing the solid circulation rate (Figure 3.36). This is perhaps due to the increased fluidisation of the solids achieved as result of larger interfacial area of gas bubbles. It is thought that under actual fermentation conditions, contaminated solid particles will fluidise more readily in light of the microbial fermentation taking place in their lattice. This has been already observed on a small scale with a variety of support particles in a packed column (see section 2.4.4).

3.4.3 Desorption of Ethanol

The results for gas humidification of air due to water vapour removal from the vessel follow the predicted behaviour whereby an increase in the dehydration rate with superficial gas velocity was observed (Figure 3.37). The negative gradient at the highest value of J_G is most likely due to a decrease in the interfacial area of the bubbles brought about by slug flow. This was not visually observed due to the very dense bubble

population in the riser. Similar pattern for the desorption of ethanol with a maximum value at J_G= 1.27 cm/s is observed (Figure 3.41). The predicted values of the desorption rate of ethanol obtained from the penetration theory provide grossly over estimated results (Figure 3.42). By correcting for the turbulent flow regions in the reactor, values in the same order as the observed rates are obtained. This confirms the earlier argument with regard to the mass transfer in the turbulent bubble regime of the reactor vessel. It is also notable that the predicted values based on the interfacial area of the bubbles, show a linear increase in the desorption rate with increasing J_G.

The above observations pose yet another limitation towards the design of the fermenter. In order to maximise turbulence and hence mass transfer in the reactor, the energy input is limited by the bubble flow behaviour in the vessel. Optimum rates are observed only during homogeneous bubble flow. In a three-phase system the size of the draught tube is also limited by the size which would allow minimum fluidisation in the reator. As a result in order to effectively employ a GLF similar to the one described for *in situ* recovery of ethanol by desorption, a design based on minimum ratio of cross-sectional area of downcomer to the cross-sectional area of riser is recommeded.

3.5 General Discussion

The hydrolysates of hemicellulose degradation are water soluble (Tsao *et al* , 1978) and may be readily used as the carbon component of a simple growth mrdium such as MCR. The means by which xylose, the main sugar monomer of hemicellulose, may be converted to ethanol is discussed in the earlier Chapters. The choice of a gas-lift fermenter for thermophilic solvent fermentation became obvious when the combined advantages of this system were considered.

The ability of *Clostridium thermosaccharolyticum* to ferment xylose was examined as an indicative measure for the organism's potential industrial use. From the results and the discussion presented in Chapter 2 it is evident that such potential may not be met and fully exploited at the current level of understanding of this organism. In comparison to the ethanol productivity of yeast or Zymomonas based on glucose, certainly the observed maximum productivity level of 0.5 g/l/h is much lower and considerably higher levels would be desired. It is therefore fair to assume that the low alcohol production and tolerance level of this organism, and many other xylose fermenting organisms, has posed the greatest question towards the economy of hemicellulose utilisation. The inhibitive nature of ethanol on yeasts and bacteria is well documented and the accumulated data highlight the complexity of the inhibitory mechanisms and routes for strain improvement.

Under conditions of thermophilic fermentation, the inhibitive action of organic end-products could be reduced by their continuous removal. Such measures were observed to be readily achieved in a gas-lift fermenter by the way of desorption of the volatile components into the gas-phase. Thus not only is the suitability of the gas-lift fermenter for this particular fermentation system demonstrated, but also a new feature for the use of GLFs is presented which may be employed with other fermentation systems.

The basic hydrodynamic study of gas-lift fermenters revealed how easily the fermenter may be adapted for two- or three-phase systems. Moreover it was indicated how changes in the reactor geometry and the physical properties of the liquid system can be employed to alter the flow behaviour of the fermenter to suit the desired conditions.

In the light of the information obtained from the studies of pentose fermentation and fementer system, the large scale conversion of hemicellulose may be considered. Fermentations based on pure culture of *C.thermosaccharolyticum* or in coculture with other fementative organism(s) are feasible. As a pure culture, suspended or immobilised cells may be grown on a xylan containing medium, and provided the optimum conditions for maximum productivity of ethanol are maintained, a similar kinetics as depicted in Figure 2.21 is anticipated. It is thought that under the steady-state conditions of continuous growth, the liquid properties of the broth would remain constant, which would allow the prediction of the flow behaviour of the reactor. Under conditions of excess substrate the growth rate would be maximal and any minor hexose contaminant of hemicellulose hydrolysis or otherwise are readily removed from the system without any major change in the growth behaviour. For the optimum operation of the fermenter, a two-phase gas-liquid system may prove more beneficial. This conclusion arises from a number of observations made in the course of this study. In general the use of solid particles in the fementer vessel promotes slug flow regime, which has been noted to decrease the rate of desorption in fermenter system. Moreover the circulation of solids in the fermenter introduces geometric restrictions, which may not be desirable. Finally due to the porous structure of the support particles, any gas formation within the particles may lead to adverse density changes and result in the particles floating on the surface of the broth.

In a coculture, the growth of *C. thermosaccharolyticum* is often considered concurrent with the growth of one or more ethanol producing organism(s) unable to metabolise the full range of carbon sources in the medium. Provided the organisms share common optimum conditions a similar fermenter system as described for the pure culture system may be employed. However with such a system two problems are envisaged. Firstly owing to the preferential growth of *C. thermosaccharolyticum* on different carbon sources, the pentose utilisation may not commence until complete exhaustion of the hexose supply. Hence the overall substrate consumption rate is only affected with respect to the removal rate of hexoses. Secondly, should the organism(s) in coculture be able to produce or tolerate higher concentrations of ethanol than *C.thermosaccharolyticum* , they may come to predomianate as the growth of the latter is inhibited or retarted due to environmental stress factors.

As an alternative to a single fermenter coculture system, a two-(or multi-) stage sytem is often considered whereby the medium may feed from one fermenter system into another for selective utilisation of the carbon source. A medium regulation module in between the stages can be employed for adjusting the nutrient content of the medium. Incorporation of a preliminary product recovery system such as membrane filters, or flash vaporisers, can also reduce the inhibitory effect of the medium due accumulation of the end-products. In this mode of operation the fermenter containing *C. thermosaccharolyticum* may be treated as the pure culture system described earlier.

As well as the future investigation of the above systems in the proposed GLF, the flexibility of the fermenter may be examined by undertaking of other fermentation systems. The acetone/butanol fermentation by *Clostridium acetobutylicum* may be a promising commercial fermentation which can certainly employ the the advantages of GLF for a possible scale-

up strategy. The aerobic efficiency of the GLF may also be used for cell mass production e.g fermentation of *Penicillium sp.* or cell tissue cultures.

Appendix One

Design of the Pilot Gas-Lift Fermenter

A : The engineering drawings of the stainless steel sections of the pilot gas-lift fermenter. The vessel was pressure tested by Alval Engineering.

B : The outline diagram of the baffles used in the annular region of the fermenter. The baffles were made from perspex and supported by the bolts form the top plate.

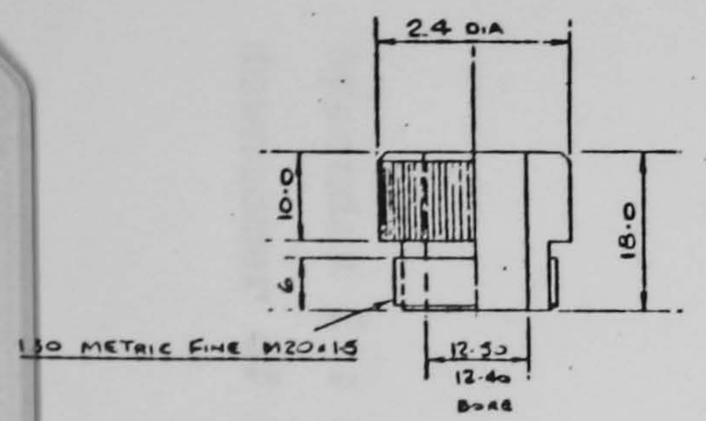

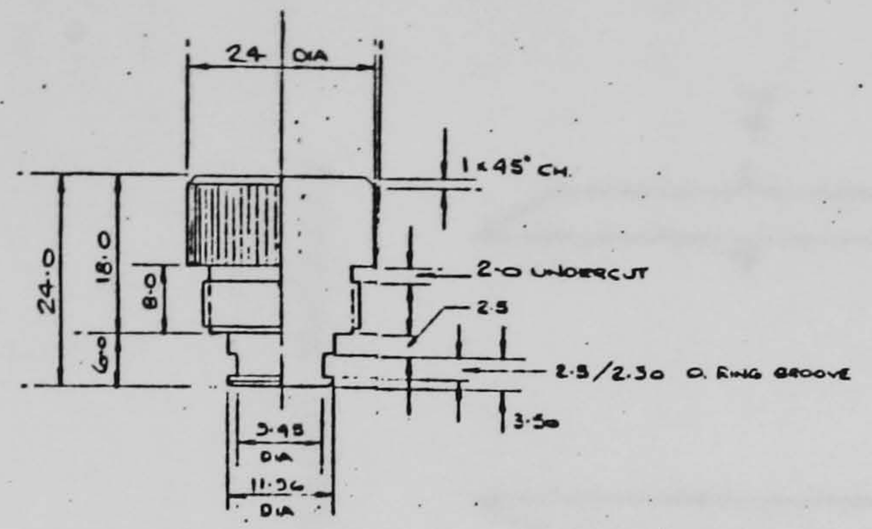

① DETAIL OF PROBE HOLDER

5 REQD

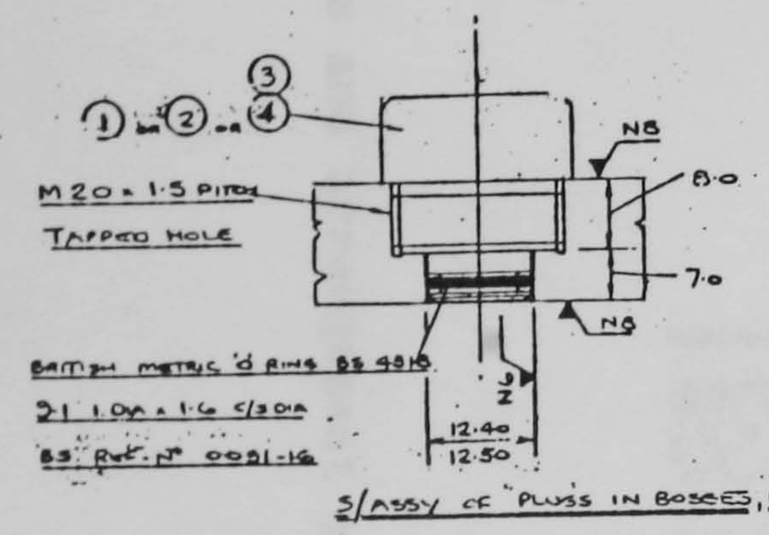

② DETAIL OF BLANK PLUG

▽7 REQD

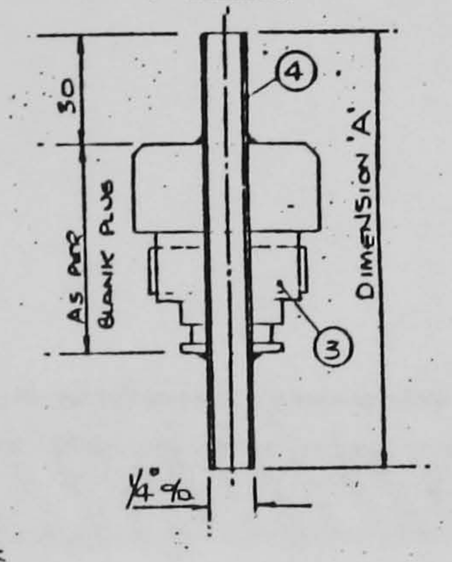

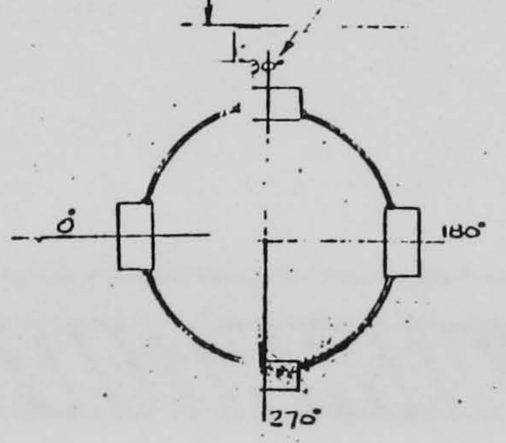

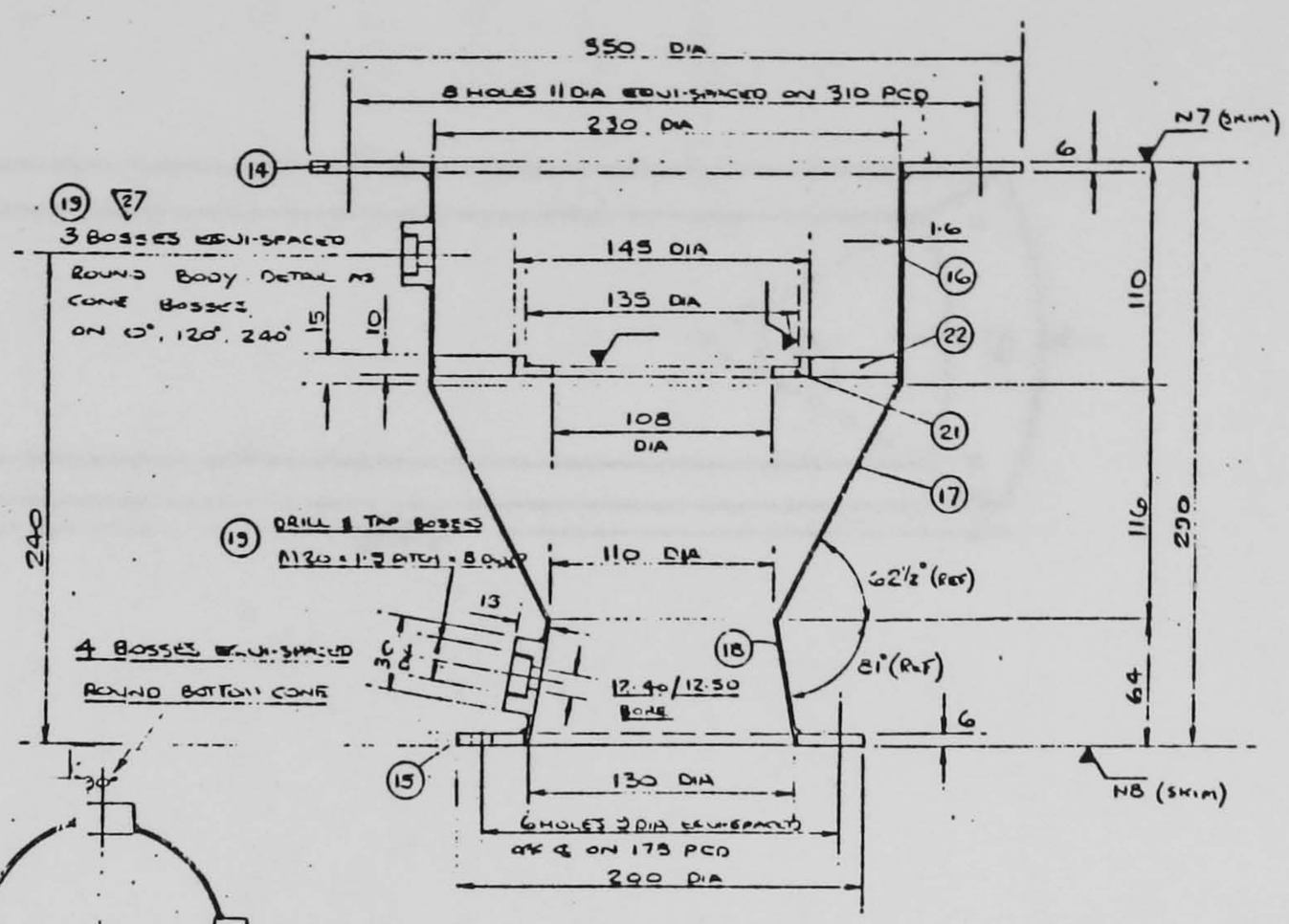

SUPPORT WEBS EQUI-SPACED ROUND CARRIER

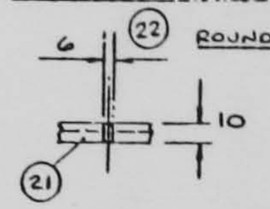

INTERNAL TUBE CARRIER

DETAL OF 5ᵀᵀ BOTTOM SECTION

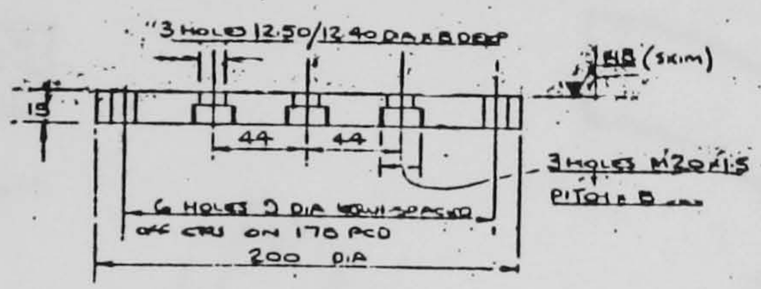

20 DETAL OF BOTTOM PLATE

③④ DETAIL OF IN/OUT CONNECTOR

▽7 REQD DIMENSION A = 64

1 REQD DIMENSION A = 65 (FOR INLET NOZZLE)

5/ASSY OF PLUGS IN BOSSES, ETC

DETAIL OF CONDENSER ℄ TOP COVER PLATE

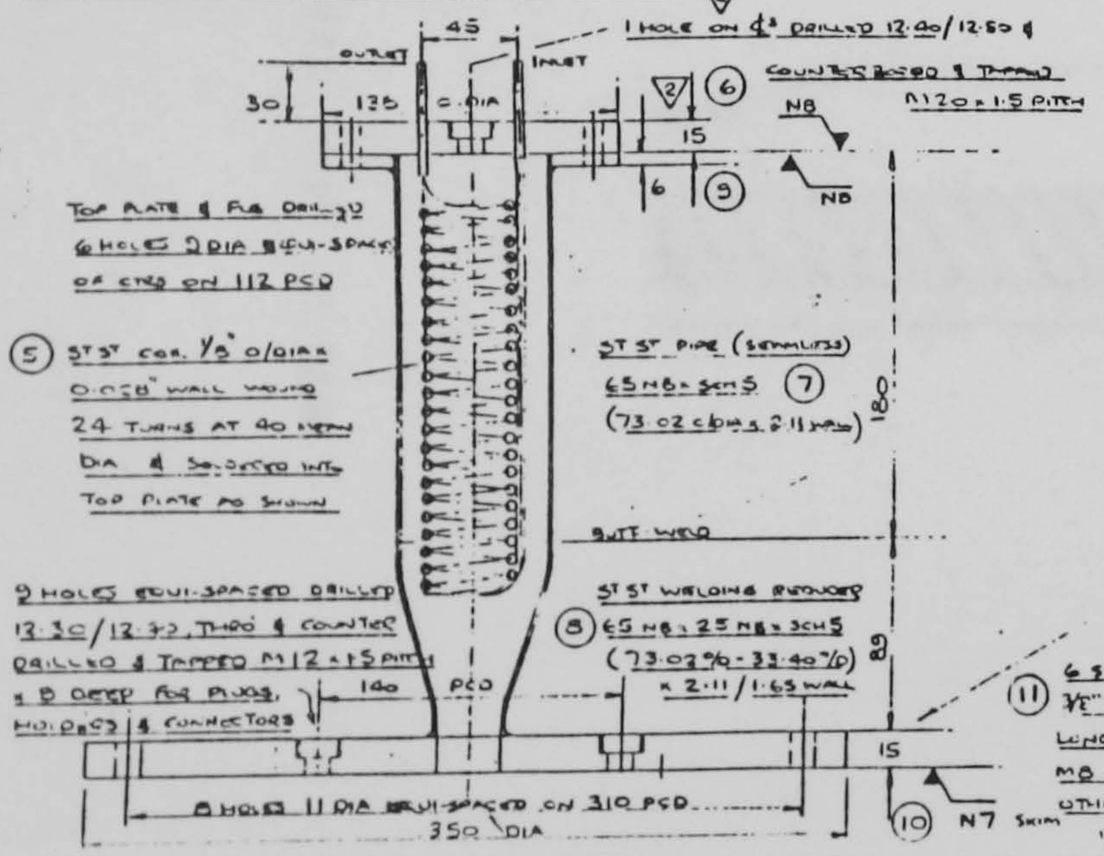

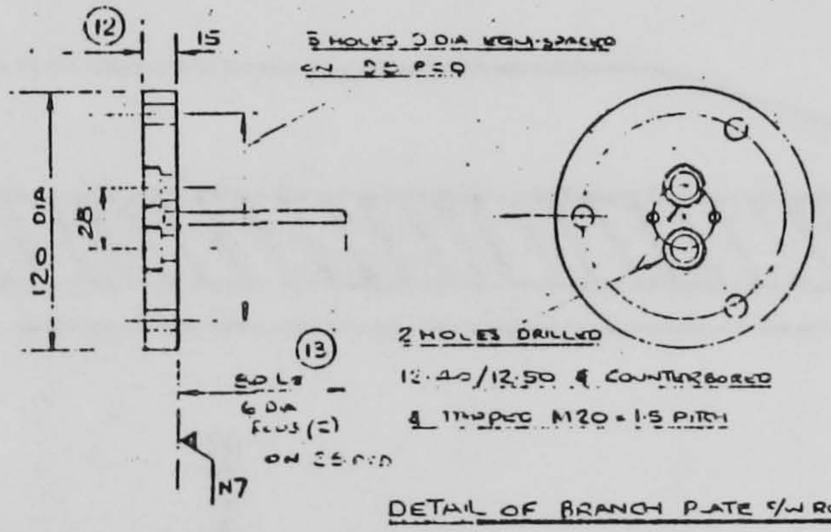

DETAIL OF BRANCH PLATE S/W RODS

MATERIAL :- STAINLESS STEEL AISI 316

FINISH :- FLANGE FACE TO HAVE A SURFACE FINISH OF MINIMUM 2·5 µ Ra (N7). NOT TO BE FREE FROM DEEP SCRATCHES ℄ ABRASION. FLATNESS TO BE WITHIN 0·1 mm.
FACE OF FLANGES TO BE CONCENTRIC ℄ SQUARE TO PIPELINE AXIS

ALL MINOR OF 5ᵀᵀ5ᵀ COMPONENTS TO BE DESCALED ℄ FREE FROM WELD SPATTER WELDS TO BE CONTOUR FREE

ISS No	DATE	DESCRIPTION	ISSUED TO	NAME
3	4.1.88	Complete cover with MTK. O.R.S.	MJ	Dunn
		Cover on Top Spool Components Added		
		2 Bolts added to 25 DN Inlet		
1	15.8	ORIGINAL	M.J.	Dunn

MODIFICATIONS

CUSTOMER :- HERIOT - WATT UNIVERSITY (CHEM ℄ PROCESS ENG)

CUSTOMERS ORDER No. :-

TITLE :- DETAL OF 5ᵀᵀ5ᵀ COMPONENTS FOR G.L.F. DESIGN : FERMENTORS

DO NOT SCALE IF IN DOUBT - ASK! | DIMENSIONS IN MM UNLESS STATED | SCALE :- 2:1 1:2

ALVAL ENGINEERING Co. Ltd.
Leven, Scotland, KY8 5HD.
Telephone (0333) 27220 Telex 728230

	NAME	DATE
DRAWN	MAJER	MAY 8
CHECKED		
APPROVED		

JOB No. :- 50-017 | DRG. No. :- 50-084-1 | ISSUE 2

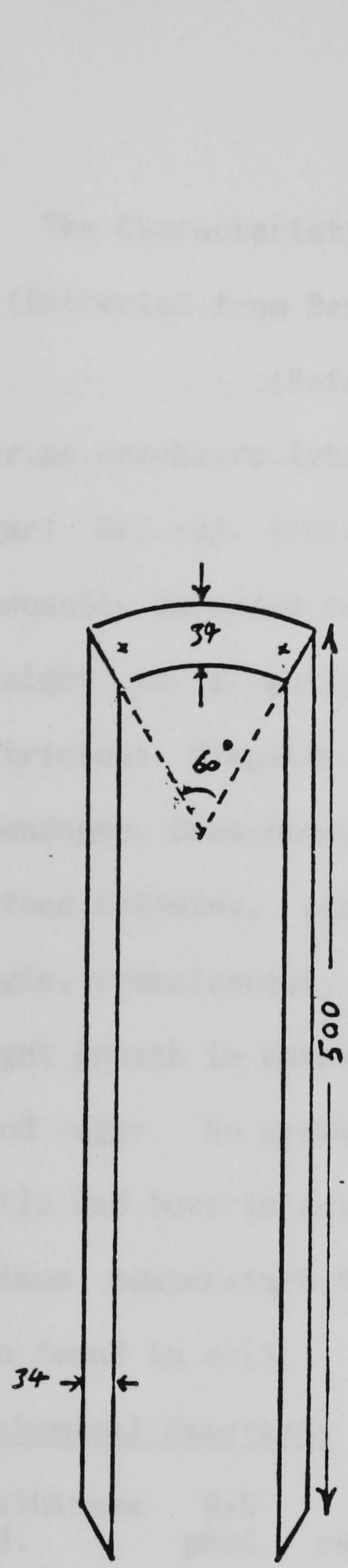

Perspex baffle

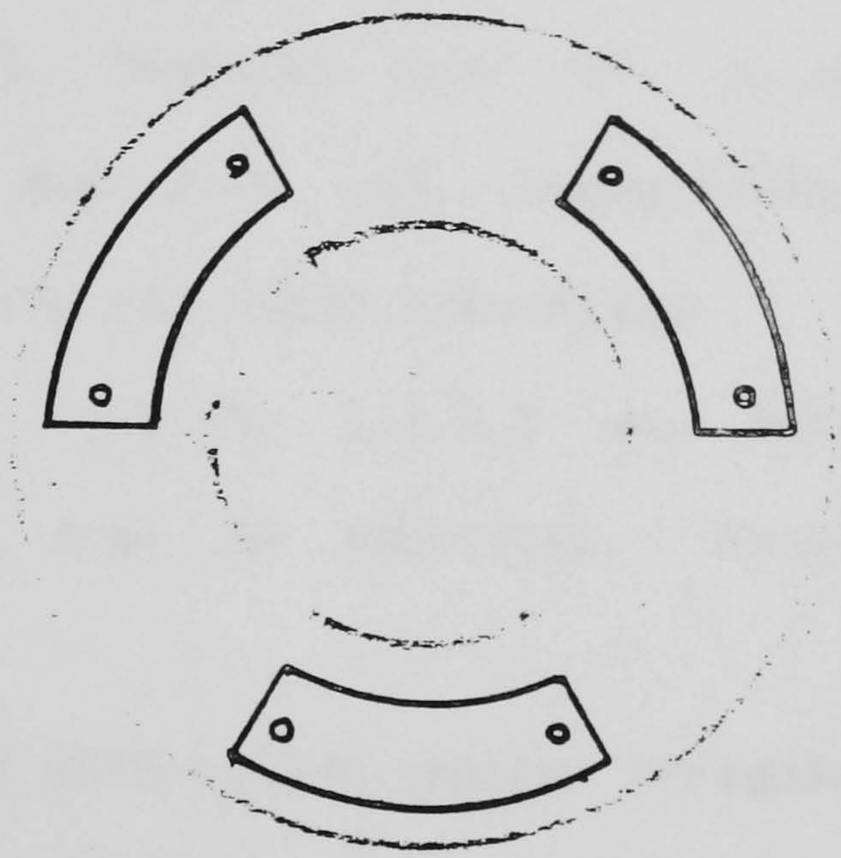

Top view

Side view

Appendix 2 : Dimensions and arrangement of baffles employed in the downcomer of the GLF

Appendix Two

The Characteristic Features of *Clostridium thermosaccharolyticum*

(Extracted from Bergey's Manual of Determinative Bacteriology, 1974)

(Reference strain ATCC 7956, NCIB 9385)

ther.mo.saccha.ro.lyti.cum. Gr. adj. thermus: hot; Gr. n. saccharum: sugar; Gr. adj. lyticus: disolving; M.L. neut. adj. thermosaccharolyticum presumably intended to meanthermophilic and sugar fermenting.

Straight to slightly curve rods, o.5 by 3.1-5.5 μm. Motile with pertrichous flagella. Spores are oval to spherical, terminal; no appendages. Gram-negative.

Surface colonies, circular, low flat with raised centre, irregular lobate margin, transluscent, grayish, glossy surface.

Slight growth in nutrient broth with or without carbohydrate. No growth on blood agar. No growth on egg yolk agar. Fermentation products include acetic and butyric acid.

Optimum temperature for growth is 55 °C; no growth below 45 °C. It has been found in soil.

Biochemical Reactions

Lecithinase prod.	H_2S prod.	NO_3^{-1} reduced	Acetyl methyl carbonyl prod.	Toxin prod.	pathogenic	Blood hemolysed
-	-	-	-	-	-	-

Carbohydrates Fermented

Adonitol	-	Fructose	+	Maltose	+	Salicin	+
Amygdalin	+	Galactose	+	Mannitol	-	Sorbitol	-
Arabinose	+	Glucose	+	Mannose	+	Sorbose	d
Cellobiose	+	Glycerol	-	Melezitose	-	Starch	+
Cellulose	-	Glycogen	+	Melibiose	-	Sucrose	+
Dulcitol	-	Inositol	-	Raffinose	d	Trehalose	d
Erculin	d	Inulin	-	Rhamanose	-	Xylose	+
Erythritol	+	Lactose	+	Ribose	d		

+: growth; -: no growth; d: slight growth

Appendix Three

Computer Programme for Determination of the Area under a Curve

The programme was written in BASIC language for a BBC model B (32 K expanded) computer. The following features were included;

- Data logginig for experimental conditions
- Data retrival from the "Vela Data Logger"
- Calculations of the area under the curve by Simpson's rule
- Determination of Peaks and troughs by gardient analysis
- Smoothing routine for reducing background noise
- Calculation of the mean residence time, and the standard deviation of the distribution by the method outlined by Levenspiel (1972), and thus determination of the percentage dead space in the reactor.
- Filing of the summary of the results including a list of all the peaks observed.

```
+>LIST
   10 MODE 0:CLS:PRINT''"*************************************************************
*********************"''"                              T R A C E     A N A L Y S I S "
   20 PRINT''"            M.Janekeh    20 July 1987""          Heriot-Watt Universi
ty"
   30   PRINT''"*************************************************************
*************":FOR I=1 TO 3000 :I=I:NEXT I
   31 CLS:PRINT''"      Background notes"''
   32 PRINT'"      This program integrates the area under the curve for a recorde
r output. The data is read from a VELA disc (40 track) one file at a time."
   33 PRINT'"The program adjusts for the baseline and correction factor. A smoot
hing routine (option) eliminates the background noise and groups the data ten at
 a time, also determining peaks and the area under the curve."
   34 PRINT'"The mean residence time distribution is evaluated using the respons
e data. The method used is that of LEVENSPIEL,O which also includes an estimate
of the standard deviation of the distribution."
   35 PRINT'"A data file records all the inputed information plus the reported r
esults under the heading R.filename."
   36 PRINT''''"   H I T   A N Y   K E Y   T O   C O N T I N U E":Z=GET
   40 CLS:PRINT '"DO YOU WISH TO SEE THE DIRECTORY ? ":Z$=GET$:IF Z$="N"THEN 80
   50 INPUT'"ENTER 1 FOR SIDE 1 AND 2 FOR SIDE 2 ";S:IF S=1 THEN *CAT 0
   60 IF S=2 THEN *CAT 2
   70 PRINT''"ANY MORE ? ":Y$=GET$:IF Y$="Y" THEN 50 ELSE 80
   80 FIRST=0:LAST=0:H=0:J=1:SIG=0:DIM X(12) ,MVOLT(103),PEAK(30),PTIME(30),A(7)
 :CLS:INPUT''"File name "Source$:PEAK1=0:PEAK2=0
   90 CLS:INPUT''"DATE ";D$'"EXP : ";E$''"SAMPLE VOLUME (ml) ";SV''"MAX OR MIN C
ONC (micro S) ";CM''"VOLUME OF TANK (Liters) ";VOL''"LIQUID FLOWRATE (l/min)  ";
LF
  100 INPUT ''"GAS FLOWRATE (l/min) ";GF''"TEMPERATURE  'C ";TEMP
  110 Source=OPENIN("D."+Source$):FOR I=1 TO 7:A(I)=BGET#Source:NEXT:TME=A(4)*25
6+A(5):CLS:PRINT''"NUMBER OF DATA BYTES = ";A(1)*256+A(2)
  120 PRINT'"PROGRAM NUMBER ";A(3)''"PARAMETER VALUE ";TME,''"DATA BLOCK NUMBER
";  A(6)''"CHANNEL GAIN ";A(7),''''" H I T  A N Y  K EY   T O  C O N T I N U E"
:Z=GET
  130 IF A(3)=1 THEN TME=TME*0.000001
  140 IF A(3)=2 THEN TME=TME*0.001 ELSE 150
  150 Xn_1=0:Scale=(900)/255:FOR I=1TO12:X(I)=BGET#Source:NEXT:FOR I=3TO12:S=S+X
(I):DIF=(SQR(X(I)*X(I))-X(2))+DIF:NEXT:BLINE=S/10:DLINE=DIF/10:MVOLT(1)=S/10
  160 CLS:  BL=BLINE*Scale:Pointn_1=BGET#Source:PRINT"PLOT OF VOLTAGE VERSUS TIME
          CALCULATIONS OF AREA UNDER THE CURVE":PRINTTAB(63,11)"TPEAK = "
  170 I=0:Xn=10:MOVE 0,BL:DRAW 0,900:DRAW 1000,900:DRAW 1000,BL:DRAW 0,BL:DRAW 1
11,BL:PRINTTAB(63,5)"AREA = ":PRINTTAB(63,7)"TIME = ":PRINTTAB(63,9)"PEAK "
  180 REPEAT:MOVE Xn_1,Pointn_1*Scale:Pointn=BGET#Source:T=T+TME:CT%=CT%+(Pointn
-BLINE)*TME:T2=(Pointn-BLINE)*TME*T+T2:T3=(Pointn-BLINE)*TME*T*T+T3:N=N+1
  190 PRINTTAB(70,5);CT%:PRINTTAB(70,7);T:FIRST=Pointn:IFABS(FIRST-LAST)>.06*FIR
ST THEN PROCPEAK
  200 PRINTTAB(70,9);PEAK(H):PRINTTAB(70,11);PTIME(H):PROCSMOOTH :Xn=Xn+1
  210 IF Xn<=1000 THEN DRAW Xn,BL
  220 IF Xn<=1000 THEN DRAW Xn,Pointn*Scale ELSE 230
  230 Xn_1=Xn:Pointn_1=Pointn
  240 UNTIL Xn=1023 OR EOF#Source
  250 CLOSE#Source
  260  MT=T2/CT%:SD=(T3/CT%)-MT*MT:TACT=VOL/(LF*60):DSP=100*TACT/(MT)
  270 PRINTTAB(0,BL/30)"DO YOU WISH TO SEE THE ANALYSIS OF RESULTS":YN$=GET$:IF
YN$="Y" THEN PROCPANA ELSE 290
  290 PRINT''"DO YOU WISH TO LOOK AT SMOOTH CURVE":YN$=GET$:IF YN$="Y" THEN PROC
PMOOTH ELSE 320
  310 PRINT"DO YOU WISH TO HAVE AN ANALYSIS OF THE RESULTS FOR SMOOTH CURVE":YN$
  =GET$ :IF YN$="Y" THEN PROCPANA ELSE 320
  320 PRINT'''"DO YOU WISH TO STORE THIS DATA  ?":YN$=GET$:IF YN$="N" THEN STOP
  330 F=OPENOUT("R."+Source$):PRINT#F,Source$,D$,E$,SV,CT%,CM,VOL,MT,LF,GF,TEMP,
TME,SD,H,MVOLT(90):FOR I=1 TO H:PRINT#F,PEAK(I),PTIME(I):NEXT
  340 CLOSE #F
  350 DEFPROCSMOOTH:I=I+1 :SIG=SQR(Pointn*Pointn)+SIG
  370 IF I=10 THEN J=J+1
  380 IF I=10 THEN MVOLT(J)=SIG/10
  390 IF I=10 THEN SIG=0
  400 IF I=10 THEN I=0
  410 ENDPROC
  430 DEFPROCPEAK:IF (FIRST-LAST)>ABS(DLINE) THEN PEAK2=FIRST
  440 IF ABS(FIRST-LAST)<=ABS(DLINE) THEN 480
  450 IF PEAK2>PEAK1 THEN H=H+1
  460 IF PEAK2>PEAK1 THEN PEAK(H)=PEAK2
  470 IF PEAK2>PEAK1 THEN PTIME(H)=T
  480 LAST=FIRST: PEAK1=PEAK2:ENDPROC
  490 DEFPROCPANA:CLS:VDU 14:PRINT''"NUMBER OF PEAKS OBSERVED =";H
  500 PRINT'"            PEAK No                VOLTAGE (mV)              TIME (sec.)"''
  510 FOR I=1TO H:PRINT"                    ";I;"                  ";PEAK(I);"
      ";PTIME(I) :NEXT:PRINT'"BASELINE AT ";BLINE;" VOLTS"
  540 PRINT'"CORRECTION FOR NOISE =";DLINE;" VOLTS":PRINT'"AREA UNDER CURVE = ";
CT%'''"MEAN RESIDENCE TIME = ";MT/3600" hours"''"STANDARD DEVIATION = ";SD/(3600
*3600)" hours^2"''"THEORETICAL RTD = ";TACT" hours"''"DEAD VOLUME % = ";DSP
  570 ENDPROC
  580 DEFPROCPMOOTH :CLS:H=0:MOVE 0,BL:DRAW 0,900:DRAW 1010,900:DRAW 1010,BL:DRA
W 0,BL:DRAW 11,BL:PRINTTAB(63,5)"PEAK ":PRINTTAB(63,7)"TPEAK "
  600 FOR I= 1 TO (J-1):SM=SM+10:SAREA=TME*10*(MVOLT(I)-BLINE)+SAREA:DRAW SM,MVO
LT(I)*Scale:FIRST=MVOLT(I):T=SM*TME:PROCPEAK
  610 PRINTTAB(70,5);PEAK(H):PRINTTAB(70,7);PTIME(H):Z=GET:NEXT I:ENDPROC
```

References

Adler, I., Deckwer, W.D, and Schügerl, K., *Chem Eng Sci*, **37**: 271, (1982)

Adler, I., Deckwer, W.D, and Schügerl, K., *Chem Eng Sci*, **37**: 417, (1982)

Adler, I., W.D, and Schügerl, K., *Biotechnol Bioeng*, **25**: 417, (1983)

Aduse-Opoku, J., *Unpublished report*, Heriot-Watt University, (1987)

Aduse-Opoku, J. and Michell, W.J., *FEMS Mircobiol Letters*, **50**: 45, (1988)

Aiba, S., Shoda, M. and Nagatami, M., *Biotechnol Bioeng*, **10**: 845, (1968)

Aiba, S. and Shoda, M., *J Ferment Tech*, **47**: 790, (1969)

Akita, K., and Yoshida, F., *Ind Eng Chem Proc Des*, **12**: 76, (1973)

Anonymous, *Biotechnol Bioeng*, **24**: 495, (1982)

Atkinson, B., *Biochemical Reactors*, Pion Press, London, (1974)

Atkinson, B. and Davies, I.J., *Trans IChemE*, **52**: 248, (1974)

Atkinson, B., Black, G.M. and Pinches, A., in *Biological Fluidised Bed Treatment of Water and Waste Water*, Eds. Cooper, P.F, and Atkinson, B. (Ellis Horwood, Chichester) (1980)

Atkinson, B., Mavituna, *Biochemical Engineering and Biotechnology Handbook*, (Macmillan, London) (1983)

Atkinson, B., Black, G.M. and Webb, C., *Chem Eng Res Des*, **62**: 154, (1984)

Barker, S.B. and Summerson, W.H., *J Biol Chem*, **138**: 535, (1941)

Barker, T.W. and Worgan J.T., *Euro J Appl Microbiol Biotechnol*, **13**: 77, (1981)

Barretts de Menezes, T.J., *Proc Biochem*, **17**: 32, (1982)

Bazua, C.D. and Wilke, C.R., *Biotechnol Bioeng Symp*, **7**: 105, (1977)

Bello, R.A, *A Characterisation Studies of Airlift Contactors for Application to Fermentations*, Ph.D Thesis, Univ. of Waterloo, Ont (1981)

Bello, R.A, Robinson, C.W., and Moo-Young, M., *Advances in Biotechnology Vol. 1* ", Moo-Young, M., Robinson, C.W., Vesina, C. (Eds), Proceedings 6th International Fermenter Symposium, Toronto, Pergamon Press, 547, (1981)

Bello, R.A, Robinson, C.W., and Moo-Young, M., *Can J Chem Eng*, **62**: 573, (1984)

Bello, R.A, Robinson, C.W., and Moo-Young, M., *Biotechnol Bioeng*, **27**: 369, (1985)

Benedek, and Heideger, *Biotechnol Bioeng*, **13**: 663, (1971)

Bernhardt, W., *The Futurist*, **14**: 27, (1980)

Black, C., *Chem Eng Progress*, **76**: 78, (1980)

Black, G.M., Webb, C., Matthews, T.M. and Atkinson, B., *Biotechnol Bioeng*, **26**: 134, (1984)

Blakebrough,N., McManamey, W.J., and Walker, M., *Chem Eng Res Des*, **61**: 264, (1983a)

Blakebrough,N., McManamey, W.J., and Walker, M., *Chem Eng Res Des*, **61**: 369, (1983b)

Blenke, H., *Adv in Biochem Eng Vol 13* , Ghose, T.K., Fiechter, A., Blakebrough, N. (Eds), Springer-Verlag, 121, (1979)

Blenke, H., *Biotechnology Vol 2*, Brauer, H. (Eds), Vch Verlagsgesellschaft, **21**: 465, (1985).

Booth, I.R. and Mitchell, W.J., in *Sugar Transport and Mertabolism in Gram-Positive Bacteria*, Reizer, J. and Peterkofsky, A., (Eds), Ellis Horwood, Chichester, (1987)

Brown, T.D.K., Jones-Mortimer, H.L. and Kornberg, H.L., *J Gen Mircobiol*, **102**: 327, (1977)

Brown, L., *Food or Fuel : New Competition with the world's Cropland*, World Watch Institute Paper 35, Washington DC, (1980)

Brown, S.W., Oliver, S.G., Harrison, D.E.F., Righelato, R.C., *Euro J Appl Microbiol Biotechnol*, **11**: 151, (1981).

Buchanan, R.E and Gibbons, N.E *Bergey's Manual of Bacteriology 8th edition* , Waverley Press Inc. (1974)

Buchholz, H., Luttmann, R., Zakrzewski, W., and Schügerl, K., *Chem Eng Sci*, **35**: 111, (1980)

Bucke, C., in *Process Engineering Aspects of Immobilised Cell Systems*, Webb, C., Black, G.M. and Atkinson, B. (Eds), IChemE (Pergamon Press Publs), (1986)

Bu'loch, J.D., *Cellulosic Materials as a U.K Resource*, Weizmann Microlbial Chemistry Labarotory, Manchester, (1983)

Bu'loch, J.D., Comberback, M.D, Ghommidh, C., *Chem Eng J*, **29**: B9 (1984)

Calderbank, D.H., *Trans, IChemE*, **36**: 443, (1958)

Calderbank, D.H., Moo-Young, M., Bibby, R., *Third European Symp on Chemical Reaction Eng*, Pergamon Press (1964)

Campbell, I.M., *Adv Microbial Physiol*, **25**: 1, (1984)

Casey, G.P., Ingledew, W.M., *CRC Critical Rev Microlbiol*, **13**: (1986)

Chakravarty, M., Begum, S., Singh, H.D., Baruah, J.N., and Iyengar, M.S., *Biotechnol Bioeng Symp*, **4**: 363, (1973)

Chan, M., Himes, R.H. and Akagi, J.M., *J Bacteriol*, **106**: 876, (1971)

Charm, S.E., *Fundamentals of Food Engineering 3rd Ed*, Avi Publ. Co Inc, (1978)

Chen, H.C., Zall, R.R., *Proc Biochem*, **17**: 20, (1982)

Chichester, C.O., Netto, A.G., Prebluda, H. J., *The Biotechnology Challange In Brazil* , The Nutrition Foundation New York (1981)

Chung, I.S. and Lee, Y.Y., Enz Mircobial Tech, **17**: 217, (1985)

Clark, N.N., Flemmer, R.L., *AIChE J*, **31**: 500, (1985)

Cooper, P.F, and Atkinson, B., (Eds) *Biological Fluidised Bed Treatment of Water and Waste Water*, Ellis Horwood, Chichester, (1981)

Clift, R., Grace, J.R. and Weber, M.E., *Bubbles, Drops, and Particles*, Academic Press, (1978)

Coulson, J.M., Richardson, J.F., Backhurst, J.R. and Harker, J.H., *Chemical Engineering Vol 2, 3rd Ed*, Pergamon Press (1978)

Curatolo, W., Kanodia, S., Roberts, M.F., *Biochemica et Biophysica Acta*, **34**: 336, (1983)

Dale, B.E., Moreira, M.J., *Biotechnol Bioeng Symp*, **12**: 31, (1982).

Dale, M.C., Okos, M.R. and Wankat, P.C., *Biotechnol Bioeng*, **27**: 932, (1985a)

Dale, M.C., Okos, M.R. and Wankat, P.C., *Biotechnol Bioeng*, **27**: 943, (1985b)

Datta, P. and Zeikus, J.G., *Appl Environ Microbiol*, **49**: 522, (1985)

Daugulis, A.J., Swaine, D.E., *Biotechnol Bioeng*, **29**: 639, (1987)

Dekker, R.F.H., *Biotechnol Letters*, **4**: 411, (1982)

Dekkar, R.F.H., *Biotechnol Bioeng*, **29**: 605, (1986)

Detroy, R.W., Cunningham, R.L., Herman, A.I., *Biotechnol Bioeng Symp*, **12**: 81, (1982)

Dunning, J.W., Lanthrop, E.C., *Ind Eng Chem*, **37**: 24, (1945)

Dussap, G., and Gross, J.B., *Chem Eng J*, **25**: 151, (1982)

Ennis, B.M., Gutirrez, N.A., Maddox, I.S., *Proc Biochem*, **21**: 131,

(1986)

Erickson, L.E., Patel, S.A., Glasgow, L.A. and Lee, C.H., *Proc Biochem*, **18**: 16, (1983)

Esser, K. and Karsch, T., *Proc Biochem*, **18**: 116, (1983)

Esser, K. and Schmidt, U., *Proc Biochem*, **17**: 46, (1982)

Estey, J.R. and Meyer, K.F., *J Infect Dis*, **31**: 650, (1922)

Euzen, J.P., Trambouze, P., van Landeghem, H., *Chemical Reaction Eng* - 5th Int Symp (ACS Symp Ser No. 65), (1978).

Fan, L.S., Hwang, S-J. and Matsuura, A., *Chem Eng Sci*, **12**: 1677, (1984)

Fan, L.S., Ramesh, T.S., Tang, W-S and Long, T-R., *Chem Eng Sci*,**42**: 543, (1987)

Fan, L.S., Fujie, K., Tang, W-S and Long, T-R., *Biotechnol Bioeng*, **30**: 4, (1987)

Fang, H-Y., *MSc Thesis*, MIT, USA, (1980)

Faust, U., Präve, P. and Schlingmann, M., *Proc Biochem*, **18**: 31, (1983)

Fields, P.R. and Slater, N.K.H., *Chem Eng Sci*, **38**: 647, (1983)

Gammack, G. and Brown, C.M., *Heriot-Watt University*, Edinburgh, (1986)

Gareth Morris, J., *Biochem Soc Symp*, **48**: 147, (1983)

Gasner, L.L., *Biotechnol Bioeng*, **16**: 1179, (1974)

Ghose, T.K. and Tyagi, R.D., *Biotechnol Bioeng*, **21**: 1401, (1979)

Gibbs, D.F., *Trends in Biotechnol*, **1**: 12, (1983)

Godbole, S.P and Shah, Y.T in *Encyclopaedia of Fluid Mechanics, Gas-Liquid Flows, Volume 3* , Cheremisinoff, N.P., (Ed), Gulf Publ Co, Houston, (1986)

Gõdia, F., Casas, C., Sola, C., *Proc Biochem*, **22**: 43, (1987).

Hatch, R.T., *Experimental ans Theoretical Studies of oxygen Transfer in the airlift fermenter* , Ph.D. Thesis, M.I.T., (1973).

Hattori,H. and Takeda, K., *J Chem Eng Japan*, **2**: 125, (1978)

Herraro. A.A., Gomez, R.F., *Appl Environ Microbiol*, **40**: 571, (1980)

Herraro, A.A., Gomez, R.F., Roberts, M.F., *Biochemica et Biophisica Acta*, **693**: 195, (1982)

Herraro, A.A., *Trends in Biotechnol*, **1**: 49, (1983)

Herraro, A.A., Gomez., R.F., Roberts, M.F., *J Biol Chem*, **260**: 7442,

(1985)

Higbie, L., *Trans AIChE*, **31**: 365, (1935)

Hinshelwood, C.N., *The Chemical Kinetics of Bacterial Cells*, Oxford University Press, London, (1946)

Hines, D.A., *DECHEMA-Monograph*, **82**: 55, (1978)

Hinze, J.O., *AIChE J*, **1**: 289, (1955)

Ho, C.S., P*roc. 6th Biochem Eng Symp*, **1:** (1976)

Ho, C.S., Erickson, L.E., and Fan, L.T., *Biotechnol Bioeng*, **19**: 1503, (1977)

Ho, C.S., *Proc Biochem*, **21**: 148, (1986)

Holzburg, I., Finn, R.K. and Steinbraus, K.H., *Biotechnol Bioeng*, **9**: 413, (1967)

Hoppe, G.K. and Hansford, G.S., *Biotechnol Letters*, **4**: 39, (1982)

Hsu, E.J, and Ordal, Z.J., *J Bacteriol*, **97**: 1511, (1969a)

Hsu, E.J, and Ordal, Z.J., *Appl Bacteriol*, **18**: 958, (1969b)

Hsu, E.J, and Ordal, Z.J., *J Bacteriol*, **102**: 369, (1970)

Hsu, Y.C., Dudukovic, M.P., *Chem Eng Sci*, **35**: 135 (1980)

Humphreys and Glasgow Ltd, in *The Alcohol Economy*, Rothmans, H., Greenshields, R., Callé, F.R. (Eds), Frances Pinter (Publs.), London (1983)

Hungate, R.E., in *Methods in Microbiology*, Norris, J.R. and Ribbons, D.W. Eds, Vol 3B, Academic Press Inc, New York, (1969)

Hwang, S.J. and Fan, L.S., *Proceedings of the 16th Annual Meeting of the Fine Particle Society*, (1985)

Hwang, S.J. and Fan, L.S., *Chem Engng J*, **33**: 49, (1986)

Ingran, L.O., Buttke, T.M., *Microbial Physiol*, **25**: 254, (1984)

Jiménez, A. and Chávez, O., *Chem Eng J*, **37**: B1, (1988)

Jones, D.T., van der Westhuizen, A., Long, S., Allcock, E.R., Reid, S.R. and Wood, D.R., *Appl Environ Microbiol*, **43**: 1125, (1982)

Jones R.P., *J Appl Biotechnol*, **63**: 153, (1987)

Jöbses, I.M.L., Roels, J.A., *Biotechnol Bioeng*, **28**: 554, (1986)

Kalter, R.J., Boisvert, R.N., Gabler, E.C., Walker, L.P.,Pellerin, R.A, Rao, A.M., and Hang, Y.D., *ERDA report No.* 81-7, 136-144, (1981)

Kamp. F., Wase D.A.J., McManamey, W.J., Mendoza, O. and Thayanithy,

K., *Biotechnol Bioeng,* **30**: 179, (1987)

Kemblowski, Z. and Kristiansen, B., *Biotechnol Bioeng,* **28**: 1474, (1986)

Khan, A.W., Murray, W.D., *Biotechnol Letters,* **4**: 177, (1982)

Kiese, S., Ebner, H.G., and Onken, U., *Biotechnol Letters,* **2**: 345 (1980)

Kim, S.D., Baker, C.G.J. and Bergougnou, M.A., *Can J Chem Eng,* **50**: 695, (1972)

Klecka, G.M. and Maier, W.J., *Appl Environ Microbiol,* **49**: 46, (1985)

Kolot, F.B., *Proc Biochem,* **19**: 7, (1984)

Koide, K., *J Chem Eng Japan,* **16**: 413, (1983)

Koide, K., Sato, H., and Iwamoto, S.J., *J Chem Eng Japan,* **16**: 407, (1983)

Koide, K., Horbie, K., Kawabata, H., and Ito, S., *J Chem Eng Japan,* **3**: 248, (1985)

Korn, S.R., Harper, J.M., *Biotechnol Letters,* **4**: 417, (1982)

Kosaric, N., Duvnjak, Z., and Stewart, G.G., *Adv Biochem Eng,* Springer Verlag, New York, **20**: 119, (1981)

Kubota, H., Hosono, Y. and Fujie, K., *J Chem Eng Japan,* **11**: 319, (1978)

Lamont, A.G.W., *Can J Chem Eng,* **31**: 153, (1958)

Landuyt, S.L., Hsu, E.J. and Lu. M., *Annals New York Acad Sci,* **413**: 473, (1983)

Landuyt, S.L.and Hsu, E.J., in *"Fundamental and Applied Aspects of Bacterial Spores"* (Eds), Academic Press, New York, (1984)

Lee, C.K. and Ordal Z.J., *J Bacteriol,* **94**: 330, (1967)

Lee, J.C. and Buckley, P.S., in *Three Phase Catalytic Reactors* , Ramachandran, P.A. and Chandhari, R.V., Gordon and Breach Science Publishing, New York, (1983)

Lefrançois, L., Mariller, L.G., and Mejane, J.S., *French Patent* 1102200 (1955)

Lefrançois, L., *Problems of aeration and circulation in aerobic fermentation vats.* , 34th Int Conf Ind Chem, Belgrade, Sect. **14**: (1963)

Levenspiel, O., *Chemical Reaction Engineering 2nd Ed* , John Wiley and Sons Inc, (1972)

Levenspiel, O., *Biotechnol Bioeng,* **22**: 1671, (1980)

Lewis, D.A. and Davidson, J.F., *Trans IChemE,* **60**: 283, (1982)

Lewis, D.A., Nicol, R.S. and Thompson, J.W., *Chem Eng Res Des*, **62**: 334, (1984)

Lin, C.H., Fang, B.S., and Wu, C.S., *Biotechnol Bioeng*, **18**: 1557, (1976)

Linden, J.C. and Moreira, A.R., in *Biological Basis of New Developments in Biotechnology*, Hollaender, A.H., Laskin, A.I. and Rogers, P., (Eds), Plenum, New York, 377, (1983)

Ljungdahl, L.G., *Microbial Physiol*, **19**: 149, (1979)

Lovitt, R.W., Longin, R., Zeikus, J.G., *Appl Envior Microbiol*, **48**: 171, (1984)

Luong, J.H.T., *Biotechnol Bioeng*, **27**: 280, (1985)

Luttmann, R., Thoma, M., Lehmann, J., and Shügerl, K., *Biotechnol Bioeng*, **24**: 1851, (1982)

Luttmann, R., Thoma, M., Bucholz, H. and Shügerl, K., *Comp Chem Eng*, **7**: 43, (1983)

Lyons, T. P., *Process Biochem*, **18**: 18, (1983)

Maiorella, B.L., Wilke, C.R. and Blanch, H.W., *Adv Biochem Eng*, **20**: 43, (1981)

Maloney, M.T., Chapman, T.W. and Baker, A.J., *Biotechnol Progress*, **2**: 192, (1986)

Manderson, G.J., *IEA/FE CPD-5 Report No 1* ,(1985)

Margaritis, A., and Sheppard, J.D., *Biotechnol Bioeng*, **23**: 2117, (1981)

Margaritus, A., Bajpai, P., *Biotechnol Bioeng*, **24**: 941 (1982)

Marucci, G., *Chem Eng Sci*, **24**: 975, (1969)

Matsumara, M., Märkl, H., *Biotechnol Bioeng*, **28**: 534, (1986)

Matsuoka, H., Koba, Y., Ueda, S., *J Ferment Technol*, **60**: 599 (1982)

Merchuk, J.C., and Stein, Y., *AIChE J*, **27**: 377 (1981)

Merchuk, J.C., and Stein, Y., *Biotechnol Bioeng*, **23**: 1309 (1981)

Merchuk, J.C., and Stein, Y., and Mateles, R.I., *Biotechnol Bioeng*, **22**: 1189 (1980)

Merchuk, J.C., *Hydrodynamics and Hold-Up in Airlift Fermenters*. In: Encyclopaedia of Fluid Mechanics, Vol. 3 (Cheremisinoff, N.P., ED.) Gulf Publ., Houston, 1485 (1986).

Merchuk, J.C., and Siegel, M.H., *J Chem Tech Biotechnol*, **41**: 105,

(1988)

Metz, B., Kosen, N.W.F. and van Suijdam, J.C., *Adv Biochem Eng,* **11**: 103, (1979)

Michaels, St. L. and Blanch, H. W., *Acta Biotechnologica,* **1**: 351, (1981)

Miller, D.G., Griffiths-Smith, A.E. and Scopes, R.K., *Biotechnol Letters,* **4**: 601, (1982)

Miyahara, T., Hamaguchi, M., Sukeda, Y., Takahashi, T., *Can J Chem Eng,* **64**: 718 (1986)

Monod, J., *Ann Rev Microbiol,* **79**: 390, (1949)

Moresi, M., *Biotechnol Bioeng,* **23**: 2537, (1981)

Moreira, A.R., *UN DO Workshop on Fermmentation of Alcohol DOC ID/WG* 293/2, Vienna (1979)

Moreira, A.R., Dale, B.E. and Doremus, M.G., *Biotechnol Bioeng Symp,* **12**: 263, (1982)

Moss, M.O and Smith, J.E., *Industrial Applications of Microbiology,* Surrey University Press, London, (1977)

Moulin, G., Boze, H., Galzy, P., *Biotechnol Letters,* **3**: 351, (1981)

Nauman, E.B. and Buffham, B.A., *Mixing in Continuous Flow Systems* , Wiley and Sons Inc, (1983)

Nauman, E.B., *Chemical Reactor Design* , Wiley and Sons Inc, (1987)

Nicol, R.S. and Davidson, J.F., *Chem Eng Res Des,* **66**: 152, (1988)

Núñez, M.J., Lema, J.M., *Enzyme Microbial Technol,* **9**: 642, (1987)

Onken, U, Weiland, P., *J Appl Microbiol Biotechnol,* **10**: 31, (1980)

Onken, K., and Weiland, P., *Advances in Biotechnology Vol 1* , Moo-Young, M., Robinson, C.W., Vezina, C., (Eds), Oxford, Pergamon Press, 559, (1981)

Onken, K., and Weiland, P., *Advances in Biotechnological Processes, Vol 1* , Mizrahi, A., Van Wezel, A.L., (Eds), Alan R Liss Inc New York, 67, (1983)

Onken, K., and Jostmann, Th., *Biotechnol Letters,* **6**: 413, (1984)

Orazem, M.E., and Erickson, L.E., *Biotechnol Bioeng,* **21**: 69 (1979)

Orazem, M.E., Fan, L.T., and Erickson, L.E., *Biotechnol Bioeng,* **21**: 1579 (1979)

Parekh, S.R., Parekh,R., Wayman, M., *Proc Biochem,* **22**: 85, (1987)

Perry, H.R. and Green D., *Perry's Chemical Engineers Handbook 6th Ed* ,

McGraw-Hill, (1984)

Pheil, C.G. and Ordal, Z.J., *Appl Microbiol*, **15**: 893, (1967)

Pieber, M. and Toha J.C., *J Ferment Technol*, **60**: 247, (1982)

Pitt, Jr, W.W., Haag, G.L. and Lee, D.D., *Biotechnol Bioeng*, **25**: 123, (1983)

Rogers, P., *Adv Appl Microbiol*, **31**: 1, (1986)

Rose, A.H. and Beaven, M.J., in *Trends in Biology of Fermentation for Fuels* , Plenum, New York, (1981)

Rothmans, H., Greenshields, R., Callé, F.R. (Eds), *The alcohol economy* , Frances Pinter (Publs), London (1983)

Rothstein, D.M., *J Bacteriol* , **165**: 319, (1986)

Rousseau I., and Bu'loch, J.D., *Biotechnol Letters*, **2**: 475, (1980)

Schügerl, K, *Proceedings of International Symposium on Fluidisation* , Eindhoven, **9.4**: 102, (1967)

Serra, A., Poch, M., and Sola, C., *Proc Biochem* , **22**: 154, (1987)

Shah, Y.T. and Sharma, M.M., *Trans IChemE* , **54**: 1, (1976)

Shah, Y.T., *Gas-Liquid-Solid Reactor Design* , McGraw Hill, New York, (1979)

Shah, Y.T., Kelkar, B.G., Godbole, S.P. and Deckwer, W.D., *AIChE J* , **28**: 353, (1982)

Shieh, W.K and Chen, C.Y., *Chem Eng Res Des* , **62**: 133, (1984)

Siegel, M.H., Merchuk, J.C., Schügerl, K., *AIChE J*, **32**: 1585, (1986)

Sittig, W., Faust, U., *Chem Engineer*, 230, June, (1982)

Sjolander, N.O., *J Bacteriol*, **34**: 419, (1937)

Skoog, K.and Hahn-Hägerdal, B. *Enzyme Microbiol Technol*, **10**: 66, (1988)

Sleyter, U.B., Thorne, K.J.I., *J Bacteriol*, **126**: 377, (1976)

Sonnleitner, B. and Fiechter, A., *Tends in Biotechnol*, **1**: 74, (1983)

Suppelco Reporter, *GC Bulletin 816 A* , Suppleco Inc, (1984)

Taya, M., Suzuki, Y. and Kohayashi, *J Ferment Technol*, **62**: 229, (1984)

Treybal, R.E., *Mass-Transfer Operations 3rd Ed*, McGraw-Hill Inc, London, (1980)

Tsao, G.T., Ladisch, M.R., Voloch, M., Bienkowski, P., *Proc Biochem*, **17**: 34, (1982)

Tsao, G.T., Ladisch, M.R., Ladisch, C., Hsu, T.A., Dale, B., Chou, T., *Annual Reports On Fermentation Proceses Vol. 2,* Academic Press Inc. (1978)

van Uden, N., *Adv Microbial Phys*, **25**: 195, (1984)

Vancanneyt, M., De Vos, P. and De Ley, J., *Biotechnol Letters* , **9**: 567, (1987)

Vega, J.L., Navarro, A.R., Clausen, E.C., Gaddy, J.L., *Biotechnol Bioeng,* **29**: 633, (1987)

Verlaan, P., Tramper, J., Van 'T Riet, K., *Chem Eng J* , **33**: B43, (1986)

Viswanthan, K., in *Encyclopaedia of Fluid Mechanics, Gas-Liquid Flows, Volume 3* , Cheremisinoff, N.P., (Ed), Gulf Publ Co, Houston, (1986)

Wallis, G.B., *One-Dimensional Two-Phase Flow,* McGraw Hill , New York, (1969)

Wardell, J.N., *Personal Communication*, Heriot-Watt University, (1985)

Wase, D.A.J., McManamey, W.J. and Raymahassay, S., *Biotechnol Bioeng,* **27**: 1166, (1985)

Webb, C., Fukuda, H. and Atkinson, B., *Biotechnol Bioeng,* **28**: 41, (1986)

Webb, C., Black, G.M. and Atkinson, B. (Eds), *Process Engineering Aspects of Immobilised Cell Systems*, IChemE, (Pergamon Press), (1986)

Weiland, P., Onken, U., *Ger Chem Eng*, **4**: 174, (1981)

Weiland, P., *Ger Chem Eng,* **7**: 374 (1984)

Wecker, M.A., Zall, R.R., *Proc Biochem* , **22**: 135, (1987)

Wodinski, R.J., Gennaro, R.N., Scholla, M.H., *Adv Appl Microbiol*, **32**: 37, (1987)

Woods, D.R. and Jones, D.T., *Adv Microbial Phys*, **28**: 1, (1986)

Zajic, J.E., Maddux, N.L. and Jones, L.P., *Acta Biotechnologica*, **4**: 307, (1982)

Zeikus, J.G., *Ann Rev Microbiol* , **34**: 423, (1980)

Zertuche, L. and Zall, R.R., *Biotechnol Bioeng,* **24**: 57, (1982)

Ziffer, J., Iosif, M.C., *Biotechnol Letters,* **4**: 573, (1982)

Zuber, N., Findlay, J.A., *J Heat Transfer,* Nov, 453, (1965)